A Model-based Method for Optimising Emissions of Diesel Engines Through Non-linear Model Predictive Control

DISSERTATION

Presented in Partial Fulfilment of the Requirements for
the Degree Doctor of Philosophy
in the University of Gloucestershire

By

XIAOMING WANG

Cheltenham, United Kingdom, June 2019

Faculties and Schools:
School of Business and Technology

Supervisors:
Professor Shujun Zhang
Professor Kemal Bechkoum

DECLARATION OF AUTHORSHIP

I certify that the work presented here is, to the best of my knowledge and belief, original and the result of my own investigations, except as acknowledged, and has not been submitted, either in part or whole, for a degree at this or any other University.

Xiaoming Wang

02.06.2019

ABSTRACT

For diesel engines, based on the legislative emission limits set by Euro I to Euro VI, the reductions required in particulate matter and nitrogen oxide are 80% and 90%, respectively. Meanwhile, fuel-consumption efficiency is still an important consideration for customers due to ever-increasing fuel prices. Modern diesel engines employ advanced fuel-injection systems which can efficiently reduce emissions and fuel consumption, as they have good fuel distribution in the combustion chamber and produce a close-to-homogeneous charger-compression ignition. However, ideal combustion conditions can be achieved only in combination with optimal control of the air-path system of the engine. Therefore, the aim of this study is to research, design and develop a new algorithm for the nonlinear, model-predictive control of air-path systems of diesel engines. In this study, which is conducted on the basis of measurements taken from a virtual test-bench under near-real load conditions, a linear parameter-varying model is created and parameterised by dynamical system identification. The results of simulation show that a linear parameter-varying modelling approach can be used to represent this air-path system more precisely than is possible with other, more conventional methods. The data-based modelling approach through an engine-simulation platform and the model-based optimisation framework developed in this study are used to design an innovative, non-linear, model-predictive controller for a diesel-engine air-path. The idea behind the proposed non-linear model-predictive control strategy is to represent the plant model as a linear parameter-varying model, and the control-objective function in searching for an optimal solution to the quadratic programming problem is extended to the parameter-varying cost function by utilising the given linear parameter-varying model. This concept is aimed at optimising the efficiency of engine-air-path systems with respect to intake-manifold pressure and air-mass flow tracking in transient operations. The problems of a prediction-model mismatch and the cross-coupling effects of two actuators are overcome by the application of a multiple-input, multiple-output linear parameter-varying model. The results reveal that, compared to existing approaches, the proposed non-linear model-predictive control method significantly improves the accuracy and computational efficiency of engine-air-path system control—even in large, transient operations. Finally, significant potential exists to improve the performance of the control. Thus, emissions and fuel consumption in the certification driving cycle of the vehicle can be optimised on the basis of the model.

ACKNOWLEDGE

I am indebted to many supportive people for their encouragement which provide invaluable for the research work presented.

First of all, I want to thank the people who guided and supported my thesis during my study at the University of Gloucestershire. I would like to thank my supervisor Professor Shujun Zhang for his restless encouragement in the field of engineering science, full of ideas and guiding me from beginning to the end of my thesis. His patience and support allowed me to spend time on the focus and finally to write this thesis. It has been a great honour to be his PhD student. Furthermore, I would like to thank Professor Kemal Bechkoum who kindly reviewed this thesis. His expertise in scientific research was a great help. I also thank my company colleagues from BRP-Rotax GmbH & Co KG for all the technical discussions, in particular the head of structural mechanics, Dipl.-Ing Karl Glinsner, the manager of virtual powertrain, Dipl.-Ing Michael Gumpesberger, and the head of thermodynamics, Dipl.-Ing Stefan Leiber, who teach and support me from the beginning of my work. Special thanks go to Dipl.-Ing Jean-Charles Pouillard and Dipl.-Ing Johann Schamberger for the proofreading and advice. This thesis would not have been possible without their helps. The advices of Dipl.-Ing Andre Sell from SGE Engineering GmbH on optimisation and visualisation issues are greatly appreciated.

The final words I want to dedicate to my family, who made it possible for me to complete my PhD study. The encouragement and support they gave me throughout the duration of my overseas life in different countries and the words to describe my deep appreciation fail me. Special thanks go to my wife Cheng Li for her dedication and confidence in me. Her generosity and support gave me enough time to work on my thesis but also for provided moments of distraction necessary to for me to do my work with the intensity and passion needed for completion.

June 2019

Xiaoming Wang

TABLE OF CONTENTS

List of Notations and Abbreviations

Notation	**Meaning**	**Unit**
A	State (or System) Matrix	
A_{plant}	System Matrix Plant	
A_{dist}	System Matrix Disturbance	
A_{EGR}	Open Section Exhaust Gas Recirculation	%
$A_{CloseLoop}$	System Matrix Close Loop	
A_{tube}	Intake Tube Area	
a	Coefficient in State (or System) Matrix	
B	Input Matrix	
B_{dist}	System Matrix Disturbance	
B_{plant}	System Matrix Plant	
$B_{CloseLoop}$	System Matrix Close Loop	
b	Coefficient in Input Matrix	
C	Output Matrix	
C_{plant}	System Matrix Plant	
C_{dist}	System Matrix Disturbance	
C_{o2a}	Oxygen Mass Concentration Ambient	%
C_{o2x}	Oxygen Mass Concentration Intake	%
C_{o2i}	Oxygen Mass Concentration Exhaust	%
$C_{CloseLoop}$	System Matrix Close Loop	
c	Coefficient in Output Matrix	
ci	Position Compressor Intake	
c_p	Specific Heat Capacity Constant Pressure	
c_v	Specific Heat Capacity Constant Volume	
D	Feedthrough (or Feedforward) Matrix	
d	Coefficient in Feedthrough (or Feed-forward)	
E	Expectation	
e	System Error	
ex	Position After Cylinder	

f	Gradient	
g	Function of Linear Regression	
H	Hessian Matrix	
$H(t)$	Enthalpy Equation	kj/kg
ie	Position Intake Manifold	
is	Isentropic	
J	Cost Function	
k	c_p/c_v	
MAF	Intake Manifold Air Flow	kg/h or mg/st
MAP	Intake Manifold Air Pressure	bar or mbar or hpa
l	Length of the Intake Tube	m
m	Mass	kg or g
m_f	Fuel Injection	mg/st or kg/h
NOx	Nitrogen Oxides	ppm
n	Rotation Speed	rpm
nT	Position After Turbine	
n_{PH}, PH	Prediction Horizon	
n_{CH}, CH	Control Horizon	
$OPAC$	Opacity	%
PM	Particulate Matter	%
P_{ex}	Exhaust Manifold Pressure	bar or mbar or hpa
p	Pressure	bar or mbar or hpa
p_r	Ratio Between Intake and Exhaust	
p_i	Scheduling Variables	
Q	Output Weight	
Q_{NMPC}	NMPC Output Weight	
$Q_{KalmanFilter}$	Kalman Filter Output Weight	
R	Input Weight	
R_{NMPC}	NMPC Input Weight	
$R_{KalmanFilter}$	Kalman Filter Input Weight	
T	Temperature	k or c°
TL	Turbocharger	
u	System Input	

v	Volume	m^3 or cm^2
vT	Position Before Turbine	
W	Mass Flow	
W_f	Injection	mg/cyc or kg/h
w	System Input Matrix	
xi	Position Exhaust Gas Recirculation	
xt	Position Intake Turbine	
x_{EGR}	Rate Exhaust Gas Recirculation	%
x_{VGT}	Rate Variable Turbocharger	%
y	System Output	
y_{ref}	Reference Output	
$\hat{y}$	Estimated System Output	
φ	System Input Vector	
θ	System Parameter Vector	
$\hat{\theta}$	Estimated Parameter Vector	
$\emptyset$	System Input Matrix	
ε	System Error	
ω	Relaxation Parameter	
η	Efficiency	%
τ	Turbo Time Constant	second
lb	State Under Limit	
ub	State Up Limit	
$\mathcal{A}$	System Matrix	
$\mathcal{B}$	System Matrix	
$\mathcal{C}$	System Matrix	
$\mathcal{G}$	System Matrix	
$\mathcal{K}$	System Matrix	
$\mathcal{S}$	System Matrix	
$\mathcal{T}$	System Matrix	
λ	Air Fuel Ratio	
λ^T	Lagrange Multipliers	
∇L	Hessian of the Lagrangian	
Δu	Rate System Input	

$\Delta\theta$	Variation of System Parameter	
Δz	Chang of z	
δ	Chang/Rate	
dU	Change of Internal Energy	w or kw
δQ	Rate of Heat Transfer	w or kw
δW	Rate of Total Work	w or kw
$(.)_c$	Index of Compressor	
$(.)_{ci}$	Index of From Compressor to Intake Manifold	
$(.)_e$	Index of Engine Cylinder	
$(.)_f$	Index of Fuel	
$(.)_t$	Index of Turbine	
$(.)_{TL}$	Index of Turbocharger	
$(.)_m$	Index of Mechanical	
$(.)_x$	Index of Exhaust	
$(.)_{xi}$	Index of From EGR to Intake manifold	
$(.)_{xt}$	Index of Exhaust to Turbine	

Abbreviation	**Meaning**
ACEA	European Automobile Manufacturers' Association
Ar	Argon Gas
ARMAX	Autoregressive Moving Average Exogenous Input
ARX	Autoregressive with Exogenous Input
CO2	Carbon Dioxide
DEQ	Differential Equations
DOC	Oxidation Catalysts
DOE	Design of Experiment
DPF	Diesel Particulate Filter
ECU	Engine Control Unit
EGR	Exhaust Gas Recirculation
ESC	European Stationary Cycle
Euro	European Emission Standards
FTP-75	EPA Federal Test Procedure
GPC	Generalised Predictive Control
HCCI	Homogeneous Charger Compression Ignition
HiL	Model in the Loop
Hinf	H Infinity Methods
KKT	Karush Kuhn Tucker
LMI	Linear Matrix Inequalities
LPV	Linear Parameter Varying
LQR	Linear Quadratic Regulator
LS	Least Square
LTI	Linear Time Invariant
MAF	Air Mass Flow
MAFref	Reference of Air Mass Flow
MAP	Manifold Pressure
MAPref	Reference of Manifold Pressure
MiL	Model in the Loop
MIMO	Multiple Input Multiple Output
MISO	Multiple Input Single Output
MPC	Model Predictive Control

N_2	Nitrogen Gas
NEDC	New European Driving Cycle
NMPC	Non-linear Model Predictive Control
NOx	Nitrogen Oxides
O_2	Oxygen Gas
OEM	Original Equipment Manufacturer
OPAC	Opacity
DPF	Diesel Particulate Filter
PI	Proportional Integral Controller
PID	Proportional Integral Derivative Controller
PM	Particulate Matter
QP	Quadratic Programming
RQ	Determination Coefficient
RMSE	Root Mean Square Error
SCR	Selective Catalyst Reactions
SERM	Software Engineering Research Methodology
SISO	Single Input Single Output
SQP	Sequential Quadratic Programming
VAF	Variance Account For
VGT	Variable Geometry Turbocharger
VVT	Variable Valve Train
VW	Volkswagen
WG	Wastegate

LIST OF FIGURES

LIST OF TABLES

Chapter 1. INTRODUCTION

1.1 Background

The European car market is currently experiencing a strong business growth towards the end of 2017, and prospects for 2018 and 2019 look cautiously optimistic. New passenger-car registrations, which reached 1,088,498 units in 2017 increased by 3.4% to a six-year high according to data published by the European Automobile Manufacturers' Association (ACEA) in December of 2017. The five major car markets in Europe have all contributed to solid growth, with Italy and Spain leading the way with 7.9% and 7.7%, respectively (ACEA, 2018). However, the overall market volume may remain at a lower level despite this positive trend (Integer Research, 2018).

Note that the emissions industry has been dominated by news of the Volkswagen Group (VW) emissions scandal ever since it broke in September of 2015. Industry stakeholders have commented that they feel that the entire industry not just the passenger car sector is under intense scrutiny from regulatory officials, the media and the public. It leads to increasingly stringent in-service conformity limits to prevent any similar situations (Integer Research, 2018). Whether customers will trust the performance of diesel vehicles is in question, as is the potential for such vehicles to face heavy restrictions or to be banned from some urban areas of big cities such as London and Shanghai. The reputation of the emissions-control industry is under question, and swift action is being taken—and will continue for the foreseeable future—to assure the public and regulatory officials that emissions-control manufacturers can be trusted to develop low-emissions, fuel-efficient technology and vehicles (Integer Research, 2018).

In recent years, climate change has often dominated the headlines of newspapers and television broadcasts all around the world. The result is an increased environmental awareness—especially in industrialised countries (Jacob, Goettel, Kotlarski, Lorenz, & Sieck, 2008; WWF, 2018).

Diesel engines offer many advantages over gasoline engines in many respects (Song, 2015; Zhao, 2010); however, the weakness of emissions cannot be ignored. Diesel vehicles bore the brunt of recent bad press surrounding emissions, and the admission of VW has only compounded this. Nitric oxides (NOx) and particulate matter (PM)[1] are the main ingredients of air emitted by the tailpipe of the vehicles. Due to their specific combustion characteristics, the diesel engines release more NOx and more PM as compared to gasoline engines. These emissions are known to cause cancer as well as severe respiratory issues (WWF, 2018).

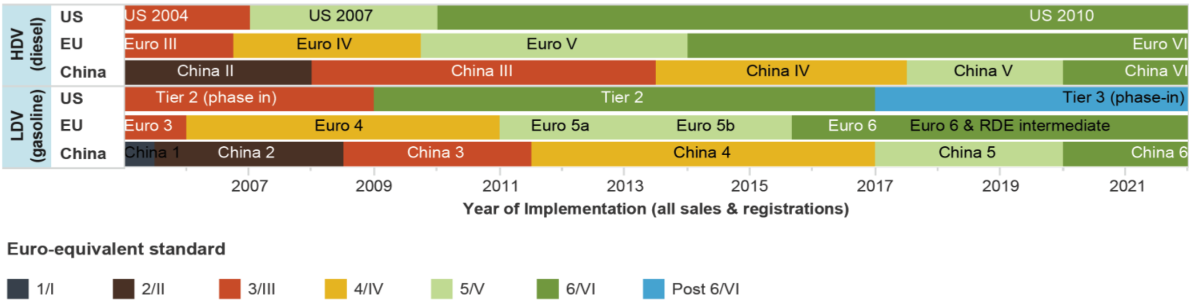

Figure 1.1: US, EU and China vehicle emissions standards (Transport Resources Interational Limited, 2017)

As shown in Figure 1.1, for Euro VI (Transport Resources Interational Limited, 2017) regulations and vehicles, the mandatory standards for new type approvals and registrations have been in place since 2016 and are showing good results in vehicles in the reduction of critical pollutants. For example, good results have been noted with respect to NOx and PM from diesel engines and overall vehicle efficiency.

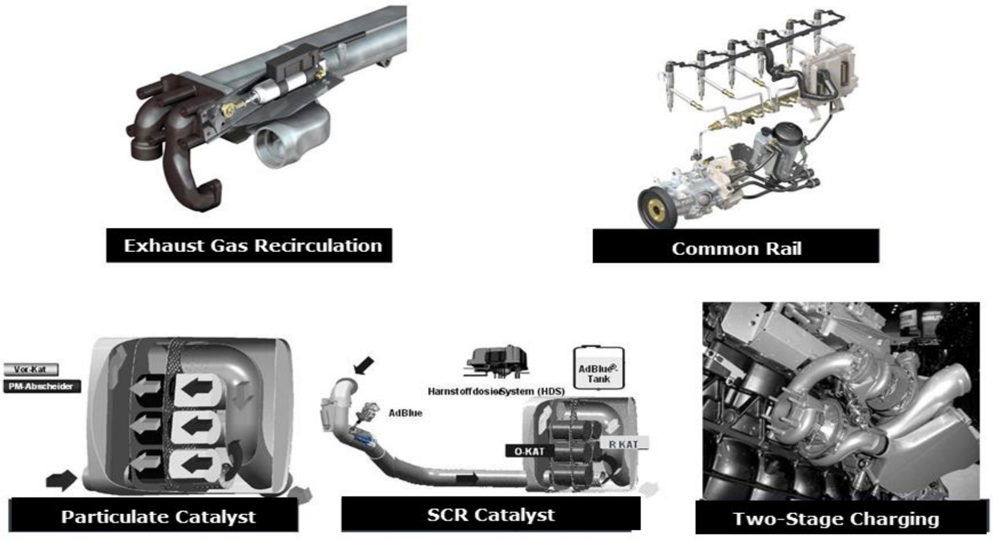

Figure 1.2: Key technology for clean and economical diesel engine (Azam, Ali, & Iqbal, 2016)

[1] Using the AVL micro-soot sensor and opacimeter, the PM can be measured as opacity (OPAC) in % to describe the opacity of contaminated air (in particular, of diesel-engine exhaust emissions).

Further reduction in pollutants can be made by improving engine-control systems and after-treatment systems, as shown in Figure 1.2. Advanced control method in engine control unit (ECU), diesel particulate filters (DPF) and selective catalytic reduction (SCR) are widely used in vehicle applications to solve space issues and improve vehicle efficiency. The harmonisation and the development of a common product is a priority for vehicle, engine and technology manufacturers. The aim of the manufacturers is to develop and sell a common product through the global market; however, differing regulations and staggered advancements in different countries make this goal hard to achieve (Integer Research, 2018).

From an engineering aspect, there is some concern that global legislative emission targets are becoming increasingly stringent more quickly than the technology can be developed. Electric and hybrid vehicles are making inroads, but there two main problems. One is that the higher-complexity system architecture of a combustion system leads to higher vehicle weight and manufacturing costs. The other is that the battery still has a limited capacity and regularly requires time-consuming charging. So far, there is no significant improvement and reasonable solution. Therefore, periodic inspections must rely on improved engine hardware and control systems to enforce and act on emissions results. However, some engine-management technology manufacturers are lobbying against enforcement, as the technology needed to support this is not ready (JRC, 2016). Given the relatively close deadline for compliance with further emission standards, the industry focus has already turned to producing engines with advance control systems and after-treatment technology.

To achieve these targets, exhaust after-treatment systems such as DPF and SCR have made considerable progress in improving efficiency and decreasing emissions in recent years. However, the heart of the engine system is still the combustion itself, which has to be controlled as well as possible. Modern diesel engines employ advanced fuel-injection systems which can efficiently reduce emission and fuel consumption, as they have a better fuel distribution in the combustion chamber and produce a nearly homogeneous charger compression ignition. However, this ideal combustion condition can only be met by cooperating with an optimally controlled engine-air-path system[2]. There has been a strong trend toward developing an improved engine-air-path system for diesel engines, combining the advance turbocharger technology and optimised air-path control system on diesel engines,

[2] Engine-air-path system refers to diesel engine-air-path system in this whole document, unless otherwise noted.

which boast space-saving, increased efficiency and improved emissions reduction and thermal management. To reduce diesel-engine emissions, advanced control strategies are needed to adjust the transient peaks when the engine changes from one working state to another. However, as reviewed in Chapter 2, the diesel engine-air-path is a highly coupled, nonlinear, multi-input multi-output (MIMO) system with constraints, hysteresis and a limited feasible working range (Baines, 2005; Robert Bosch, 2006; Wang, Waschl, Alberer, & Del Re, 2012; Yang, Winward, Zhao, & Stobart, 2016; Skarke, Auerbach, Bargende, & Berner, 2017)—all of which make engine control more difficult. In a modern diesel engine, a turbocharger consists of two parts: a compressor and a variable geometry turbine (VGT). The compressor pumps the fresh air to the engine intake manifold to boost the pressure. The fuel is directly injected into the combustion chamber by a high-pressure fuel injection unit and is burnt with the delivered air. Part of the exhaust gas is re-circulated into the intake manifold by an exhaust-gas-recirculation (EGR) system that is aimed to reduce the NOx emission. VGT absorbs the heat energy from the exhaust gas and propels the compressor. An inter cooler is used to lower the fresh-air temperature, and an EGR cooler is used to lower the re-circulated gas temperature (Wei, 2006). The main control targets of the engine-air-path are to adjust the VGT vane position and the EGR valve, thereby regulating the compressor speed and exhaust-gas circulation rate to meet the standards for manifold air pressure (MAP) and air-mass flow (MAF), thereby producing as much energy per fuel unit as possible while keeping emissions below a given threshold.

The applications of diesel engine-air-path control have been presented in many works, Nieuwstadt, Moraal, Kolmanovsky and Stefanopoulou (1998) report a multivariable design for VGT and EGR control in combination with a gain scheduled approach. Atam (2018) develops an extended linear parameter-varying (LPV) model to design an LPV controller for engine-air-path system control in diesel engines. Analytical model-based control approaches and data-driven disturbance observers for the diesel-engine air-path are applied in (Aran & Unel, 2017). Different treatments of the nonlinear modelling and fuzzy control of the engine-air-path are applied in (Abidi, Bosche, & El Hajjaji, 2013). They are applied more in detail in (Zhao & Pan, 2012), in which a fuzzy proportional–integral–derivative (PID) controller is performed by real-time system with a guaranteed robustness property and coupled with a GT-Power engine model. Lyapunov-based nonlinear control is presented in several works (Jankovic & Kolmanovsky, 2000; Jung, 2003; Liu & Wei, 2007). Wei (2006) presents linear parameter-varying (LPV) techniques for an air-path H-infinity (H_{inf}) controller.

Recently, the application of model predictive control (MPC) for engine control has attracted much interest due to its ability to handle constrained MIMO control problems and to explicitly minimise emissions, fuel consumptions and control errors by a cost function. In contrast to classical feedback controllers, MPC could provide a promising control technique for the air-path system due to its ability to handle disturbances, system constraints, time-delay processes and MIMO systems. Several engine controls based on linear MPCs have been proposed in the literature (Kristoffersson, 2006; Maruyama, Shimura, Ejiri, & Ikai, 2011; Zhao, 2013; Wissel, Talon, Grangier, Lansky, & Uchanski, 2016). However, the improvement of technology-and-control theory facilitates the application of MPC to problems that often require a nonlinear MPC (NMPC) because of the complicated transients involved (Grüne & Pannek, 2017). Therefore, NMPC is a logical extension of MPC in which the linear model is substituted by a nonlinear one (Wang, Waschl, Alberer, & Del Re, 2012). But integrating the nonlinear model into the MPC optimisation task normally leads to a non-convex quadratic-programs (QP) problem, which is computationally expensive and is accordingly hard to solve in a short time for practical applications (Diehl, Bock, & Schloeder, 2005).

Fortunately, some faster optimisation algorithms have been developed, and more computing power is available for ECU. Therefore, it is now feasible to adopt and implement an NMPC approach to the engine-control system. An explicit MPC strategy for air-path control is implemented in (Ortner, Langthaler, Ortiz, & del Re, 2006). The explicit MPC design considers multiple models, which are selected by way of a performance cost for each engine-operating region. But what should not be neglected is that the explicit MPC has to search in the polyhedral partition, which needs long time, when many regions are present. In (Ferreau, 2006) a fast method of QP-solver is presented. The results show that an upper computation bound of optimal problem can be ensured in real-time, which is very suitable for the air-path control application. But implementing a more precise prediction modelling to MPC is still a challenge task. In further developments, Wang, Waschl, Alberer and Del Re (2012), Wang, Zhang and Bechkoum (2016) and Wang, Zhang and Bechkoum (2019) develop a cost function combined with LPV structure for air-path control. The advantage of the LPV structure is that the cost function is evaluated at each iteration by using the current external parameters. However, until now, most LPV models used in MPC are independently identified as single-input single-output (SISO) and multi-input single-output (MISO) forms with limited range of inputs and outputs. So far as the author knows, no global engine-air-path model exists which is suitable for NMPC in terms of model quality and computational performance.

Based on the above discussion, in this study, a more efficient NMPC solution for air-path control is proposed and developed by way of a model-based development process combined with a consistent test strategy to ensure the development quality. The problems of prediction model mismatch are overcome by the application of a MIMO LPV model. Compared with a general MPC, this new NMPC can be used to achieve optimum closed-loop performance by using only one plant and one controller combination in the whole engine operation area—even during plant operation in regions with some distance from the linearisation point. Besides, the controller-development time could be reduced significantly, as the switching strategy between different linear controllers is avoided. Last but not least, impressive improvement can also be expected with respect to MAF and MAP tracking, thereby optimising the exhaust emissions and fuel consumption in the driving cycles while maintaining high engine power and efficiency performance.

1.2 Research Questions and Objectives

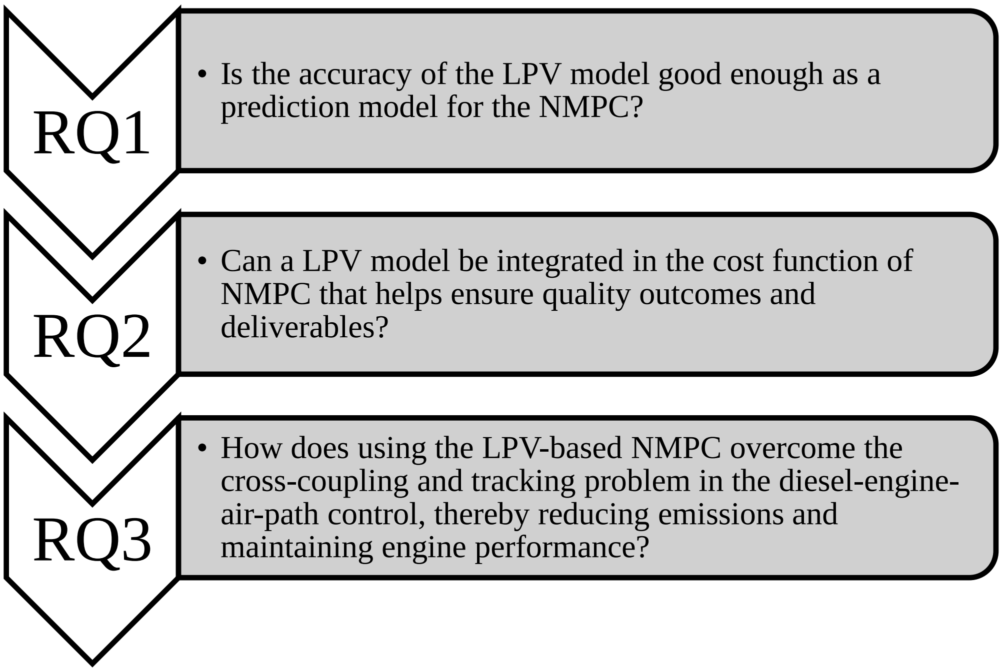

Figure 1.3: Research questions

Research is a process of accessible disciplined inquiry. The process described here is essentially generic, but it should be framed and customised by the particular discipline and subject area (Cray & Malins, 2004). The process is usually shaped by three apparently simple words: *what*, *why* and *how*. Based on the finding on literature review, the research questions (RQs) in this research project are defined (see Figure 1.3).

Corresponding to the three research questions, four main objectives of this research are as follows:

1. Analyse and evaluate the LPV system-identification method with an emphasis on the theory and applications of LPV method to identify the engine-air-path system.

2. Analyse and evaluate the existing engine-air-path control methods with an emphasis on using the theory and applications of NMPC to identify the research problems and best practices of existing methods.

3. Design a new algorithm for the NMPC controller based on the LPV model, with the objective function of high fuel consumption efficiency and low emission, by mapping the intermediate variables of the air-path.

4. Implement the NMPC controller on a mean-value model of engine-air-path in the simulation environment to reduce the emissions while maintaining engine performance. Then critically evaluate the new algorithm by simulation and comparison of various configurations of the controllers.

The overall aim of this thesis is to research, design and develop a model-based design approach to optimising emissions of diesel engines through nonlinear model-predictive control. Various modern control techniques are used for the diesel engine to optimise the VGT and EGR control and finally to reduce emissions and fuel consumption. The tasks are carried out in simulation according to the model-based design approach, but they are mainly conducted at the virtual engine-test-bench presented in Chapter 4. The engine management structure of a modern engine is not constant but changes with the operation state. This thesis does not consider special engine-operation states like cold start, warm up, idle speed and smoke-limitation operation. Only the control of the air-path is considered, which is essentially about the path which provides a mixture of fresh air plus additional substance (typically recirculated exhaust gas from EGR). Control of the fuel path and control of exhaust gas after treatment are not exploited in the proposed controllers and are not further elaborated in this thesis.

1.3 Contributions

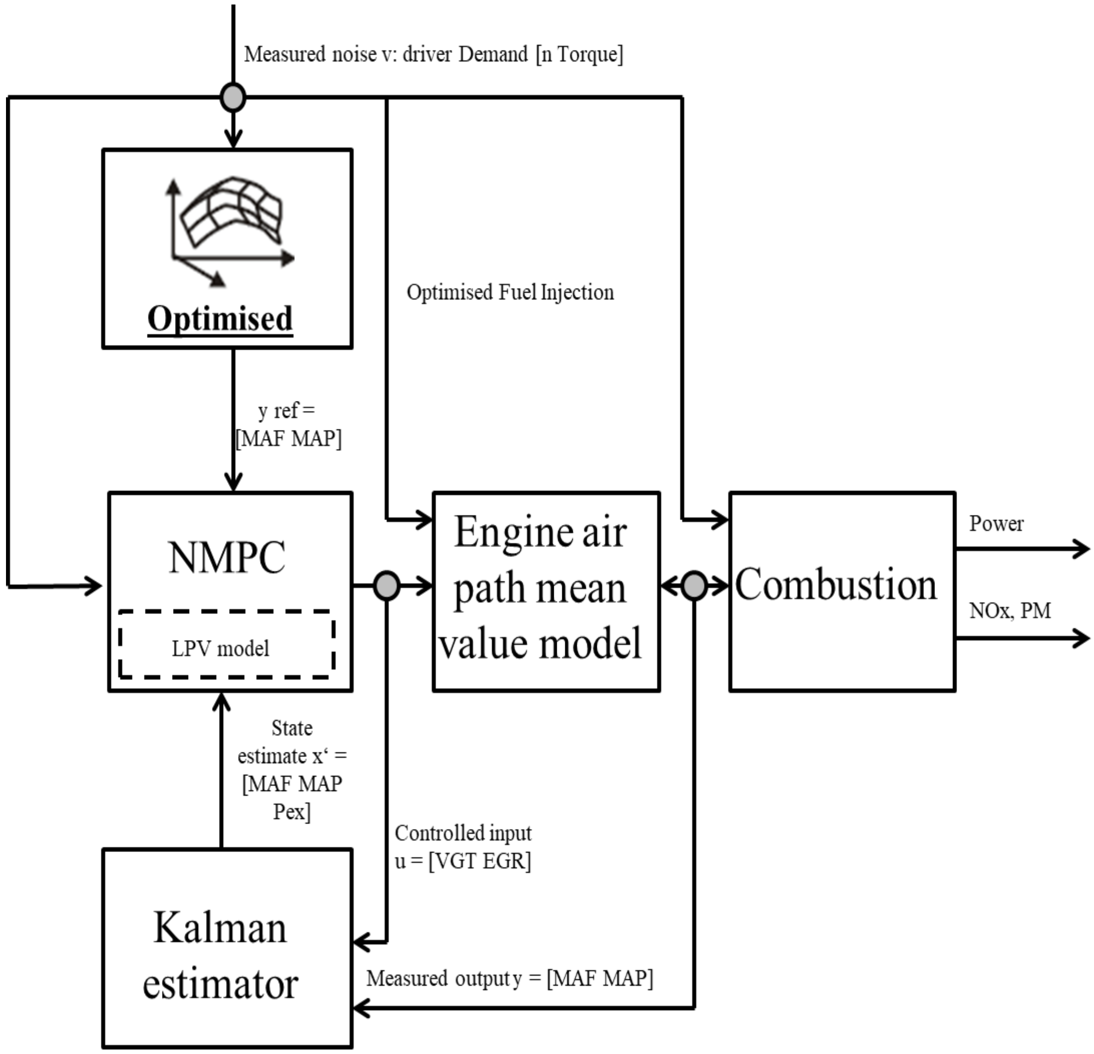

Figure 1.4: The purposed engine-air-path control structure

The purposed engine-air-path control structure is illustrated in Figure 1.4. It results from work related to this thesis, whereas the purposed control layout is based on the following key understandings:

1. The important quantities of engine-air-path control are the MAF, MAP, exhaust-gas pressure and emissions. The main characteristics of these can be captured by the

mean-value model and the data-base modelling approach for faster computing speed and higher accuracy.

2. NMPC - an optimal control method for the highly nonlinear, MIMO-constrained, engine-air-path system - is the right choice for this setup, and the NMPC internal mathematical model can be improved even more by using a nonlinear LPV model.

3. MAF and MAP as selected control references play an important role in achievable emission performance. For emission optimisation, they can be determined by numerical approaches based on the dynamical emission model.

The main contributions of this thesis are in the purposed control structure, which is itself new and contains completely new elements, including the following

1. Accurate system identification. The LPV system-identification and data-based modelling approach is developed for engine-air-path and emissions.

2. New NMPC control strategy. NMPC is for engine-air-path control, which derives from the coupled VGT and EGR control problem. The extension of classical linear MPC to new NMPC makes it possible to include a nonlinear LPV model into the optimal cost function and to thereby obtain substantial performance increases.

3. Time-efficient optimisation procedure. The optimal determination of reference of MAF and MAP by offline numerical methods based on the dynamical emission model opens a new aspect for emission and fuel-consumption optimisation which is not yet ready for production, but which nevertheless shows impressive potential for small-scale problems.

1.4 Structure of the Thesis

This thesis is structured as follows: First, Chapter 2 introduces the control objective by discussing problems and solutions for emissions via a systematic literature review. In Chapter 3, the research proposition, methodology and design are presented. And a new model-based method for optimising emissions of diesel engines through nonlinear-model-predictive control is explicitly proposed. Chapter 4 is about modelling. It gives insight into the physical nature of the plant and the possibility of data-based modelling. Chapter 5 shows the new formulation of NMPC and different control strategies on a diesel engine-air-path. Chapter 6 discusses a model-based emissions and fuel-optimisation approach to engine-air-path control.

Chapter 2 – Literature Review

This chapter reviews existing literature about engine-air-path control methods with an emphasis on the theory and applications of MPC—in particular, on the state-of-the-art concerning diesel-engine emissions. Different control methods, which have been applied to engine-air-path system, are classified in different groups. Detailed surveys are introduced to each group. The performances of MPC are compared with other existing air-path control methods. The critical factors affecting MPC performances in air-path control are reviewed based on different literature concerning prediction models, cost functions, optimisation, constraints, feasibility and stability. Gaps in the NMPC-based engine-air-path-control study are identified, and research directions are highlighted.

Chapter 3 – Research Proposition, Methodology and Design

Based on existing modelling and control strategies, a new model-based method for optimising the emissions of diesel engines through nonlinear model-predictive control is proposed. This chapter covers the research proposition, methodology and design of the project, which includes consideration of testing, system modelling and analysis and simulation methods. A variety of methodological viewpoints are discussed for collecting and analysing data toward developing a systematic understanding to this specific research project. In addition, a mastery of the project proposal design is demonstrated with respect to the practical issues of RQs, data-collection methods, data presentation and ethical issues.

Chapter 4 – Simulation Model for Engine-air-path

This chapter presents a mean-value model of a three-cylinder diesel engine. Adapting this model to other engines is possible without great extra effort. After describing the control-oriented model structure, the typical engine-air-path characteristics are described by physical equations; afterwards, the emissions and torque are modelled via a data-based approach. A comparison of measurement from the test-bench and simulation results from the engine model is provided in this chapter.

Chapter 5 – Nonlinear Model Predictive Control of a diesel Engine-air-path System

NMPC is one of the latest and widest research fields of model predictive. First, this chapter considers the theory and gives the fundamentals of the MPC by focusing on the state-space formulation-based prediction model, the cost function, the QP problem and the optimisation algorithms. Because of the nonlinearity of the plant, the linear MPC is extended to NMPC. The main difference from the linear case is the inclusion of a nonlinear prediction model in the NMPC algorithm. An LPV model structure for the internal prediction model has been investigated. The new mathematical formulation of the NMPC control problem is presented based on the LPV model structure. This chapter investigates a NMPC for the control of a diesel engine-air-path. The control object is the virtual engine-test-bench developed in Chapter 4 with actuators VGT and EGR, which measures disturbances in engine speed and fuel injection and target quantities MAF and MAP. Due to the possibility of treating constraints and nonlinear MIMO systems directly, the NMPC is chosen for this feedback-control problem. Afterwards, the application of NMPC to the air-path is compared to the nominal MPC and standard ECU functions. Various tracking-performance measures of MAF and MAP are analysed and evaluated by simulation on the virtual engine-test-bench.

Chapter 6 – Application of Model-based Emissions and Fuel Optimisation on Engine-air-path Control

This chapter implements the data-based emission model for NOx and PM to complete the software simulation environment in Matlab/Simulink with the design-of-experiment (DOE) method. Afterwards, a model-based optimisation approach to computing the ideal references is shown. The optimal references of MAF and MAP are determined based on the emission models. The NMPC developed in Chapter 5 is used to validate the potentials of this optimisation method with the aim of reducing the emissions and fuel consumption of the driving cycle.

Chapter 7 – Conclusions and Further Work

Chapter 7 draws conclusions and presents the main achievements of this study, including its contribution to the new knowledge generation. In addition, areas of further research and investigation are discussed.

Chapter 2. LITERATURE REVIEW

This chapter presents a review of literature on engine-air-path control methods with an emphasis on the theory and applications of model-predictive control. Research in this field is actively ongoing. Different control methods which have been applied to engine-air-path system are identified from a wide range of literature. However, because of their simplicity, PID control structures are still used in many engine-air-path systems, thereby resulting in the inconsistent performance of such systems. With advances in computing technology and data-processing devices, it is now feasible to adopt and implement an advanced control approach to overcome the issues inherent to engine-air-path control. The focus of this chapter is on a survey of control methods of engine-air-path systems using VGT and EGR. Emphasis is placed on the MPC approach because research on MPC methods in nonlinear system control (such as engine-air-path systems) has intensified in recent years due to its many inherent advantages.

However, a comprehensive literature review of MPC approaches for engine-air-path systems is still lacking. In particular, selected trends and issues related to engine path and controller design must be identified. This literature review is followed by a structured process to ensure that all relevant input concerning the defined RQs are shown in Figure 1.3. First, a review of engine-air-path systems and emissions of diesel engine are presented to outline the spectrum of control tasks in engine-air-path systems. Then, a review and classification of previous surveys related to engine-air-path control is given. Furthermore, the performance of MPC is compared with that of other existing air-path control methods, and the critical factors affecting MPC performances are discussed concerning the prediction model, cost function, optimisation, constrains, feasibility and stability. Despite considerable work on engine-air-path control development, areas that require further investigation still exit and are summarised in this literature review. Therefore, the final section includes a summary of important factors that govern MPC design and outlines open design problems for engine-air-path control. The gaps in MPC-based air-path control are identified, and research directions for extension the MPC to NMPC are highlighted. The investigation of techniques for comprehensive nonlinear model, accurate estimates of disturbances, integrating dynamical optimisation techniques and their impact on NMPC performance in engine-air-path control have to be done in this research.

2.1 Diesel Engine-air-path

The engine-air-path is one of the most important parts of diesel engine system. It is responsible for the management of intake and exhaust-air quality, combustion efficiency and emission reduction. Robert Bosch (2006) publishes an overview paper which details the state-of-art of the engine-air-path principle. It reports that, for the performance and emission of the engine, control of the VGT and EGR is critical. It explains that, in a typical gas exchange process inside the diesel engine-air-path, fresh ambient air is aspirated through an air filter and compressed by the turbocharger, which is driven by the exhaust gas. The compressed fresh air is cooled by the intercooler to provide higher air density and thereby to increase air mass inside the cylinders. After the combustion process, the exhaust gas leaves the cylinders through the exhaust manifold. Part of the exhaust gas is recirculated by the EGR path and cooled by the EGR cooler. It is finally mixed with the compressed fresh air in the intake manifold. The rest of the exhaust gas-flows go through the turbine into the exhaust pipe. Therefore, the VGT and EGR naturally form a coupled system. The control targets are to adjust the VGT and EGR valves for regulating the compressor speed and exhaust-gas recirculation rate, thereby to meet the required manifold pressure and the expected air-mass flow.

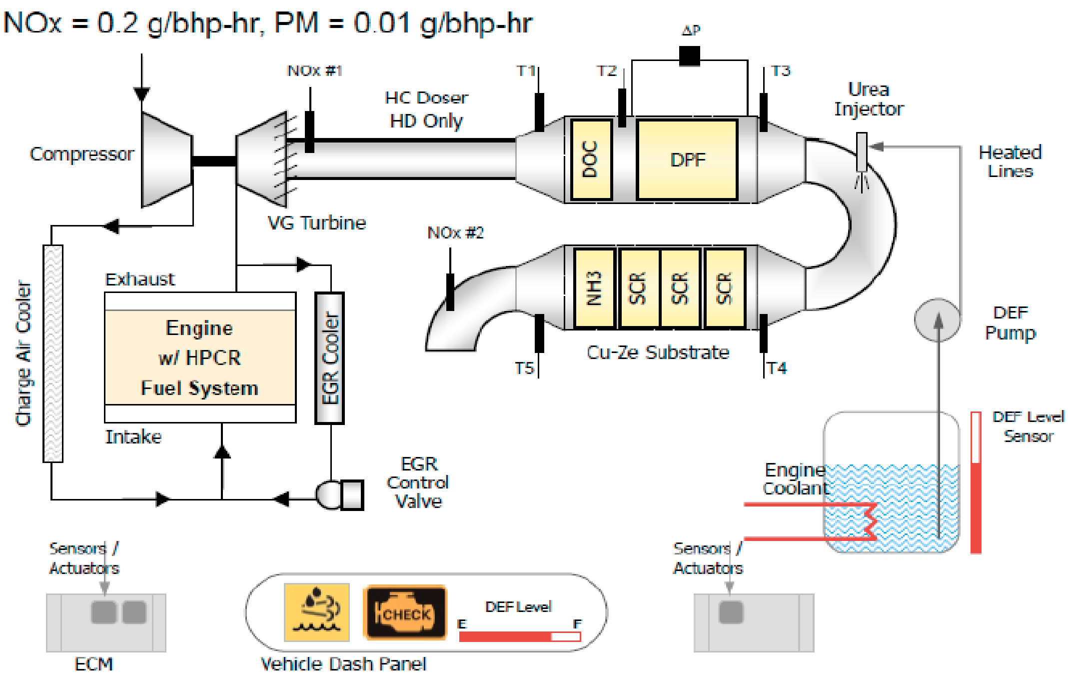

Figure 2.1: Diesel engine-air-path layout (Dorling, 2016)

Abidi, Bosche and El Hajjaji (2013) offer an overview of the dependencies of the two actuators, EGR and VGT, and the outputs, MAF and MAP. It is believed that the diesel engine-air-path is a strongly nonlinear MIMO coupled system in which both actuators influence both output variables. However, these effects are still not fully considered in a production-car ECU. Figure 2.1 shows a typical layout of a modern diesel engine, which includes an intake and exhaust manifold, a common rail-fuel injection module, an EGR, an EGR cooler, a VGT and an after-treatments system. The following sections present a review of literature on the major subsystems of a diesel engine-air-path.

2.1.1 Variable Geometry Turbocharger

A variable-geometry turbocharger (VGT) is a turbocharger that can change the angles of the turbine vanes to control engine air flow on turbine blades. This helps the engine-air-path control to balance the mass flow of air with the fuel along the entire engine-operation range. Baines (2006) has shown that the modern turbocharger is a highly-developed industrial product that has become almost indispensable to diesel and gasoline engines. The first turbocharged diesel-engine passenger car is brought to the market by VW in 1981 (Srinivasan, 2014). Since then, the focus of turbocharger development is not primarily on performance improvement but on reducing fuel consumption and emissions. In 1988 in Japan, Honda has produced the first VGT-equipped diesel engine (Wan, 2017). Since then, the VGT has been successfully used on modern diesel engines—primarily due to its ability to reduce ‘turbo lag’ at low engine speed by using adjustable guiding vanes and to its ability to reduce emissions in combination with EGR. It can be deduced that the focus of attention is now on ever more complex engine-boosting systems that are used to match the engine with high boost and maintain good exhaust-energy utilisation over wide ranges of load and speed operation. This includes VGT, EGR, enhanced materials and a high degree of sophistication in control systems.

Baines (2005) mentions one way to improve the turbine performance. By adjusting the angle of the VGT guiding vanes, the flow through the turbine can be more or less restricted. The compressed fresh air is then cooled by the intercooler to provide a higher air density and thereby an increased air mass inside the cylinders. Baines (2005) explains that one goal of a VGT is to expand the usable flow-rate range in practical applications while maintaining a high level of efficiency. A VGT system usually consists of three main parts: the compressor, the turbine with a variable vane, and the rotor that connects the compressor and turbine wheels. It may be assumed that the thermodynamic behaviour of the turbocharger is quasi-stationary phenomena event such that steady-state maps can precisely describe its process. Thus, the angle of the inlet guide vanes of the turbine can be adjusted to follow a required turbine mass flow, as shown in the Figure 2.2 (Wan, 2017).

a) VGT close

b) VGT open

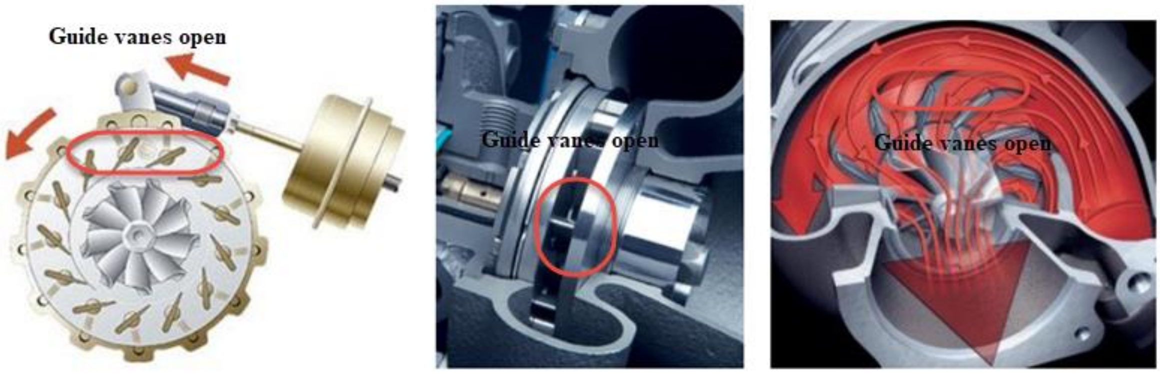

Figure 2.2: a) VGT close at low engine speed and b) VGT open at high engine speed (Wan, 2017)

The effect of VGT is almost the same as can be reached with the wastegate (WG), but the efficiency is much higher—especially at the low rotor speed condition of the engine—due to a relatively large bearing friction in the low-temperature lubrication circuit. Compared with conventional turbochargers, the advantage of VGT is that the entire exhaust mass flow is always directed through the turbine and can be converted to energy. Adjustment of the VGT guide vanes can be controlled by a series of different pneumatic or electrical regulators. This leads to a higher mechanical-structure demands than conventional turbochargers provide, since the rotary vanes need to move functionally as a highly precise controlled actuator (Nguyen-Schaefer, 2013). Compared with the WG-EGR diesel engine, the EGR rate of the VGT-EGR diesel engine has a significant increase and the VGT turbocharger has a certain effect on controlling the EGR rate (Baines, 2005). In the low load region, the increase of EGR rate has a very significant effect on the decrease of fuel consumption. At the same engine speed, the increase of VGT opening degree is conducive to reducing the pumping loss without affecting the combustion process. Therefore, the VGT opening degree increases with the decrease of the load, which reduces the effective fuel consumption of the diesel engine. VGT-EGR also reduces NOx emissions and PM emissions and improves the trade-off relationship for NOx and PM emissions of diesel engines. Using controlled VGT can improve the intake performance of the engine as well as the combustion conditions in the cylinder, thereby reducing PM emissions; the VGT turbocharger is more capable of utilising exhaust energy than the WG turbocharger.

Generally, VGT engines with the same original power can save nearly 10% on fuel consumption by reducing the cylinder volume by 25% (Nguyen-Schaefer, 2013). The direct effect of this boost in pressure is to increase the intake air density such that a turbocharged engine of smaller capacity can be used to achieve the same power output. This reduces the engine size and weight with a consequent improvement in power-to-weight ratio that is strongly advantageous—particularly, but not exclusively, in vehicle applications (Baines, 2005). The aerodynamics of a vehicle can be improved with a small and light engine, which leads to efficient fuel combustion and low emission. Furthermore, in modern diesel engines, the VGT is usually combined with EGR, which means that a part of the exhaust gas is mixed with fresh air and brought back to the combustion chamber to decrease the peak temperature during combustion. Indirectly, the greater intake air density combining with EGR allows for a leaner mixture, and lower combustion temperatures lead to a favourable influence on NOx emissions.

Wahlstrom, Eriksson, Nielsen and Pettersson (2005) describe the non-linear effect of the VGT and the MAP. Decrease of the VGT raises the resistance for the exhaust gas. This results in an acceleration of the turbine rotor and a higher MAP. Furthermore, the higher resistance for the exhaust gas also causes a higher pressure inside the exhaust manifold and thereby causes a higher re-circulated gas flow through the EGR valve. As discussed above, this higher re-circulated gas pressure can reduce the MAF again. If the EGR valve is closed, all the exhaust gas must pass the turbine. These non-linearities make control of the engine-air-path more difficult.

In summary, a significant challenge with a VGT system is the control of the angles of the turbine vanes to control air mass flow and to obtain low fuel consumption and emissions. Given the engine-air-path characteristics and the coupling effect with MAP and MAF, range-limit constraints and hysteresis in the VGT mechanisms can lead to a strong non-linearity. Therefore, the development and implementation of effective control techniques for engine-air-path control is of primary importance.

2.1.2 Exhaust Gas Recirculation

In automotive applications, modern diesel engines work with EGR, which means that a part of the exhaust gas is mixed with fresh air and brought back to the cylinder to reduce the NOx emissions (Sher, 1998). By means of this method, the burning temperature peak of the exhaust is lowed, thereby reducing NOx. The first application of EGR to a gasoline engine is made by Chrysler in 1973. With an exhaust gas re-circulation unit, the engine reached favourable operation temperatures to reduce NOx emissions. In 1990 in the United States, Ford fires the first production diesel engine equipped with EGR. Due to the high exhaust-gas temperature, a cooler installed after the EGR valve is needed to ensure high air density inside the cylinder (Sher, 1998). Additionally, the EGR cooler increases the re-circulated flow density where the effects of heat capacity and oxygen again provide benefit (Ladommatos, Balian, Horrocks, & Cooper, 1996). Hence, the cooled EGR has become very common in heavy-duty diesel engines in the United States. However, Ladommatos, Balian, Horrocks and Cooper (1996) experimentally analyse the influence of EGR on the reduction of NOx, and find that, through the EGR cooler, the exhaust gas acts as an inert gas in the cylinder and thereby decreases the peak temperature during combustion. They believe that too low a combustion temperature leads to a low oxidation rate and probably to higher soot when EGR increases. So, they suggest that, during the design of EGR, NOx reduction should be considered, and efforts should be made to achieve PM-NOx trade-off and fuel economy. But they have not further investigated how to achieve this trade-off. This means that it is necessary to study a control method that can be used to reduce both NOx and PM without also reducing engine-power efficiency. After 2008, the application of EGR is expanded to passenger cars, and not only for NOx reduction but also for PM-NOx trade-off and fuel economy.

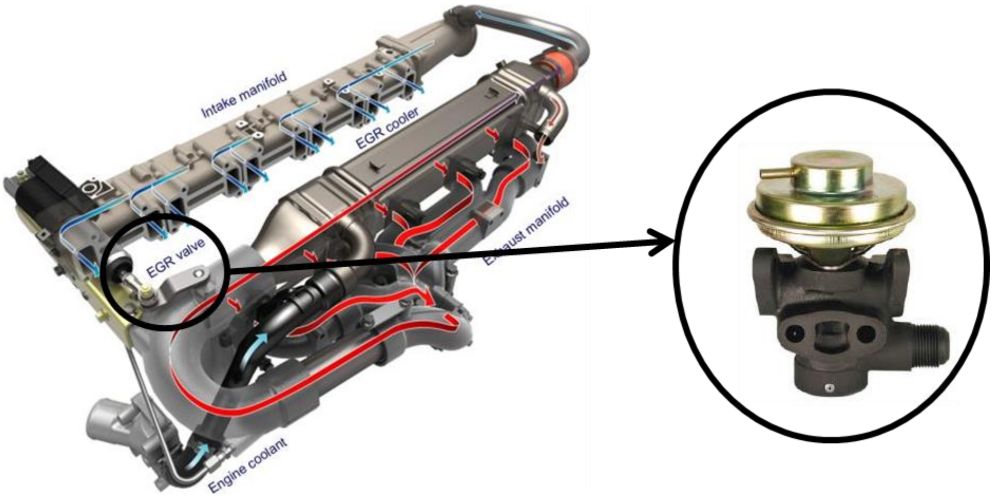

Figure 2.3: EGR system for diesel engines (Jaeskelaeinen, 2017)

Figure 2.3 shows a VGT diesel engine with EGR in which the exhaust gas partly returns to the engine with a maximum of 50% EGR before entering the turbine (Jaeskelaeinen, 2017). The EGR rate is defined by the ratio of the recirculation mass flow to the exhaust mass flow. A typical, modern diesel-engine EGR system includes an EGR control valve, an EGR cooler and piping. According to ECU control, the EGR valve is an electro-pneumatic actuator which affects the rate of re-circulated exhaust gas. The EGR valve uses a vacuum to open the valve and to regulate re-circulated exhaust gas-flow. The EGR valves are mainly electrically operated and can be opened in various increments so that NOx emission fulfils the current emission requirements (Grimm, 2010). In case of a turbocharger with EGR, the re-circulated exhaust gas-pressure after the EGR cooler must be higher than the charge-air pressure at the compressor intercooler outlet. It can be assumed that the pressure ratio of the turbine is required to be high enough to overcome the charge air pressure. This obviously shows that the engine must work against the high exhaust gas-pressure at the engine exhaust manifold. It is believed that the high exhaust gas-pressure leads to an increase of emissions and fuel consumption when the engine is under a full load. Therefore, they suggest that, to improve the emissions and fuel efficiency, the EGR valve can be controlled so as to be opened as soon as the exhaust gas-pressure reaches the required maximal pressure limits (Nguyen-Schaefer, 2013). This means that in engine-air-path it is required to improve the existing control strategy to optimise the EGR control.

In case of an engine with EGR and VGT, the pressure of the re-circulated exhaust gas behind the EGR cooler must be high enough to overcome the charge-air pressure (Nguyen-Schaefer, 2013). Research shows that an opening of the EGR valve will increase the re-circulated gas flow; otherwise the re-circulated exhaust gas-pressure works against the compressed charge-air pressure at the compressor outlet. As a result, the MAF through the compressor can be reduced by gas flow from the EGR (Guzzella & Onder, 2004). Meanwhile, by means of a lower MAF in the cylinder, the exhaust gas-pressure at the EGR inlet and turbine inlet is reduced. Furthermore, the lower pressure gradient at the turbine inlet reduces the turbine rotor speed and thereby reduces the MAP in the intake manifold.

Jung (2003) has analysed the non-linear dependency of EGR on MAF in detail. The EGR valve regulates the re-circulated gas flow. Variation of the EGR valve at a lower rate can cause a higher variation of the re-circulated gas flow through the EGR valve than variation at a higher EGR rate. The mathematical formulation of this problem delivers the non-linear valve equation presented in Section 4.4.3 As described in the previous sections, a higher re-circulated gas flow can reduce the MAF in the intake manifold. This means that the MAF is reciprocal proportional to the re-circulated gas flow.

Furthermore, as mentioned in (Wahlstroem, 2006), the non-linear behaviour of EGR and MAF also depends on the position of the VGT. If VGT is opened further, the resistance to the exhaust gas-flow becomes less, which results in a reduced exhaust gas-pressure and thereby in a decreased pressure drop between the exhaust and intake manifolds. Consequently, the non-linear effect decreases by a smaller VGT rate.

In the engine-air-path system, another non-linear effect is the dependency of MAF on the VGT. Ortner (2006) analyses the influence of VGT on MAF for different positions of the EGR valve. If the VGT rate is less than 50%, the increasing of the VGT leads to a higher MAP in the intake manifold. A higher MAP results in an increased MAF. Additionally, the pressure drops over the EGR valve reduces the re-circulated gas flow. Meanwhile, this circumstance raises the MAF as well. The second circumstance, which is part of the cross-coupling control problem, is the non-linear dependency of the EGR and the MAP. This behaviour is tangentially identical to the relationship between EGR and MAF. A closing of the EGR valve can raise the MAP because all the exhaust gas must pass the turbine, and the resulting acceleration of the compressor rotor increases the MAP.

From the above discussion, it can be seen that, to meet the more stringent emission law in diesel engine applications, engine manufactures must continually adopt new technologies such as those using advanced-control strategies, increase of fuel-injection pressure, diesel-oxidation catalysts and so on.

2.2 Emissions of Diesel Engine

However, the biggest drawback of diesel engines is pollution. Song (2015) shows that diesel engines are too noisy and produce a lot of unburned soot, which is dirty and hazardous. According to (The European Parliament, 2007), based on the legislative emission limits specified from Euro I to Euro VI, the reduction of PM and NOx are 80% and 90% for diesel engines, respectively. Meanwhile, fuel-consumption efficiency remains an important consideration for customers due to ever-increasing fuel prices. To reach these targets, after-treatment systems such as oxidation catalysts (DOC) (Duprez & Cavani, 2014), diesel-particulate filters (DPF) (Czerwinski & Zimmerli, 2015) and SCR (Nova & Tronconi, 2014) have in recent years made huge steps in efficiency and provide tools necessary to decrease emissions. Many engine manufactures have pursued after-treatment technology as their main emissions-control solution, but the increasing cost of using after treatment will likely affect vehicle sales once further emission standard is implemented. However, the heart of the engine system is still the combustion itself, which has to be controlled as optimally as possible. Therefore, a further important contribution can be offered by improved engine control, which can lead to an abatement of raw emissions and a reduction of consumption. Criens (2014) shows that engine control generally concerns two different paths: the so-called air-path (which is essentially the path that supplies the combustion chamber with a mixture of fresh and re-circulated combusted air at the given temperature and pressure), and the fuel-injection path (which is typically regulated by the rail pressure and the opening time of the injectors). Modern diesel engines allow for advanced injection system which can dramatically reduce noise, emissions and fuel consumption, as they allow for a better distribution and produce a close to homogeneous charger-compression ignition (HCCI) that can only be met by cooperating with an exactly controlled air-path system which includes a throttle, valve-timing, VGT and EGR (Reif, 2014). It is suggested that using advanced combustion with optimised engine-air-path control is currently the best solution for emission control in diesel engines. Therefore, to improve the control system, this section provides a review of the principles of NOx and PM formation in diesel engines and of how the emission can be affected via the available actuators in the diesel engine-air-path.

2.2.1 Nitrogen Oxides

Nitrogen oxide is one of the main pollutants of diesel engines. Van Basshuysen and Schäfer (2004) provide an overview detailing the NOx-formation reaction during combustion. While the main purpose of the combustion process in a thermal engine consists in the oxidation of carbon and hydrogen, the oxygen can be provided only together with nitrogen, which is present in high quantities of the fresh intake air, so that secondary reactions inevitably happen in which nitrogen is oxidised in different ways.

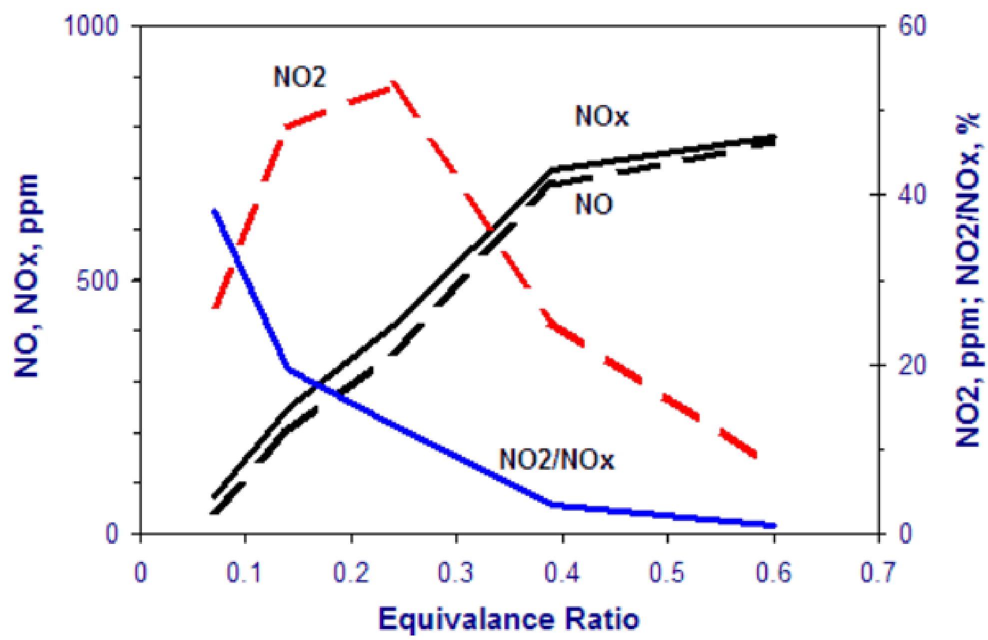

Figure 2.4: Effect of air fuel equivalence ratio on NOx concentration in diesel engines (Jaeskelaeinen, 2018)

Song (2015) explains that the production of NOx is mainly in the form of NO. NO has a larger enthalpy than oxygen and nitrogen; therefore, it can be produced only if external energy is supplied. In fact, the production of NOx is strictly related to the temperature of the combustion flame. During combustion under high-temperature and oxygen-rich conditions, an increase in temperature of 1% increases the formation rate of NOx by 20%. Analogously, under low temperatures and oxygen-lean conditions, it produces very little NOx (California Environmental Protection Agency, 2015). These reactions are also known under the name of the Zeldovich model. Schwerdt (2006) emphasises that the Zeldovich equations are confirmed by the dependency of NO on the fuel-to-air equivalence ratio and on the combustion temperature. Figure 2.4 shows differences in NOx dependency on the air-to-fuel ratio. The higher equivalence ratio is more the NOx emissions.

Therefore, in practice, combustion peak temperature and the availability of oxygen (intake air flow) have to be controlled to reduce the NOx formation rate. Schwerdt (2006) states that the main method of NOx reduction in combustion engines involves the use of EGR in the engine-air-path system. Figure 2.5 shows the dependency on the EGR rate. EGR does increase the initial mixture temperature, but it increases the thermal capacity as well and reduces the oxygen concentration such that NOx is reduced. More details about the EGR used for the emission control can be found in Section 2.1.2.

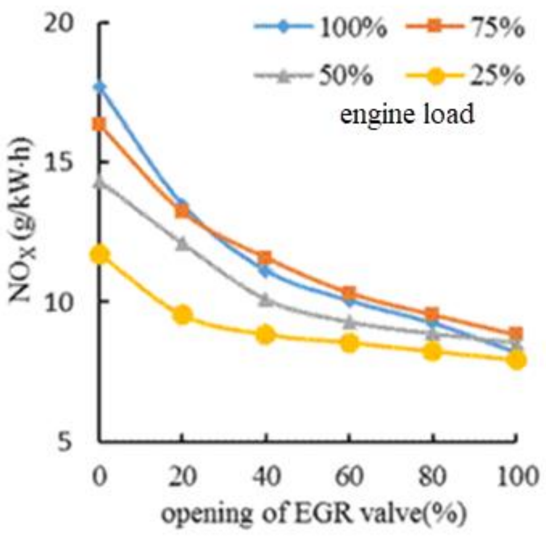

Figure 2.5: Effect of EGR rate on NOx emission in diesel engine at different load (Zhu, Ren, & Luo, 2015)

2.2.2 Particulate Matters

The other main pollutant of diesel engines is particulate matter (PM). Saggese (2012) investigates that, PM, usually called soot, consists mainly of fuel drops which have not burnt as expected but have been subjected to a process similar to the production of coal (external heat and flame, but not enough oxygen to burn). The California Environmental Protection Agency (2015) claims that PM is mainly a problem in diesel engines. However, GDI engines also have the problem, and it is possible to produce soot with standard SI engines just by requiring a high load at low temperatures and rotating speeds. In practice, PM consists of different elements, among which are the following: lubricant oil, soot from fuel, sulphates, bound water and unburnt fuel.

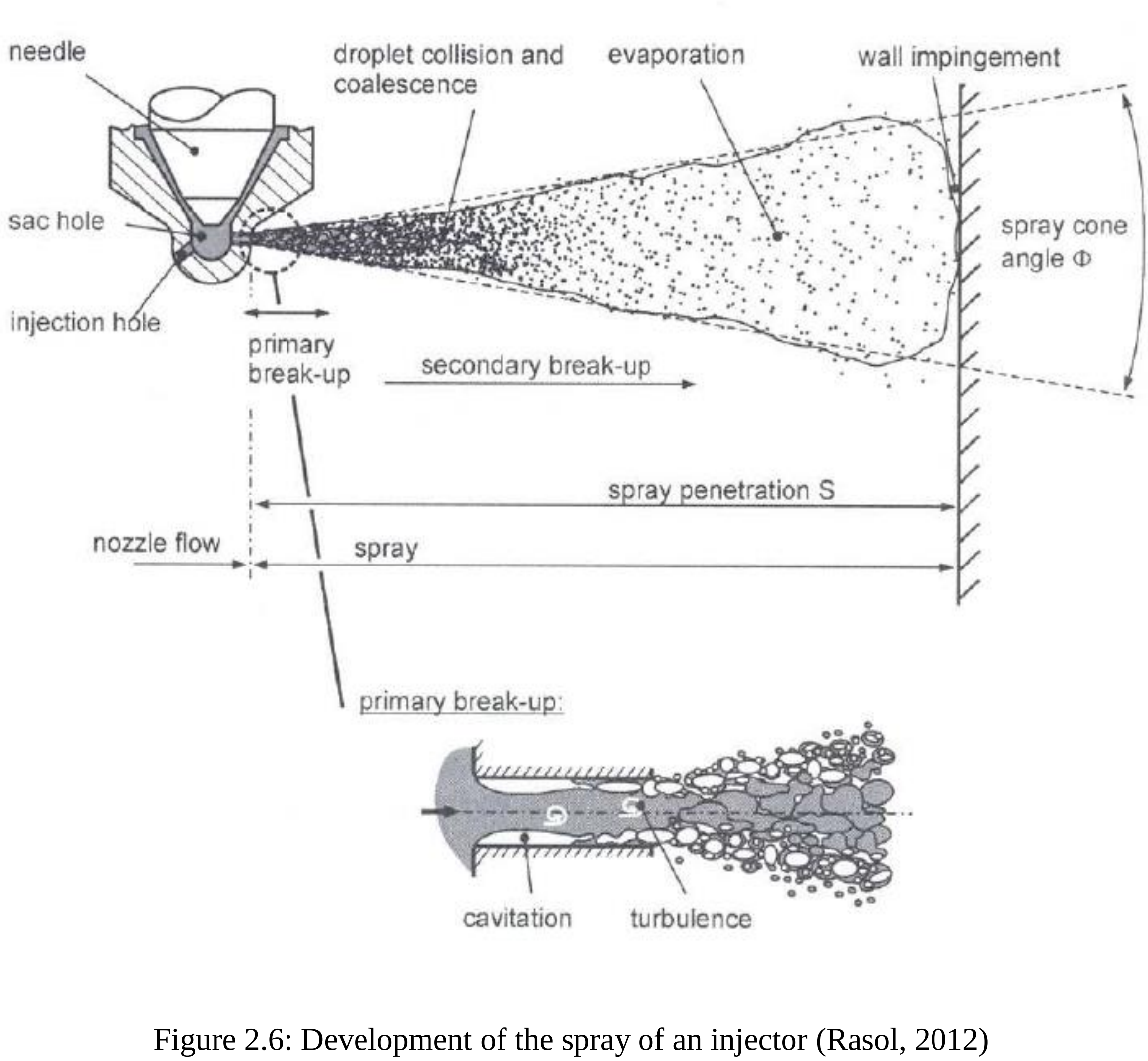

Figure 2.6: Development of the spray of an injector (Rasol, 2012)

In (Rasol, 2012), the principle of PM formation is further researched. Figure 2.6 shows the development of the spray of an injector. Ideally, the whole fuel should reach the evaporation phase without hitting the wall. In practice, requirements for injectors (which must provide for both very small and rather large amounts of fuel) lead to compromises, which can lead to a partial evaporation - small droplets can remain or re-build. A droplet essentially burns anaerobically, and this is the main cause of soot. Standard particulate catalysts help reduce the size by partly removing this layer, but they do not remove the soot itself. Criens (2014) suggests that, in conventional diesel engines, the best way to reduce the PM emissions, rather than to prevent soot formation, is to improve the combustion conditions to accelerate the soot-oxidisation rate, which includes increasing the injection pressure, advancing the start of the injection angle and optimising air-path control to improve the air-to-fuel ratio.

2.2.3 Emission Control Legislation and Technology

Song (2015) explains that a key benefit of diesel engines is that they efficiently compress fuel to make it burn relatively completely. However, diesel engines emit high levels of PM and NOx, which are major contributors to air pollution and have negative health impacts. A major concern for vehicle and engine manufacturers is the lack of an effective emission-control technology for diesel engines such that they remain significant sources of pollutants.

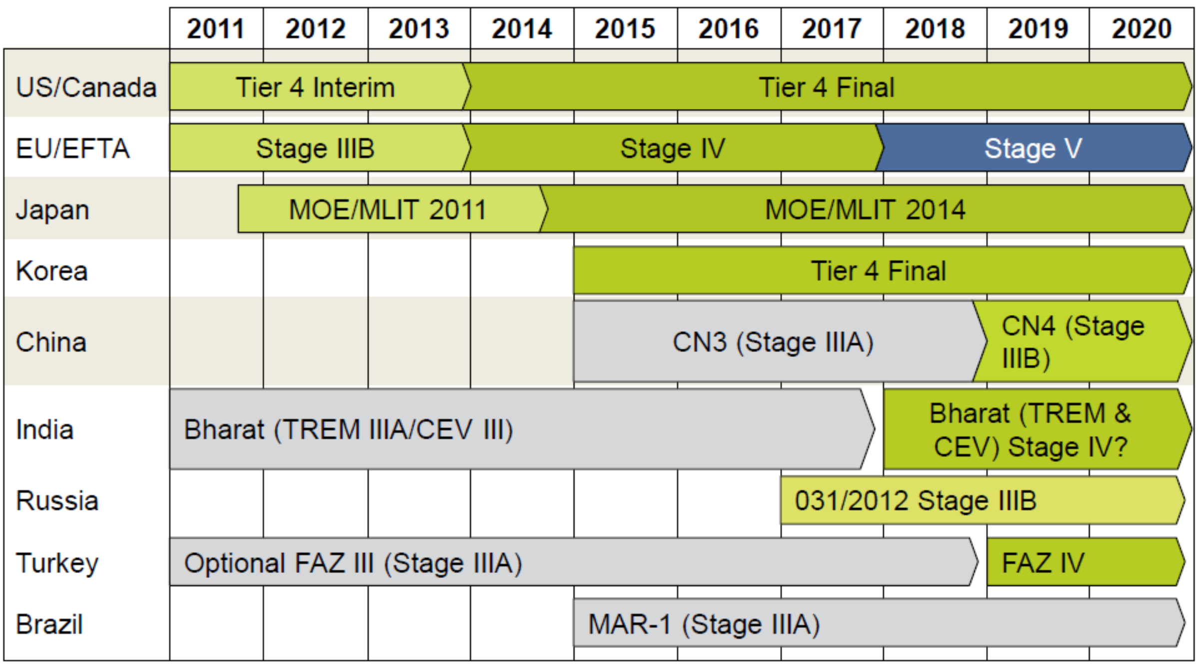

Figure 2.7: Harmony between global NOx and PM limits (Dorling, 2016)

As is explained in (European Union, 2011) and Figure 2.7, in 2011, the EU sends a draft version of Stage V emission legislation for non-road vehicles and machinery for public consultation. Though there is no timeline for the legal implementation, the industry is optimistic that stricter regulation will soon be implemented. Stage V will require new and advanced technologies for engine combustion, emissions control, after treatment and auto electrical control. Currently, international manufacturers are planning their next stage of emission control technology upgrades, while domestic OEMs are being more conservative. Research indicates that EGR and DOC systems will provide the main route for domestic OEMs to achieve Stage V.

Nova and Tronconi (2014) state that SCR systems can provide the most effective solution for Stage V emission-control legislation and the best way to meet Stage V. They also suggest that the increased use of natural-gas engines, which have the advantage of lower prices and better results on the WHTC testing cycle, can reduce PM emissions. Reis (2005) claims that engine manufacturers may have already understood the technical requirements of emission legislation but that the practical application after upgrading is a matter of major concern. It is said that many manufactures have pursued SCR technology as their main emissions-control solution but that the increasing cost of using SCR after treatment will likely affect truck sales once the new legislation is implemented. It is expected that the implementation and enforcement of new emission-control legislation would lead to an improvement in emissions control. The panellists agree that it is the social responsibility of all industry players to comply with the stricter emission legislation; however, vehicle and engine manufacturers may still be hesitant to move forward given the higher cost of production and investment.

Nieuwstadt and Kolmanovsky (2000) explain that EGR is one of the most urgently needed improvements in the engine-air-path to control the NOx emissions. Part of the exhaust gas is re-circulated by the EGR valve and cooled and mixed with the fresh compressed air in the intake manifold. After combustion, the exhaust gas leaves the cylinders through the exhaust manifold. Here, a part of the hot gas is reused via the EGR path into the cylinder, and the rest flows through the turbine into the exhaust pipe. In (Bennett, 2014), to achieve a reasonable EGR rate and reduce NOx emissions, the EGR system is used to design and optimise the wastegate EGR system. Circulating exhaust gas from EGR can dilute the oxygen concentration in the cylinder and reduce the rate of chain reactions during combustion, thereby decreasing adiabatic flame temperature. These factors significantly reduce the NOx emissions of the WG-EGR diesel engine. On the other hand, they also exacerbate the regional hypoxia and prompt the generation of PM. Meanwhile, the decrease in the combustion temperature in the cylinder also affects oxidative decomposition after the formation of PM, which significantly increases the PM emissions of the WG-EGR diesel engine. It is therefore necessary to consider the NOx-PM trade-off in the air-path control.

Ni, Liu and Shi (2016) explain that the VGT turbocharger can reduce the turbine nozzle opening when the engine is running at low speed, thereby increasing the exhaust back pressure and flow rate and improving exhaust energy efficiency. The VGT nozzle opening can be adjusted during the high-speed operation so that it works in the high-efficiency area of the supercharger in the whole process. When combined with an EGR system, adjusting the opening of the VGT nozzle can improve the pressure difference between turbine forward pressure and the post pressure of the EGR system and thereby reduce NOx emissions.

The combination of VGT and EGR is a key technology for emission control in diesel engines. As demonstrated, Euro V can be achieved for a heavy-duty EGR engine by using a SCR-only strategy which meets both the European Stationary Cycle (ESC) and WHTC. Euro VI can be achieved for a heavy-duty EGR engine with the addition of VGT technologies and after-treatment systems.

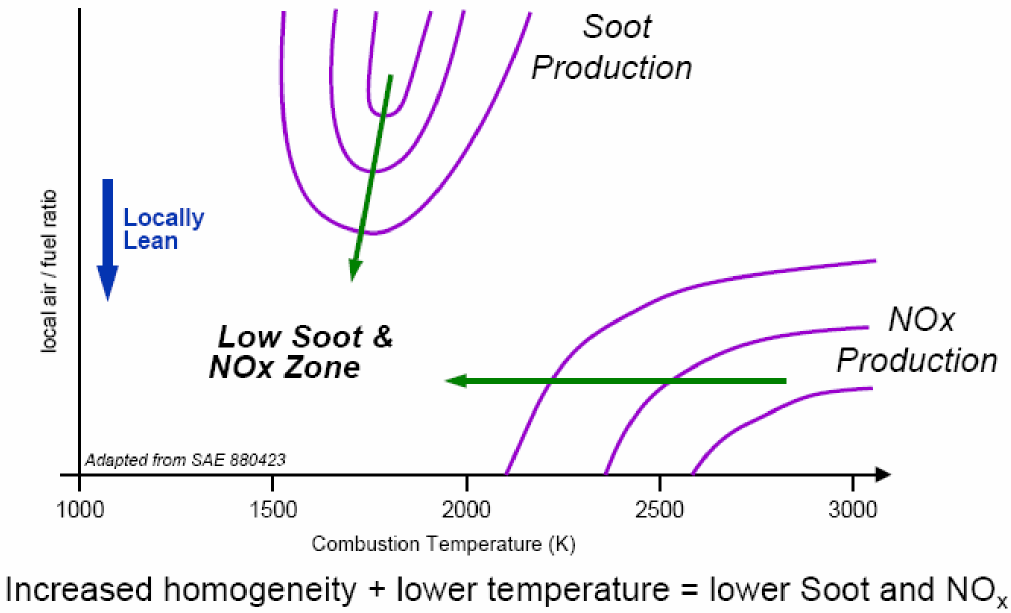

Figure 2.8: NOx and soot depend on combustion chamber temperature and air/fuel ratio (Bruckner, Grünbacher, Alberer, del Re, & Atschreiter, 2006)

However, Bruckner, Grünbacher, Alberer, del Re and Atschreiter (2006) state that arrangements in diesel engines aimed to reduce particle and NOx contain a conflict, as shown in Figure 2.8. If the aim is to lower the number of particles, the NOx emissions get worse. For the future, it is important to reduce both values to meet the laws regarding exhaust gas emissions. Figure 2.8 shows the dependence of the NOx and soot production on combustion temperature and the fuel/air ratio. It is suggested that emissions can be decreased by using optimising methods without compromising fuel economy.

2.3 Diesel Engine-air-path Control Methods

A large body of literature has been published on applications of engine-air-path control. Nguyen-Schaefer (2013), Criens (2014) and Zeng, Upadhyay and Zhu (2017) show that air-path control is one of the most important aspects of engine control. The throttle, vane position of VGT and EGR valve are used as inputs to obtain an optimised air-fuel mixture under a given reference temperature and pressure. There are three main types of mechanism for regulation of the turbocharger in a diesel engine: intake-air-controlled wastegate turbocharger (Figure 2.9), solenoid-controlled wastegate turbocharger (Figure 2.10), and electric-actuator-controlled VGT (Figure 2.11).

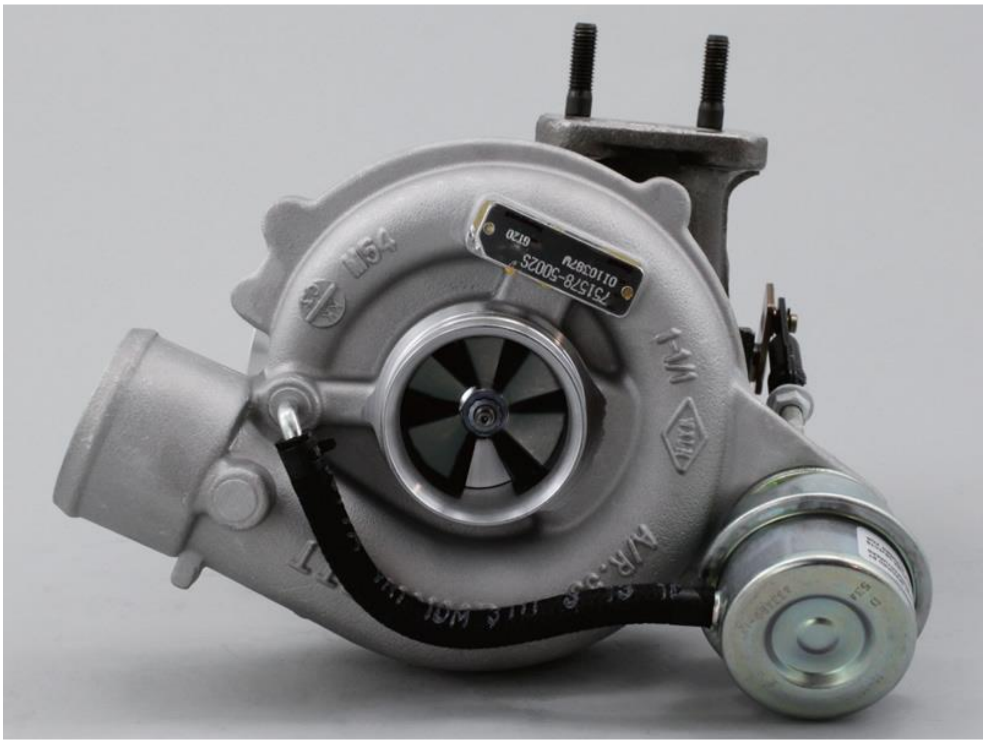

Figure 2.9: Intake air controlled wastegate turbocharger (Baines, 2005)

Figure 2.10: Solenoid controlled wastegate turbocharger (BorgWarner, 2018)

Figure 2.11: Electric actuator controlled VGT (BorgWarner, 2018)

Table 2-1: Classification of control methods for engine-air-path systems

Control	Authors	Contributions
Classical Control	(Wahlstrom, Eriksson, Nielsen, & Pettersson, 2005)	PID based emission control for diesel engines equipped with VGT and EGR
	(Ahmed, 2013)	PID controller design and tuning for EGR and VGT control in diesel engines
Non-linear Control	(Liu & Wei, 2007)	H_{inf} control for VGT and EGR
	(Kuzmych, Aitouche, Hajjaji, & Bosche, 2014)	Constructive Lyapunov control design for turbocharged diesel engines
	(Atam, 2018)	LPV based control for air-path system control in diesel engines
Hybrid Control	(Zhao & Pan, 2012)	Fuzzy PID control for VGT
	(Kim, Choi, & Jin, 2016)	Hybrid control approach of a diesel engine air-path system
Model Predictive Control	(Maruyama, Shimura, Ejiri, & Ikai, 2011)	Model predictive control with dead zone in engine control
	(Wang, Waschl, Alberer, & Del Re, 2012)	Independent LPV MISO MPC control for VGT and EGR
	(Zhao, 2013)	Explicit MPC application in a turbocharged diesel engine
	(Huang, Zaseck, Butts, & Kolmanovsky, 2016)	Rate-based model predictive control (RB-MPC) for a diesel engine-air-path
	(Dahl, et al., 2018)	Model predictive control of a turbocharged engine

The system to be studied here is a diesel engine equipped with an electric-actuator-controlled VGT and EGR. As mentioned in sections 2.1 and 2.2, in production ECU, the diesel engine-air-path is controlled by two SISO control loops. The desired MAF is controlled by the EGR valve and the MAP is controlled by the angle of the VGT guide vanes. The problem is that the influences from EGR on MAP and VGT on MAF, which are called cross-coupling effects, are not directly considered by the controller. Engine-air-path is a typical MIMO system. To control a MIMO system with the help of two SISO controllers requires a strong restriction on the performance of engine. An overview of model-based control of the VGT and EGR approaches that cover the system structure, modelling of the diesel engine and controller design are presented in (Ammann, Fekete, Guzzella, & Glattfelder, 2003). Dekker and Sturm (1996) and Truscott and Porter (1997) have reviewed the classical control techniques for air-path systems that use a decentralised SISO approach. Multivariable design for VGT and EGR control for diesel engines is comprehensively studied in (Nieuwstadt, Moraal, Kolmanovsky, & Stefanopoulou, 1998). A review of different treatments of fuzzy modelling and fuzzy control for engine-air-path is provided in (Abidi, Bosche, & El Hajjaji, 2013).

The optimal control approach of an air-path system for a diesel engine is reviewed in (Yan, Benjamin, & Wang, 2009). A hybrid control approach for the air-path controller design is provided in (Kim, Choi, & Jin, 2016). In addition, a survey of model-predictive control for the turbocharged diesel-engine air-path is given in (Dahl, et al., 2018). Additionally, a survey of model-predictive control for the diesel engine-air-path is given in (Ortner, 2006). Brief details are introduced to each method in the following sections. These control methods can be divided into classical control, non-linear control, hybrid control and model-predictive control. A classification for these control methods for engine-air-path systems is illustrated in Table 2-1.

2.3.1 Classical Control

The controller used in production ECU usually consists of feedback modules, look-up tables and parameters (Wahlstrom, Eriksson, Nielsen, & Pettersson, 2005; Ahmed, 2013). As mentioned in Section 1.1, to reduce system complexity, MIMO interactions among subsystems have typically been neglected in classical engine-control design. Figure 2.12 illustrates the hierarchical function environment into which the classical air-path controller has been integrated. Langthaler (2007) and Ahmed (2013) show that, in the SISO PID controller structure, the set point values of MAF and MAF are stored in two lookup tables which are usually optimised with respect to emissions, torque and fuel consumption in the steady-state by field test; however, the important optimisations during transients are neglected. A feedback loop in which the actual MAP is subtracted from the desired MAP is used, and the result is passed into the inner loop. Then the inner loop uses a PID controller to regulate the MAP based on the VGT position. The second control loop from EGR to MAF acts in the same way by controlling MAF with the EGR valve.

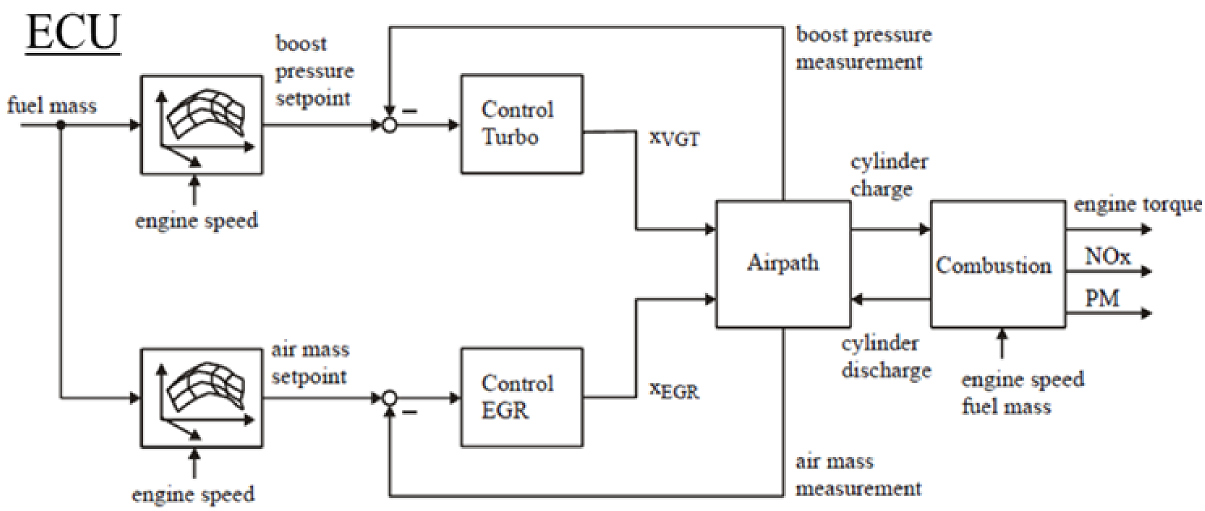

Figure 2.12: Classical air-path controller within the ECU (Langthaler, 2007)

As mentioned above, the engine-air-path is a typical MIMO system, and there is a strong cross-coupling effect between MAF and MAP control loops (Jung, 2003; Ahmed, 2013). Obviously, to control a MIMO system with gain scheduling, a SISO PID controller provides a strong restriction on the control performance. Furthermore, the feedback PID control type can only move along the NOx-PM trade-off curve. It is impossible to minimise both emission NOx and PM quantities at same time (Nieuwstadt & Kolmanovsky, 2000). In addition, one must often consider the fact that the calibration work of gain scheduling PID control of VGT and EGR is very time consuming and, in certain application (such as transient operation), the scheduling PID controller may be unacceptable due to high engine non-linearity (Wahlstrom, Eriksson, Nielsen, & Pettersson, 2005).

2.3.2 Non-linear Control

Research shows that, due to strong non-linearity, the high-performance requirement and the rapidly growing complexity of the system, non-linear control techniques are widely researched for engine-control systems. Robust non-linear control for air-path systems is a logical extension of classical PID control methods. Liu and Wei (2007) introduce an alternative LPV-modelling approach based on a system-identification technique. In this work, a gain scheduled LPV H_{inf} controller is applied to a diesel engine, the guarantees robustness considering varying exogenous variables, engine speed and VGT position. Its advantage is that the non-linear controller utilises the varying characteristics and thus can provide better performance than that of a linear controller. The control development is done and tested on a mean-value model. But this kind of control approach is still very difficult to integrate into an air-path system due to its additional specification of a H_{inf} controller. However, the author points out that LPV modelling is one of the promising control techniques for non-linear systems such as the engine-air-path.

In (Kuzmych, Aitouche, Hajjaji, & Bosche, 2014), a Lyapunov control function based on a nonlinear controller is applied to a turbocharged diesel engine. The model-based tests in simulation and experiment perform well in certain operational regions. However, the constructive Lyapunov control parameters must be improved if they are to provide acceptable performance for a wide variety of engine-operation regions. Atam (2018) develops an extended LPV model to design an LPV controller for air-path system control in diesel engines. This work uses a mathematical model of an engine air-path with the extension of an engine exhaust-manifold pressure and compressor air-mass flow for model-based control design. The plant model includes the external inputs of fuel mass and engine speed and the controlled outputs of exhaust-manifold pressure and compressor air-mass flow. A non-linear controller for this system is derived from the LPV interpretation of the plant. However, due to the high computing time of the gain-scheduling controller, the calibration work is very time-consuming.

2.3.3 Hybrid Control

Hybrid control is one of the newest control techniques. It usually consists of two or more kinds of control techniques. Several hybrid controllers have been proposed for engine-air-path control.

In (Bengea, DeCarlo, Corless, & Rizzoni, 2002), a hybrid control for diesel engine EGR and VGT is implemented. The non-linear physical model is linearised in different regions. For each operation region, a third-order non-linear error model is generated in polytypic form, which is later used for control design as a set of linear matrix inequalities (LMI). To solve this equilibrium problem, considerable computing time is required (up to five seconds for each step). This leads to unacceptable control performance.

In (Zhao & Pan, 2012), a fuzzy PID-based hybrid control is established to track EGR reference values. At first, a non-linear mean-value model which consists of combustion chamber, an EGR system, and an intake and exhaust manifold is developed to evaluate the performance of control strategy. Afterwards, according to the fuzzy rules, a hybrid gain-scheduled controller for varying the state of the EGR system is presented and overshot without any oscillations. The non-linear-control problem is solved by the hybrid controller instead of by each technique separately.

In (Kim, Choi, & Jin, 2016), a hybrid control of VGT and dual-loop EGR is implemented. The non-linear physical model of pressure and mass flow is linearised in different regions. For each operation region—i.e., for all high-pressure-EGR and low-pressure-EGR areas—a coordinated controller based on the control-oriented model is designed. To solve this chronic problem using conventional pressure-based controllers, considerable computing time is required. This leads to unacceptable control performance.

Although hybrid control exhibits a combination of advantages from different kinds of control techniques, it also inherits many problems that must be faced in air-path system control, such as computing time, the disturbance rejection, constraint handling, difficulty tuning over a wide range of operation regions and a stability problem.

2.3.4 Model Predictive Control

Despite the similarity of engine-air-path system control to other types of non-linear-process control, certain features exist that are unique and challenging with respect to engine-air-path system control, including the following:

- a coupled MIMO control problem,

- a non-linear time-varying system,
- boundary of inputs, and
- multiple time-varying delays and disturbances.

These requirements lead to more advanced MIMO controllers. MPC has already been applied to air-path control. The objectives of cost function in MPC for air-path systems can include minimisation of emissions, fuel consumptions and control errors. Examples of MPC in air-path control can be found in (Ferreau, Ortner, Langthaler, Del Re, & Diehl, 2007; Maruyama, Shimura, Ejiri, & Ikai, 2011; Wang, Waschl, Alberer, & Del Re, 2012; Zhao, 2013; Huang, Zaseck, Butts, & Kolmanovsky, 2016; Dahl, et al., 2018), etc. The MPC is based on linear or non-linear models with constraints, because the relatively new fast-quadratic-problem-solver (QP-solver) algorithm can formulate the online optimal problem to yield a suitable formulation of the control law.

MPC is an optimal control method based on open-loop optimisation, which uses a model of the process and minimises an objective function. In contrast to classical feedback controllers, MPC is a more advanced control technique. It is able, due to its predictive character, to take future reference signals and known future disturbances into account. Furthermore, input and output constraints can be handled easily. This section provides a comprehensive survey of MPC in which the main focus is on MPC-based linear models with constraints because the relatively new algorithms can formulate the online optimal control law to a non-linear formulation of the control law.

2.3.4.1 Linear MPC

MPC describes a class of control algorithms that imply a prediction model for the plant to be controlled. This model is used to predict future system outputs.

The MPC algorithm determines a sequence of manipulated variable settings in each time step by optimising a specified cost function (Gruene & Pannek, 2017). The first value of the optimal solution vector is then used as a plant input for control. This sequence is repeated in each control interval. Originally, it is developed for petroleum refinery and power-plant control applications. Because it involves sampling times in the range of minutes and near steady-state conditions, the online-optimisation-control problem of MPC can be performed without strong constraints on computing power. Over the last 35 years, MPC has evolved to dominate the process industry—as in petroleum-refinery and power-plant control applications. One of the first predictive controllers is described in the literature of the 1970s by (Richalet, Rault, Testud, & Papon, 1978). It is called model-predictive heuristic control. In the 1980s (Cutler & Ramaker, 1980), the first dynamic matrix control is proposed to compute the effect of control inputs.

Next, a generalised predictive control (GPC) is introduced by (Qin & Badgwell, 1997) in the 1990s, which is a technique based on transfer function models with input, output and white noise. This special control form is widely accepted in the industry because of model descriptions that became popular toward the end of the decade. A further development of stability theory by Lyapunov makes state-space model description more attractive than the GPC method (Camacho & Bordons, 2007).

Several air-path controls using linear MPC have recently been proposed. To control MAF and MAP in an air-path system, a MIMO-model-based MPC is developed to control the air-path actuators (Cheng & Maloney, 2018). A standard design framework for linear MPC using Matlab/Simulink's model predictive control toolbox is shown for air-path control. In the simulation, the SISO PID controller proves to be insufficient due to the coupling problem in the air-path system. In contrast to PID control, it is observed that the MPC control can be used to meet the multiple-optimisation objective-control problem (e.g., transient power demands) and change the engine operation point while minimising emissions.

Gelso and Dahl (2016) compare a linear MPC control of VGT and EGR with an air-path baseline controller from engine electronic control unit (ECU). The results confirm the good performance of the MPC controller. The responses of the MPC controller are nearly independent of step amplitude. In contrast, overshoots of the baseline controller increase significantly for a higher deviation from the linearisation point. The manipulated variables, VGT and EGR, vary much more in the case of the baseline controller. This can lead to problems—especially with respect to the EGR valve control.

The conclusion to be drawn from the linear MPC review can be summarised in a few words. The chosen MPC-control technique can control the coupled EGR and VGT systems in an optimal MIMO form—at least in nearly steady-state conditions.

2.3.4.2 Non-linear MPC

The benefits of MPC also imply a demand for a more precise plant model and increased computational effort. NMPC is a logical extension of MPC in which the linear model is substituted by a non-linear one (Wang, Waschl, Alberer, & Del Re, 2012). In recent decades, the number of MPC applications has increased permanently. The improvement of technology and control theory facilitates the application of MPC in new problems which often require NMPC because of the large transients involved (Thoma, Allgöwer, & Morari, 2009)—as has already been seen in industry sectors like food processing, automotive, aerospace, etc. Therefore, there is now great interest in introducing MPC in the control of complex non-linear systems such as the engine-air-path system. Unfortunately, the implementation of NMPC still requires an increased computational effort in contrast to the classical control structures. In the past, this type of controller is not suitable for all fields of application (Maciejowski, 2000)—especially in fast dynamic-process control with a high sampling rate. Inserting this non-linear model into the MPC optimisation task, which is called QP, leads in general to a non-convex problem which is difficult to solve in a short time (e.g. by a sequential approximation with QP at each time step, which is computationally expensive) (Wang, Waschl, Alberer, & Del Re, 2012). With advances in data storage, computing, and communication hardware, it is now feasible to adopt and implement an NMPC approach to overcome the inherent issues, because faster optimisation algorithms (Chen, et al., 2018) are available and more computing power (of ECU) is also available.

In (Zhao, 2013), work on turbo-charged diesel engines with EGR has realised the MPC for engine control under small disturbances and achieved some valuable results. It is proven by the author that the MPC control scheme is feasible under small disturbance; but it will produce greater deviation under large disturbances if the internal prediction not accurate enough. Furthermore, it has been pointed out that the turbo-charged diesel engine is mainly to provide power to heavy-duty vehicles. When the engine-operation points change, the MAP and MAF in the engine-air-path contain the most favourable information about engine dynamics, and this indirectly represents the power demand of the vehicle. Therefore, MAP and MAF provide reasonable assurance for engine-air-path control.

Ortner (2006) implements an explicit MPC strategy originally proposed by (Bemporad, 2001) for air-path control. The explicit MPC approach has a large advantage over the linear MPC, as it is able to select a stored linear-control law instead of solving a quadratic optimisation problem at each sampling instant. As the test-bench results show, MAF and MAP can be tracked with this new MIMO controller better than they can be tracked with the standard SISO and general MPC controllers, thereby leading to lower emissions. But what must not be neglected in this work is that the explicit MPC has to search for the optimal solution in the polyhedral partition, which takes time when many regions are present. In the QP-solver used here, the search is implemented only by a simple loop that makes searching very inefficient. Use of faster search algorithms can enormously accelerate the problem solution.

A fast QP-solver that is based on an online active-set strategy is shown in (Ferreau, 2006). This solver is basically intended for linear MPC problems, but it can be enhanced for varying QP matrices. The idea is to move on a straight line in the parameter space from one QP to the next. Along this path, a sequence of optimal solutions is produced. Interrupting this sequence because of limited time results in a sub-optimal solution. In the next sampling, a new homotopic path to the next solution is calculated. This approach provides enough computing power for general non-linear problems with input and state constrains. Ferreau, Ortner, Langthaler, Del Re and Diehl (2007) report that this fast QP-solver-based MPC has been carried out on the engine-test-bench. The results show that an upper computation bound on the order of milliseconds per QP solution can be guaranteed in real-time. In this work, prediction of MAF and MAP is also included in the controller with linear form only in a very short time interval. But the question of including more precise future information for the control has to be investigated more in detail.

Dahl, et al. (2018) develop an NMPC technique for the VGT-EGR diesel engine. The motivation is to control the air-path system and, in particular, the exhaust energy, thereby to achieve satisfaction of the exhaust-after-treatment-system (EATS) requirements and assess the fuel economy. The proposed MPC controller reaches mass-production maturity level and has a margin similar to that of the EURO VI emission regulation and the PID control in the ECU. Wei (2003) develops a control-oriented modelling technique for a non-linear system which uses an LPV-model structure. This technique is based mainly on the Kronecker product technique. In the context of LPV, the discrete LPV system is described well by the scheduling variable, which is usually measurable. In (Lu & Arkun, 2000), the time variation of the scheduling variable is available in real-time, and it is bound by the rate of change in the scheduling parameter which results in better feasibility and performance. Furthermore, in

(Casavola, Famularo, & Franze, 2003), the constant of the control horizon is cancelled such that the length of control horizon can be applied with close-loop instead of open-loop prediction. This reduces conservativeness and improves feasibility, but it significantly increases the computational burden more than non-scheduling approaches do. The stability issue of LPV MPC is discussed in (Hanema, Lazar, & Toth, 2017), where the robust asymptotic stability is given by interpolation-based LPV MPC. This method improves the performance with respect to moderate computational expense.

Wang, Waschl, Alberer and Del Re (2012) investigate a non-linear approach for air-path control. A fast QP-solver using an online active-set strategy is applied to the LPV MPC. In the simulation platform, the combustion engine is modelled with two actuators, two measured disturbances and two target quantities. The output-prediction model, required by the NMPC, is designed as two independent MISO systems by using LPV techniques. Due to the possibility of treating constraints and non-linear MIMO systems directly, an NMPC is chosen for this feedback-control problem. The simulation and comparison of various configurations shows a satisfying closed-loop performance of the two target quantities, MAF and MAP. Compared to general MPC, this approach provides better tracking performance—even during plant operation in regions at some distance from the linearisation point. The same conclusion is made by comparing the NMPC with two SISO PI controllers, as they are utilised in production engines. Therefore, the LPV-NMPC-control approach can achieve adequate closed-loop performance in air-path control. However, the prediction model structures used in this NMPC are two independent MISO models. The disadvantages are no interaction of the coupled effect of EGR and VGT, and twice the time consumption required for two MISO system models. The design effort can be improved significantly by a general MIMO LPV plant model.

2.3.4.3 Factors Affecting MPC Performance

The most commonly used performance criterion for evaluating the performance of various controllers is the stabilisation and reference tracking of a dynamic system. Therefore, in the following sections, the critical factors which affect MPC performance in air-path control are reviewed from different literatures concerning the prediction model, cost function, optimisation, constraints and QP problem.

2.3.4.3.1 Prediction Model

In MPC, a mathematical model is used to predict future system outputs based on past inputs, outputs and predicted inputs. The deviation between the reference trajectory and predicted outputs is then minimised by means of an optimisation algorithm that considers possible constraints and the defined objective function.

An overview of MPC technique that covers the prediction model is presented in (Camacho & Bordons, 2007). Some linear model-based MPCs have been tested for air-path systems in (Maruyama, Shimura, Ejiri, & Ikai, 2011; Cheng & Maloney, 2018; Dahl, et al., 2018), e.g., the impulse-response model, ARX, ARMAX and the state-space model. But the benefits of an MPC controller also imply the demand for a more precise plant model. Non-linear models can be used to represent the process more precisely, but the optimisation problem becomes more complicated.

In recent years, the study of LPV systems has received much attention. In (Gunes, Wingerden, & Verhaegen, 2018; Schulz, Bussa, & Werner, 2016; Wang & Steiner, 2011; Wei, 2006), several approaches have been tested, among which the linear parameter-varying method seems a good alternative in terms of complexity and performance. The LPV model-identification technique is not a main topic of this proposed study, but it can be an essential part of the NMPC controller. The LPV method is reviewed in Section 2.4.

2.3.4.3.2 Cost Function

Camacho and Bordons (2004) introduce that, an MPC controller computes future optimised-control sequences for the output. The optimised-control sequence is called a control horizon, and it specifies the degree of freedom of the controller. After reaching the control horizon, the control value is set constant. The optimisation task is to minimise a criterion—usually in form of a cost function of quadratic errors between the predicted output signal and the reference trajectory, but also the limitations of control values and their changing rate are considered in the optimisation task.

In linear MPC air-path control (Cheng & Maloney, 2018; Ferreau, Ortner, Langthaler, Del Re, & Diehl, 2007; Maruyama, Shimura, Ejiri, & Ikai, 2011), the prediction model is used to calculate the system output for MAF and MAP. Then the difference between the output and the reference values is minimised by the cost function. Thus, the cost function has a linear formulation whose system matrixes stay constant in each time step. An alternative to solving the optimisation task online in air-path control is to use an explicit MPC approach (Oravec, Jiang, Houska, & Kvasnica, 2017). This explicit formulation can be implemented to reduce the online computational effort. This can be achieved by pre-calculating the solution of the state-feedback control law and storing the results in tables for the online controller selection (Ortner, 2006). Wang, Waschl, Alberer and Del Re (2012) develop a cost function combined with LPV structure for air-path control. The results clearly show that the advantage of the LPV structure is that the cost function is evaluated at each time step with the current external parameters. This kind of structure gives the cost function an efficient solution to the QP problem.

2.3.4.3.3 Constraints

Studies in (Gruene & Pannek, 2017) show that, in MPC, the optimal problem can be easily solved if the cost function is quadratic and the prediction model is linear without any constraints. The constraints make the optimisation problem difficult due to the complex and non-convex problem. Unfortunately, most automotive systems have constraints. These constraints can be input, state or output constrains. In case of the engine-air-path control, the constraints are the minimum and maximum positions and the rate for closing and opening the EGR and VGT actuators (Jung, 2003). The EGR valve position is limited to between 0% and 100%. But the maximum position of VGT depends on the engine operation areas, because too much closing of the VGT valve at high power points can damage the manifold by high pressure (Wang, Waschl, Alberer, & Del Re, 2012). In addition, the MAP is also limited under the physical boundary due to safety reasons (Van Basshuysen & Schäfer, 2004).

2.3.4.3.4 QP Problem

In MPC, the optimisation of cost function can be transformed into a QP problem which can be solved by a QP-solver. In the linear case, algorithms for QP-solver configurations are state-of-the-art. The QP describes the standard convex quadratic-optimisation problem. However, the complex structure of a non-linear problem can complicate the formulation of a NMPC. For the class of unconstrained, input-affine non-linear systems, an analytical solution can be derived which also guarantees closed-loop stability (Ferreau, Ortner, Langthaler, Del Re, &

Diehl, 2007). But the introduction of constraints into the cost function makes it necessary to follow other approaches to a solution. Multi-parametric non-linear programming (Bacic & Cannon, 2003; Findeisen & Allgoewer, 2006), for example, provides sub-optimal solutions for general non-linear problems with input and state constraints. Findeisen and Allgoewer (2006) give a summary of algorithms for the implicit solution of NMPC problems. Dimitris, Gianluca, Andrea and Moritz (2018) introduce an alternative fast-method QP-solver. The results lead to the conclusion that an upper computation bound of optimal problem can be ensured in real-time by an advanced QP-solver, which is very suitable for the NMPC air-path control application.

2.3.5 Summary

This section shows very different approaches to improving engine-air-path control and to lowering emissions and fuel consumption of engines. The results of the review lead us to the conclusion that. Considering the air-path system characteristics, if a new air-path control concept is developed, it should exhibit less time-consuming tuning procedures and deal with constraints, high non-linearity and time-delay. Apparently, the reviewed air-path control concepts have difficulty meeting all the requirements. Alternatively, as discussed above, the MPC can be a very promising control technique for the air-path system due to its ability to handle system constraints, time delay processes, MIMO systems and integration of disturbance models for disturbance rejection.

2.4 System Identification of Diesel Engine-air-path

The air-path control of the diesel engine is the basis of every engine-control structure and has a direct impact on vehicle performance and emissions. To design the engine-air-path control, it is essential to perform a measurement or at least estimate the engine-air-path physical qualities. As the direct measurements for each engine subsystem are too expensive, several approaches have been proposed to estimate engine-air-path physical qualities based on observed input and output data.

Li, Li, Huang, Lai and Zheng (2010) show that modelling the drive train, control units, engines, vehicle dynamics and communication networks in automobiles allows engineers to evaluate design alternatives and predict results (such as fuel consumption and driving performance) before the vehicles are built. The model-based development combined with a consistent test strategy—from model in the loop (MiL) to hardware in the loop (HiL)—allows error correction to occur much earlier in the development phase and thereby reduces prototype tests. There are two broad ways to model engine-air-path systems that are suitable for control: physical modelling (Unver, Koyuncuoglu, & Gokasan, 2016; Yin, Su, Guan, Chu, & Meng, 2017), and modelling by means of system identification (Sequenz, 2013; Cornetti, 2014). Physical modelling based on the law of conservation of energy or the mass-conservation law has attractive intuitive component-based features, but it suffers from complexity issues with adverse effects in application (Bengtsson, 2007). System identification is useful when the only available information from a system is input and output data, and it has proven to be a very effective modelling method for control system when it is too difficult to describe a system using known physical laws in many real-world situations (Lauer, 2018; Tangirala, 2014; Wei, 2003). In such cases, the system-identification method can be used to perform black-box modelling. The purpose of this section is to provide a survey of state-of-the-art system identification techniques in engine-air-path control, giving particular attention to LPV system identification.

An important task in system identification is to find the relationship between input and output by using any measurement data that exist in a set of variables when at least one is random or unknown. The standard treatment of linear- system identification and detailed descriptions are found in (Lauer, 2018; Tangirala, 2014), Many system-identification methods are developed for linear systems (for example in (Lennart, 1999; Mareels & Polderman, 1996; Gruenbacher & Schrems, 2007; Johansson, 1993)). Some studies of automotive engines that are based on linear identification models have been developed in recent years (Kamaruddin & Darus, 2012; Serrano, 2014; Nickmehr, 2015) etc. However, these methods have serious disadvantages, as the precision of the estimates they provide depends very strongly on the engine parameters. These, in turn, are usually known only approximately, because important factors like operation areas or production tolerances (Wei, 2006), which cannot be known in advance, strongly influence the model output. Therefore, it seems appropriate to look for a suitable model structure which can be easily identified from data.

In the last decade, the study of LPV systems has received much interest. Several approaches have been tested, of which the linear parameter-varying method seems a good alternative in terms of complexity and performance. Corno, Wingerden and Verhaegen (2012) explain that LPV stands for “linear parameter-varying”, which means that the model has a linear model structure though the coefficients in this structure can vary over time depending on one or more external parameters. This provides an opportunity to describe systems with non-linear behaviour. The external parameters can be inputs, outputs, system states or any other parameters. The only condition on the parameter is the characteristic description of the change of system properties. This type of structure is suitable for non-linear system control.

The LPV system control method originates from the gain-scheduling practice where the controlled non-linear plants are modelled by linear models in many local operation regions and for which each linear time-invariant (LTI) model linear-control strategy is applied (Wei, 2003). While the plant operates in different operation areas, the controllers are switched from one to another or the control output is weighted from all the controller outputs.

Nemani and Ravikanth (1995) address the first report of LPV identification. This paper proposes a method for the identification of a full-state measurable method. Chou and Verhaegen (1997) have developed an identification method for LPV systems in which the outputs are the noisy measurements of the state, and Hubert (1997) proposes an identification method to identify an LPV system without the limitation of full-state measurability. In the series works by Verdult (Verdult, 2000; Verdult & Verhaegen, 2001; Verdult, 2001), LPV identification issue is considered under the subspace identification framework. In this approach, the subspace-identification method for the linear time-invariant (LTI) system is extended to the LPV system.

As in (Santos, Romano, Azevedo-Perdicoulis, & Ramos, 2017), the LPV model can be formulated as a linear regressive form. Some classical identification algorithms can be directly applied to LPV systems, such as the iterative regularisation methods described in (Engl, Hanke, & Neubauer, 1996; Hanke & Hansen, 1993). Using digital computers, iterative methods become powerful ways to find the solution to a non-linear-system identification problem. If these methods are observed a bit more carefully, it can be seen that many iterative methods exhibit a “self-regularising property”. This means that, with increasing iteration index, the solution goes to the non-regularised solution. One advantage of iterative methods is that only matrix-matrix or matrix-vector multiplications are needed. These can be implemented very easily and effectively. It can be said that the iteration index has a meaning similar to that of the regularisation parameter.

Chen, Jiao, Liu, Yu and Xu (2018) introduce a further development of the control-oriented identification of the LPV system using a new model structure. It is mainly based on a Kronecker-product technique. The classical least-square parameter-estimation algorithms are transformed into linear forms which can be directly applied with a change of regression. Wang, Waschl, Alberer and Del Re (2012) implement the LPV method to track MAF, and MAP is used as a prediction model for MPC control. The LPV model used for control design consists of two MISO sub models. Each sub model consists of four inputs (engine speed, fuel injection, VGT and EGR) and one output (either MAF or MAP). The LPV models which use VGT and EGR as scheduling variables describe the engine dynamics. However, the prediction model structures used in this NMPC are two coupled MISO models. A disadvantage is that two MISO system models take twice as much time. The development time can be reduced significantly by employing a general MIMO LPV plant model.

2.5 Engine Optimisation Methods

Modern internal combustion engines have to meet constantly increasing demands on fuel consumption, performance and emission behaviour. Therefore, Reif (2014) explains that the classic manipulated variables of injection volume and injection timing are joined by further manipulated variables, such as EGR, VGT, injection pressure in common rail systems, variable valve train (VVT) and injection modulation. These control variables affect engine torque, consumption and emissions. This creates a complex, non-linear, multivariable system with about five to nine input variables and six to seven output quantities. This variety of control options and their interactions make it increasingly difficult for engine designers to find an optimal engine setting.

Obviously, the previous working procedure used by experienced test-bench engineers (Unland, Stuhler, & Stuber, 1998; Renninger, Daudel, & Hohenberg, 2000; Friedrich, Compera, Auer, & Stiesch, 2017) for engine application requires a lot of time and is difficult to implement when the number of manipulated variables rises. Such methods are no longer suitable for such multidimensional optimisation problems in engine calibration. Model-based optimisation methods are therefore required for further development of electronic engine-management systems which allow for both the steady and dynamic behaviour of combustion engines to be determined as accurately as possible by means of mathematical models and computer simulation. Xie, Kistner and Bleile (2018), Wang Y. (2015), Bodenstein, Lohse and Zimmermann (2010), Li, Li, Huang, Lai and Zheng (2010) summary the benefits of efficient development through model-based methods, as follows:

- before experiments, off-line simulation platforms can help us select the highest potential solutions and specify the necessary experimental campaign;
- during experiments, off-line and on-line simulation platforms can help us to complete and reduce the number of experiments; and
- after experiments, off-line simulation platforms can help us to gather the project knowledge and perform after-project tests.

In (Hafner, Schueler, & Isermann, 2000), an example of a system-identification method that can detect the stationary influence of engine-control variables on emissions is applied to engine application. Based on the black-box mathematical model of HC and NOx, the influence of the manipulated variables (injection timing and VTG and EGR) on engine emissions is given. Despite slight variations in the validation results, the system-identification method has qualitatively established the mathematical relationship of the engine input and output. Offline stationary-engine optimisation can be performed on this mathematical model to determine the optimum manipulated variables. This model-based method shows very great potential in engine optimisation.

Zhou, Fiorentini and Canova (2016) use a model-based optimisation method of individual engine-operation points to optimise the engine performance and ensure the stability of the compressor during transient. This optimisation is performed on a cost function for the fuel consumption and emissions. In this case, this cost function can be minimised, depending on the manipulated variables, by EGR, fuel injection, engine speed and VGT, and it can be presented as a mathematical model. Using an advanced constrained-quadratic algorithm, the model-based optimisation solution can be solved in a short time.

AVL GmbH (2017) presents a way to optimise engine performance by using a global DOE: namely, a drive-cycle approach to the optimisation of emissions. This optimisation approach is based on the selection of DOE points that represent the standard drive cycle to be optimised. In such operating points, the influence of the control variables—including real driving emissions (RDE)—is measured on the test-bench and on vehicle variants and legislation cycles. Using the data recording, the main emission operating points and their corresponding weights are calculated in CAMEO software and used for the optimisation of fuel consumption and emission. The disadvantage of this method is in the limitation of a few operating points; thus, optimisation for a wide range of operating points is still hardly feasible due to the high non-linearities.

2.6 Conclusions

The aim of this study is the development of a NMPC with MIMO structure for a diesel engine-air-path system. A systematic literature review has been conducted to appraise the research that has already done in this context. The literature review suggests that, if a new NMPC concept for engine-air-path control is developed, the following important points should be considered:

1. Different air-path control methods in the form of classical control, non-linear control, hybrid control and model-predictive control have been reviewed. Considering the air-path system characteristics, the advantages and disadvantages of each control method are highlighted. In contrast to the reviewed methods, there are several advantages that make MPC a powerful alternative to classical engine-air-path control approaches. In the engine-air-path system, the control objectives, VGT and EGR, are constrained: Values must be within 0% and 100%. The MPC is able to include such constraints on the control value, but it also constrains changing rates of the control value and the output values in the optimisation task.

   System constraints lead to problems with control structures that include an integral part, like conventional PI or PID controllers. By reaching physical boundaries, a persistent difference between the reference signal and the measured plant output can lead to a permanent increase of the integral value. The inclusion of constraints in the controller synthesis of an MPC, which automatically leads to an “anti-windup” behaviour, constitutes the most significant difference from conventional control methods. The optimisation task in MPC can be solved by integrating a MIMO prediction model into the controller. Furthermore, the plant behaviour can be considered over a future horizon by the controller. This allows the MPC to reduce deviations from the desired trajectory.

The main difference of an NMPC from the linear MPC is in the inclusion of a non-linear prediction model in the MPC algorithm. This provides increased prediction accuracy compared to the linear case. As already mentioned, the use of non-linear models also complicates the solution of the optimisation problem. In both cases, a QP has to be solved in each step of the prediction horizon. In the linear case, these two calculation steps have to be performed once for each optimisation procedure.

For non-linear problems, output prediction and the condensing must be performed for each step of the prediction horizon again. This additional effort significantly increases the required computational power. However, as shown in the above literature, the development of fast QP-solver and LPV structure have created the right conditions for NMPC application in engine-air-path control.

2. A large challenge to implementing a NMPC is the need for an accurate model. The term *accurate* is hard to quantify: The model must be able to reflect the real dynamics in a sufficient way. The LPV identification algorithms delivered in the reviewed papers are successfully applied to different system modelling and control issues. The conclusion is that LPV identification techniques provide a new way to model dynamical systems. Compared to linear models, LPV models offer several advantages which make them good alternatives in non-linear system-control application.

   However, until now, most LPV models used in MPC are only identified as MISO forms with limited ranges of inputs and outputs. A global MIMO engine-air-path model has still not been obtained. If a new NMPC control approach can achieve adequate closed-loop performance in the whole engine operation area combined with one prediction model, the controller-development time can be reduced significantly and no switching strategy between different linear controllers would be required. LPV prediction is one of the targets in this research project. Further theoretical research and experiments should be investigated. Furthermore, it is suggested by the investigation that good LPV system-identification results can be reached by combining non-linear control methods. This makes these methods possible for purposed NMPC application.

3. In air-path control, the high non-linearity and constrains increase the complexity of the optimal problem (QP problem of cost function) in NMPC. As mentioned in the literature review, the online active-set strategy has already greatly improved the ability of MPC to run on a fast application (Ferreau, Ortner, Langthaler, Del Re, & Diehl, 2007). This strategy is inspired by the expectation that the active set does not change much from one QP solution to the next, which is very suitable for air-path control design. A more elegant formulation of combined MIMO-LPV structure should be defined in this research project, whereas the optimal problem of NMPC is overcome by the application of online active-set strategy. The feasibility and stability of NMPC must be ensured. The literature suggests that a parameter-dependent Lyapunov function can be used to construct a poly-quadratically stable control law to guarantee the feasibility and stability of the non-linear control system. The study of feasibility and stability analysis of NMPC should be proposed.

Chapter 3. RESEARCH PROPOSITION, METHODOLOGY AND DESIGN

3.1 Introduction

This chapter presents the research proposition, methodology and design for this study. Previous chapters reviewed and highlighted the advantages and disadvantages of a wide variety of methods for engine air-path control. Despite considerable work on engine air-path control, a controller that completely meets all technical demands does not exist so far as the author is aware. In this study, a new model-based method is proposed for optimising the emissions of diesel engines through non-linear model-predictive control.

In addition, a control-design method with a low design effort is introduced. Compared with other control methods, this new NMPC provides superior performance under varying conditions with respect to transient response and robustness to disturbances. The main contributions of this work can be summarised as follows: This work provides a new, accurate LPV system-identification method for the MIMO system; it contributes a new NMPC diesel-engine air-path control strategy which combines the NMPC algorithm with the LPV model; and it offers a new, time-efficient, model-based emission-optimisation method and a model-based simulation-and-verification approach applied to the diesel-engine air-path controller design.

The most important thing in research methodology and design is that the choice of topic, research questions, definitions, hypotheses, statements, methods for data collections and analysis (etc.). All need to be correlated to each other (Cray & Malins, 2004). As discussed in previous chapters, the topic of this thesis is the research, design and development of a model-based design approach for optimising the emissions of diesel engines through non-linear, model-predictive control. It is shown in Figure 1.3 that three RQs are to be answered in this study. It is important to repeatedly refer to the RQs and important definitions and hypotheses during the research. The study of research methodology and design conducted within this chapter shows that the methodological schools that characterise research in engine-air-path control and allied disciplines are reviewed and critiqued to establish the applicability of each. This chapter covers research in engine-air-path control research, including thermodynamic theory, control theory, testing methods, system modelling, analysis and simulation methods. Furthermore, a variety of methodological viewpoints for collecting, analysing and using experimental data in developing a systematic understanding of this specific research project is discussed. Finally, a mastery of the project proposal design is demonstrated with respect to the practical issues of RQs, data collection methods, data analysis and ethical issues.

The organisation of this chapter is as follows. Section 3.2 introduces the research proposition of a new model-based method for optimising emissions of diesel engines through NMPC. Section 3.3 describes the research methodology based on the existing engine-air-path control. Section 3.4 describes the research design, how the proposed modelling and model-predictive control techniques can be used to achieve the controller design requirements in engine-air-path. Section 3.5 presents an approach to verify and validate the NMPC control. Sections 3.6 and 3.7 introduce the data-collection and data-analysis methods. In Section 3.8, the ethical issue is discussed.

3.2 Proposition of a New Model-based Method for Optimising Emissions of Diesel Engines through NMPC

The propositions of this research are explained below in more detail.

3.2.1 A New Model-based Method for Optimising Emissions of Diesel Engines through NMPC

A new model-based method for optimising emissions of diesel engines through NMPC is proposed on this section. In the diesel engine-air-path, the VGT and EGR have a direct relation with the performance of the diesel engine. This new designed controller is aimed at improving the robustness and performance of the VGT and EGR control with particular emphasis on emission reduction. In the context of this project, the robustness and performance of the air-path control can have two interpretations. The first involves maintaining the closed-loop stability and sensitivity in case of large process dynamics during changing the engine operation points. The second involves maintaining the ability to track reference signals and to compensate for external disturbances while maintaining engine performance (engine power, fuel consumption and emissions). This research shows that the new NMPC controller MIMO structures can trade-off the robustness and performance in a more efficient way than the existing ones. Due to its advanced controller structure, the non-linear control problem, such as coupling effect on VGT and EGR control in engine-air-path, can be solved more efficient than standard control function in ECU, and this controller is efficient to implement and calibrate, which reduce controller development time and the complexity. This is a significant improvement over the existing control methods used in the automotive industry. Another key originality of this work is to determine a new LPV-identification method with a particular emphasis on modelling suitable for NMPC control design. Compared with previous identification approaches found in the literature (Wei, 2004; Wang & Steiner, 2011; Verdult & Verhaegen, 2001), the accuracy of the resulting LPV model and the possibility for MIMO structure are improvements. In addition, the LPV methods also calculate Kalman filters for the state estimation.

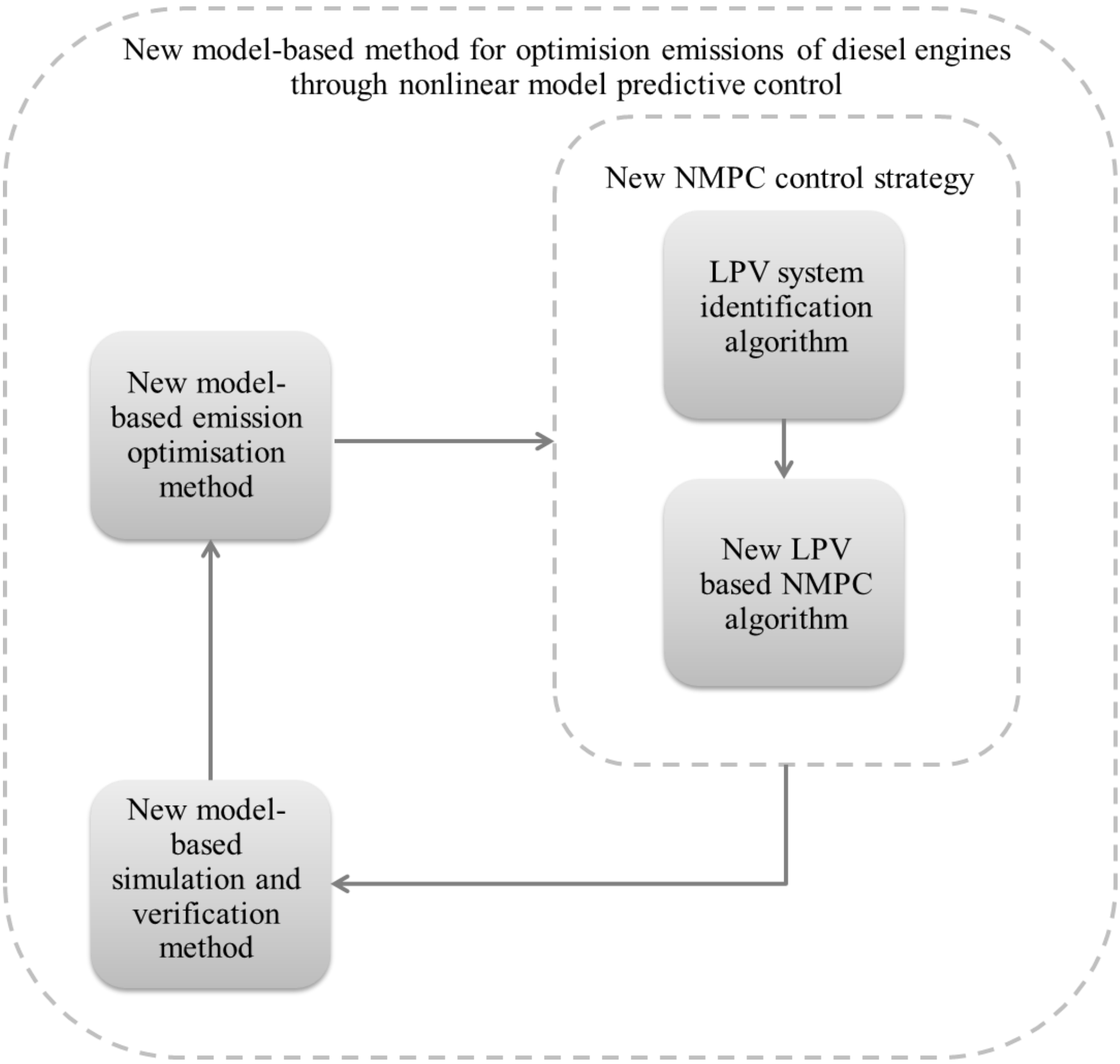

Figure 3.1: Relationship of the research originalities

Moreover, because of the NOx-PM emission and fuel-consumption trade-off problem, a new, model-based, multi-criteria optimisation is made for the optimisation of such “opposite” outputs. A Matlab/Simulink engine-air-path model equipped with a dynamical emission model is used during the optimisation. It is found that, by using the MAP and MAF as turning parameters, an automatic optimisation for engine performance is possible. Combined with the dynamical emission output from the model, direct optimisation of the emissions and fuel consumption can be achieved. The controller design and verification processes presented in this study are demonstrated mainly through a model-based approach. The mean-value engine-air-path model includes thermodynamic and gas-dynamic characteristics, which are important for controller design and optimisation tasks. Compared with alternative modelling approaches found in the literature (Li, Li, Huang, Lai, & Zheng, 2010; Unver, Koyuncuoglu, & Gokasan, 2016; Yin, Su, Guan, Chu, & Meng, 2017), the ability of modelling the dynamic emission is an advantage. Figure 3.1 illustrates the hierarchical relationship of the research contributions with which the proposition to be proved is concerned.

3.2.2 LPV System Identification

A new non-linear system identification that uses the LPV method is used as an accurate and time-efficient method for generating the NMPC prediction model. In recent years, great progress has been made in the field of LPV-system identification (Hirsch, 2011; Wang & Steiner, 2011; Kamaruddin & Darus, 2012; Santos, Romano, Azevedo-Perdicoulis, & Ramos, 2017; Chen, Jiao, Liu, Yu, & Xu, 2018). Apparently, many system-identification methods display several shortcomings with respect to non-linear systems. For instance, the optimisation in the identification method often requires a very long time to handle a high-order system, which can lead to instability for an open-loop, stable system, and which requires massive amounts of data for training and reinforcement. Analysis requires extensive time. Alternatively, to improve system-identification accuracy and efficiency and to use it to address the engine-air-path modelling and NMPC control issue, a new LPV-identification method suitable for NMPC control is first proposed. A system interpretation based on a constant-transfer function is extended to a polynomial function by introducing scheduling variables. Compared with the classical system-identification methods, this LPV approach provides for more accurate output prediction and computing capacity and is more robust in the presence of engine-operation disturbances. The significant advantage approaches and details of the LPV model developed for NMPC engine-air-path control are presented in Chapter 5.

3.2.3 NMPC for Air-Path Control

A new NMPC controller is designed that is aimed at maintaining engine performance while reducing NOx and PM emissions. When considering engine-air-path system characteristics, NMPC control offers many advantages. Many processes in engine-air-path systems are complex, non-linear, multi-variable systems with time-varying and strongly non-linear coupling effects and disturbances to the system. The system undergoes a wide range of operation ranges. The VGT and EGR exhibit rate- and range-limit constrains. Therefore, it is very hard to use the standard ECU-PID-control algorithm and linear-control methods to achieve target value tracking, adaptability and control precision. According to the literatures review, only few studies have been conducted on NMPC in engine control; those which exist are mainly aimed at the SISO engine-control system (Ferreau, Ortner, Langthaler, Del Re, & Diehl, 2007; Langthaler, 2007). The main problem is in the time-consuming nature of modelling non-linear systems and in difficulties with integrating the non-linear model into the NMPC algorithm. In the presence of all these challenges, a new LPV-based NMPC algorithm is proposed for implementing the diesel engine-air-path system control. This is of great significance. The contribution of NMPC for air-path control can be divided into two main segments, as discussed below.

1) The NMPC controller can use data-based models to predict the system output. A new MIMO LPV model is first proposed in the design of the NMPC controller to simulate the control of the diesel engine-air-path. The focus of this part is primarily on LPV modelling for MAF, MAP and control signals. The LPV algorithms are presented and applied to measured data to estimate the MAF and MAP of the engine-air-path and control input. The coupling effect of VGT and EGR, which is neglected by the SISO model structure, is modelled properly for the accurate control of MAF and MAP. It is expected that this proposed LPV engine-path model is then integrated into the NMPC controller. In terms of model quality, the proposed model structure can be used to significantly improve the accuracy of the prediction output and is more applicable to NMPC control. Therefore, LPV modelling for engine-air-path will be given the special attention in this thesis.

2) A new NMPC algorithm which is based on the LPV model will be proposed and implemented. The design effort of the controller could be reduced significantly by the MIMO structure, and no switching strategy between different linear controllers is required. For engine-air-path control, the VGT and EGR are constrained to operate within 0% -100% of their ranges. After the formulation of the LPV modelling of the engine-air-path and constraints, a dynamical cost function for optimisation is used in the minimisation of fuel consumption and emissions. Compared with a linear MPC and a standard automotive ECU, the NMPC shows superior performance in terms of transient rise time, settling time and percentage overshoot. The calculation of NMPC cost-function optimisation is accelerated by adopting a new, specially tailored, online, active-set strategy algorithm for the fast calculation of quadratic-optimisation program problems arising in the NMPC. On an engine-air-path simulation platform, this new NMPC algorithm is developed and evaluated in terms of controller-response time, robustness, different operation areas and external disturbances.

3.2.4 Model-based Emission Optimisation

A new model-based multi-criteria optimisation is used as an accurate and time-efficient method for optimising the controller set points at all engine-operation points. In the diesel-engine operation areas under different working conditions, proper control parameters are required to achieve optimum power, emission, and economy (Guzzella & Onder, 2004; Ferreau, 2006). The traditional optimisations via the engine-test-bench require a heavy workload, and the calibration accuracy and repeatability are relatively poor. The classical gradient-based techniques are usually designed to work with linear functions and may not even be used to find the global optimisation minimum of the engine. To this end, a model-based optimisation method for emission reduction is adopted and developed in this research. An engine-emission model is obtained through regression analysis of test-bench measurement by system identification. The mathematical model establishes the relationship between the parameters of engine, the control variables and the diesel response in the whole operation range of the diesel engine. The minimisation of emissions and fuel consumption is formulated as a non-linear quadratic-optimisation program, which is solved by using a sequential QP algorithm. Compared with conventional optimisation, a model-based, sequential, QP-based optimisation is able to search for the optimum more efficiently and thereby make the diesel engine achieve the highest efficiency and smallest emission under nominal conditions. The whole optimisation process achieves a better solution in fewer iterations compared with the standard optimisation, which greatly reduces the design effort.

3.2.5 Model-based Simulation and Verification

To conduct the studies for engine-air-path control, a simulation platform and verification procedure are generated, with particular emphasis on a method suitable for model-based control, by taking into account the pressure and air-mass flow dynamics in and between different subsystems of the engine-air-path. Compared with other thermodynamic simulation models, the mean value engine model and data-based emission model with real-time performances are highlighted and can well meet the requirements of the NMPC controller-design process.

The main research originality of this section is summarised as follows:

1) Model-based control syntheses requiring dynamic models and turbocharged diesel engine with emissions are estimated by system identification and physical modelling. The physical model is created by using the mean value method. It aims to describe the major thermodynamic and chemical interactions that occur during the operation of a combustion engine. The described models are implemented and simulated in Matlab/Simulink. The proposed NMPC can be interfaced with comprehensive models built in engine-simulation platforms to simulate control performance for a real engine under actual operation conditions. Chapter 4 provides the details of the simulation platform.

2) To control the development quality, a verification process is used to ensure that the NMPC controller performance is achieved as expected. The verification of the new NMPC controller performance is demonstrated experimentally on the simulation platform. Using this simulation platform, different air-path control methods are implemented and then evaluated and compared in terms of controller performance for variables such as response time, robustness against uncertainty, response to external disturbances and load variations. Experimental evaluation and verification are approached by way of qualitative comparison with respect to predictive accuracy and statistical error analysis to serve as a basis for high-

precision NMPC engine-air-path control. Please refer to Section 3.5 for the details of the verification process.

3.3 Methodology

A research methodology is the general approach a researcher takes in carrying out the research project. To some extent, this approach dictates the particular tools the researcher selects (Bryman & Bell, 2011). The methodology used for this study is a combination of theoretical derivation of the NMPC control algorithm and effective validation using computer software. Modern diesel engines contain many complex mechatronic systems, each of which may incorporate a large number of subsystems. As complexity increases, development cycles are under pressure and have to be short so that controller designers can deliver the latest in safety, fuel efficiency and convenience to consumers in a highly competitive industry (Hellestrand, 2005). At the same time, quality and reliability remain of paramount concern. As reviewed in Section 4.2, the benefits of using model-based techniques for the development of complex mechatronic systems controllers have been clearly shown (Li, Li, Huang, Lai, & Zheng, 2010; Unver, Koyuncuoglu, & Gokasan, 2016; Yin, Su, Guan, Chu, & Meng, 2017). The model-based methodology speeds up development and allows the project to handle more complex systems; therefore, model-based methodology is applied in this study, as it provides an efficient and cost-effective way to develop engine-air-path control algorithms. The complexity and expense of automotive controller design has motived the development of simulation tools and techniques which facilitate the conversion of high-level languages such as Matlab/Simulink into model-based design processes. In this study, the NMPC controller design is developed in the Matlab/Simulink environment. And after the designed NMPC is developed, controller performance is evaluated on the air-path simulation platform by using Matlab/Simulink simulation.

The waterfall methodology (V-model) is widely accepted as a comprehensive design methodology for large-scale projects (Ammann, Fekete, Guzzella, & Glattfelder, 2003; Ferrari, Fantechi, Gnesi, & Magnani, 2013; Aarenstrup, 2015). As Figure 3.2 shows, the left side of the V-model includes the design activities while the right side includes the verification activities. However, as explained in (Aarenstrup, 2015), the main disadvantage of the V-model is that the entire system design plan is well defined at the beginning. This makes it hard to work with complex systems, such as engine-air-path control systems, in which development steps and changing requirements might not be known until later in the process. But in a model-based approach, simulating a model instead of an actual physical system makes the V-model easier to manage by showing the interactions between components in simulation.

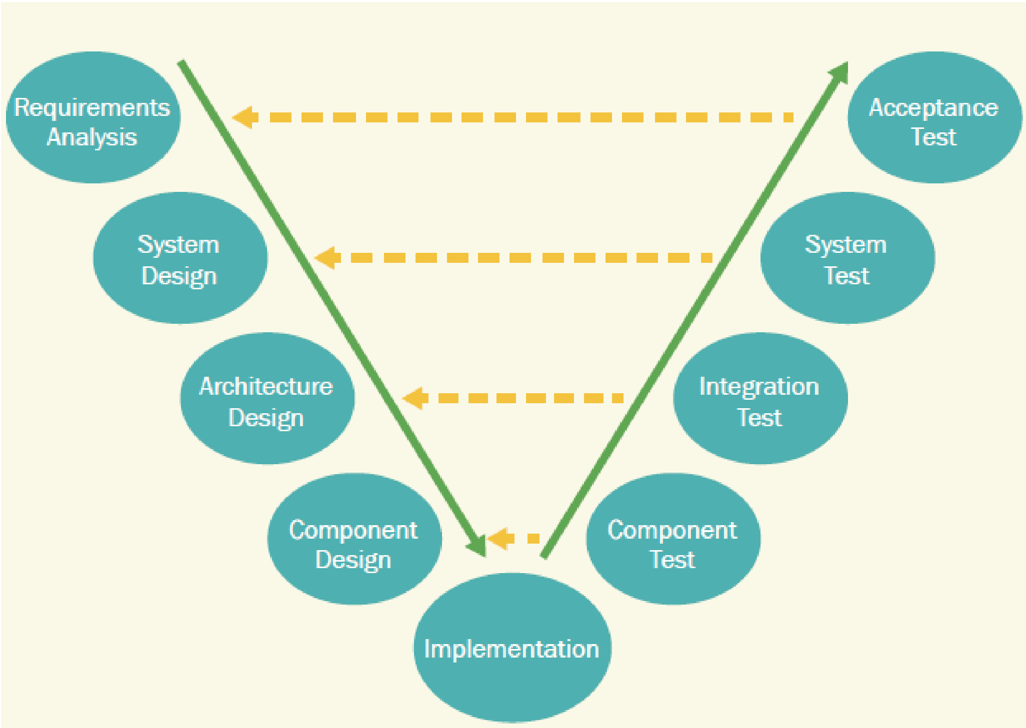

Figure 3.2: V- Model (Aarenstrup, 2015)

Engine-air-path control function development is one of the most important parts in automotive software design for control unit. As this engine-air-path study grows in size and complexity, its correct behaviour becomes increasingly hard to ensure. For this reason, this research project requires a new development workflow that can handle more complex software development projects. Considering all the above-mentioned advantages of V-model processes and model-based designs, an enhanced V-model process based on a model-based design is adopted for this particular project. Based on a diesel-engine air-path simulation platform, this research project implements a front-loaded development process with shortened development cycles and minimised rework, thereby making it possible to evaluate control designs much earlier in the design process and to proceed with great confidence to model-in-the-loop (MIL) testing. Based on this enhanced V-model process, there are three steps to follow in the design process: modelling the engine-air-path system, synthesising the NMPC engine-air-path control concept and developing and testing the controller on the plant model. To achieve the goals of this study, a diesel-engine air-path simulation platform is used to create the primary data for system identification, to design and develop the control algorithms and to evaluate the performance of the controller. The output-prediction model, which is required by the NMPC, is designed by adopting an LPV approach.

3.4 Research Design

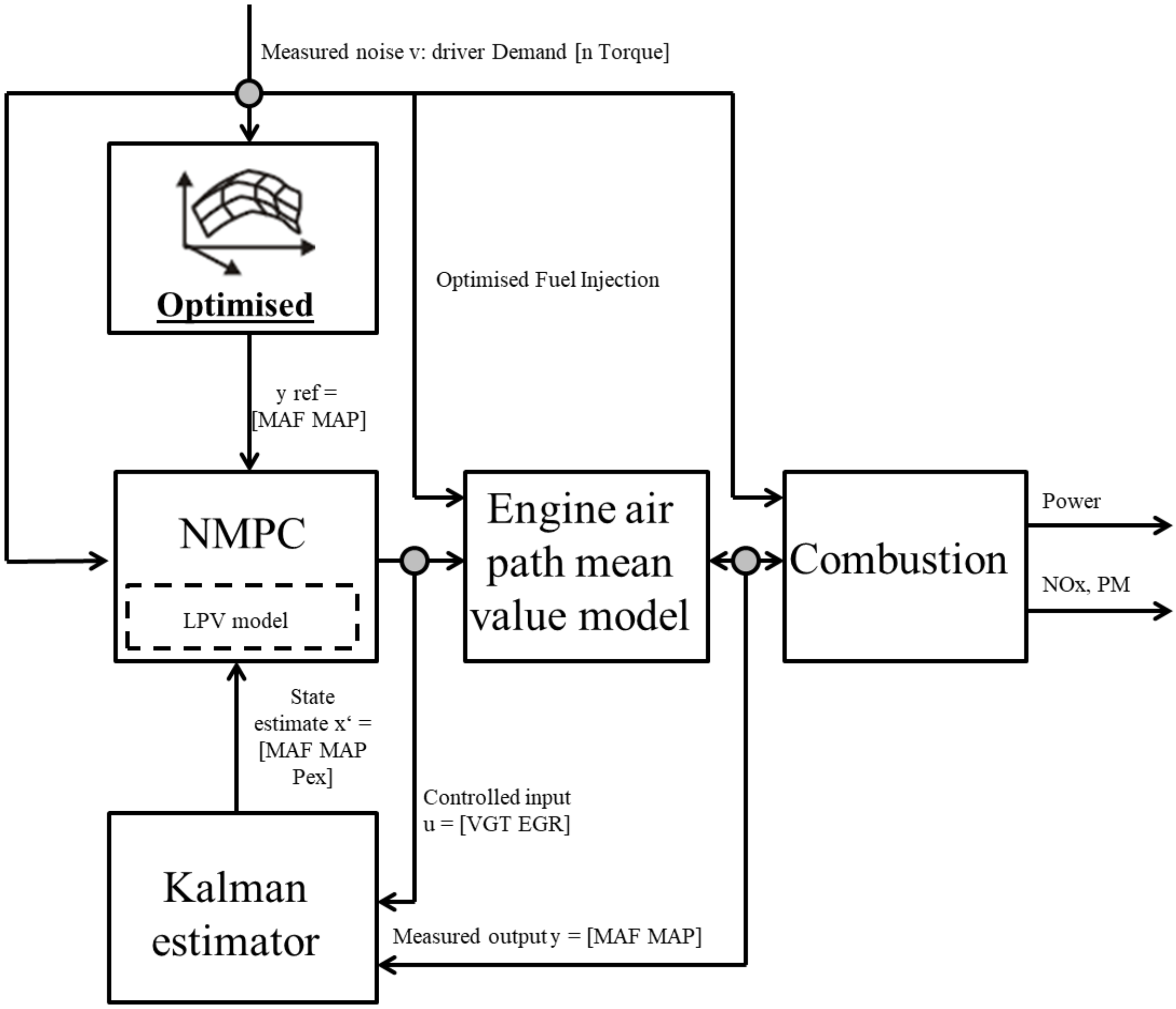

Figure 3.3: An overview of the proposed control scheme

In this thesis, the control structure, which is illustrated in Figure 3.3, consists of five parts: first, steady-state engine maps defining emission optimised MAF and MAP reference values based on corresponding engine operation points, engine speed and engine fuel injection;

second, a LPV model-based NMPC controller to improve the tracking performance of the MAF and MAP during the engine transients operation; third, a non-linear Kalman filter to estimate the controller states of MAF, MAP and exhaust pressure and to reduce the effects of disturbances; fourth, a mean-value engine-air-path model to simulate the engine behaviour and to validate the NMPC controller; and fifth, a data-based torque-and-emission model to determine the actual performance and emissions of the engine. This control concept does not include placing the emissions feedback directly into the control loop. The direct control of emissions faces difficulties in the high nonlinearity of the process. Apart from very few exceptions, concepts that include reference to the feedback of the emissions have not been published. The reasons for this include both the unavailability of fast emission sensors in production-type vehicle systems and the demanding mapping of engine measurements to the emissions. Therefore, the control objectives are replaced by intermediate variables (MAF and MAP) which are able to indirectly describe the emissions of the engine (Langthaler, 2007). Steady-state engine maps—which are maps with input settings, engine speed and fuel injection, for all engine operations points—are determined by optimal trade-off between NOx, PM and fuel efficiency. Their designs are discussed in Chapter 6. It is shown that the model-based optimisation procedure generated in Chapter 6 offers a time-efficient possibility.

The NMPC controller is the main part of the new controller design. Its purpose is to control the VGT and EGR to make the engine output match as closely as possible to the optimised MAF and MAP reference values, thereby to ensure tight compliance with emission legislation. By applying the NMPC controller, the effects of uncertainties and disturbances are compensated for by using the Kalman filter. When the NMPC controller keeps the outputs close to their respective reference values, the effects of changing conditions on emissions and engine performance are countertraded. During the transient operation, to ensure a fast response and reduce the difference between the actual output and the desired value, an LPV-based NMPC controller implemented. This kind of controller makes additional estimates for the future based on the LPV model. This speeds up the response time of VGT and EGR. The design and validation of the NMPC controller in engine-air-path is further discussed in chapters 5 and 6. By combining the optimal calibrated engine maps with NMPC controller, it is possible to achieve desirable engine emissions and performance and improve transient engine behaviour. Apart from the performance of the controller, it is obvious that it is necessary to develop a conceptual framework that clusters the process of NMPC controller design for engine-air-path system in logical steps.

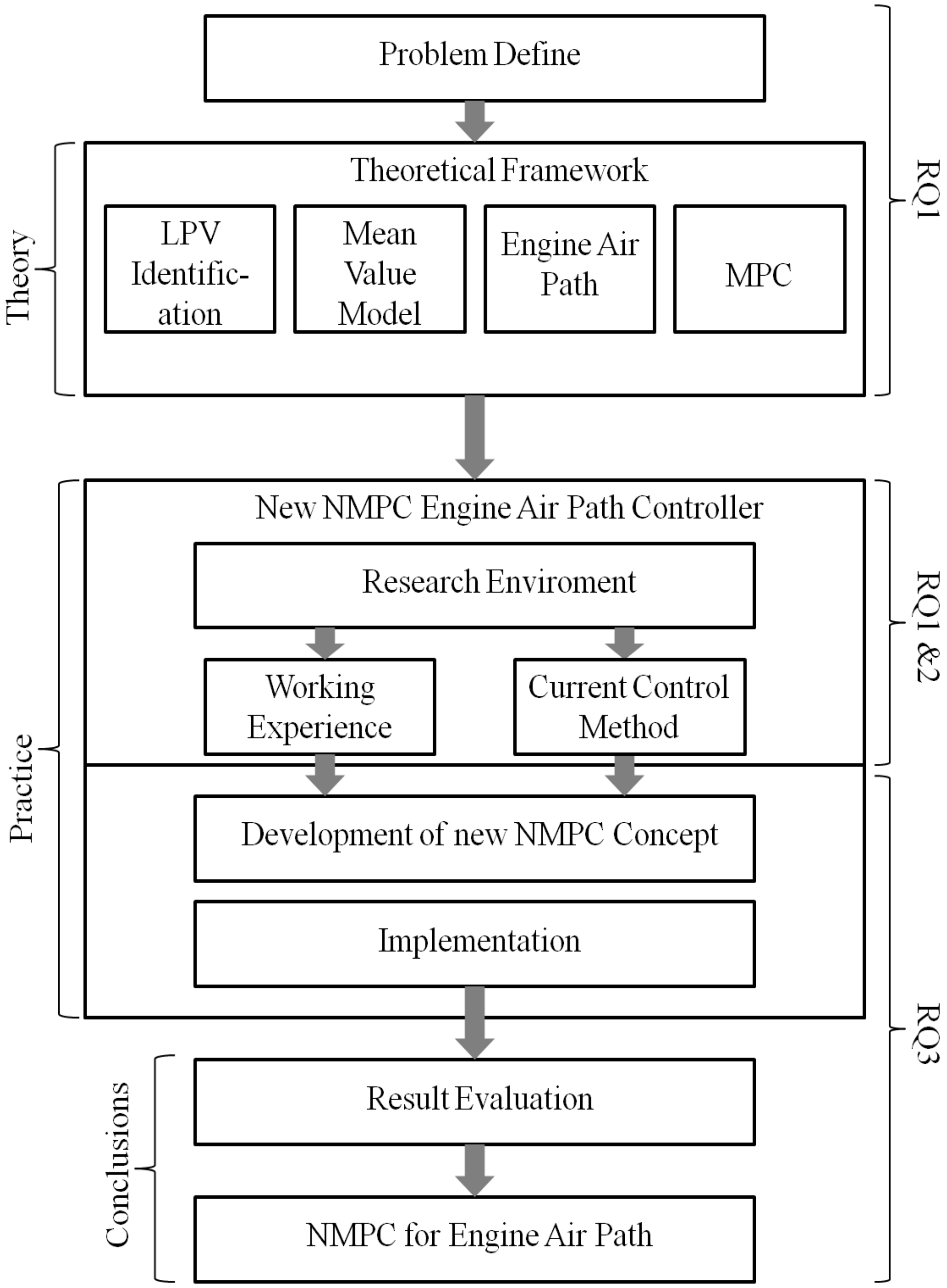

Figure 3.4: Air-path controller design framework

Figure 3.4 offers a high-level description of the NMPC engine-air-path controller development process, which provides the connections and contexts with the theory and practice. The steps at the top portion of the diagram indicate some theory studies that are required for improvement of the engine-air-path control. The “practice blocks” illustrated in the middle of the diagram indicate, are considered the most important in the whole development process using theory, simulation tools and processes. The purposed NMPC control algorithms are developed as controller models in Matlab/Simulink platform. The controller could be interfaced with an engine-air-path model to evaluate the control performance for real engine-air-path conditions by using computer simulation. The proposed engine-air-path controller design method is an advanced control, calibration, and optimisation process that provides comprehensive engine control, aids engine control in all essential tasks during function design and control unit calibration and evaluates the control results.

3.5 Approach to Verification and Validation

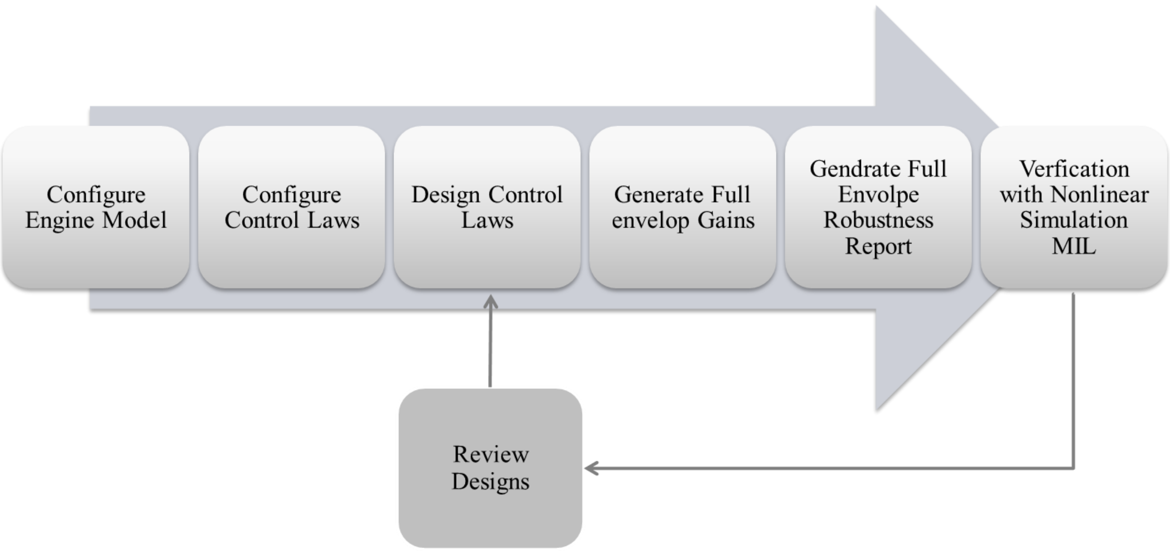

Figure 3.5: Illustration of the engine-air-path control development process

Verification and validation are approached via qualitative analysis of model accuracy, predictive accuracy and control performance and of capacity to serve as a basis for high-precision NMPC air-path control. Figure 3.5 illustrates the engine-air-path-control development process with a design-review iteration path. In the verification and design-review phase, the developing air-path control may be progressively tested on the engine-air-path model by simulation. The iteration loop and review-designs step are performed interactively with the verification and design-control steps. This indicates any further work required for fixing problems or other required improvements in the development. In the simulated engine environment, the engine speed and injection quantity are varied and the two reference values for MAF and MAP are changed around the linearisation point. Based on the simulation, the NMPC will be compared with a conventional air-path controller to validate the significance and advantages of NMPC approaches. Considering the non-linear characteristics of the engine-air-path system, the following comparison metrics are used to evaluate the performances of the purposed controller: transient response (rise and settling time, percentage overshoot), steady-state response and robustness to disturbances in changing operation conditions. The simulation results will be quantitatively analysed and evaluated using Matlab with descriptive statistics including correlation, covariance, Fourier analysis and histogram to determine how well the designed control function interacts to deliver the desired performance.

3.6 Data Collection Methods

The method of data collection depends on the research topic. There are qualitative methods, quantitative methods and mixed methods. Researchers typically select a quantitative approach to respond to research questions which require numerical data, a qualitative approach for research questions requiring textural data, and a mixed-methods approach for research questions requiring both numerical and textural data. The data used for this study are derived from a combination of qualitative and quantitative methods, which are presented in the form of secondary and primary data. The collection of secondary data is mainly undertaken by a systematic literature review with a focus on engine control to examine its utility and to analyse and evaluate the various approaches undertaken by researchers in this field. The primary data is mainly generated, presented and analysed in sections on experiment, modelling, simulation and validation. The careful attention must be paid to ensure the effective data analysis, to make sure that the reference to the research question is clear and to guarantee that the desired results are achieved.

3.6.1 Methods for Collecting the Secondary Data

In this project, the secondary data is gathered mainly through literature review. As has been shown in Chapter 2, a wide range literature on air-path control is reviewed to examine its utility and to illustrate the various approaches undertaken by researchers in this field. The data collection is focused on automatic-control engineering reported by several leading journals, organisations and conferences: Automatic, International Federation of Automatic Control (IFAC), Institute of Electrical and Electronics Engineers (IEEE), *International Journal of Vehicle Mechanics and Mobility*, Conference on Decision and Control, *International Journal of Oil and Gas Science* and Technology and Society of Automotive Engineers (SAE). The time frame for the articles covered in this report is from 1978 to 2018. Initially, articles are selected based on a study of the Ankle Brachial Index (ABI) using keywords such as *model-predictive control, diesel engine-air-path*, *mean-value engine modelling*, *VGT*, *EGR*, and *LPV*. On the topic of diesel engine-air-path control research, 120 articles are identified. The 120 articles have been reviewed and categorised according to research methodology (shown in Table 3-1) and scanned to see if they consider relevant engine-air-path control studies.

Table 3-1: Research methodologies (Gregg & Kulkarni, 2001)

	Methodologies
1	Qualitative
2	Experimental
3	Survey
4	Simulation/modeling
5	Concept/discussion
6	Secondary data

A software-engineering research-methodology (SERM) framework provides a well-defined perspective with which to understand design research in automotive control systems (Purao, 2002). It ensures that the intended behaviour of the control system is explicated in accepted forms. Therefore, this study follows the SERM framework. The SERM framework defines three phases for a software-engineering research methodology: the conceptual phase, the formal phase and the developmental phase (Gregg & Kulkarni, 2001). In the conceptual phase, the requirements of the study are defined. In the formal phase of the SERM framework, a mathematical or logic-based explanation is developed based on the requirements specified in the conceptual phase to describe and verify the software system. In the developmental phase, a prototype is developed to demonstrate the validity of the solution. As in SERM—based on the rating system by (Gregg & Kulkarni, 2001), as shown in Table 3-2, which involves assessing to what extent the study is conceptual, formal and developmental—every paper is rated *high*, *medium*, *low* or *none* on each of the three rating dimensions.

Table 3-2: Rating categories in three research dimensions: conceptual, formal and developmental (Gregg & Kulkarni, 2001)

Rating	Conceptual	Formal	Developmental
High	Major extensions or generalisation of an existing concept or a totally new concept	Defined in math and logic terms; formal definition or proofs; mathematical decription.	Prototype or model with validation and verification
Medium	In cremental extension and/or generalisation of an existing concept	Definitional without the math and/or logic proofs; establishes correctness criteria.	Prototype or modell with limited functionality
Low	Existing concept with limited extensions	Descriptive details and conjectures	Discussion of program requirements
None	No new concept	No formal definitions	No implementation described

Table 3-3 shows the rating results for 120 research papers according to Gregg's rating system per Table 3-2. Only 30 of the 120 articles received a high rating on all three dimensions. These 30 articles constitute the basis of this literature review.

Table 3-3: Rating results

Rating	Count
High rating on conceptual, formal and developmental	30
Others with medium, low and none rating	90

3.6.2 Methods for Collecting the Primary Data

In this study, the primary data for this NMPC engine-air-path control study can be divided into experimental and simulation categories. In the model-based design method, the accuracy of the created model depends largely on the quality of the data collected from the system. The collected data should capture most characteristics of the system and exhibit high accuracy, low disturbance and appropriate resolution to capture the process dynamics correctly. Of particular interest, the data is collected from the test-bench under typical engine-operation conditions.

Figure 3.6: A typical engine test-bench experiment setup (FEV, 2017)

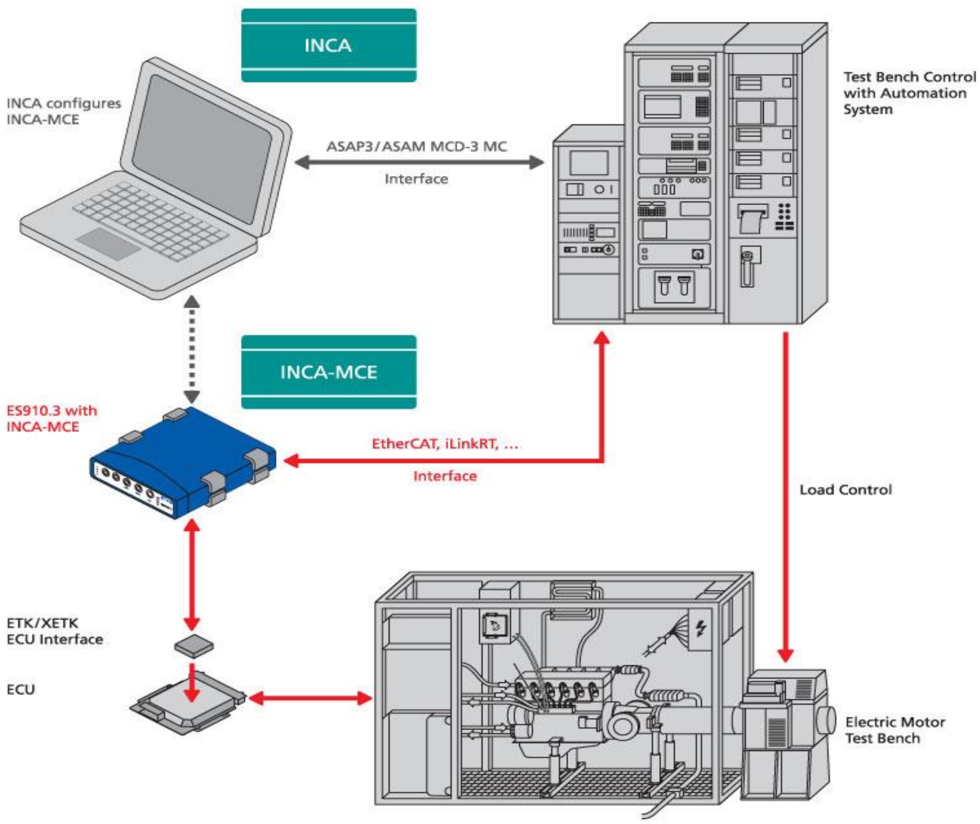

Figure 3.7: Data collection system schematic for engine dynamometer testing (ETAS, 2017)

In this regard, multiple test campaigns were conducted on a modern 1500ccm diesel-engine test-bench. This test-bench is comprised of the engine, an EGR valve, and a turbocharger. The engine was mounted on test-bench dynamometer equipment. This dynamometer controls the engine speed and provides measurements of engine torque and output power. The flow characteristics of both of these systems are presented in Chapter 2. For all measurements, the data which should be recorded and stored are presented in Section 4.3 (Table 4-3), and a legend for the measurement equipment and sensor positions on the engine is given in Table 4-2. The general engine test-bench setup and the system connection for data collection used in this study are shown in figures 3.6 and 3.7. The test-bench experiment setup is discussed in more detail in Section 4.3.

On the test-bench, the measurement system, produced by ETAS, is used to record engine test data and to monitor relevant engine parameters while the engine is running. The operator laptop is equipped with a data-processing card that allows for communication with the engine ECU. Communication is conducted via the CAN calibration protocol network. INCA provides a software interface for the engine operation. This allows the engine operator to adjust parameters such as throttle position and fuel-injection timing. Additional experimental sensors can be read from the laptop with custom INCA-MCE modules. The experimental data is generated on the test-bench under given conditions by using experiments. To this end, engine testing is kept to a minimum and complex interactions are visually realised to better understand the engine system. The collected data is used to analyse the engine performance, to conduct model validation and to generate the simulation platform. On the simulation platform, various simulations in Matlab/Simulink have been conducted. In the simulation experiments, we are interested in the steady-state and dynamical behaviour of the engine system. In the steady-state experiments, the controller performance under different load disturbances is an important criterion. In this case, the default input profile is defined for a particular time period. The load change request ranges from 900 to 3200 rpm, and fuel injection ranges from 13 to 27 mg/cyc under normal operation conditions. The time between the set-point changes is set to 15s to ensure that the air-path system studies the steady-state. In recent decades, dynamic driving cycles have evolved into a standard tool for various vehicle-testing purposes. The most prominent involves fuel consumption and emissions measurement, in which dynamic driving cycles like the FTP-75, which is developed by California’s Air Resources Board, have found wide usage (California Environmental Protection Agency, 2015). The FTP-75 driving cycle is one of the most commonly used dynamic driving cycles for fuel consumption and emissions tests. For this reason, in dynamical-simulation experiments, the FTP-75 driving cycle is used to validate controller performance. More details about the FTP-75 driving cycle can be found in Section 4.3.2.2. The transient behaviour is recorded during the simulation in Matlab/Simlink and compared with different configurations of air-path controllers. To show the significance and advantage of NMPC approaches, details of the developed NMPC engine-air-path controllers are presented within the simulation platforms in Chapter 5.

3.7 Methods for Data Analysis

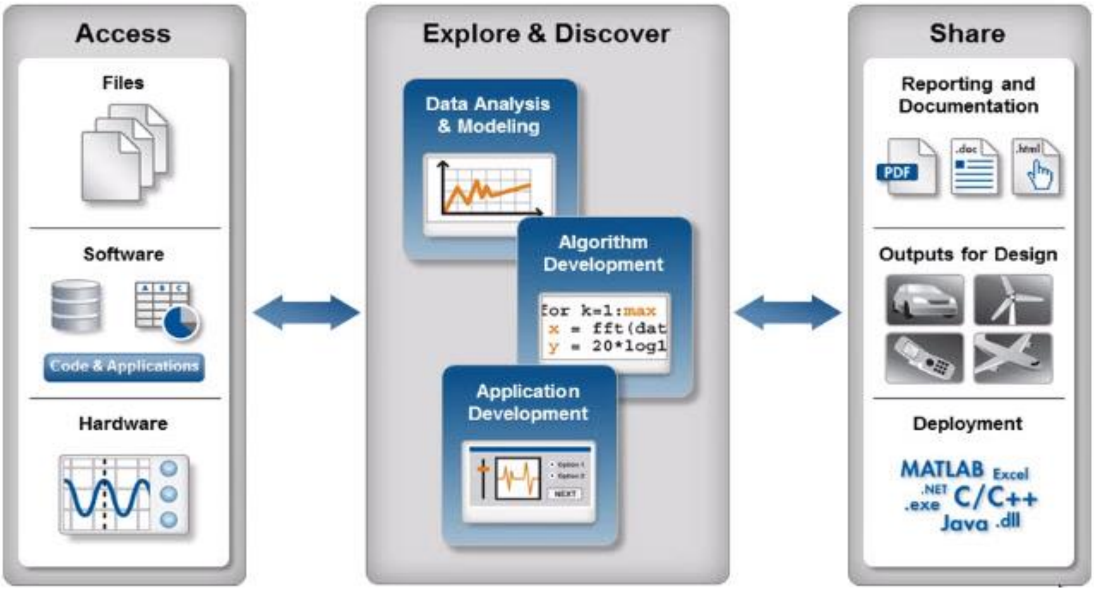

Figure 3.8: Steps of data analysis (MathWorks, 2018)

The data analysis in this study comprises three steps, as displayed in Figure 3.8. The first step is to access the data and import it into the analysis platform. This data might be stored in a specific format, such as in Excel, text or CSV files. It may have to be retrieved from a database or be directly streamed from instruments. Once the data is imported into the analysis platform, extensive statistical analysis, algorithm development work and visualisation are performed. Finally, the results and analysis are shared in a report and are available for further development. In this study, statistical and curve-fitting functions from MATLAB and Simulink are used for data analysis.

With the support of functions of mathematical analysis in Matlab/Simulink, the graphical and mathematical representation of data collected from qualitative and quantitative approaches and the characteristic value of the design performance is given. The following three mathematical methods are used to analyse the data in this study.

Scatter Diagrams

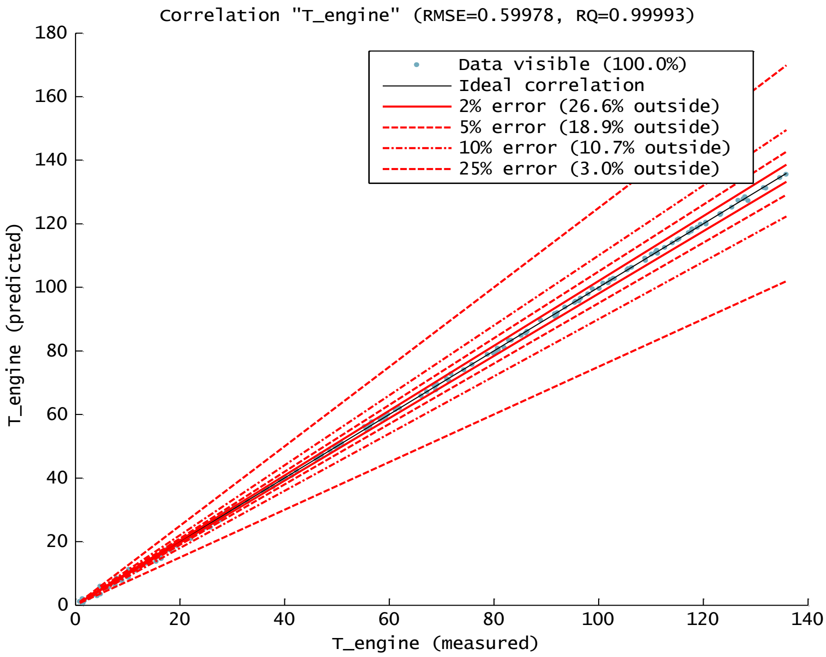

Figure 3.9: Scatter diagram

The scatter diagram (Figure 3.9) is used to deduce regularities and relations from the basic data to prove unclarities about potential causes of a problem by experiments. The scatter diagram is very helpful if both the influence quantities and the describable quantities of the problem are measurable. It is usually an X-Y diagram with the influence quantity on the abscise and the quantity of the problem on the ordinate.

Root mean-square error (RMSE) is regularly employed in model-validation studies. It is suggested in (Willmott & Matsuura, 2005) that RMSE is a good indicator of average model performance. The RMSE describes the variance to be expected (standard deviation) from the model, and it measures the difference between the estimates $\hat{y}(i)$ and the realised actual observations $y(i)$. The RMSE is defined by the following equation (Chai & Draxler, 2014):

$$RMSE = \sqrt{\frac{1}{n}\sum_{i=1}^{n}(y(i) - \hat{y}(i))^2} \;, \tag{3-1}$$

where y denotes the measurement, $\hat{y}$ is the model output and n is the number of data samples.

The determination of coefficient RQ is defined by the following equation:

$$RQ = \frac{\sum_{i=1}^{n}(\hat{y}(i)-\overline{\hat{y}(i)})^2}{\sum_{i=1}^{n}(y(i)-\bar{y}(i))^2} \quad , \tag{3-2}$$

where $\bar{y}$ is the mean value and n is the number of data samples. RQ is a relative measure for evaluating the model error; it indicates which portion of the total variance of the measuring data is described by the model. Chai and Draxler (2014) note that the RQ measure results in the following evaluations: If 0 < RQ < 0.5, the model is not suitable for reliable predictions; if 0.6 < RQ < 0.8, the model is suitable for qualitative predictions; if 0.9 < RQ < 1, the model is very good and is therefore suitable for quantitative predictions.

Control Chart (Chai & Draxler, 2014)

The control chart is used to observe processes and to recognise problems of a process punctual. Spot-checks are made at a per-defined interval, and statistical parameters are registered in the control chart (Figure 3.10).

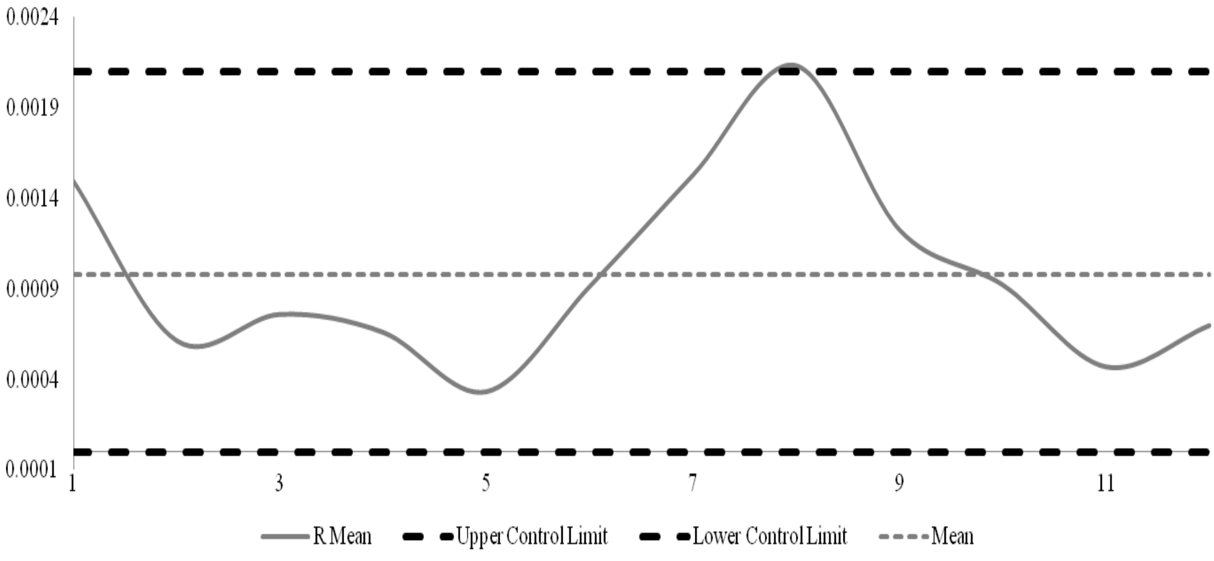

Figure 3.10: Control chart

The standard deviation is explained in the following equation:

$$s = \sqrt{\frac{\frac{1}{n}\sum_{i=1}^{n}(x(i)-\bar{x})^2}{n-1}} \ , \tag{3-3}$$

where x denotes the measurement and $\bar{x}$ is the mean value of the measurement. Furthermore, the upper control limit and lower control limit are defined as follows:

$$X_{upper} = \bar{x} + 3s , \tag{3-4}$$

$$X_{Lower} = \bar{x} - 3s . \tag{3-5}$$

Variance Accounted For (VAF) Value (Chai & Draxler, 2014)

The variance-accounted-for (VAF) value has been widely used as a validation method for system identification. As mentioned in (Wei, 2006; Wang, Waschl, Alberer, & Del Re, 2012; Wang, Zhang, & Bechkoum, 2019), the VAF is useful to apply a benchmark criterion for the comparison of the simulation model output and the measurement from test-bench. In a typically quantitative data analysis, the qualities of the output signals generated by the model are measured by using the VAF, which is calculated using Equation (3-6):

$$VAF = max\left\{1 - \frac{var(y_k - \widehat{y_k})}{var(y_k)}\right\} \times 100\% , \tag{3-6}$$

where y_k denotes the accompanying output of the validation data set, and $\widehat{y_k}$ is the estimated output of the estimated model for the validation data. The $var(.)$ denotes the variance of a quasi-stationary signal. The result provides a percentage between 0% and 100%. The closer the value is to 100%, the better the model coincides with the measurements. Chai and Draxler (2014) claim that if 0 < *VAF* < 40%, the model is not suitable for reliable predictions; if 40% < *VAF* < 70%, the model is suitable for qualitative predictions; if 70% < *VAF* < 100%, the model is very good and is therefore suitable for quantitative predictions.

3.8 Ethical Issue

Research ethics educates and monitors scientists' research to ensure that high ethical standards are maintained. In this section, the specific ethical issues of this study are identified. According to (Minnesota, 2003), a researcher should be able to view himself or herself as a member of a university community and promote critical thinking and the prerequisites for research. I conduct this research in the context of diesel engine-air-path control under the guidance provided by the *Handbook of Principles and Procedures* from the University of Gloucestershire (Research Committe, 2008). There are legal requirements for confidentiality (data protection acts, freedom of information, human rights). Under the requirements of the Data-Protection Act (Research Committe, 2008), I have signed a confidentiality agreement. I shall neither disclose to any third party nor use for other purposes any information that the research project has designated to be "confidential." This applies to the confidential information of any other person, company or community. Confidential information includes personal researcher information, engine- and part-supplier information, company financial information and strategies, marketing information, and research and development activities. All confidential information shall be disposed of in a secure manner by using shredders at a secure document destruction facility or other means to ensure that the study’s confidential information cannot be discovered. Furthermore, the specific guidance in (Research Committe, 2008) concerning how to maintain the anonymity of qualitative and quantitative data will be followed. For confidential reasons, all the commercially sensitive and identifiable information from engine and part suppliers will be kept at a reasonable level of anonymisation. I will always check to see if there is another way of gathering the data that takes particular care in research with fabrication, falsification and plagiarism.

Chapter 4. SIMULATION MODEL FOR ENGINE-AIR-PATH

4.1 Introduction

Technological developments in the automotive industry are increasingly driven by a decrease in fuel consumption and a drastic reduction in emissions. This context has led to the emergence of complex technologies while making development cycles shorter and shorter. For example, the engines are being built from increasingly advanced technologies, and mechanical, electronic, and control systems are growing in number and becoming more complex. The model-based approach provides an accurate representation of complex systems in the virtual world throughout the whole product-development process – starting from development, pre-design and testing. It also facilitates the structured data management of simulation results and the use of measurement as a basis for the verification and validation of controller design of mechatronic systems. As discussed in Section 3.3, model-based design is a prominent trend for improving product development efficiency, see (Aarenstrup, 2015; Bodenstein, Lohse, & Zimmermann, 2010; Ferrari, Fantechi, Gnesi, & Magnani, 2013). Therefore, to analyse the engine-air-path system and evaluate the benefits of the new engine-air-path control method with respect to emissions and fuel consumption, a digital model of the diesel engine-air-path is developed in a Matlab/Simulink simulation platform. The different components of the engine-air-path—manifolds, turbocharger, and EGR—are modelled in the Matlab/Simulink with the help of one-dimensional gas dynamics to represent the flow and heat transfer of the engine. The emissions and torque are modelled thanks to an existing, non-linear regression approach. The data used in the simulation platform is based on geometrical parameters of engine sub-systems, measurement, and manufacture specifications. This simulation model would allow us to virtually study the behaviour of the engine-air-path system and would support the development of engine-control algorithms and the model-based optimisation task.

To present this approach, this chapter is organised as follows: A description of the reason for a model-based test for engine-air-path control is given in Section 4.2. The experimental set-up and design are described in Section 4.3. Next, in Section 4.4, the physical dynamic of each part of the engine-air-path is studied and modelled. Finally, in Section 4.5, the results of the simulation are discussed, and a validation phase is performed to compare the models with measurements.

4.2 Model-based Testing: Why, What, How

Two different testing methods (physical-experiment and model-based) can be used for engine-air-path control. Kiencke and Nielsen (2005) introduce classical development steps of engine design, starting with basic engine design, through the measurement and control optimisation, and on to the emission tests at the engine test-bench. However, because of the high number of interacting control functions from different vehicle domains, the testing of engine control systems at the engine test-bench has become a challenge. Functional engine testing is seen as a part of the optimisation, validation and verification phases at the end of the V-development process, and it is mainly facilitated by use of measuring and testing tools. Errors in software functions found during the engine testing phase have caused major time delays. This pushes up testing effort and expenses for equipment in terms of test engines.

For these reasons, the air-path control testing work is shifted towards the earlier stages of the development in this study. The requirements are tested via models in virtual environments, initial control function testing begins during function design, and pre-calibration is done at the same time as the integration of the optimisation function of emission and fuel consumption. The methods such as design of experiments (DOE), data-based modelling, and automated calibration are used to support the controller design during development process.

Compared with the real test-bench, the engine simulator as a virtual test-bench has several advantages: 1) It offers efficient support for the EGR and VGT system behaviour understanding via computer simulation; 2) it reduces controller development and calibration development time and risk, as the testing on the virtual test-bench can be done long before real hardware is available; 3) it is possible to perform wide range and large number of tests, including some test that cannot be run at the real test-bench without cost-intensive field tests.

However, even with the potential benefits of using model-based testing, we should often consider the risks of the accuracy of the models. It should always be remembered that the simulation models are here to represent some reality, and these models can be used in the model-based testing only if they show compliance with the represented reality. Therefore, in this study, the virtual test-bench model needs to be verified and validated for each context. For this purpose, the model has to be critically evaluated by simulation. The accuracy of this model needs to be assessed in comparison to the experimental data registered, both in the stationary test and in the dynamic test. Please refer to Section 4.5 for the details of the validation of the engine-air-path model.

4.3 Experiments

The information provided by engine manufacturers is usually given in the form of steady-state maps and curves. This information typically lacks some of the required details to compute behaviour in engine operation conditions which are far from steady-state. Therefore, different measurements are needed during the experiments if detailed information is acquired regarding the different engine subsystems that confirm a high-quality and comprehensive engine model. The experiments reported in this work focus on the thermodynamic characterisation of engines; they involve measuring the temperature and pressure of the different parts of the engine and engine performance and emissions under different operations.

This section provides a review of the engine test-bench facility, including a review of engine configuration, sensor positions and experimental plan.

4.3.1 Engine Test-bench Setup

The test engine is a modern, four-stroke, three-cylinder, 1.5 litre diesel engine equipped with a common-rail injection system, EGR and VGT. Detailed technical specifications for this engine are listed in Table 4-1.

Table 4-1: Specification of the engine

Name	Data
Fuel Type	Diesel
Displacement	1500 ccm
Number of Cylinder	3
Maximum Torque	295 Nm
Maximum Power	80 kW

As shown in Figure 3.6, the engine is mounted on test-bench dynamometer equipment. This dynamometer controls the engine speed and provides measurements of engine torque and output power.

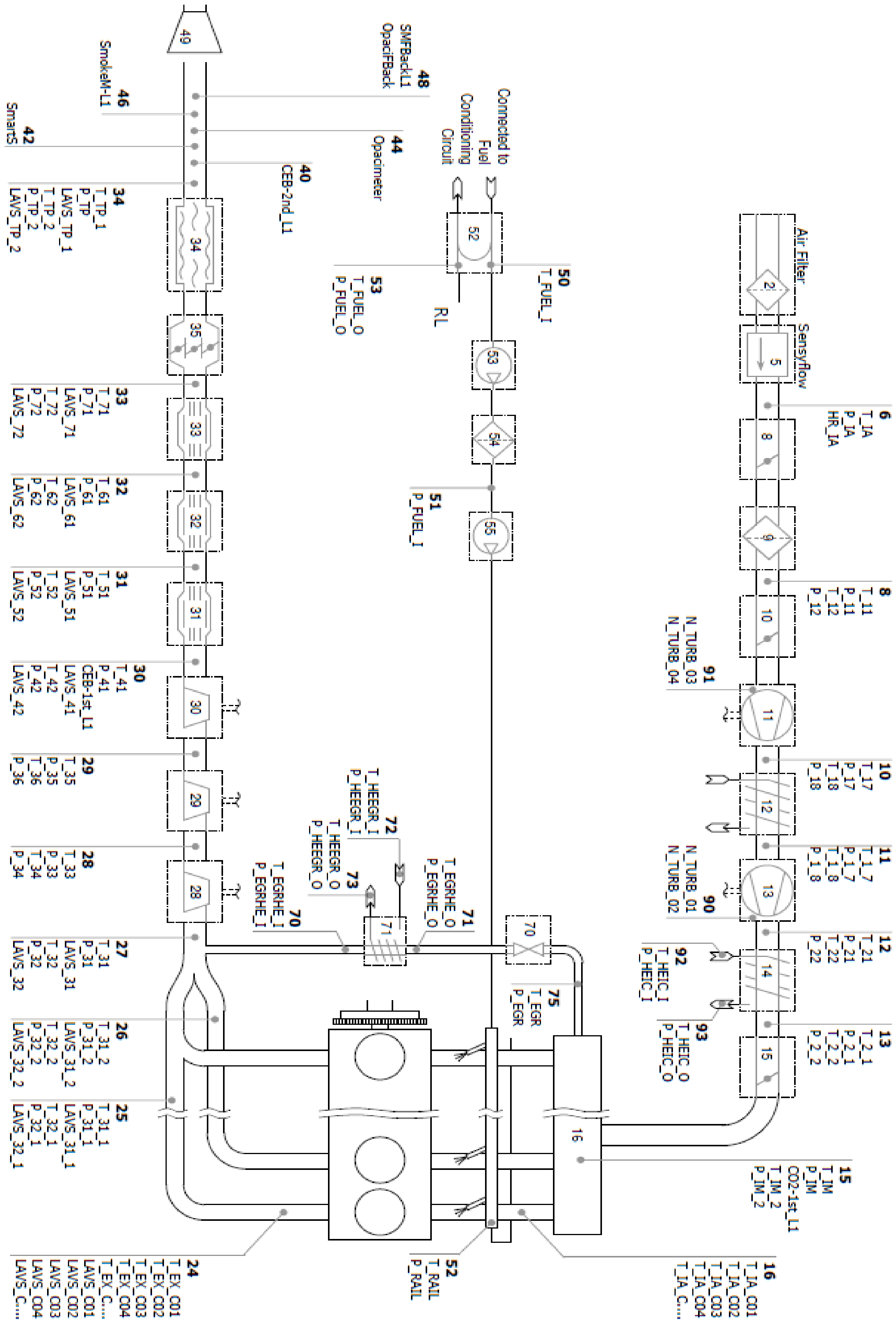

Figure 4.1: Standard sensor location (AVL List GmbH, 2014)

Figure 4.1 shows a general schematic representation of the engine test-bench which focuses on the sensor positions. In this test-bench, temperatures and pressure sensors are installed on the inlet and the outlet pipes of the engine according to (Kiencke & Nielsen, 2005). An optical speed sensor is located on the turbocharger housing to measure the turbo speed. Inlet mass-flow rate is measured by a mass air-flow sensor upstream of the compressor.

Two five-gas analyser systems determine the exhaust gas composition. Both are Horiba systems. The first is a MEXA-9100-analyser system which uses un-heated sample lines; the second is a 9130 system with a heated sample line. Both of them are used to measure HC, THC, NOx concentrations to within +- 1% Full Scale (FS) accuracy. FC accuracy is represented with respect to the full-scale variation of the instrument. Thus, *+- 1% FS* means that the value of any reading of this measurement may be off by 1% in either direction. The second system is used in general four-stroke engine development where HC concentrations are more than 15000 ppm. The 9100 system is used for engine emissions development, with un-heated lines going from each test cell to the analyser and a water trap prior to the analyser bench. The emissions method used for both analysers involves the use of flame ionisation detectors (FID) for THC, non-dispersive infra-red (NDIR) for CO and CO_2, and chemiluminescence for NOx. For transient NOx investigation, a fast-response gas analyser (CLD500 from CAMBUSTION) is applied (CAMBUSTION, 2018) to measure the transient NOx concentrations. This equipment has a specified accuracy of +-1% FS. When rapid transients occur, the fast NOx analyser can capture the fast-dynamic nature of the engine's emissions.

In addition, two measurement systems are used to measure the concentration of particle matter from the engine. Both are produced from AVL. The first is an AVL smoke meter sensor for steady-state operation. It measures the reflection of visible light from a soot loaded filter surface. Its measurement accuracy is +-1% FS. The exhaust gas will be directed through a measuring chamber and draw is through a clean filter paper. The filtered "soot" caused blackening of the filter paper which is detected by an optical measuring head (see Figure 4.2 a).

A good correlation is achievable between the blackening grade and the concentration of particle matter is achievable if particle losses are taken into account (AVL List GmbH, 2014). The second system is an AVL opacimeter senor is used to determine the continuous smoke (particle matter) concentration in the raw exhaust gas from the diesel combustion engines. This sensor operates based on the optical measurement principle (AVL List GmbH, 2008). The accuracy and reproducibility of this equipment are based on its initial system calibration. In the exhaust pipe, the loss of light intensity between a light source and a reference light is measured (see Figure 4.2 b), and the opacity of the exhaust gas is calculated from the difference of the light intensity based on the Beer-Lambert law (Miller, Vandome, & McBrewster, 2009).

a) AVL Smoke Meter

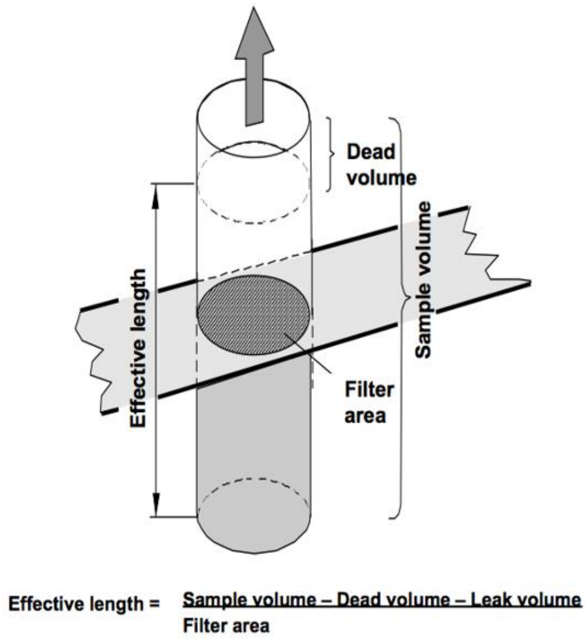

b) AVL Opacimeter

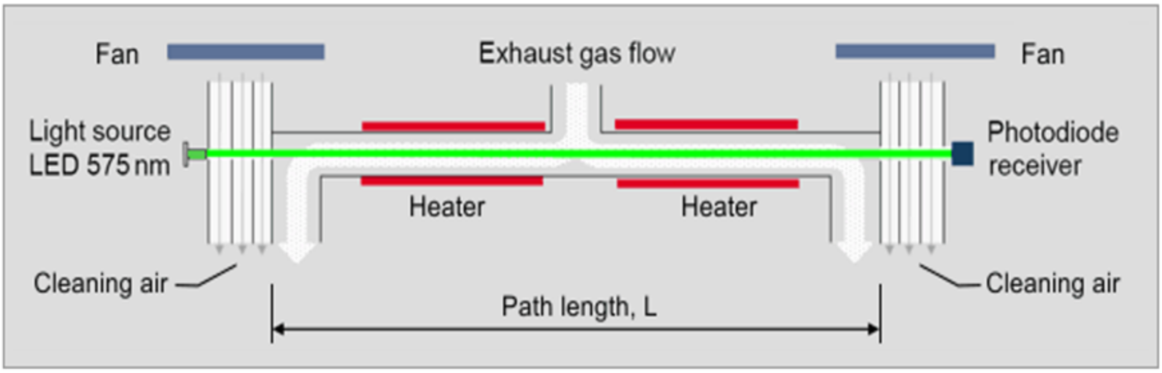

Figure 4.2: PM measurement principle a) AVL smoke meter (AVL List GmbH, 2014); b) AVL opacimeter (AVL List GmbH, 2008)

Table 4-2: Legend of sensor positions

Part Intake Air Treatment	**Part Engine Intake Air**
1 Heat Exchanger Intake Air	9 Air Filter
2 Air Filter	10 Throttle upstream Compressor
3 Volume Flow Measurement Device	11 Additional Compressor
4 Vessel	12 Additional Intercooler
5 Mass Flow Measurement Device	13 Main Compressor
6 Fan	14 Main Intercooler
7 Air Funnel	15 Thottle downstream Compressor
8 Intake Air Pressure Regulation Flap	16 Intake Manifold
Part Exhaust	**Part Fuel Supply**
28 Main Turbine	52 Bypass
29 Additional Turbine	53 Fuel Supply Pump
30 Additional Turbine	54 Fuel Filter
31 First-Aftertreatment System (e.g. Pre-Catalyst)	55 Injection Pump or High Pressure Fuel Supply Pump
32 Second-Aftertreatment System (e.g. Main Catalyst)	
33 Third-Aftertreatment System (e.g. DPF)	**Part Exhaust Gas Recirculation**
34 Muffler	70 EGR-Valve
35 Exhaust Backpressure Regulation Flap	71 EGR-Cooler
49 Test-bench Exhaust System	

Table 4-3: Channel of measurement

Name	**Unit**	**Name**	**Unit**
engine speed	[rpm]	EGR position	[%]
engine torque	[Nm]	NOx emission	[ppm]
pedal	[%]	Opacity (OPAC, particle matter) emission	[%]
throttle	[%]	P_11 (pressure after air cleaner)	[hPa]
mass flow air	[kg/h]	P_21 (pressure after compressor)	[hPa]
mass flow fuel	[kg/h]	P_2_1 (pressure after inter cooler)	[hPa]
intake pressure	[hPa]	P_IM (pressure before cylinder)	[hPa]
intake temperature	[°C]	P_31 (pressure after cylinder)	[hPa]
exhaust pressure	[hPa]	P_41 (pressure after turbine)	[hPa]
lambda exhaust	[-]	P_51 (pressure after catalyst)	[hPa]
coolant temperature	[°C]	T_11 (temperature after air cleaner)	[°C]
oil temperature	[°C]	T_21 (temperature after compressor)	[°C]
ambient pressure	[hPa]	T_2_1 (temperature after inter cooler)	[°C]
ambient temperature	[°C]	T_IM (temperature cylinder)	[°C]
Particle matter emission	[g/kwh]	T_31 (temperature cylinder)	[°C]
turbo charger speed	[rpm]	T_41 (temperature after turbine)	[°C]
VGT position	[%]	T_51 (temperature after catalyst)	[°C]

A legend for the sensor positions on the engine is listed in Table 4-2. As described in Section 3.6.2, for modern controlled test-benches, a fully automated test run is available which generates all necessary data in a fully automated way.

An automatic ETAS data acquisition and processing system is established in the engine test-bench to measure engine parameters. The engine operation conditions (speeds, loads and EGR and VGT openings) are controlled by test-bench operation software, which is connected to the engine ECU. For all measurements, the data in Table 4-3 should be recorded and stored.

4.3.2 Measurement Plan

4.3.2.1 Stationary Cycle

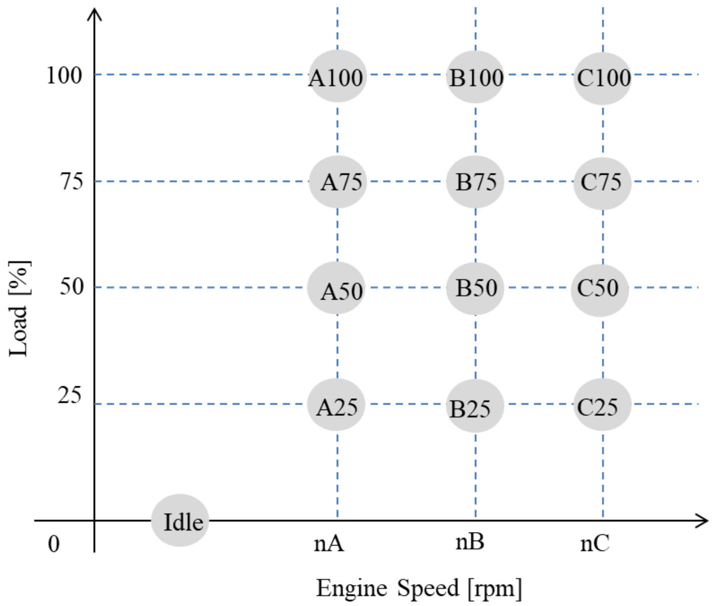

Figure 4.3: European stationary cycle (ESC)

One of the focuses of this study is the optimisation of diesel-engine emissions performance. According to the (Martyr & Plint, 2011), the European stationary cycle (ESC) is introduced as one of the standard methods for emission measurement from diesel engines. In this test, the engine is tested on an engine dynamometer over a sequence of 13 steady-state modes (Table 4-4, Figure 4.3). The details of the test-bench setup are described in Section 4.3.1. During a prescribed cycle of warmed-up engine-operating conditions, the engine must be operated for the prescribed time in each mode, completing engine-speed and load changes in the first 20 seconds. The main variables of the test procedure are engine speed and engine load. The variation of the defined speed must be held to within ±50 rpm, and the defined load must be held to within ±2%. As mentioned in Section 4.3.1, NO_x, HC, CO and CO_2 emissions are all measured by a Horiba emission-measurement system, and the particulate-matter emissions are sampled by the AVL smoke meter in the raw exhaust gas. The test conditions and test results are as shown in Table 4-4. The duration of each test mode is two minutes. The A25 means that the engine operates at 25% of the full load torque with engine speed $n_A = 2000\,rpm$. Engines running in idle do not have output power; therefore, the torque and BSFC value in this state are empty. The weight values of NO_x and PM are specific ESC weighting factors for emission calculation.

Table 4-4: ESC measurement on test-bench

Nr.	Point	Torque	Speed	Power	Weighting	BSFC	NOx	PM
-	-	[Nm]	[rpm]	[kW]	-	[g/kWh]	[g/kg]	[mg/kg]
0	Idle	Idle	Idle	Idle	0.15	177.57	0.25	2.78
1	A25	74	2000	15	0.05	280.37	0.22	6.92
2	A50	148	2000	30	0.05	218.69	0.35	7.28
3	A75	221	2000	46	0.05	195.33	0.43	9.00
4	A100	295	2000	61	0.08	187.85	0.64	6.42
5	B25	71	2500	18	0.10	281.31	0.23	6.30
6	B50	142	2500	36	0.10	221.50	0.35	7.11
7	B75	208	2500	53	0.10	200.93	0.36	9.25
8	B100	278	2500	70	0.09	190.65	0.60	6.64
9	C25	64	3000	19	0.05	301.87	0.23	9.16
10	C50	127	3000	38	0.05	247.66	0.30	6.77
11	C75	193	3000	58	0.05	232.71	0.46	7.07
12	C100	256	3000	77	0.08	217.76	0.63	7.86
Weighted Value of ESC	-	-	-	-	-	Weighted	Weighted	Weighted
	-	-	-	-	-	g/kWh	g/kWh	g/kWh
	-	-	-	-	-	220.45	3.09	0.051

The NO_x and PM are measured for each mode and averaged over the cycle by using a set of weighting factors. Martyr and Plint (2011) recommend that the measurement begins with the lowest possible speed and that load is increased for the first speed step. By going to the next speed step, the maximum load is continued, and the load points for the second speed step are measured in descending order. At the third speed step, this procedure starts once again until the maximal speed is reached. The test plan is shown in Figure 4.3. Select 12 operating points with loads of 25%, 50%, 75% and 100% at speeds of A, B and C to form the test points. The engine speed and operating points are obtained from the engine specification and are defined as follows:

1) $n_{reference}$ = 3750 rpm is engine speed at maximal engine power,
2) n_{high} = 3500 rpm is engine speed at 70% of maximal engine power,
3) n_{low} = 1500 rpm is engine speed at 50% of maximal engine power,
4) $n_A = n_{low} + 25\% \cdot (n_{high} - n_{low}) = 2000\ rpm$,
5) $n_B = n_{low} + 50\% \cdot (n_{high} - n_{low}) = 2500\ rpm$, and
6) $n_C = n_{low} + 75\% \cdot (n_{high} - n_{low}) = 3000\ rpm$.

4.3.2.2 FTP-75 Driving Cycle

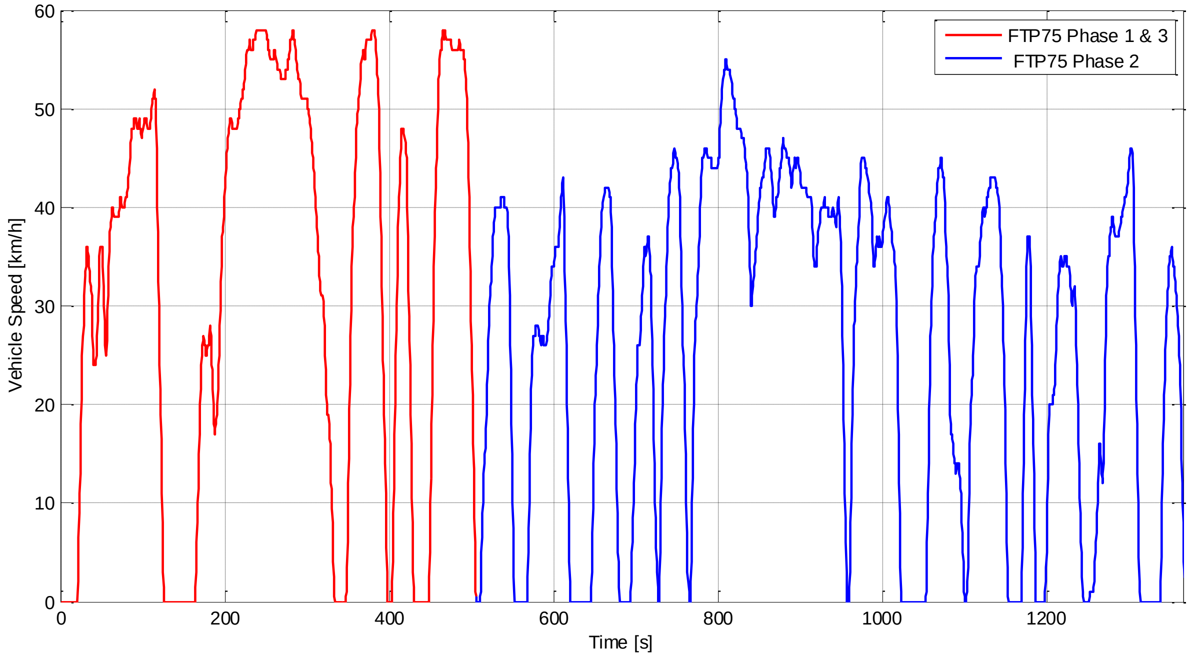

Figure 4.4: FTP-75 driving cycle speed profile

To model and validate the engine-air-path, measurements must be made of a standard dynamical driving cycle. As a baseline for engine fuel economy and emissions tests, an exactly defined driving cycle is needed. In general, the FTP-75 cycle can be used for this purpose (Martyr & Plint, 2011). It truly reflects the real driving condition of a passenger vehicle at high speed and acceleration. The FTP-75 is a driving cycle developed by workgroups of the United Nations with the intention to provide a harmonised test procedure for the development and testing of passenger vehicles in the United States with respect to fuel consumption and emissions. The driving cycle consists of the following segments: cold-start phase 0~505 seconds, stabilised phase 506~1372 seconds, and hot-start phase 1373~1870 seconds (a repeat of the first phase). Figure 4.4 presents the vehicle speed profile.

4.4 Engine-air-path Model

This section explains the mean-value modelling approach to engine-air-path modelling. One large issue in engine simulation is its complexity. For model-based control design it is important that the simulation model is able to capture all essential dynamic properties meanwhile keeps simple model structure since low order models are preferable (Bengtsson, 2007). Therefore, it is important to determine what is necessary to consider and what can be neglected because its influence on the main results vanishes. There is always a trade-off between model complexity, precision and computing time as we try to reflect reality as precisely as possible but need to do the simulation in finite time.

Two methods are often used to obtain models of diesel engine-air-path: CFD modelling and mean-value modelling. The CFD modelling, which is based on multidimensional computational fluid dynamics, has attractive intuitive component-based features. The CFD models are commonly used in thermodynamic analysis, examples of which can be found in several sources (Bengtsson, 2007; Gundmalm, 2009; Meeks, 2014). But they are too computationally expensive to serve the purpose of model-based control and the application in real-time control. Whereas the mean-value model is based on the ideal gas law, use of the law of conservation of mass and conservation of energy has proved to be a very effective modelling approach for design of control. For example, a mean-value model can accurately describe the behaviour of the engine-air-path, the cylinder pressure for the gas exchange and the engine consumption (Andersson, 2012; Dekker & Sturm, 1996; Dekker & Sturm, 1996; Mitterer & Zuber-Goos, 2002). Therefore, a mean-value model is employed in this study.

Matlab/Simulink is scientific computing software from MathWorks Inc. It is widely used in controller design, multi-domain simulations and model-based design. Please refer to (MathWorks, 2018) for the details of the Matlab/Simulink. In this study, Matlab/Simulink is used as a software tool for the modelling and simulation of the engine air-path system. The engine-air-path model uses one-dimensional gas dynamics to represent the flow and heat transfer in the components of the engine model. As a language of technical computing, Matlab is further used for the processing of data. For example, it is used to provide characteristic maps and curves and for the initialisation of constants and variables, and it is also used for the analysis and processing of simulation results. The basic structure of mathematical models for the stationary and dynamic behaviour of the engine-air-path can be gained from physical laws via the ideal-gas, energy-conservation and mass-conservation laws. However, modelling the details of torque and the development of the emissions is currently not usually possible with theoretical models. In addition, many parameters are not precisely known. It is widely accepted that data-based system identification has proven to be a very effective modelling method for such systems (Bamieh & Giarre, 2002; Hirsch, 2011; Kamaruddin & Darus, 2012). Therefore, data-based modelling of engine torque and emissions (by applying system identification methods) is required. To present this modelling approach, this engine-air-path simulation model is divided into different parts—intake and exhaust manifolds, turbocharger, EGR, emissions, oxygen concentration and torque—as shown in Figure 4.5.

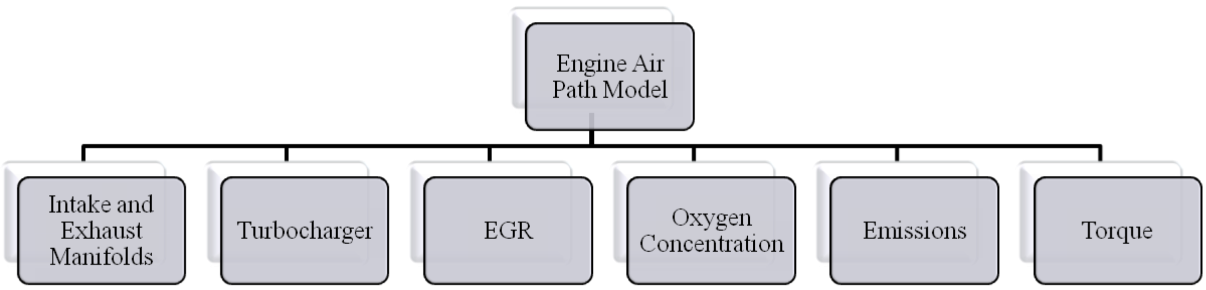

Figure 4.5: Engine-air-path model structure

Figure 4.6 illustrates the top level of the whole simulation model as it can be seen in Simulink. The inside of the model is displayed in Figure 4.7. The data required by the four sub-models in Figure 4.7 are either parameters whose values are kept constant throughout the simulation or inputs whose values change in time. The more detailed the model, the higher the number of parameters and inputs required. The engine air-path model requires four inputs, 37 parameters and 28 maps. Some parameters can be found in the engine-and-supplier technical document provided by the manufacturer; others must either be determined experimentally, as described in Section 4.3, or default values must be assumed.

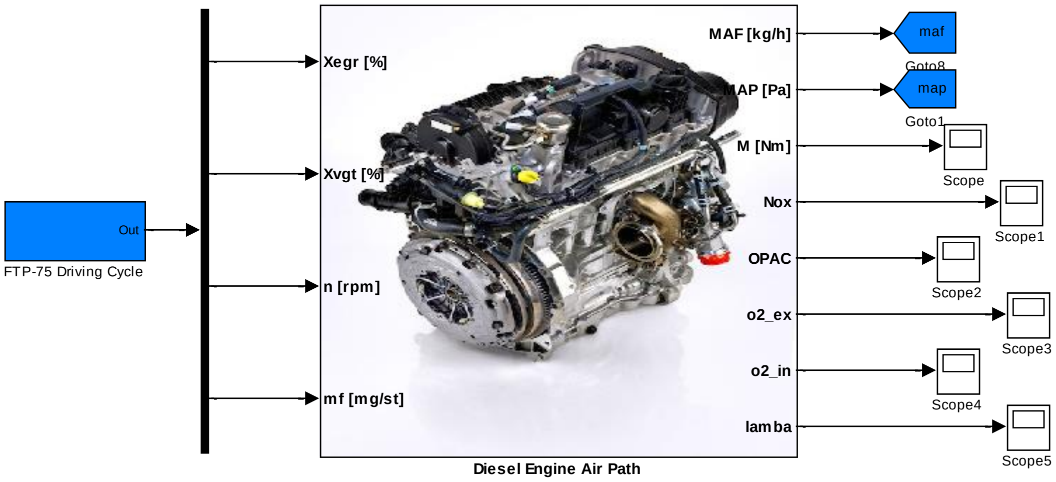

Figure 4.6: Simulink engine-air-path model top level

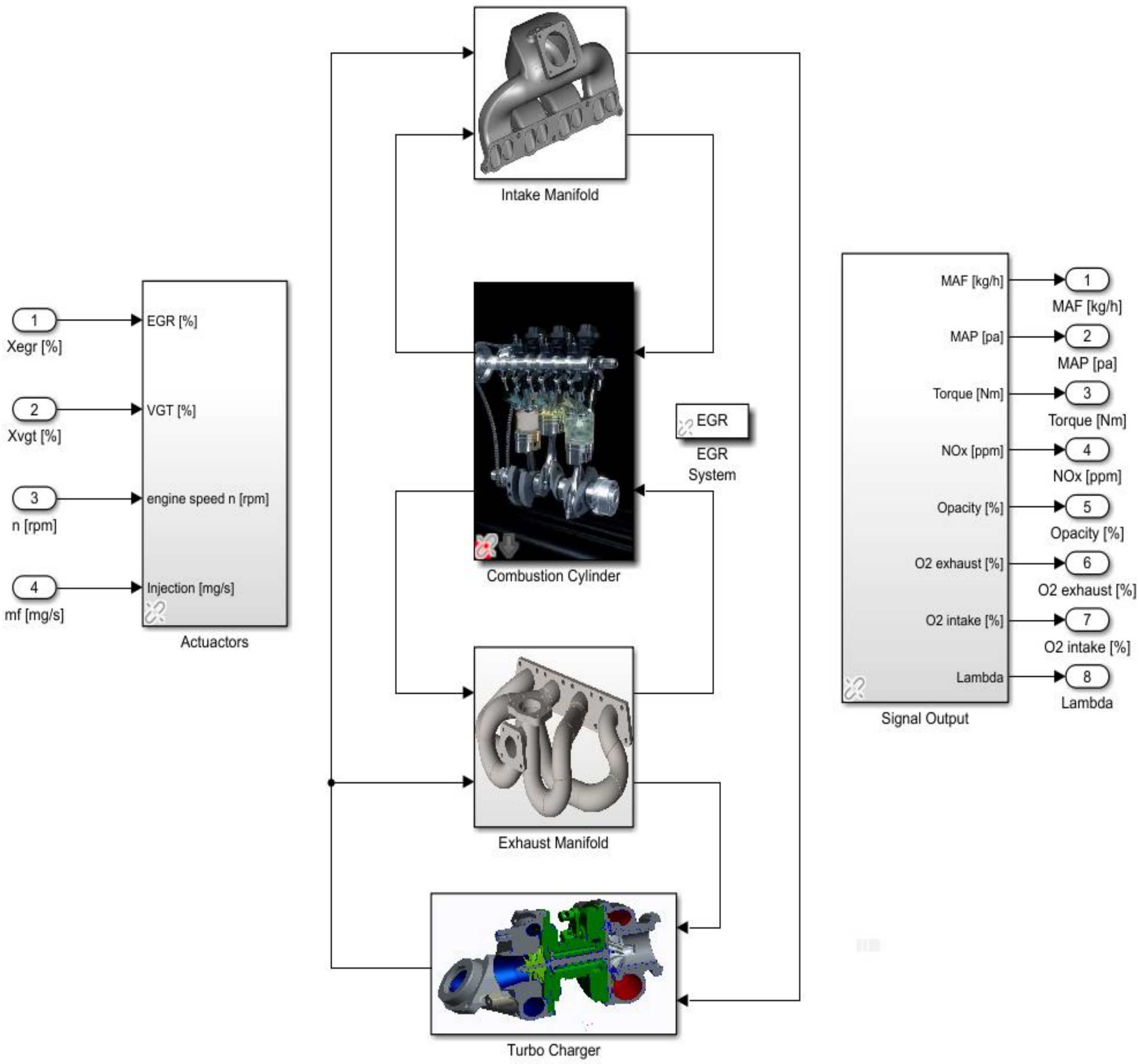

Figure 4.7: Engine-air-path model inside

Usually the standard approach to the physical modelling of the engine-air-path is to consider all the components as comprising an ideal open thermodynamic system; the air and fuel are assumed to be perfectly compressible (Eriksson, 2002). Some of the essential thermodynamic characteristics of the combustion engine must be determined for the engine-air-path modelling. Hereby, the ideal gas law, the law of conservation of mass and the law of conservation of energy can be applied.

Theorem: *Ideal gas law* (Bennett, 2014).
The ideal gas law is often written as follows:

$$p \cdot V = m \cdot R \cdot T \tag{4-1}$$

or

$$T = \frac{p \cdot V}{m \cdot R}\,, \tag{4-2}$$

where (1) p is the pressure of the gas,

(2) V is the volume of the gas,

(3) m is the amount of substance of the gas,

(4) $R = 287\,\frac{\mathrm{J}}{kg \cdot K}$ is ideal specific gas constant for air (De, Agarwal, Chaudhuri, & Sen, 2018), and

(5) T is the temperature of the gas.

Theorem: *Law of conservation of mass* (Bennett, 2014).
The mass of an object or collection of objects never changes, no matter how the constituent parts rearrange themselves.

According to the law of conservation of mass, in the engine inlet and exhaust manifold, the rate of the change of the air mass inside the volume is given by the difference between the mass flow in and out. Differential equations 4-3 and 4-4 represent the change of air flow masses in the engine manifolds:

$$\dot{m}_\imath = W_{ci} + W_{xi} - W_{ie}\,, \tag{4-3}$$

$$\dot{m}_x = W_{ex} - W_{xi} - W_{xt}\,, \tag{4-4}$$

where (1) $W\,(.)$ is the mass flow,

(2) i is index for parameters in intake manifold,

(3) ci is index for parameters in intake path after compressor,

(4) xi is index for parameters in intake path after EGR,

(5) ie is index for parameters in cylinder,

(6) x is index for parameters in exhaust manifold,

(7) ex is index for parameters in exhaust path after cylinder, and

(8) xt is index for parameters in exhaust path after turbine.

Theorem: *First law of the thermodynamics* (Guzzella & Onder, 2004).
In a closed thermodynamic system, the first law of the thermodynamics can be written as follows:

$$dU = \delta Q - \delta W, \tag{4-5}$$

where (1) dU is the change in internal energy,

(2) δQ is the heat supplied to the system from its surroundings, and

(3) δW is the total work done by the system.

Based on the law of conservation of energy, for ideal gases with constant volume, the general expression for the time differential of internal energy $U = c_v \cdot T \cdot m$ is given by (Song, 2015),

$$\frac{d}{dt}U = c_v \cdot \dot{T} \cdot m + c_v \cdot T \cdot \dot{m}, \tag{4-6}$$

where (1) U is the internal energy,

(2) $c_v = 725 \frac{\mathrm{J}}{kg \cdot K}$ is specific heat at constant volume, and

(3) T is the temperature.

For ideal gases with constant pressure, the general expression for the time differential of the enthalpy $H = c_p \cdot T \cdot m$ is given by (Song, 2015),

$$\frac{d}{dt}H = c_p \cdot T \cdot \dot{m}, \tag{4-7}$$

where (1) H is the enthalpy, and

(2) $c_p = 1014 \frac{J}{kg \cdot K}$ is specific heat at constant pressure.

In Figure 4.7, the Simulink model structure is displayed. The figure shows how the engine is divided into subsystems to facilitate physical modelling. They are the intake and exhaust manifolds, turbocharger, EGR, emissions, oxygen concentration and torque. Descriptions of the modelling of each component are given in the following sub-sections: 4.4.1 to 4.4.6.

4.4.1 Intake and Exhaust Manifolds

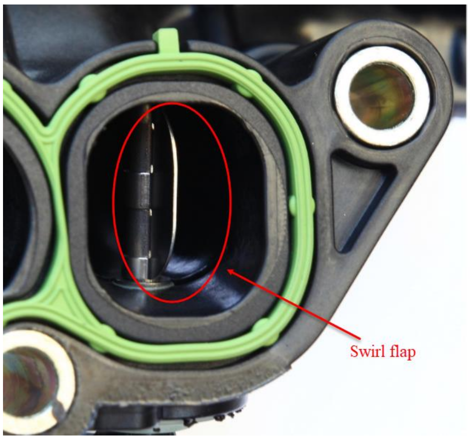

Figure 4.8: Diesel engine swirl flap

In the case of a diesel engine with direct injection, the filling of the cylinder through the intake manifold is an important quantity used to define the output torque and the power of the engine. Some modern diesel engines contain an additional actuator on the intake side of engine. This device, called swirl flap, is a part of the intake manifold; it ensures that air flows into the combustion chamber (Figure 4.8). The aim is to ensure a good mixture of air and the injected fuel drops inside the cylinder. The consequence is a homogenous combustion and, potentially, low emissions. A swirl flap is a small, buttery valve fitted to the intake manifold. It influences flows into the combustion chamber. Due to combustion deposits on the flaps and the connection part of the intake manifold, the flaps can begin to stick in one position over time such that the correct flap position cannot be achieved. Because of the missing feedback of the swirl flap position and its limited influence on MAF and MAP, the swirl flap effect can be neglected in this study without considerable effect on the accuracy of the simulation.

As mentioned in Chapter 2, the VGT rate influences the quantity of the air charging into the intake manifold and cylinder. If the VGT is not completely open, the quantity of air charging by the engine is smaller, and this reduces the torque. In addition, the quantity of air in the intake manifold depends on the EGR rate, ambient pressure and cylinder pressure (Nguyen-Schaefer, 2013). Figure 4.9 shows the section of the intake and exhaust manifolds. As discussed above, the intake and exhaust manifolds are considered to be thermodynamic systems. Thus, the ideal-gas and energy-conservation laws can be applied.

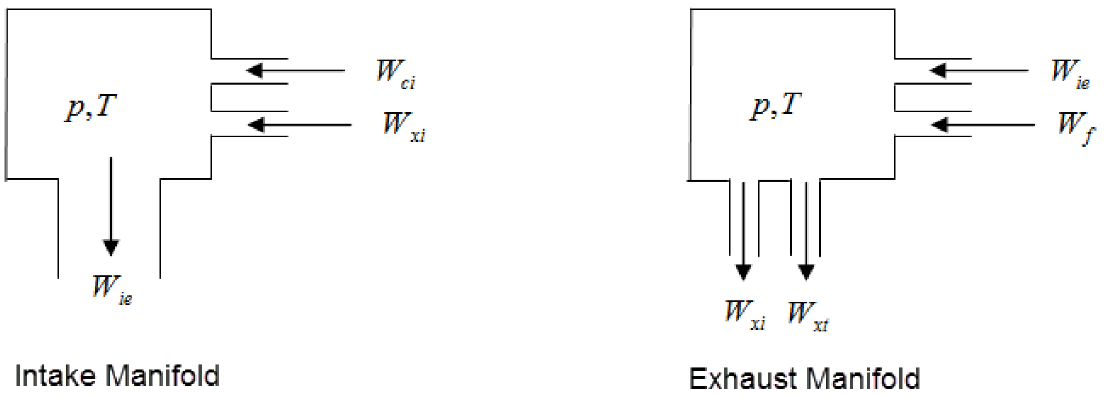

Figure 4.9: Schematics of intake and exhaust manifolds

In the intake manifold, the change of the specific internal energy and specific enthalpy can be written as follows (Isermann, 2014):

$$\dot{U}_i(t) = \dot{H}_{ci} + \dot{H}_{xi} - \dot{H}_{ie} \quad . \tag{4-8}$$

Reorganising equations 4-6 and 4-7 in Equation 4-8 leads to the following:

$$c_v \cdot \dot{T}_i \cdot m_i + c_v \cdot T_i \cdot \dot{m}_i = c_p \cdot T_{ci} \cdot W_{ci} + c_p \cdot T_{xi} \cdot W_{xi} - c_p \cdot T_{ie} \cdot W_{ie} \ . \tag{4-9}$$

Replacing m_i in Equation 4-9 with the ideal gas Equation 4-2 yields,

$$\dot{T}_i = \frac{R \cdot T_i}{c_v \cdot p_i \cdot V_i} \cdot (c_p \cdot T_{ci} \cdot W_{ci} + c_p \cdot T_{xi} \cdot W_{xi} - c_p \cdot T_{ie} \cdot W_{ie} - c_v \cdot T_i \cdot \dot{m}_i), \tag{4-10}$$

where (1) R and c_v have been explained in equations 4-1 and 4-6, and

(2) $V_i = 0.0109\ m^3$ is the intake manifold volume from engine specification.

In the ideal gas law, p_i is given by,

$$p_i = \frac{T_i \cdot m_i \cdot R}{V_i}. \tag{4-11}$$

Differentiating it leads to

$$\dot{p_i} = \frac{R}{V_i} \cdot (\dot{T_i} \cdot m_i + T_i \cdot \dot{m_i}) \ . \tag{4-12}$$

Adding the adiabatic exponent $k = \frac{c_p}{c_v}$ (Del Re, 2011) and replacing the $\dot{T_i}$ in Equation 4-12, the following equation for the change of pressure at intake manifold is obtained,

$$\dot{p_i}(t) = \frac{R \cdot k}{V_i} \cdot (T_{ci} \cdot W_{ci} + T_{xi} \cdot W_{xi} - T_{ie} \cdot W_{ie}), \tag{4-13}$$

where (1) R and V_i have been explained in equations 4-1 and 4-10, and

(2) $k = 1.4$ is isentropic expansion factor (De, Agarwal, Chaudhuri, & Sen, 2018).

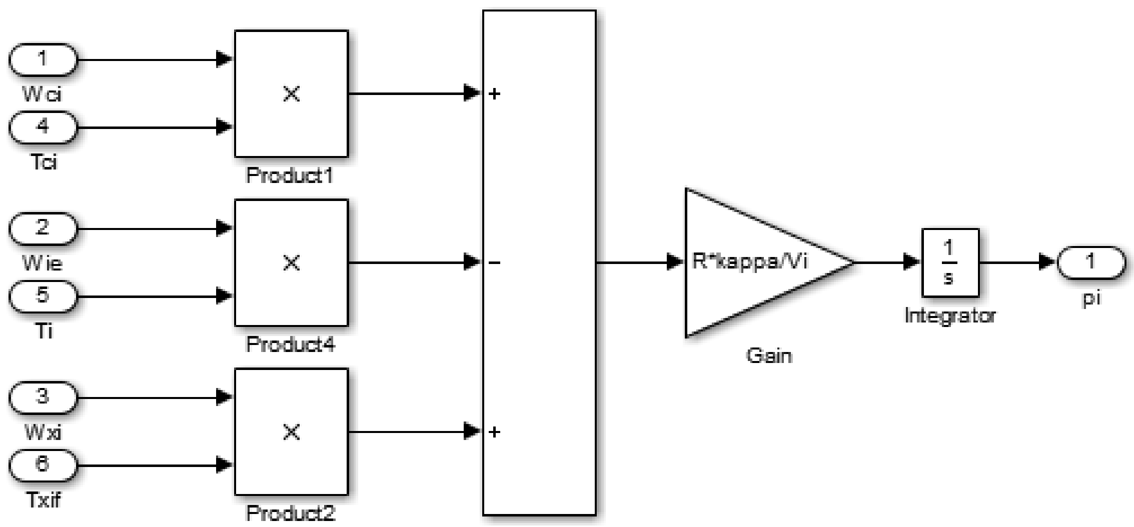

Figure 4.10: Intake manifold model

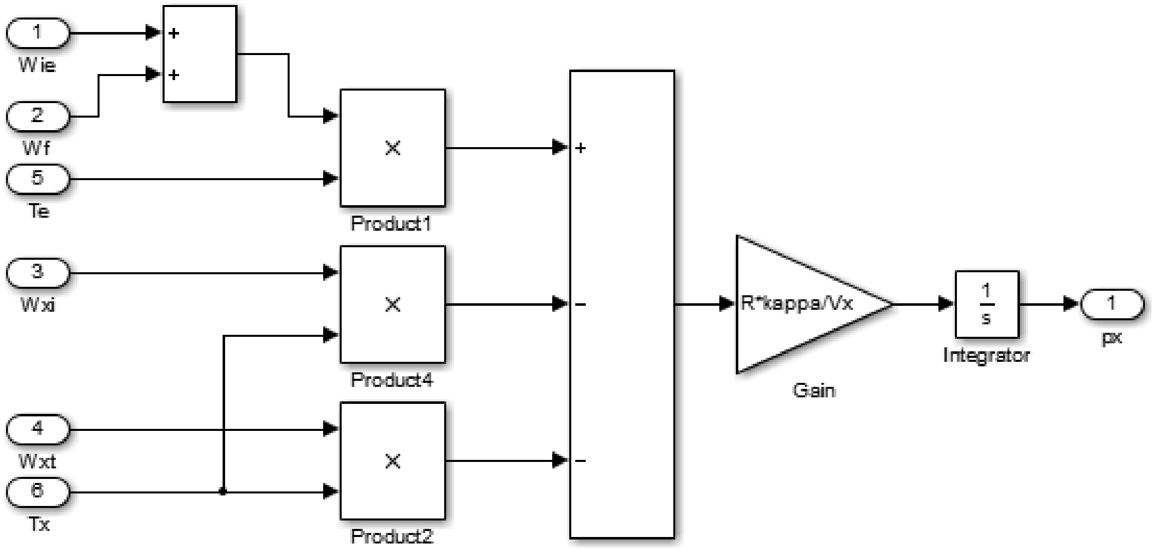

Figure 4.11: Exhaust manifold model

Similarly, the pressure change in the exhaust manifold can be determined using Equation 4-14:

$$\dot{p_x}(t) = \frac{R \cdot k}{V_x} \cdot ((W_{ie} + W_f) \cdot T_e - ((W_{xi} + W_{xt}) \cdot T_x) \,, \qquad (4\text{-}14)$$

where (1) $V_x = 0.0249\ m^3$ is the exhaust manifold volume from engine specification, and
(2) $k = 1.4$ is isentropic expansion factor (De, Agarwal, Chaudhuri, & Sen, 2018).

The Simulink models of the intake and exhaust manifolds are shown in figures 4.10 and 4.11.

4.4.2 Turbocharger

The turbocharger consists of three main parts: the bearings, the compressor and the turbine. The turbine and compressor are mounted on the same shaft, which is driven by the exhaust gas (Nguyen-Schaefer, 2013). From a physical point of view, it can be said that the energy is absorbed from the exhaust gas and transported from the turbine to the compressor by the rotation of the common shaft, whereby the energy is used to compress the aspirated air.

Each process (propelling the turbine, rotation of the common shaft and compressing the fresh air) is related to mechanical and thermal dynamic losses, which can be described in terms of state-dependent efficiency and air-mass flow maps over a wide range of operation conditions, as shown in Figure 4.12. These maps characterise the performance of a turbocharger, thereby allowing engine design engineers to choose the correct combination of turbo mechanical construction and engine.

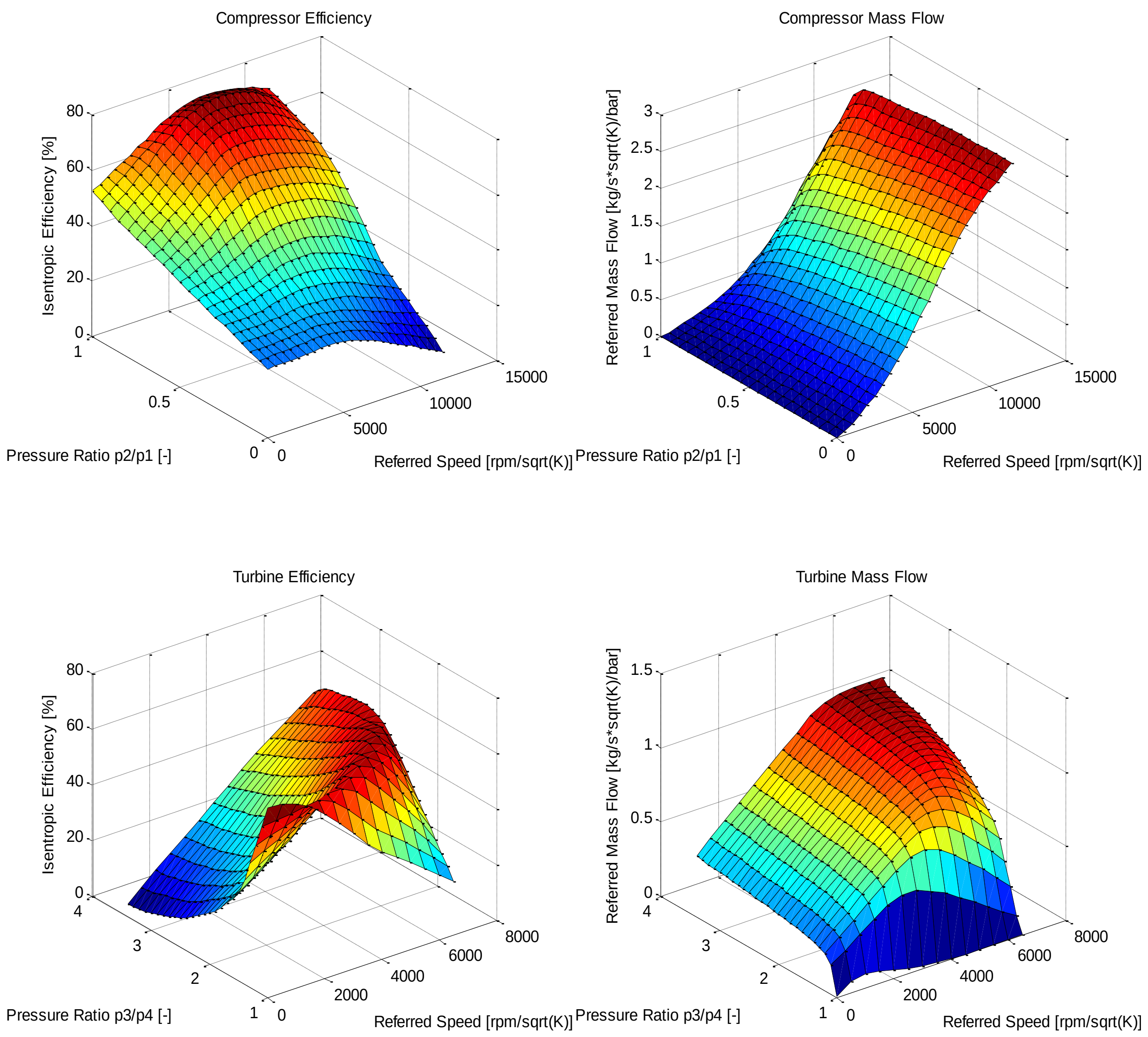

Figure 4.12: Compressor and turbine efficiency and air mass flow maps (VGT = 0%, closed)

In this study, the powertrain block sets from Matlab/Simulink are applied. The compressor and turbine maps (Figure 4.12) are delivered by the turbocharger manufactures, which are generated by specialised turbo calibration and test equipment: Turbo Test Pro. Figures 4.13 and 4.14 show the experimental setup of the test-bench and the interface of the integrated data-processing software at turbocharger manufacture.

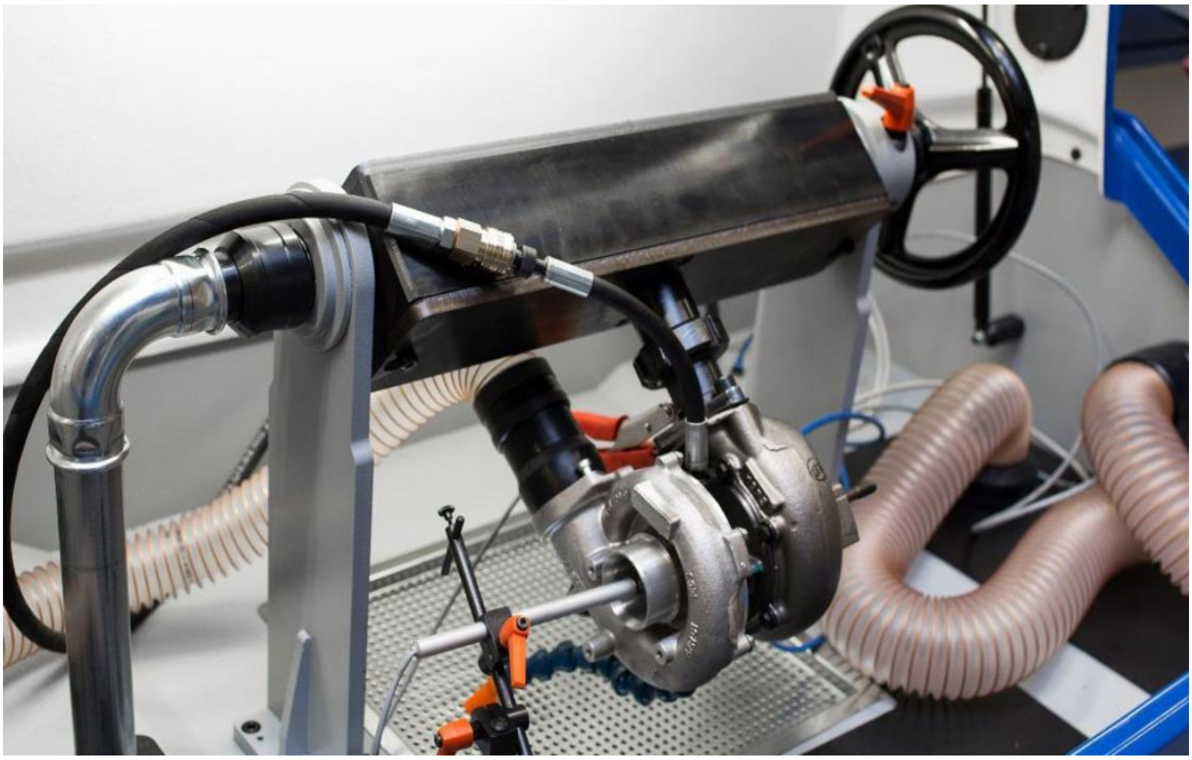

Figure 4.13: Turbo Test Pro test-bench setup (CIMAT, 2018)

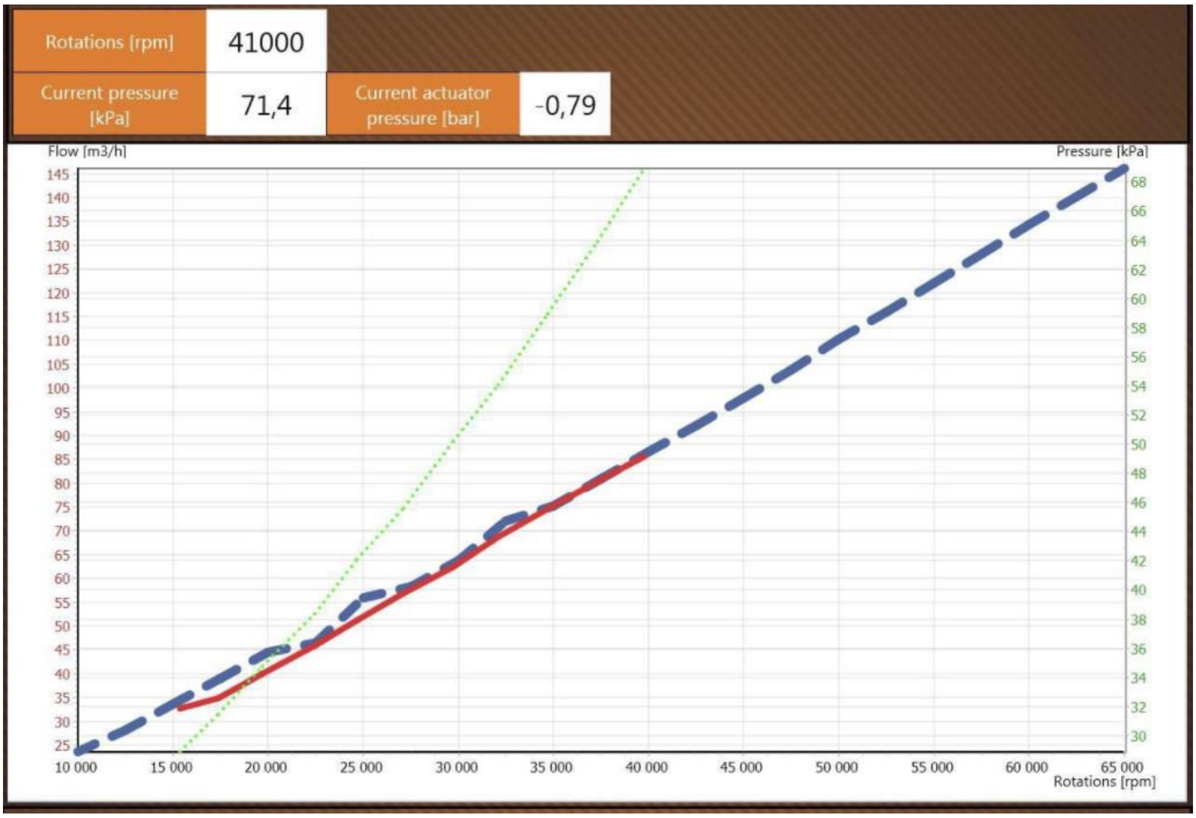

Figure 4.14: Turbo Test Pro test-bench analysis software interface (CIMAT, 2018)

However, these maps characterise the behaviour only in rarely reached steady operation regions. An alternative method is introduced in (Jung, 2003) to gain the required maps through CFD analysis. Jung's model captures the effects of combustion, in-cylinder motion and turbulence of gas, and it is much more accurate than the requirement for VGT and EGR control for the purposes of this study. It could be argued that the time required for computation in simulation is a critical factor for control tasks; thus, the speed of the simulation should be as fast as possible. It is acceptable to use a modified mean-value turbocharger model for the simulation without considering in-cylinder motion and turbulence of gas, because the analysis of the pressure oscillation in the engine-air-path is not the focus of this study.

The energy conversation of a turbocharger is given by (Eriksson, 2002),

$$w = h_{vT} - h_{nT} \ , \tag{4-15}$$

where nT is an index for parameters after the turbine, vT is an index for parameters before the turbine, and w is the mechanical work on the common shaft between the turbine and compressor.

Replacing h in Equation 4-15 with the specific enthalpy equation $h = c_p \cdot T$ yields the following:

$$w_T = c_p \cdot T_{vT} \cdot (1 - \frac{T_{nT}}{T_{vT}}) \ . \tag{4-16}$$

In an adiabatic system, $p \cdot v^k = constant$ (Batteh, Tiller, & Newman, 2003). This leads to,

$$\frac{p_{vT}}{p_{nT}} = (\frac{V_{nT}}{V_{vT}})^k \ . \tag{4-17}$$

Using the ideal gas equation, $V = \frac{R \cdot T \cdot m}{p}$, it follows that,

$$\frac{T_{nT}}{T_{vT}} = (\frac{p_{nT}}{p_{vT}})^{\frac{k-1}{k}} \ . \tag{4-18}$$

The temperature of the compressor is modelled as follows (Eriksson, 2002):

$$T_c = \frac{1}{\eta_{c,is}} \cdot \left(T_{c,is} - T_a\right) + T_a, \tag{4-19}$$

where (1) $\eta_{c,is}$ is the compressor efficiency,

(2) c is the index of compressor outlet,

(3) a is the index of compressor inlet, and

(4) *is* the index of isentropic.

Using thermodynamic equations for the isentropic process (Jung, 2003), the effective compressor power P_c results in the following:

$$P_c = W_{ci} \cdot c_p \cdot (T_c - T_a)\ . \tag{4-20}$$

Replacing T_c in the Equation 4-20 with Equation 4-19 yields,

$$P_c = W_{ci} \cdot c_p \cdot \frac{1}{\eta_{c,is}} \cdot T_a \cdot \left(\frac{T_{c,is}}{T_a} - 1\right). \tag{4-21}$$

By replacing the $\frac{T_{c,is}}{T_a}$ in Equation 4-21, the effective compressor power P_c becomes,

$$P_c = W_{ci} \cdot c_p \cdot \frac{1}{\eta_{c,is}} \cdot T_a \cdot \left(\left(\frac{p_c}{p_a}\right)^{\frac{k-1}{k}} - 1\right). \tag{4-22}$$

The modelling approach for turbochargers given in (Jung, 2003) is based on the turbo-efficiency map (Figure 4.12), $\eta_{c,is} = f^{map}\left(w_{ci}, \frac{p_c}{p_a}\right)$.

The map of the pressure ratio which are provided by the turbocharger manufacture, as shown in Figure 4.15, is given by

$$\frac{p_c}{p_a} = f^{map}(w_{ci}, n_{TL})\ , \tag{4-23}$$

where (1) n_{TL} is the turbo speed,

(2) TL is the index for turbocharger, and

(3) w_{ci} is the mass of air flow at compressor inlet.

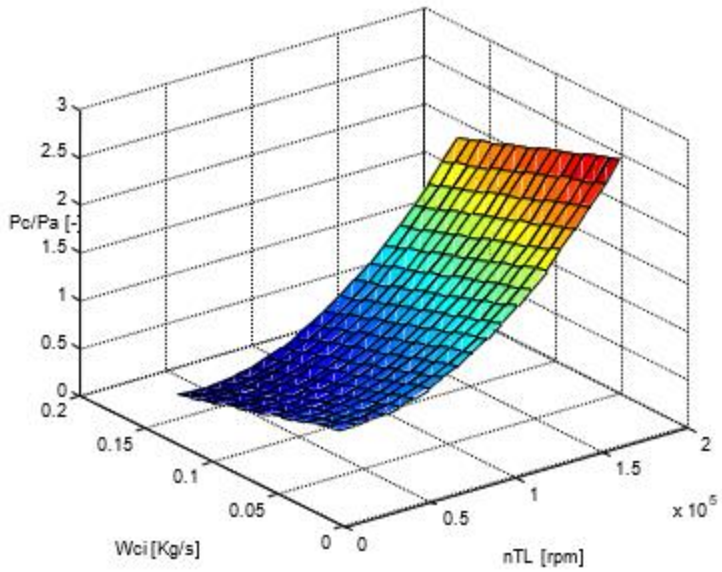

Figure 4.15: Map of p_c/p_a

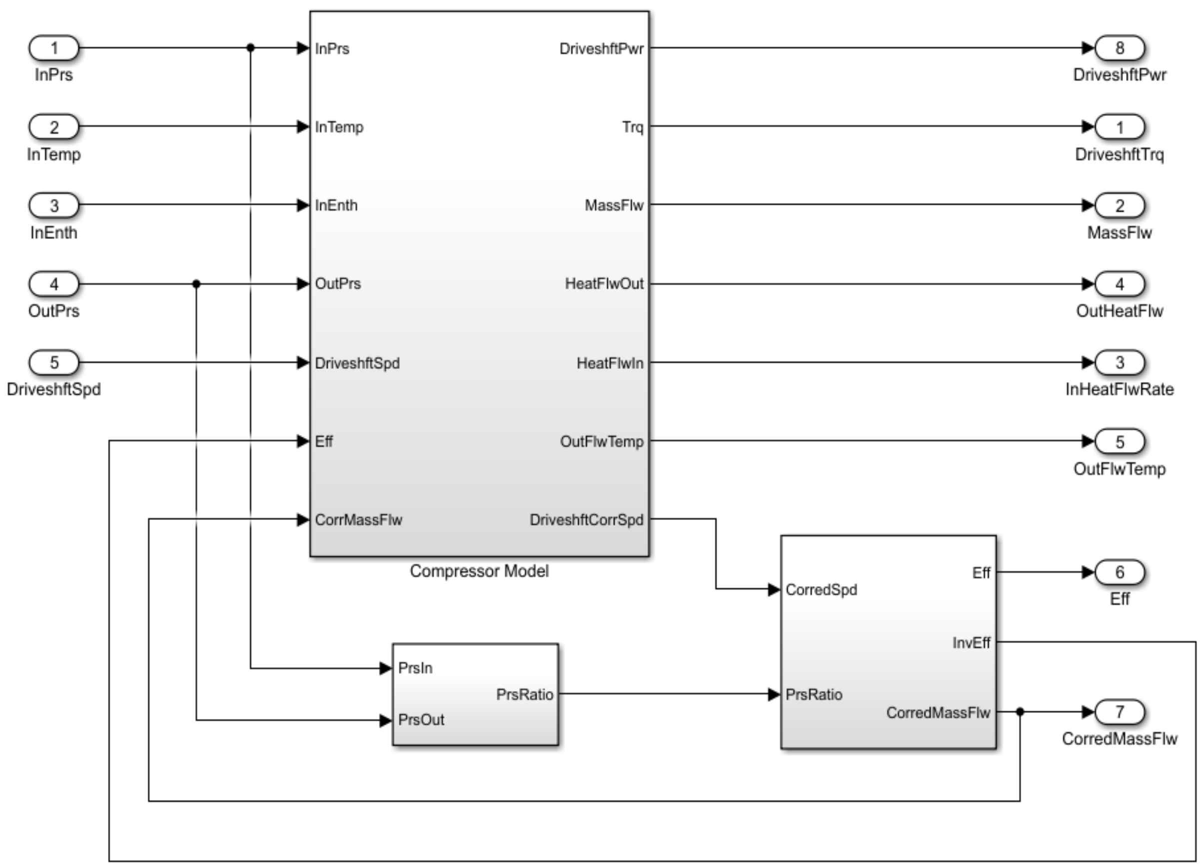

Figure 4.16: Compressor model

Figure 4.16 illustrates a model of the compressor block in Powertrain block sets from Matlab/Simulink. The compressor block simulates engine boost by using the drive shaft energy to increase the intake manifold pressure. The block uses two-way ports to connect to the inlet and outlet control volumes and the drive shaft. The control volumes provide the pressure, temperature, and specific enthalpy the compressor uses to calculate the mass and energy-flow rates. To calculate the torque and flow rates, the drive shaft provides the speed to the compressor. Both compressor and turbine are mounted on the same shaft, which is supported by the bearing system of the radial and thrust bearings (Jung, 2003). Analogously, due to the energy transfer involved in using the bearing system, the required turbine power is calculated from the isentropic turbine efficiency according to (Nguyen-Schaefer, 2013):

$$P_t = W_{xi} \cdot c_p \cdot \eta_{t,is} \cdot T_x \cdot \left(1 - (\frac{p_{nT}}{p_x})^{\frac{k-1}{k}}\right) \ , \tag{4-24}$$

where *nT* is the index of turbine outlet, and *x* is the index of turbine inlet.

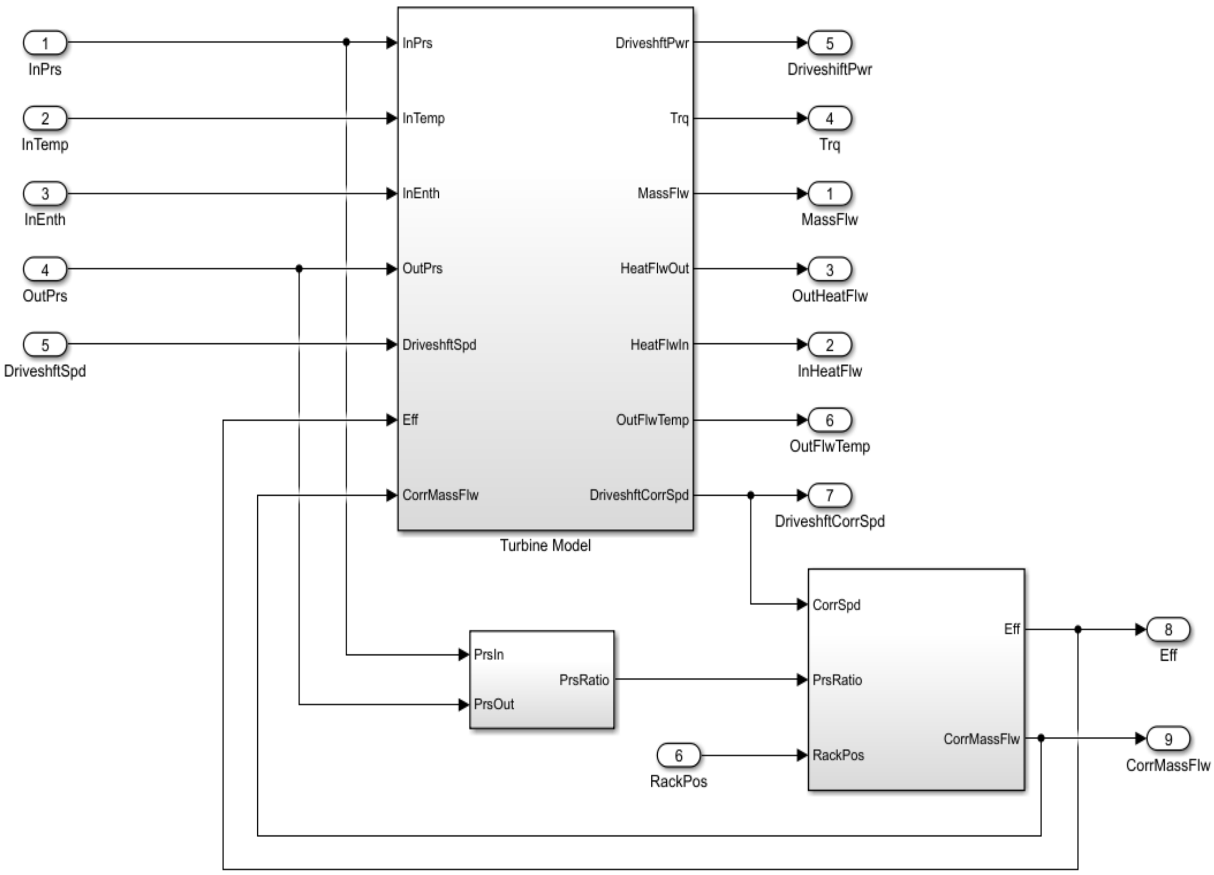

Figure 4.17: Turbine model

Figure 4.17 illustrates the model of turbine block in Powertrain block sets from Matlab/Simulink. The turbine block uses the conservation of mass and energy to calculate mass and heat flow rates for turbines with variable geometry. The block uses two-way ports to connect to the inlet and outlet control volumes and the drive shaft. The mass flow rate and turbine efficiency are calculated by lookup tables. The turbine manufacturers provide the mass flow rate and efficiency tables as a function of corrected speed and pressure ratio.

The connection of compressor and turbine can be described with the angular acceleration of the connection boost drive shaft (Jung, 2003), which is calculated from the shaft dynamics equation:

$$\dot{n}_{TL} = (\frac{30}{\pi})^2 \cdot \left(\frac{P_t - P_c}{J_{TL} \cdot n_{TL}}\right), \tag{4-25}$$

where J_{TL} denotes the turbo moment of inertia.

Figure 4.18 illustrates the model of a turbocharger dynamic block in Simulink. The boost drive shaft block uses the compressor, turbine, and external torques to calculate the drive shaft speed.

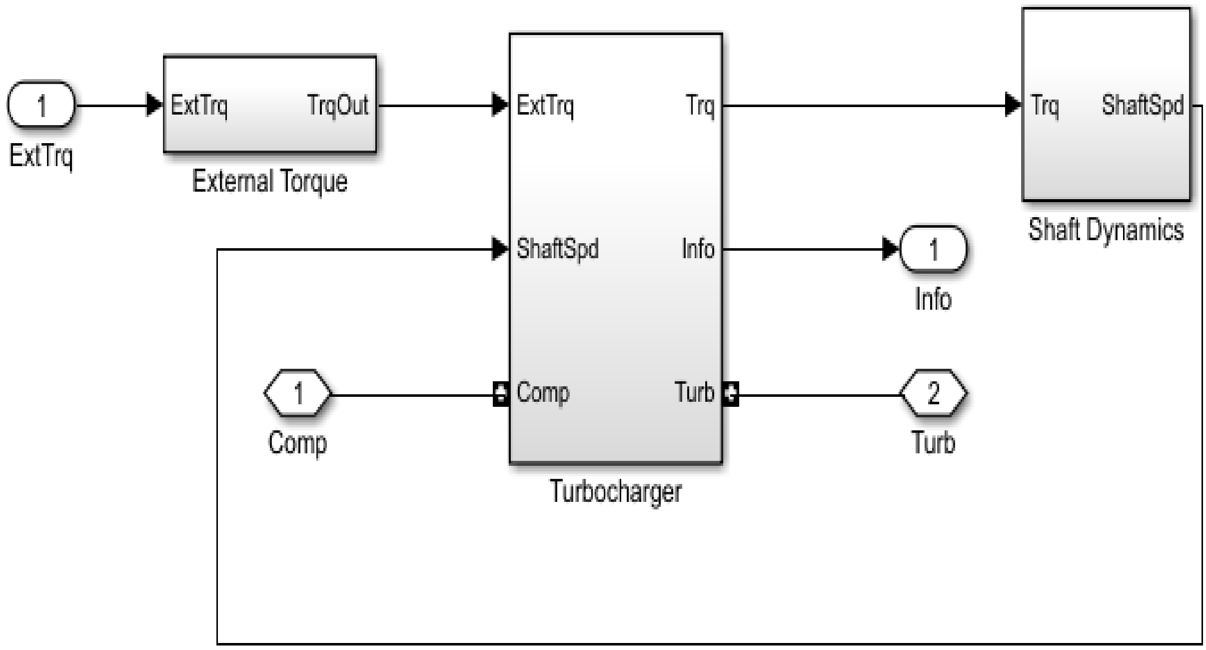

Figure 4.18: Turbocharger drive shaft model

Due to friction loss in the bearing system of the turbocharger, the turbine power results from the effective turbine power and mechanical efficiency η_m. The changing of the turbine power to the compressor is described by the differential equation according to (Cornetti, 2014):

$$\dot{P}_c = \frac{1}{\tau_{VGT}} \cdot (\eta_m \cdot P_t - P_c) \ , \tag{4-26}$$

where η_m denotes the mechnical efficiency and the time constant τ_{VGT} describes the time delay between a variation in the VGT vane position and the resulting change on the compressor power.

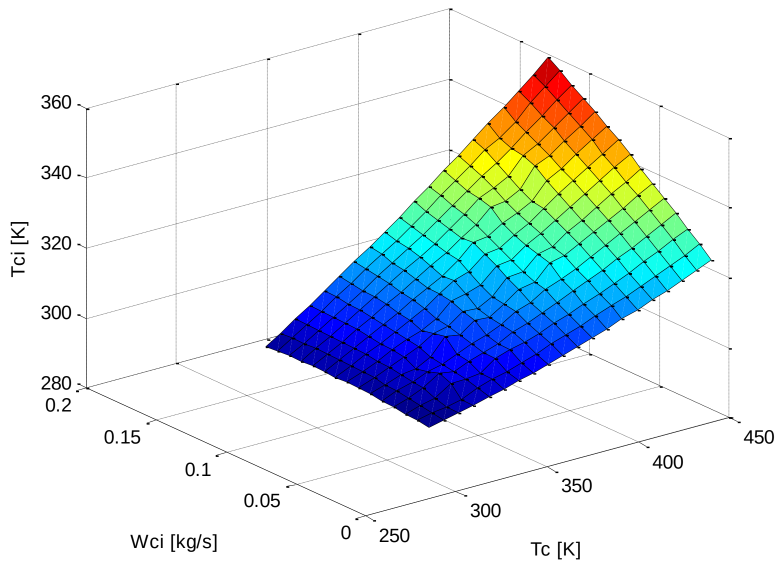

Figure 4.19: Intercooler outlet temperature

In the turbocharger system, an intercooler is usually used to cool the air that comes from the compressor because, when using a compressor, the air density increased such that the intake temperature also increases (Hamarashid, 2008). The intercooler can increase the efficiency and intake air density of the combustion by cooling the compressed air temperature after the compressor. Basically, the intercooler is an air-air cross-flow heat exchanger which consists of many small pipes through which the air flows. A derivation and discussion of how to apply the heat-transfer unit model to an automotive intercooler is given in (Eriksson, 2002). It suggests that the temperature out of the intercooler can be modelled with sufficient accuracy as a map $T_{ci} = f^{map}(w_{ci}, T_c)$ (Figure 4.19), which can be provided by the intercooler manufacture. There is a relation between the air flow mass *Wci*, cooler input temperature *Tc* and cooler output temperature *Tci*. This map includes the cooler properties and can be adjusted to match the temperature drop between cooler input and cooler output.

4.4.3 Exhaust Gas Recirculation

The literature review in Section 2.1.2 shows that the EGR model is a very important mechanism used in the engine-air-path to lower the temperature in the cylinders and through that to reduce NOx formation (Bennett, 2014). The exhaust gas acts are an inert gas, and it decreases the peak temperature during combustion to reduce the production of NOx (Sher, 1998). The EGR flow is regulated by an electro-pneumatic valve which regulates the amount of re-circulated exhaust gas. The mathematical formulation of the mass flow through EGR has two states according to (Eriksson, 2002):

1. If $p_x \geq p_i$, then

$$w_{xi} = \frac{A_{EGR}(x_{EGR}) \cdot p_x}{\sqrt{R \cdot T_x}} \cdot \sqrt{2 \cdot p_r \cdot (1 - p_r)} \text{ , and} \tag{4-27}$$

2. If $p_i > p_x$, then

$$w_{xi} = -\frac{A_{EGR}(x_{EGR}) \cdot p_i}{\sqrt{R \cdot T_i}} \cdot \sqrt{\frac{2}{p_r} \cdot \left(1 - \frac{1}{p_r}\right)} \text{ ,} \tag{4-28}$$

where (1) p_r donates the ratio of pressure between intake and exhaust manifold $\frac{p_i}{p_x}$, and

(2) $A_{EGR}(x_{EGR})$ stands for the effective area of an open section of the EGR.

The valve effective area is thus modelled by using a polynomial function of the control input x_{EGR}. This approach is introduced in (Dekker & Sturm, 1996). This is an approximation, and it captures the most important features of the valve:

$$A_{EGR}(x_{EGR}) = c_{EGR1}(x_{EGR})^2 + c_{EGR2}(x_{EGR}) \text{ ,} \tag{4-29}$$

where c_{EGR1} and c_{EGR2} are the EGR valve-specific values which are provided by the EGR manufacture.

Equations 4-27, 4-28 and 4-29 are used in the EGR model for engine-air-path model in Simulink, as shown in Figure 4.20.

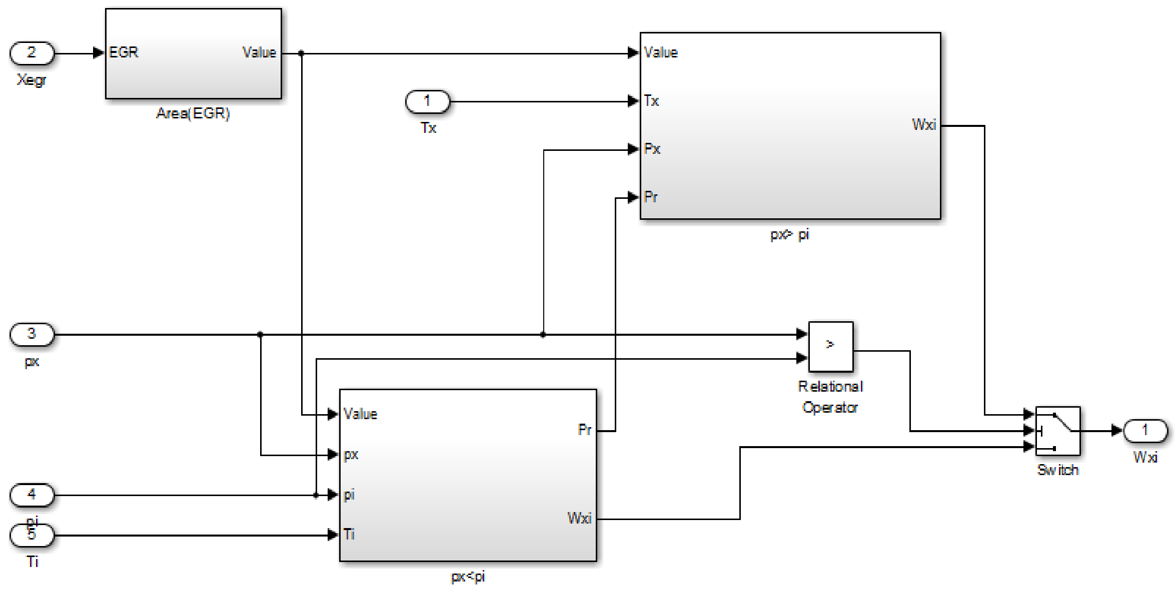

Figure 4.20: EGR model

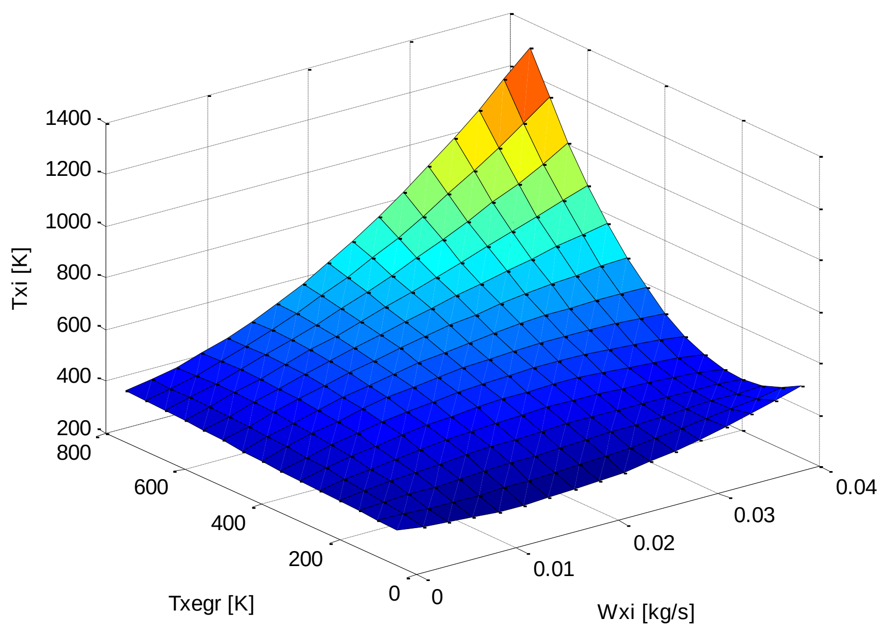

Figure 4.21: EGR cooler outlet temperature

In this system, the exhaust gas from EGR is cooled by a water-air heat exchanger. It is then, together with the intake air, led back into the engine. Analogous to the turbocharger intercooler modelling, the temperature of the EGR cooler outlet results from a map $T_{xi} = f^{map}(w_{xi}, T_x)$ (Figure 4.21), which is provided by the cooler manufacturer. The EGR valve affects the temperature of the intake manifold by releasing thermal energy depending on engine load. The change of temperature between the intake manifold and EGR can be modelled by a differential equation with time constant τ_{EGR} (Equation 4-30) (Ammann, Fekete, Guzzella, & Glattfelder, 2003):

$$\dot{T}_{xif} = \frac{1}{\tau_{EGR}} \cdot \left(T_{xi} - T_{xif}\right) \ . \tag{4-30}$$

4.4.4 Oxygen Concentration and Lambda

Oxygen is important to combustion – especially in the combustion of fuel for energy. The mechanism of the oxygen-concentration effects on the combustion and emissions of diesel engines are investigated by (Zheng & Yao, 2009; Yao & Zhang, 2009). With decrease of oxygen concentration, the peak of the average in-cylinder pressure decreases. The investigation shows that decreasing oxygen concentration is the most effective way to control NOx emissions. With the decrease of oxygen concentration, soot emissions first increase and then decrease. To model the oxygen concentration and air-fuel ratio, Computational Fluid Dynamics (CFD) provides a qualitative prediction; however, this leads to excessive computation times and is accordingly not suitable for model-based control design, therefore in this study the modelling will be generated by the mean-value modelling approach.

4.4.4.1 Oxygen Concentration

The oxygen concentration is defined with respect to the intake manifold as in reference (Guzzella & Onder, 2004) according to

$$\int (W_{ci} \cdot C_{o2a} + \ W_{xi} \cdot C_{o2x} - W_{ie} \cdot C_{o2i}) dt = m_i \cdot C_{o2i} \ , \tag{4-31}$$

where (1) W_{ci}, W_{xi} and W_{ie} are mass flows from the compressor to the intake manifold, from EGR to the intake manifold and from the manifold to the cylinder, respectively,

(2) C_{o2a} stands for the oxygen mass concentration in the ambient, it has a constant value of 23%, and

(3) C_{o2x} and C_{o2i} stand for the oxygen mass concentration in the intake and exhaust manifolds, respectively.

Differentiation of both sides of Equation 4-31 yields,

$$W_{ci} \cdot C_{o2a} + W_{xi} \cdot C_{o2x} - W_{ie} \cdot C_{o2i} = \dot{m}_i \cdot C_{o2i} + m_i \cdot \dot{C}_{o2i}. \quad (4\text{-}32)$$

The changing of the turbine power to the engine air-mass flow is described by the differential equation according to (Guzzella & Onder, 2004):

$$\dot{m}_i = W_{ci} - W_{ie} - W_{xt}. \quad (4\text{-}33)$$

Reorganising Equation 4-32 and 4-33, the oxygen concentration in the intake manifold leads to the following:

$$\dot{C}_{o2i} = \frac{1}{m_i} \cdot (W_{ci} \cdot C_{o2a} + W_{xi} \cdot C_{o2x} + (W_{xt} - W_{ci}) \cdot C_{o2i}). \quad (4\text{-}34)$$

Like the modelling of oxygen in the intake manifold, the oxygen concentration in the exhaust manifold can be determined by Equation 4-35. By *stoichiometric mixture* we understand a mixture which contains exactly as much oxygen as we need for the complete combustion of the C, H and S atoms (Isermann, 2014). This leads to

$$\dot{M}_{o2x} = W_{ci} \cdot C_{o2i} - 23\% \cdot W_f \cdot (\frac{x_{air}}{x_{fuel}})_{stoich}. \quad (4\text{-}35)$$

The mass conservation of oxygen (Guzzella & Onder, 2004) in the exhaust manifold is expressed as follows:

$$\int \left(W_{ci} \cdot C_{o2i} - 23\% \cdot W_f \cdot (\frac{x_{air}}{x_{fuel}})_{stoich} - W_{xi} \cdot C_{o2x} - W_{xt} \cdot C_{o2x} \right) dt = m_x \cdot C_{o2x}. \quad (4\text{-}36)$$

The changing of the engine air mass flow in exhaust manifold is described by the differential equation in (Guzzella & Onder, 2004):

$$\dot{m}_x = W_{ie} + W_f - W_{xi} - W_{xt}. \quad (4\text{-}37)$$

Reorganising equations 4-36 and 4-37, the oxygen concentration in the exhaust manifold leads to

$$\dot{C}_{o2x} = \frac{1}{m_x} \cdot (W_{ci} \cdot C_{o2i} - 23\% \cdot W_f \cdot (\frac{x_{air}}{x_{fuel}})_{stoich} - W_{ie} \cdot C_{o2x} - W_f \cdot C_{o2x}). \quad (4\text{-}38)$$

4.4.4.2 Lambda

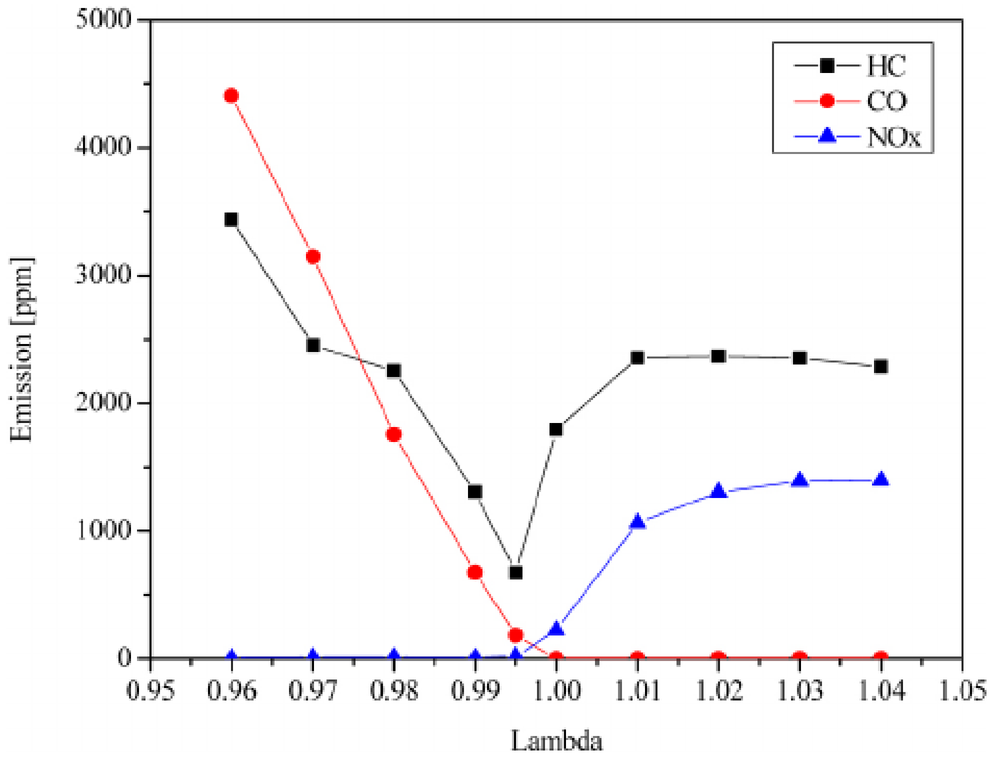

Figure 4.22: Emissions are influenced by the Air-Fuel Ratio (Shi & Seiser, 2015)

The λ is an important indicator of the combustion quality and has considerable effects on emissions. It is defined as the ratio of the actual air quantity relative to the ideal stoichiometric required quantity (Equation 4-39) according to (Eriksson, 2002). If precisely enough air is provided to completely burn all the fuel, the ratio is known as the stoichiometric ratio. A stoichiometric ratio should lead to an ideal combustion, and Figure 4.22 shows the resulting emissions with different λ. The λ of the engine is modelled using the standard model-based on the stoichiometric ratio:

$$\lambda = \frac{\frac{x_{air}}{x_{fuel}}}{(\frac{x_{air}}{x_{fuel}})_{stoich}}, \tag{4-39}$$

where (1) x is the mass flow,

(2) $\frac{x_{air}}{x_{fuel}}$ is the actual air-to-fuel ratio, and

(3) $(\frac{x_{air}}{x_{fuel}})_{stoich} = 14.5$ is the stoichiometric air-to-fuel ratio for diesel engine, which means enough air to burn all the fuel.

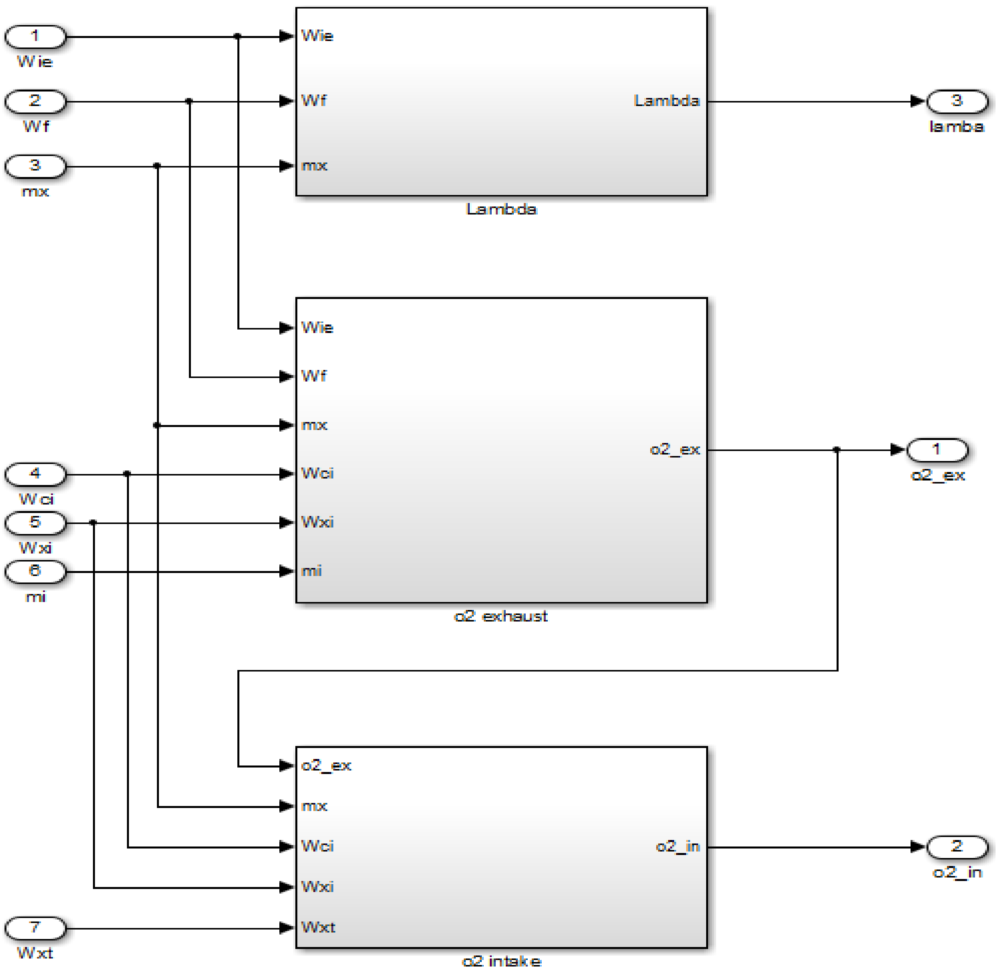

Figure 4.23: Calculation of lambda, oxygen concentration at intake and exhaust

The models of the oxygen concentration and λ implemented in Simulink are shown in Figure 4.23. Reorganising Equation 4-39 under stoichiometric condition, it follows that

$$\lambda = \frac{W_{ie} \cdot C_{o2i}}{W_f \cdot 23\% \cdot 14.5}. \tag{4-40}$$

4.4.5 Emissions

One of the main purposes of engine control is rooted in the requirement of reducing the emission output. To support this optimisation task, a dynamical emission model is generated. Several approaches can be taken to building the emission model of a diesel engine. One approach is based on the first principle according to which chemical reactions and physical phenomena are used for the description of the model. For examples, see (Cook, Pitsch, Chen, & Haweks, 2007) and (Sjoeberg & Dec, 2003).

The other approach is based on experiments and measurements; it is similar to the approach of (Hirsch, 2011) and (Ljung, 2001), where data-based models are used to optimise the system. However, because of a lack of fast emission sensors and computational technology, the modelling of the details of the development of the different emissions cannot be done with exclusively theoretical models to the present day (Langthaler, 2007). Therefore, black-box modelling by a data-based system identification method is required. The task of this modelling method is to identify models for the NOx and PM (also called OPAC for opacity) emissions based on observed input-output data. The accuracy of the identified system largely depends on the quality of the data collected from the engine system. The collected engine data for model identification should capture most of the behavioural characteristics of the emissions. With the help of the statistical experiment design (DOE), it becomes possible to describe systems by models in an efficient manner. These models are parametrised by means of measurement data; the NLARX algorithm of the system identification toolbox in Matlab/Simulink, as applied in (Ljung, Zhang, Lindskog, & Juditski, 2007), can be used for this. This section describes data-based modelling by DOE approach; the overall results of the application of emission modelling are discussed in Section 4.5.

In this section, the basics of modeling for the subsequent optimisation of emissions will be explained in detail. After a general introduction to black box modeling methods, two modeling types that appear to be particularly suitable to emission modeling are considered in more detail. Subsequently, the design of DOE measurement plan is introduced in order toreduce the data collection time for dynamic modeling, despite the increasing number of manipulated variables. Thereafter, the corresponding emission models are presented, compared and discussed.

4.4.5.1 Design of Experiment

The goal of the DOE is the model-like description of an unknown systems based on measured data. The methodology of the DOE includes the creation of the experiment plan according to statistical aspects, the creation of models and the optimisation of modelled systems. As mentioned in (Ljung, 2001), in general, the two most important issues of data-based modelling are, of course, the data itself and the DOE needed to generate the data.

Two important works about design of experiments are (Hirsch, 2011) and (Ljung, 2001). These papers must be referred to at this point. First, it is a question of which signals should be defined as outputs and which signals should be manipulated as inputs to excite the system during the experiment. It should also be stressed that there may be signals associated with the process that have to be considered as inputs – e.g., operation points, engine speed n, and fuel injection m_f in the engine-air-path system – which affect the system states. By the way, it is then still highly desirable to include these signals among the measured input signals and to consider them as measurable disturbance in the control problem afterwards. Most often, the signals are sampled using a constant sampling interval T; thus, this quantity must be chosen. The choice of input signals has a very substantial influence on the measured data. The inputs determine the operating point of the system and which parts and modes of the system are excited during the experiment. The user's "freedom" in choosing the input characteristics may vary considerably with the application. Two different aspects are associated with the input design of DOE. One concerns the spectrum of input and the cross spectrum between input and driving noise. The other concerns the shapes of the signal. It can work with the inputs as the sums of sinusoids, filtered white noise, pseudorandom signals, binary signals, etc. As a final choice for the identification experiment, the number of input-output measurements has to be mentioned.

The following definitions of input design using DOE mainly coincide with those of (Hirsch, 2011) and (Ljung, 2001). The D-optimal design is sequentially approximated if the next input $u(k+1)$ is defined, such that $d(y(u(k+1), \bar{M}(k))$ becomes maximal (For more details, see Appendix A):

$$u(k+1) = argmaxX(k+1)^T \bar{M}(k)^{-1} X(k+1) u(k+1) \in \Omega. \qquad (4\text{-}41)$$

This optimisation presents a non-convex problem with several local maxima within Ω. In this task, a multi-shot optimisation is used to cope with this issue. There, several optimisations start at random points within Ω, and the best is considered the optimum. While it cannot be guaranteed that this result is the global one, tests show that, already with a two-shot strategy, convergence towards D-optimal design is given.

4.4.5.2 Emission Modelling

The decision to build an emission model using empirical data is motivated by Section 4.4.5.1. For a good identification of data-based models, it is necessary to perform persistent excitation. So far, for non-linear systems, the DOE method is one of the best excitation methods that can be used to generate the identification data. For this identification task, the inputs of candidates of the system (m_f: total injected fuel mass per cycle, mg/cyc; n_{eng}: engine speed, rpm; MAP: manifold absolute pressure, mbar; MAF: manifold air flow, mg/cyc) should be varied such that an accurate and unique model can be identified. The outputs are NOx in ppm and OPAC in %.

According to Equation 4-41, the sequential D-optimal inputs is generated; next, the inputs and outputs are measured on the test-bench. Figure 4.24 presents the model structure, which includes all the input variations and outputs of measurements for identification. With these measurements, the system identification should be performed.

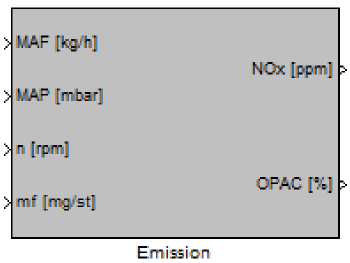

Figure 4.24: Emission Simulink model

The emissions model is identified with non-linear models. It can be assumed that a second-degree, polynomial, dynamic model (sensor dynamics is known) is sufficient for approximation (Hirsch, 2011). This system is identified with a MIMO structure to catch the interactions of all inputs and outputs, as illustrated in figures 4.25 and 4.26. The choice of the inputs is physically motivated. All the measurements are saved in this way by using a Matlab m-file. The data set is stored in a Matlab mat format. In the second step, the outliers of the original data have to be removed and the amount of data has to be reduced. This is done via signal filter in Matlab. The outlier detection and filtering are done by the Matlab function. After filtering, down-sampling to a sampling frequency of 50 Hz is performed. The filtered and resampled data is stored in a mat-file. The third step is to build a data-based identification model. The pre-processed data out of the Mat file is loaded into the system identification toolbox. The data must be detrended. Hence, the following identification is made with delta values at a defined operating point, not the absolute values.

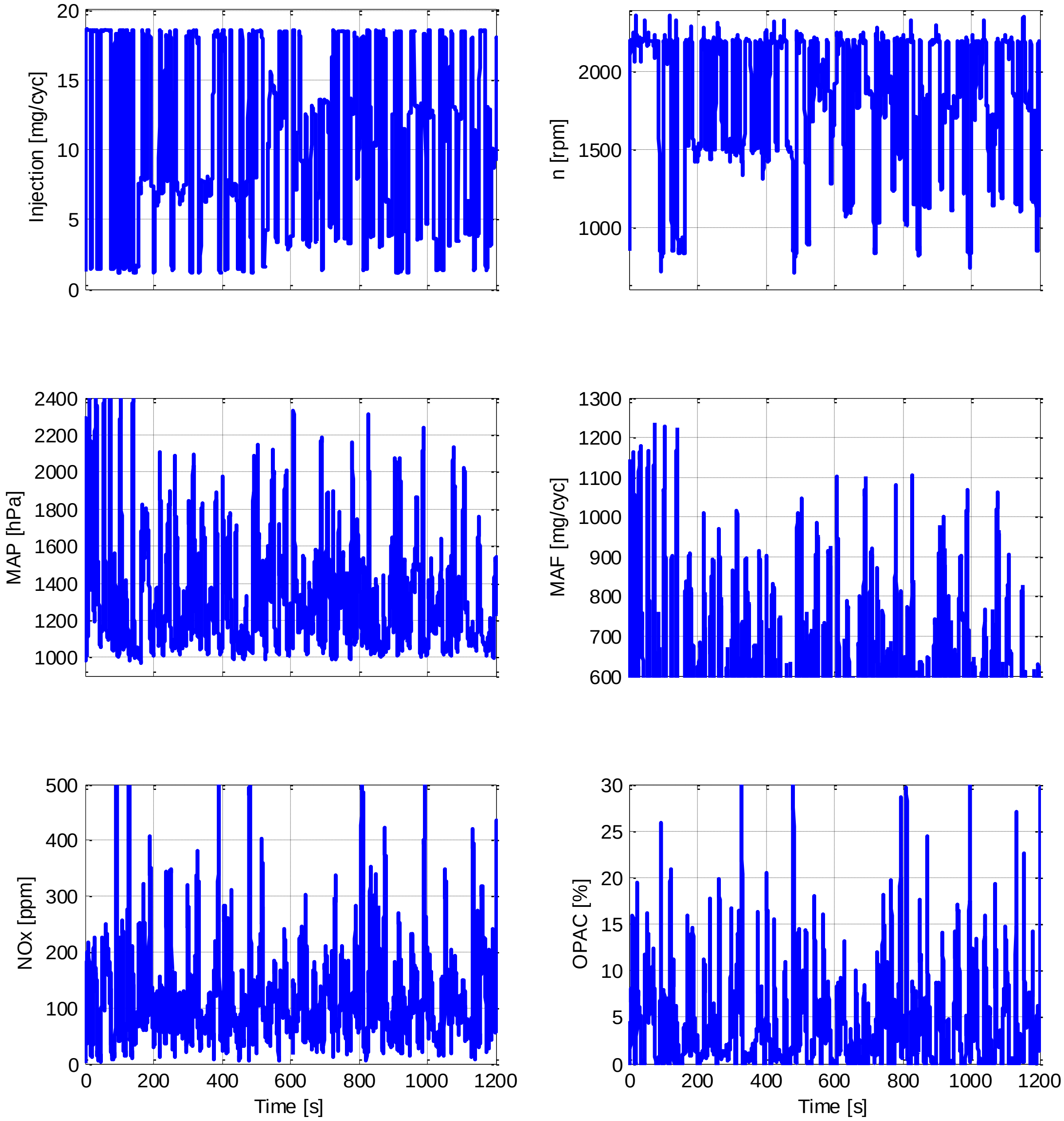

Figure 4.25: DOE input and output data

For identification, the prediction error method is applied (MathWorks, 2018), which estimates the parameters of general linear models and is able to handle MIMO and MISO model structures. The model is initialised by the well-known identification n4sid algorithm and is then further adjusted by optimising the prediction error fit. That means that the matrices are optimised until the prediction error is minimal. To estimate the order of the model, different values have been applied. From this, it can be determined that the fast MIMO system acts mainly as a system of the second order.

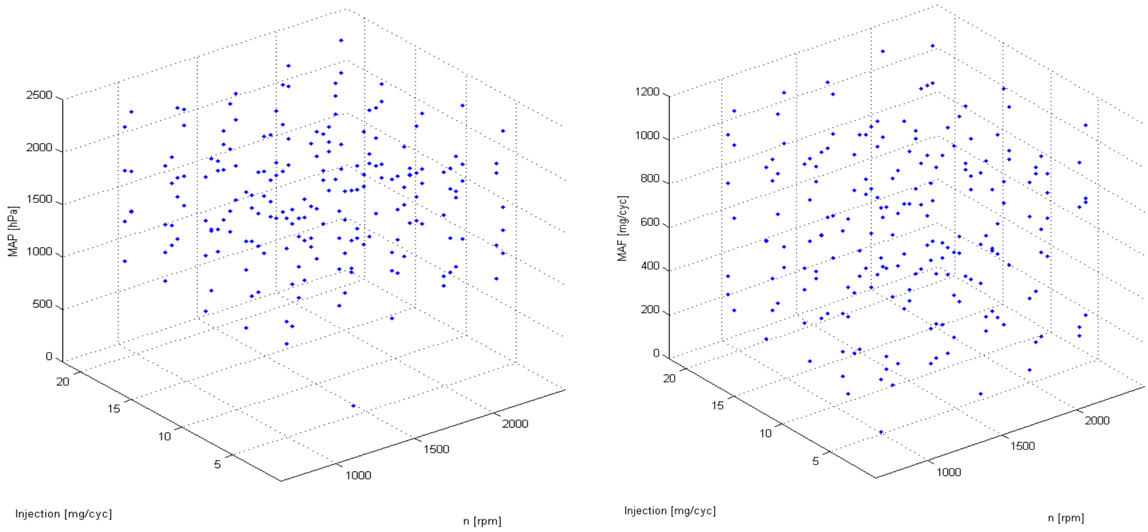

Figure 4.26: DOE data in 3D-View

A different modelling method could be performed for comparison purposes based on the ARX model. The following Figure 4.27 presents a comparison of the measured data and the simulation results based on the DOE-identified model NLARX (Equation 4-42) and the ARX (Equation 4-43) model. The VAF value is calculated by Equation 3-6. The VAF values of NOx are over 80% by NLARX DOE identification. The simulated results for OPAC reach VAF values at approximately 77% by DOE identification. In comparison to the non-linear ARX model – with a VAF value of 60% and 55% for NOx and OPAC, respectively – this is a very good result. The VAF values do not reach closer to 100% due to strong non-linearities that cannot be modelled very well by linear approximation. Another reason for the emission differences could be differences in coolant temperature and air temperature, which might cause a slightly different indicated mean pressure. The influence on emission concentrations is not quantifiable with the available data. To obtain meaningful measurements that allow prediction of driving cycle results, it must be ensured that the environmental conditions and operating point are tightly matched during data acquisition.

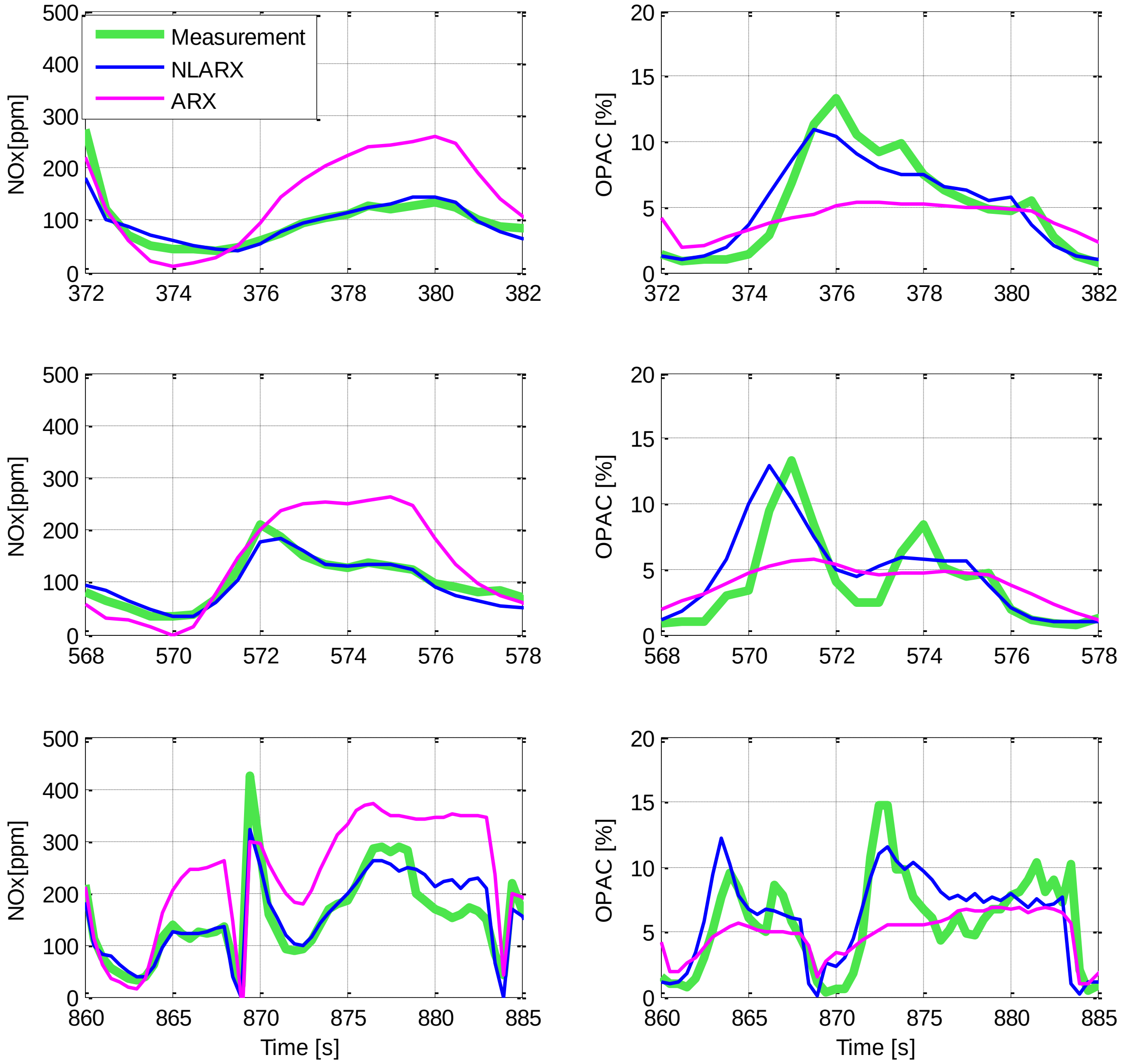

Figure 4.27: Comparison of measurement data of NLARX and ARX models (372s~382s, 568s~578s, 860s~885s)

The predicted output of NLARX emission model has the following structure:

$$y(t) = f[\,y(t-1), \dots, y(t-n_a), u(t-n_k), \dots, u(t-n_k-n_b+1)] + e(t), \qquad \text{(4-42)}$$

where (1) $y(t)$ and $u(t)$ denote the system output and input at time point t respectively,

(2) $e(t)$ represents the modelling error,

(3) the parameters *na* and *nb* are the number of past outputs and inputs,

(4) nk is the pure input delay, and

(5) f is the nonlinear function (implemented in the Matlab/Simulink Identification Toolbox (MathWorks, 2018)).

The ARX-method uses the least-squares method to estimate the parameters of the ARX emission model structure (MathWorks, 2018):

$$y(t) + a_1 \cdot y(t-1) + \cdots + a_{na} \cdot y(t-n_a) = b_1 \cdot u(t-1) + \cdots \\ + b_{n_b} \cdot u(t-n_k-n_b+1) + e(t), \quad (4\text{-}43)$$

where (1) $y(t)$ and $u(t)$ denote the system output and input at time point t respectively,

(2) $e(t)$ represents the modelling error,

(3) the parameters na and nb are the number of system poles and zeroes plus 1, and

(4) nk is the number of input samples.

4.4.6 Torque

Torque is one of the main outputs of an engine. An engine torque model is available in (Chapman, 2002) which is based on physical equations used to calculate the engine torque over the crank angle. However, this method depends very strongly on the precision of the provided engine parameters. Another disadvantage of this method is its long computation time. Langthaler (2007) shows a general workflow for obtaining a data-based model on test-benches. It seems appropriate to look for a data-based model structure for the torque model, and this model can be identified relatively easily from data. In this section, the system-identification method is used to derive and identify a Hammerstein-structure (Johansson, 1993) based engine-torque model.

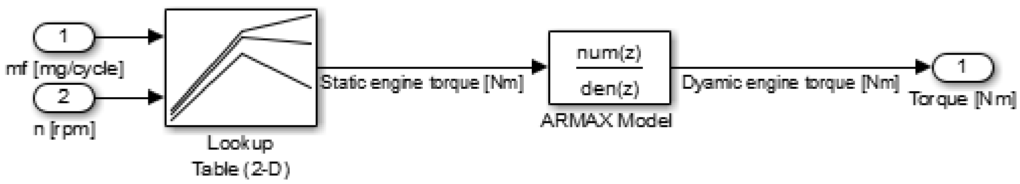

Figure 4.28: Engine torque model Hammerstein structure

The Hammerstein model is one of the most used data-based model structures for non-linear system modelling. In the Hammerstein model (Figure 4.28), the system dynamics are represented by a transfer function, and the non-linearities can be captured by using a non-linear look-up table.

In this engine-torque model, the compensation of the non-linearity can be successfully approximated by using a look-up table (Figure 4.29), and this look-up table depends on engine speed n and fuel injection m_f.

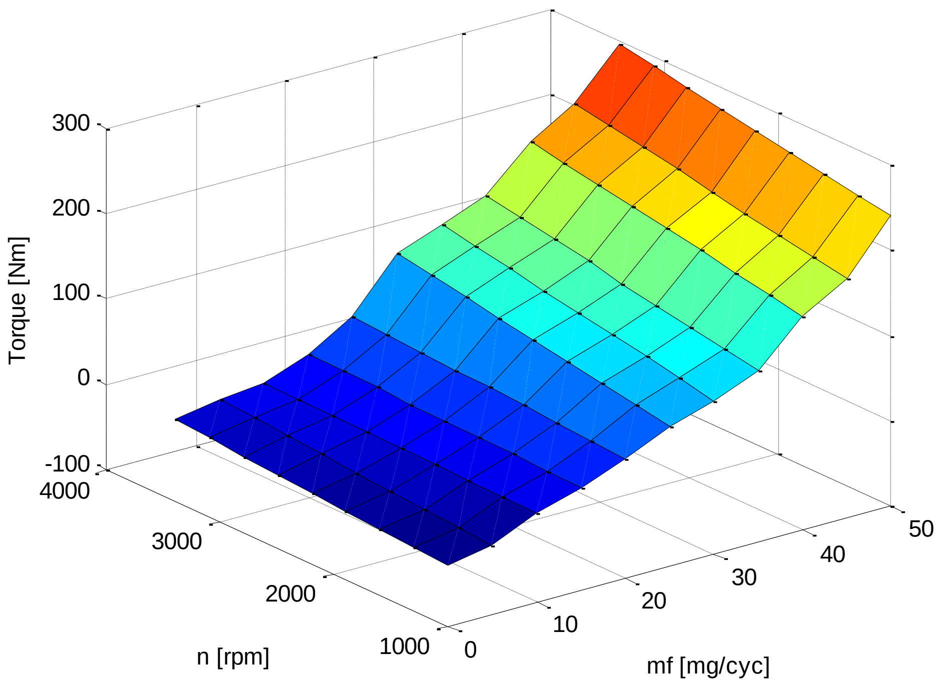

Figure 4.29: Hammerstein lookup table for torque modelling

As the linear part of the system can be described by a mathematic model, an efficient way to identify the system is to use the Matlab/Simulink product, System Identification Toolbox (MathWorks, 2018). The system can then be described using an autoregressive-moving-average-with-exogenous terms (ARMAX) model (Johansson, 1993), as shown in Equation 4-44:

$$A(q) \cdot y(t) = B(q) \cdot u(t - n_k) + C(q) \cdot e(t), \quad (4\text{-}44)$$

where (1) $y(t)$ and $u(t)$ denote the system output and input at time point t respectively,

(2) $e(t)$ describes the white-noise system disturbance value,

(3) the parameters *na*, *nb* and *nc* are the orders of the ARMAX model,

(4) *nk* is the delay,

(5) *q* is the delay operator, and

(6) *A(q)*, *B(q)* and *C(q)* can be described by a second- or high-order polynomial.

4.5 Simulation of Engine-air-path

The aim of this section is to determine whether the engine-air-path model is suitable for the simulation of the engine of interest in both stationary and in dynamic operation conditions. For this purpose, the accuracy of the simulation results needs to be assessed in comparison to the experimental data registered, both in the stationary test and in the dynamic test. The results of the model simulation and validation are discussed in this section.

4.5.1 Stationary Simulation

As shown in Section 4.3, during the ESC stationary tests, the engine is operated in steady conditions under different loads. Please refer to Section 4.3 for the details of the test-bench setup in the ESC test. The implementation of the engine-air-path model in Simulink represents the structure presented in Figure 4.6. The setup of the Matlab/Simulink simulation model is shown in Figure 4.30. The first step in running the simulation model is to store the inputs and outputs of all measured channels in new variables (see Table 4-5).

Table 4-5: Inputs and outputs of the simulation model

Inputs	Outputs
Engine Speed	MAF
Fuel Injection	MAP
VGT Position	Engine Torque
EGR Position	NOx Emission
	OPAC Emission
	Lambda
	Oxygen Concentration

During the simulation, not all of the original simulated data are stored. For example, areas with constant values are not useful for analysis, so they are omitted. All of the 13 mode simulations (see Table 4-6) are treated in this way by using stationary inputs. The simulation dataset is stored in a Matlab mat-file with the time vector. In the second step, the outliers of the original simulation results have to be removed and the amount of data has to be reduced. Outlier detection and filtering are done by the Matlab filter function. The filtered and resampled data are stored in a mat-file. After filtering, the average value of each mode simulation over the run time is calculated.

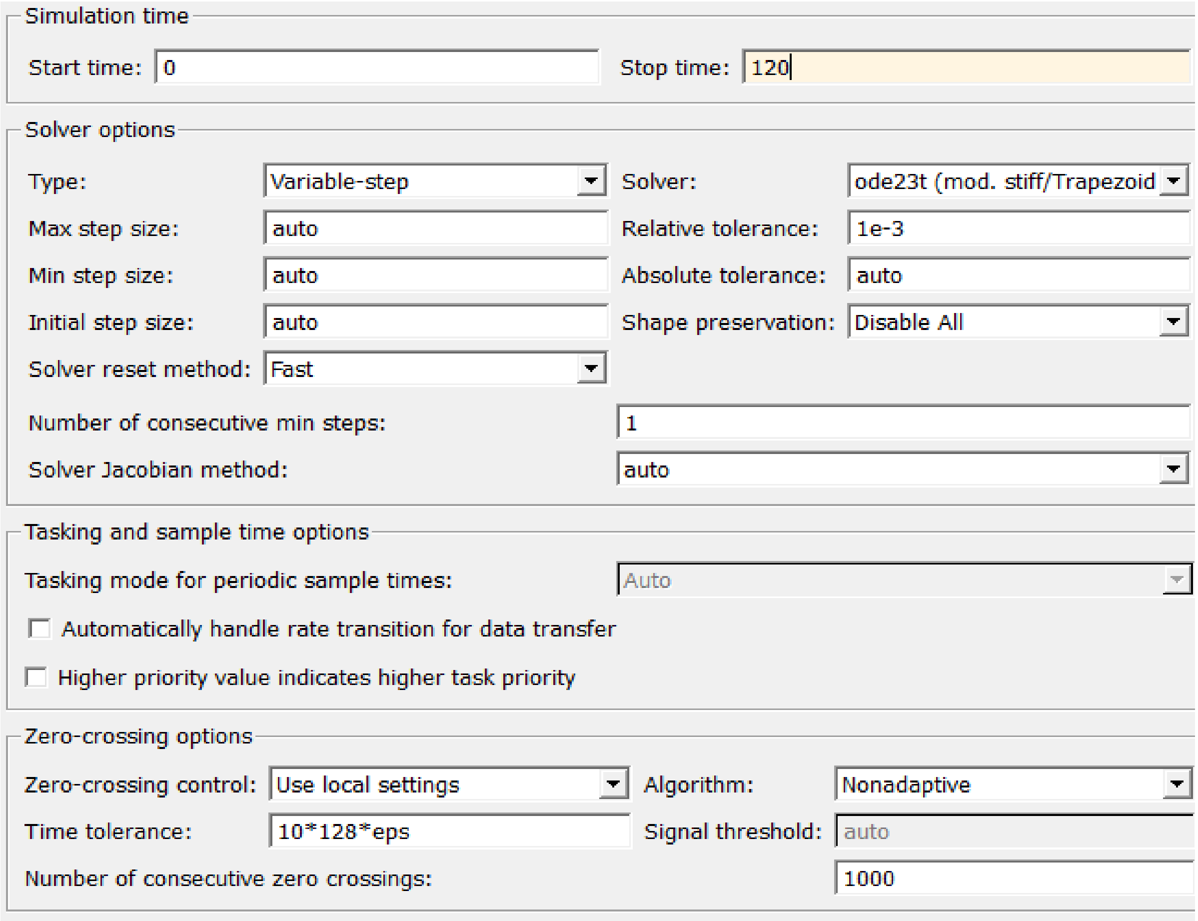

Figure 4.30: Setup of the Matlab/Simulink simulation model

The measurements are reported in Table 4-6 together with the results obtained from the simulation of the same test with the engine air-path model. Table 4-6 presents an overview of the steady-state measurement and model prediction. The experimentally measured ESC-weighted values of BSFC, NO_x emissions and PM emissions from the diesel engine are, respectively, 220.45, 3.09 and 0.051 g/kWh. For the stationary simulation, the BSFC, NO_x emissions and PM emissions simulated by the engine air-path model are, respectively, 233.27, 3.19 and 0.049 g/kWh. The relative errors of BSFC, NO_x emissions and PM emissions are, respectively, 5.5%, 3.1% and -5.2 %. As can be seen from the validation results, the proposed mean-value simulation model constitutes a good representation of the real system.

Table 4-6: ESC measurement and simulation

		Measurement			Simulation			Difference		
Nr.	**Point**	**BSFC**	**NOx**	**PM**	**BSFC**	**NOx**	**PM**	**BSFC**	**NOx**	**PM**
-	-	**[g/kWh]**	**[g/kg]**	**[mg/kg]**	**[g/kWh]**	**[g/kg]**	**[mg/kg]**	**%**	**%**	**%**
0	Idle	177.57	0.25	2.78	197.46	0.27	2.45	10.1	7.3	-13.3
1	A25	280.37	0.22	6.92	319.63	0.24	5.90	12.3	8.9	-17.2
2	A50	218.69	0.35	7.28	227.88	0.36	6.96	4.0	2.9	-4.6
3	A75	195.33	0.43	9.00	187.12	0.44	9.40	-4.4	2.1	4.2
4	A100	187.85	0.64	6.42	190.48	0.65	6.33	1.4	1.0	-1.5
5	B25	281.31	0.23	6.30	312.81	0.25	5.56	10.1	7.3	-13.3
6	B50	221.50	0.35	7.11	243.20	0.37	6.38	8.9	6.4	-11.5
7	B75	200.93	0.36	9.25	206.56	0.36	8.98	2.7	1.9	-3.0
8	B100	190.65	0.60	6.64	187.99	0.61	6.74	-1.4	0.7	1.4
9	C25	301.87	0.23	9.16	323.00	0.24	8.49	6.5	4.7	-7.9
10	C50	247.66	0.30	6.77	254.60	0.30	6.57	2.7	1.9	-3.0
11	C75	232.71	0.46	7.07	239.23	0.47	6.86	2.7	1.9	-3.0
12	C100	217.76	0.63	7.86	220.81	0.64	7.74	1.4	1.0	-1.5
Weighted Value of ESC		**Weighted**	**Weighted**	**Weighted**	**Weighted**	**Weighted**	**Weighted**	**Weighted**	**Weighted**	**Weighted**
		g/kWh	**g/kWh**	**g/kWh**	**g/kWh**	**g/kWh**	**g/kWh**	**%**	**%**	**%**
		220.45	3.09	0.051	233.27	3.19	0.049	5.5	3.1	-5.2

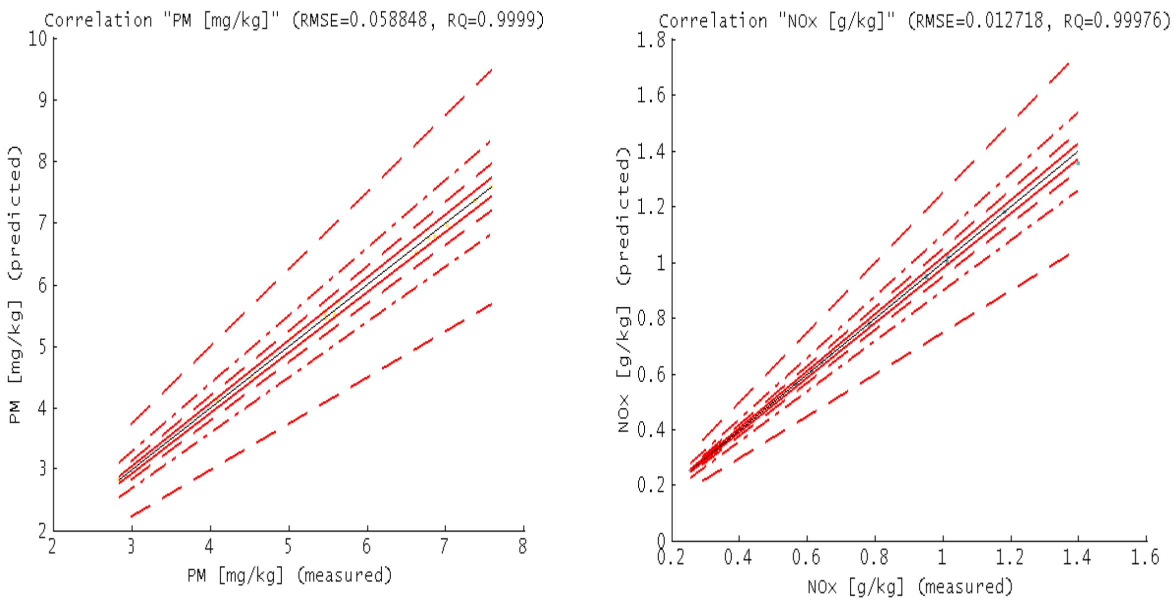

Figure 4.31: Correlation plot for NOx emissions and PM emissions

The correlation plot can be displayed for the outputs separately. The ideal correlation and some standard error lines are available for NOx emissions and PM emissions in Figure 4.31. The correlation plot provides information about the root mean-square error and the determination correlation criterion. As shown from the validation results, the purposed mean-value model is able to provide sufficient precision for the steady-state.

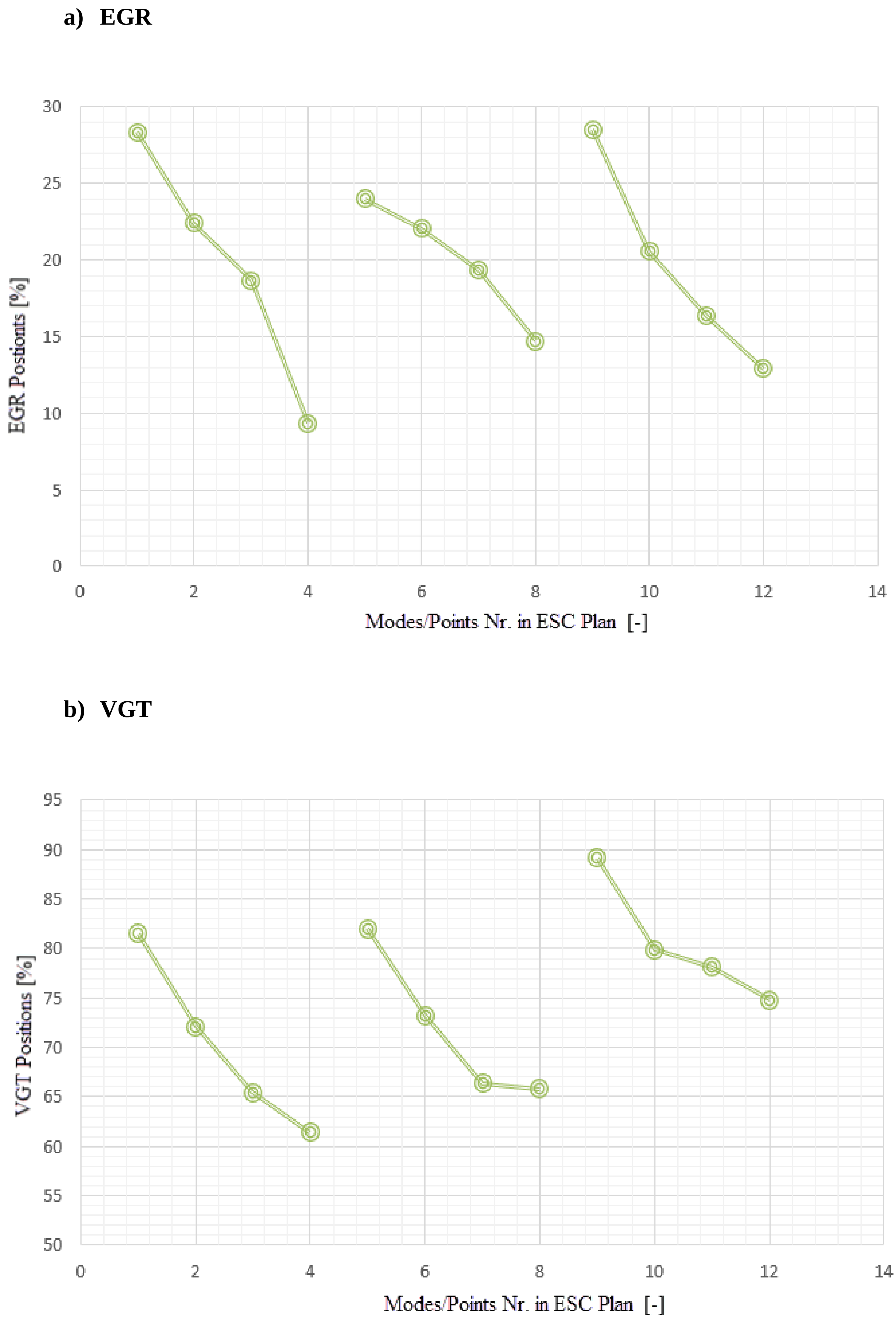

Figure 4.32: a) EGR and b) VGT positions in ESC test

When compared with the BSFC and PM, it can be seen that, indeed, the prediction of NOx is the most accurate. The overall errors in Table 4-6 might be surprisingly small, but it has to be said that transient effects are not considered in this steady-state validation. This means that these simulation results quantify errors only in the steady-state response of the engine, and the model quality has to be further validated under the dynamical operation. The comparison of the experiment and simulation results coincides with the research results in (Ni, Liu, & Shi, 2016). The EGR and VGT positions are available in Figure 4.32. Compared to a WG diesel engine with similar configuration, the BSFC of the VGT-EGR diesel engine is slightly higher than the WG diesel engine. There are two main reasons. First, the exhaust gas from the EGR heats the air inflow of the combustion cylinder to a certain degree, which reduces the fresh-air charging coefficient of the diesel engine. Second, the reduction of oxygen concentration in the cylinder by the EGR affects the combustion process. The specific heat capacity of the exhaust gas becomes large, which reduces the combustion temperature in the cylinder and the thermal efficiency of the diesel engine.

VGT-EGR system has been able to reduce the diesel emissions to a certain extent, but its EGR system fails to be adjusted on demand: as shown in Figure 4.32, the air-fuel ratio of the diesel engine is relatively large at small load which could lead to a larger EGR rate. The air-fuel ratio is great under heavy load, so the economic efficiency declines under the existing EGR rate. Meanwhile, the VGT turbocharger has low control accuracy, so it fails to meet the higher emission performance and power requirements. Therefore, the ECU control is replaced by a more advanced controller in this study. Analysis of the results shows that the raw emissions of NOx of this diesel engine can only meet the requirements of Euro IV and emissions of PM can only meet the requirements of Euro III. Therefore, further optimisation is required to reduce the emissions. In this study, the NMPC method is used on the EGR and VGT control to achieve better regulation of VGT and EGR to improve the emission performance of the engine without changing the structure of the cylinder. The engine efficiency is then improved under the premise of fuel consumption.

4.5.2 Dynamic Simulation

To validate the model in dynamical operation, the dynamic FTP-75 cycle test was performed on the engine test-bench. Please refer to Section 4.3 for details of the test-bench setup of the

FTP-75 cycle test. The same FTP-75 test has been simulated by means of the engine-air-path model to assess the agreement between the prediction of the model and the results of the measurements. The configuration of the Matlab/Simulink simulation model is the same as shown in Section 4.5.1. In the FTP-75 test, instead of the stationary mode simulation, the measured FTP-75 variables value of EGR (%), VGT (%), *n* (rpm) and *mf* (mg/cycle) are used as inputs for the model with a simulation time of 1372 seconds.

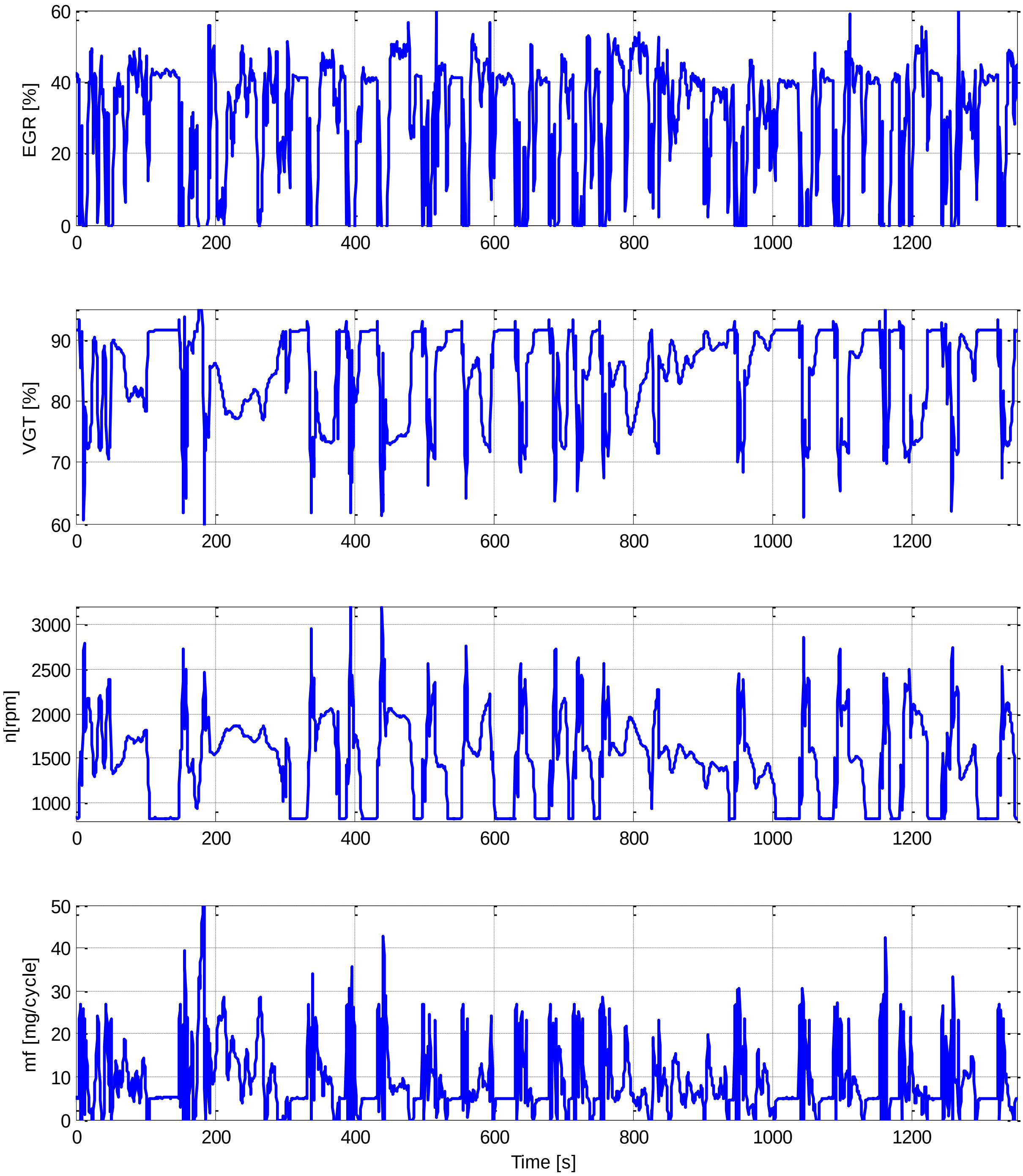

Figure 4.33: FTP-75 simulation model inputs (0~1372s)

Figure 4.33 illustrates the given variable inputs as functions of time. This engine-air-path model could also be connected with a vehicle drive-train model for calculating the speed, acceleration and gear shifting of the vehicle. However, as the main focus of this study is the control of the EGR and VGT, the calculation of vehicle dynamic is not included in this model.

4.5.2.1 MAF and MAP

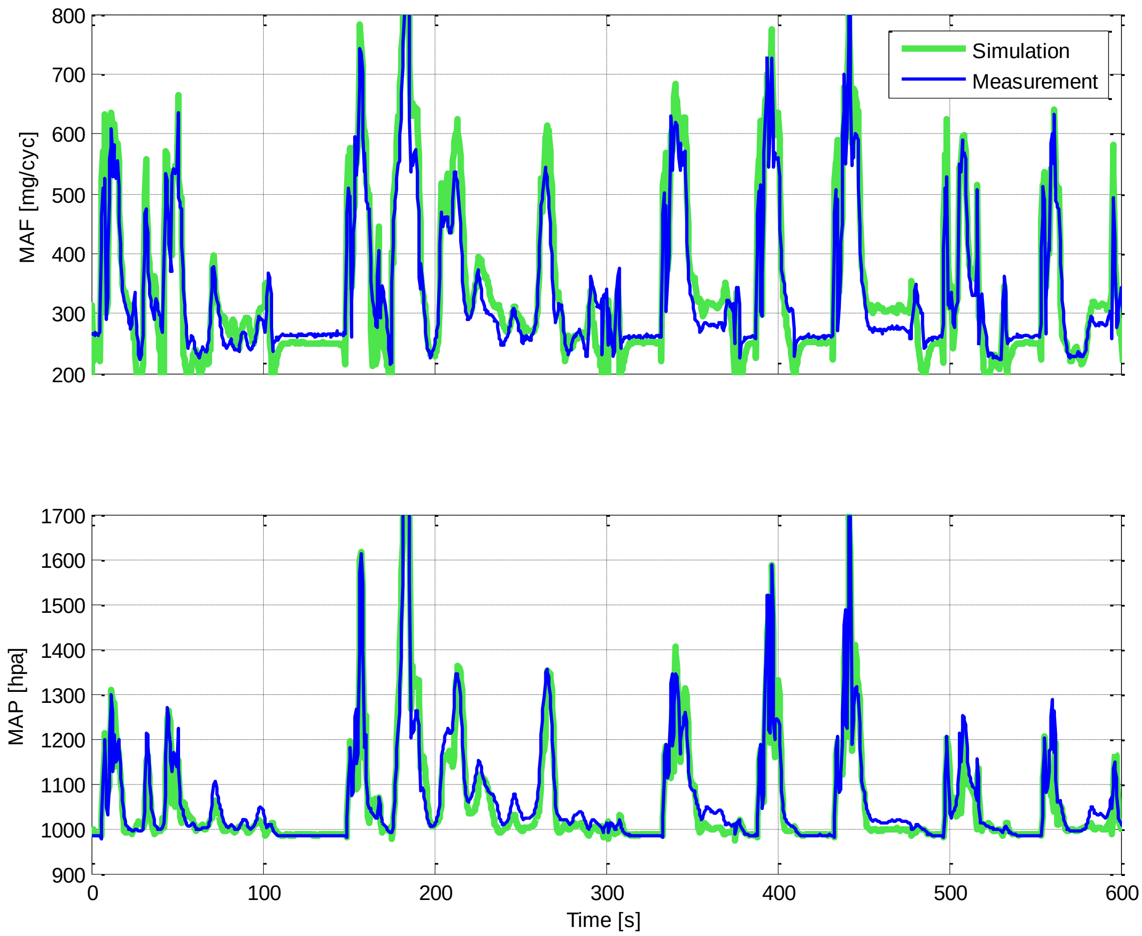

Figure 4.34: Dynamic validation of the simulation results MAF and MAP (0-600s) (VAF_{maf}=91%, VAF_{map}=90%)

As previously stated, the main purpose of VGT and EGR is the improvement of engine MAF and MAP; therefore, the MAF and MAP are modelled. For the purpose of verification, a comparison of the measurement and of the simulation results of MAF and MAP is reported in Figure 4.34. The figure clearly shows that the dynamic responses of the MAF and MAP are very well reproduced by the model: The VAF_{maf} = 91% and the VAF_{map} = 90%. The VAF values are calculated by Equation 3-6. It can be observed that the MAF and MAP are kept below 800 mg/cycle and 1700 hPa, respectively, and that the MAP increased when the MAF increased. In the experiments in which the engine is measured, the ambient pressure is 980 hPa; therefore, the simulation result of MAP never falls below 980 hPa. It can be concluded that the overall quality of the MAF and MAP models are sufficient for the qualitative tests of control deign.

4.5.2.2 Emissions

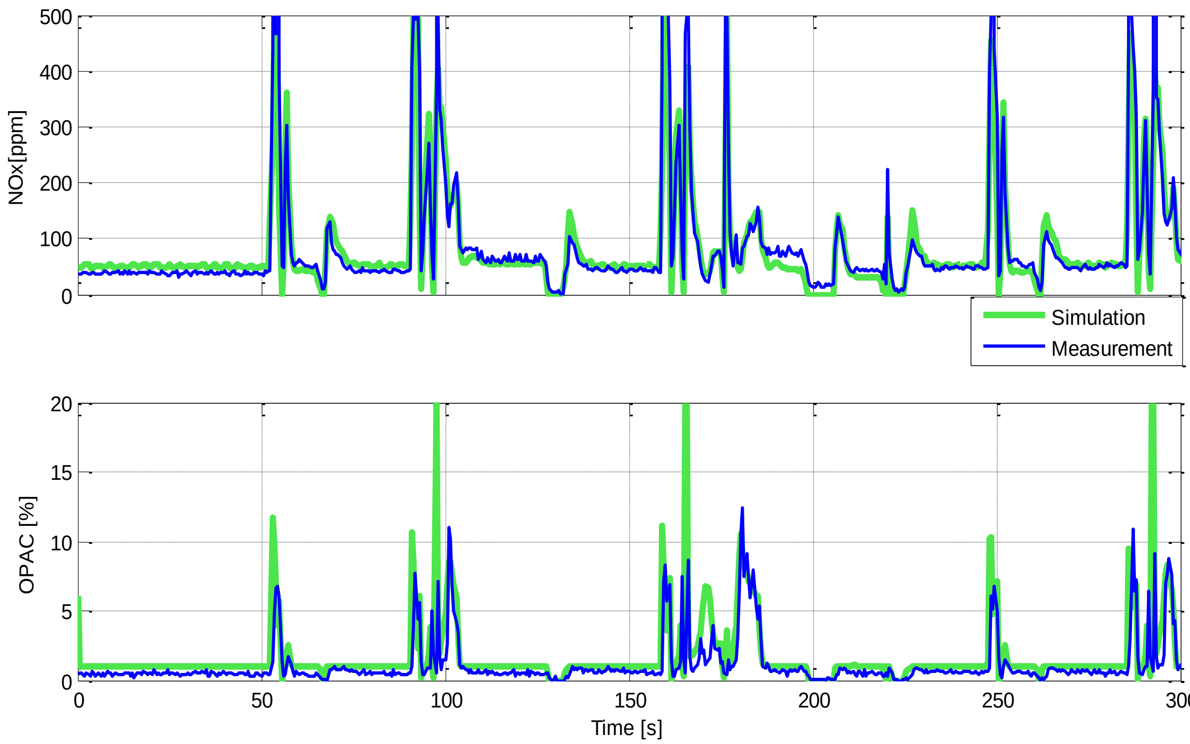

Figure 4.35: Identification of the NOx and OPAC models (VAF_{NOx}=88%, VAF_{PM}=85%)

A comparison of the identifications can be seen in Figure 4.35. The validation of NOx and OPAC is shown in Figure 4.36 with respect to how they predict efficiency. This shows that the NOx model with VAF_{NOx} = 83% agrees better with measured data than the OPAC model with VAF_{PM} = 81%. The VAF values are calculated via Equation 3-6. The cause for this behaviour is that the contribution in the production of NOx comes from the reaction of nitrogen and oxygen under the effect of the combustion. The level of NOX is strongly correlated with combustion temperature. Unfortunately, the mechanism of the particulate matter is more complex due to the unknown oxidation process during the combustion. This limited information is given as input to the system identification process; therefore, it is not surprising when NOx model exhibits better quality. However, in both cases, the relative error in VAF is in the acceptable tolerance level.

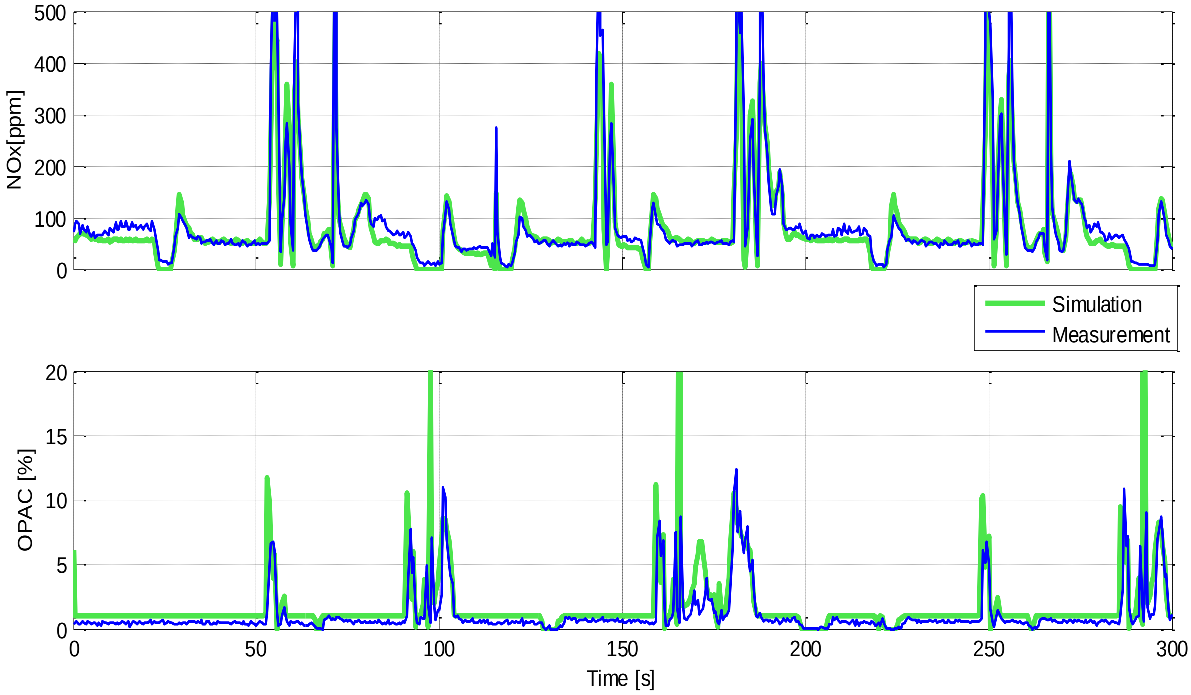

Figure 4.36: Validation of the NOx and OPAC models (VAF_{NOx}=83%, VAF_{PM}=81%)

The relationship between emissions and lambda is shown in Figure 4.37. It can be observed that the lambda value for diesel engines is either small at part load or stoichiometric at middle and full loads. However, some areas of course exhibit extreme lambda values. It seems to be the case that the engine operates sometimes in lean conditions, and the charged air is much greater than the required fuel injection at these operation points. As mentioned in Section 2.2, the combustion temperature has a significant impact on the NOx formation. However, during the combustion, high temperature is not the only reason for high NOx; temperature is also high because of a high oxygen concentration in the combustion chamber. The combination of both temperature and available oxygen is crucial.

As shown in Figure 4.37, when lambda values are close to 1 due to the high temperature caused by a favourite combustion condition, the engine produces the most emissions of NOx. The OPAC increased with lower lambda values, primarily because the mixture has too little oxygen, which means a larger number of partial combustions have occurred. Reduction of the NOx emissions of the diesel engine is mainly caused by the fact that the recirculating exhaust gas of the EGR system contains more polyatomic molecules, such as CO_2, H_2O, etc., which increase the specific heat capacity of the cylinder mixture and reduce the cylinder combustion temperature. Therefore, the conditions required by NOx formation can be controlled. Meanwhile, the circulating exhaust gas can reduce the oxygen concentration in the cylinder and reduce the rate of chain reactions during combustion, thereby resulting in a decrease in adiabatic flame temperature. These factors significantly reduce the NOx emissions of the VGT-EGR diesel engine. As for the rise of the diesel engine PM, the analysis indicates that the main reasons are as follows: The circulating exhaust gas dilutes the oxygen concentration in the cylinder, which results in the reduction of local oxygen enrichment and reduces the possibility of NOx formation. On the other hand, it also exacerbates the regional hypoxia and prompts the generation of PM. Meanwhile, the decrease in the combustion temperature in the cylinder also affects the oxidative decomposition after the formation of PM, which significantly increases the PM emissions of the VGT-EGR diesel engine. The methods used in diesel engines to reduce both particle and NOx conflict with each other. If an attempt is made to lower the number of particles, the NOx emissions become worse.

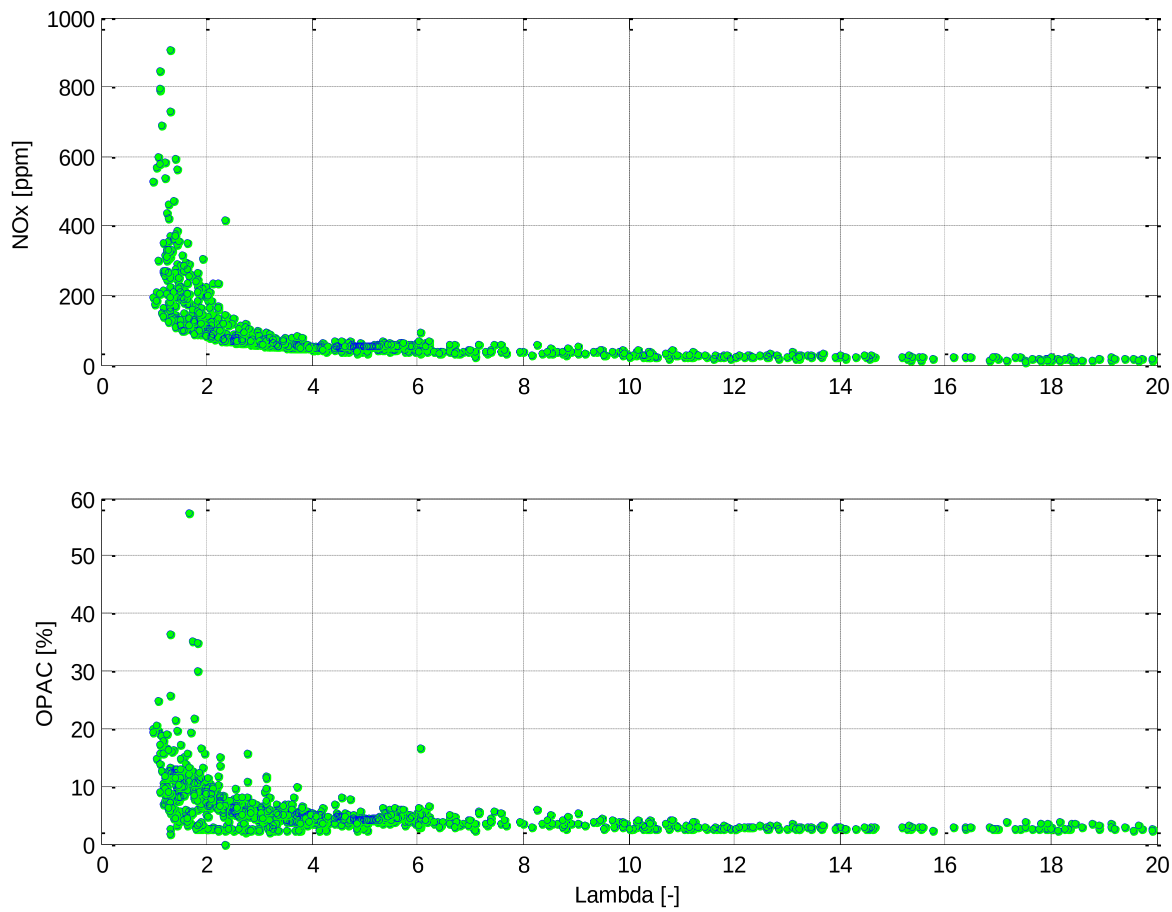

Figure 4.37: Simulation results Lambda over NOx and OPAC

For the future emission optimisation, it is important to handle the NOx-PM (OPAC) trade-off problem and reduce both values to fulfil the laws regarding exhaust-gas emissions. This is a true multiple-target optimisation that leads to a set of pareto-optimal solutions. At this point, the selection of the solution can also be performed by means of other criteria (e.g., of NOx or PM).

A NOx-PM (OPAC) pareto in Figure 4.38 is generated from the simulation. As they are coefficients to values of different units: e.g., NOx in ppm and OPAC in %. Therefore, to better illustrate the results, the NOx and PM values are shown as the normalised ratio of NOx (norm(NOx)) and OPAC (norm(OPAC)). This pareto plot shows the relation of NOx and OPAC model outputs. It allows us to judge a state in which it is not possible to improve NOx output without having to simultaneously degrade the OPAC. To solve this pareto-optimal problem with respect to the optimisation criteria, the engine-air-path model is employed to find the optimal values of MAF and MAP in different operating conditions, thereby to improve the NOx and OPAC emission performance and the premise of unchanged fuel consumption of the diesel engine.

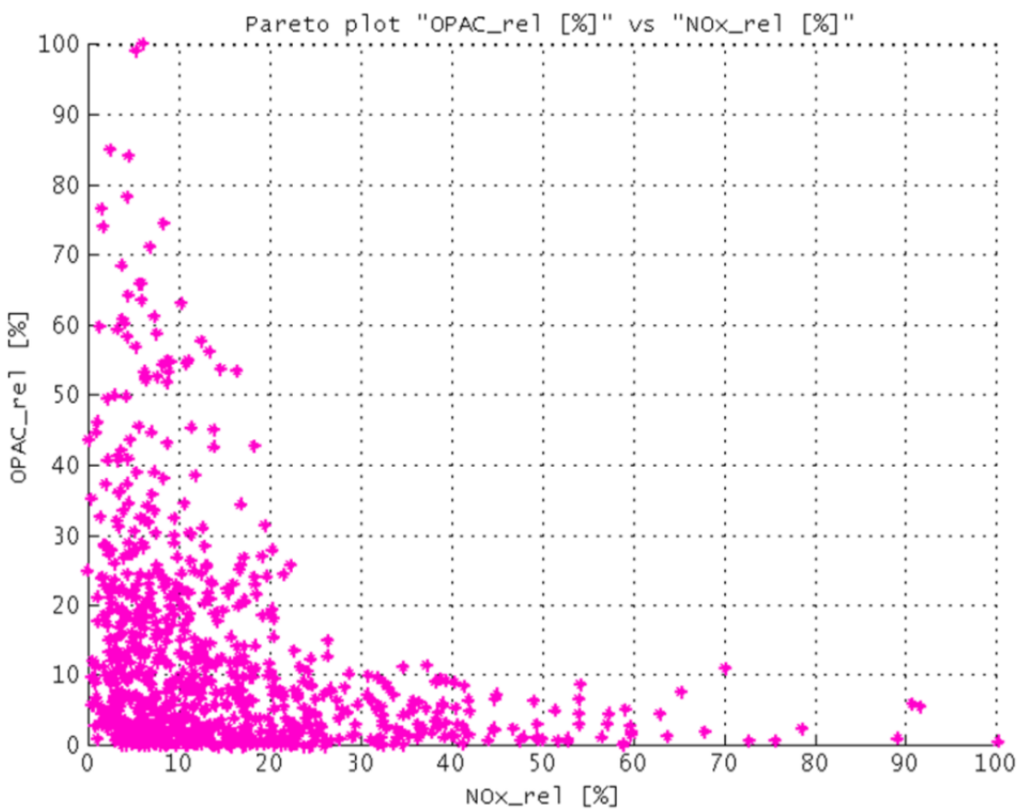

Figure 4.38: Pareto plot of NOx and OPAC

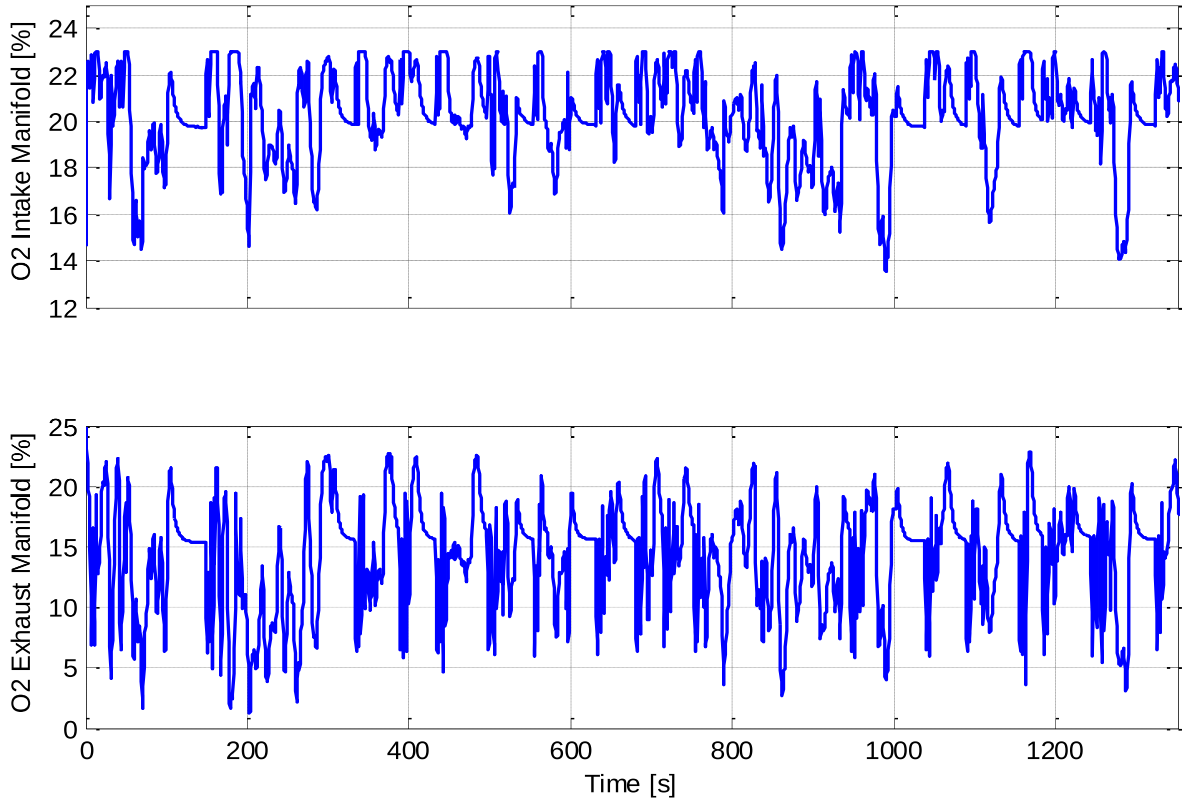

Figure 4.39: FTP-75 cycle simulation results oxygen concentration in intake and exhaust manifold (0~1372s)

Figure 4.39 shows the simulation results of oxygen concentration in the intake and exhaust manifolds. The details of the Matlab/Simulink setup in the FTP-75 cycle have been explained in Sections 4.5.1 and at beginning of Section 4.5.2. During the FTP-75 cycle simulation, the oxygen concentration in the ambient under room temperature is around 23%; in the intake manifold, the oxygen concentration is under 23%. The main reason for these results is the EGR mechanism: A part of the exhaust gas is mixed with the fresh air and brought again to the intake manifold. From 800 to 900s, the engine probably operates in a high operation area; therefore, oxygen concentration is relatively low. In the combustion, the methane and oxygen are transformed mainly into carbon dioxide and water; thus, the oxygen concentration in the exhaust manifold is clearly smaller than in intake manifold, as shown in Figure 4.39.

So far, the output emissions are modelled with the engine control variables. In addition, internal variables from the particular measurement dataset – such as MAF and MAP – can be used as the model input variables. This is useful if the aim of the optimisation introduced in the second part is not the calculation of control characteristics for the manipulated variables but command-variable mapping characteristics for secondary control, such as VGT and EGR. The identified model is able to represent the emission of the real air-path subsystem in the whole operating range. This model is also used to calculate the optimal reference values, as is mentioned in Chapter 6.

4.5.2.3 Engine Torque

Figures 4.40 and 4.41 show the torque model output together with identification and validation data. Globally, the engine torque dynamic is well predicted by the data-based model. The relative error increases in the negative torque area. The braking management system should influence the torque output. The validation results VAF value of 80% indicates that this level of model performances is satisfactory for the further study. The VAF values are calculated by Equation 3-6.

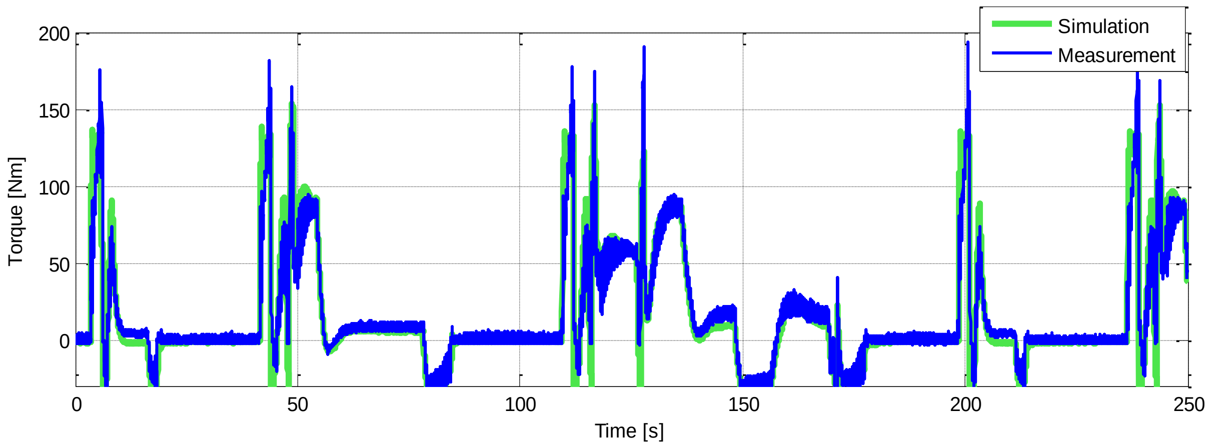

Figure 4.40: Identification of the torque model (VAF_{torque}=88%)

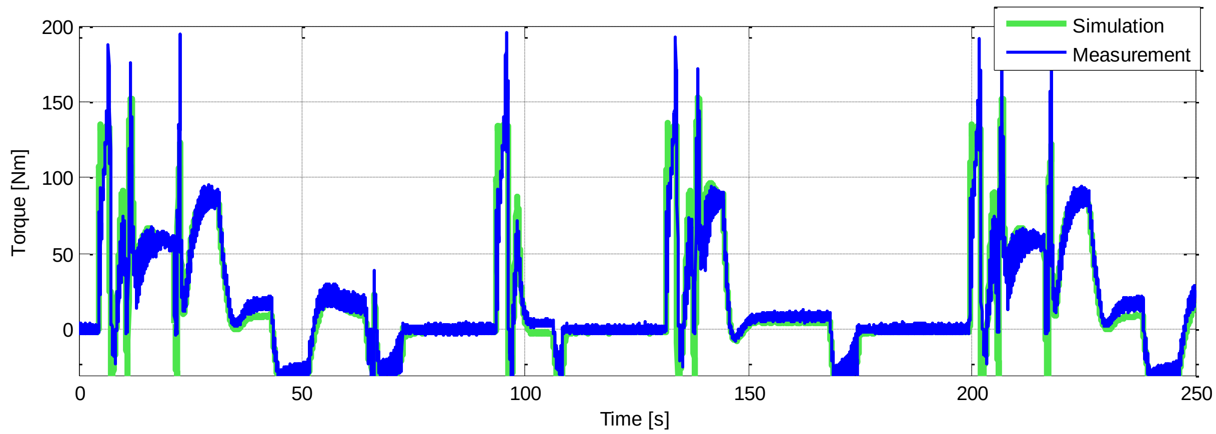

Figure 4.41: Validation of the torque model (VAF_{torque}=80%)

4.6 Summary

This chapter describes the modelling approach developed starting from experiment and thermodynamic theory of combustion engine and simulation tools, which includes a detailed simulation platform and a system identification tool. It aims to facilitate the design of equivalent fuel consumption with better emissions, both in stationary and dynamic conditions, by considering the next emission standard for sustainable and energy-effective individual mobility. The final engine-air-path model is in a good agreement with measurements such MAF, MAP, NOx, PM and the dynamics behaviour of each system. Thanks to advances in system modelling by Matlab/Simulink, this engine-air-path model guarantees fast simulation, the possibility to simulate different sub-concepts (variations-computation), an analysis of engine-air-path control concepts, and efficient identification of the best control concept under real-world driving cycles and conditions. In this study, these methods and tools have proven to provide time-effective ways to study the impact of engine-air-path control on engine emissions; thus, the established engine simulation model can be well adapted for the design and evaluation of advanced control of the engine-air-path. The next step of this study is to design and validate the NMPC air-path controller based on this engine model. It is expected that simulation results will yield a significant contribution to assess the controller performance under investigation.

Chapter 5. NON-LINEAR MODEL PREDICTIVE CONTROL OF AN DIESEL ENGINE-AIR-PATH SYSTEM

Despite currently ongoing public discussions, the modern diesel engine still represents a favourable platform for a highly-valuable future propulsion-system unit even under changing regulatory boundary conditions and an altered market environment. As emission standards for diesel engines become increasingly stringent, advanced engine-control technologies which provide improvements with respect to emissions and fuel consumption are becoming increasingly important. In automotive ECU today, the PID controller is by far the most dominating form, and more than 90% of all control loops are PID. However, in the diesel engine system, linear control rules are known to give very poor results in many non-linear control cases such as non-linearity, time varying and complex environment (Abidi, Bosche, & El Hajjaji, 2013). As mentioned in Section 2.1, the engine-air path is a typical, non-linear MIMO system, and there is a strong cross-coupling effect between MAF and MAP control loops (Jung, 2003; Nieuwstadt & Kolmanovsky, 2000). In a typical control method, two independent PID control loops are used to control the EGR valve and the VGT actuator, respectively. Obviously, to control a non-linear MIMO system with a PID controller puts a strong restriction on the control performance. As discussed in Section 2.3, the NMPC could be used with favourable properties to overcome the problems raised by non-linear system control. Previous studies (Wang & Steiner, 2011; Wang, Waschl, Alberer, & Del Re, 2012; Wang, Zhang, & Bechkoum, 2016; Wang, Zhang, & Bechkoum, 2019) have shown that the LPV modelling approach can be used to represent non-linear processes more precisely and is a good alternative in terms of model complexity and computational performance for model-based control synthesis. These benefits make NMPC possible in practice.

This chapter discusses an NMPC controller for a diesel engine-air-path based on a special, non-linear model class: LPV. The idea behind the purposed NMPC strategy (Figure 5.1) is to represent the plant model as an LPV model, and the control-objective function in searching optimal solution of QP problem is extended to the parameter-varying cost function by utilising the given LPV model. As mentioned in Section 2.3.4.3, a new online, active-set strategy for the fast solution of QP problems in MPC is developed in (Ferreau, 2014). This strategy builds on ideas from parametric optimisation and is fully suitable for fast, real-time applications. Therefore, in the new NMPC algorithms, this online active set strategy, qpOASES, is used to solve the trade-off between control performance and control effort used. Please refer to Appendix B for the details of the qpOASES.

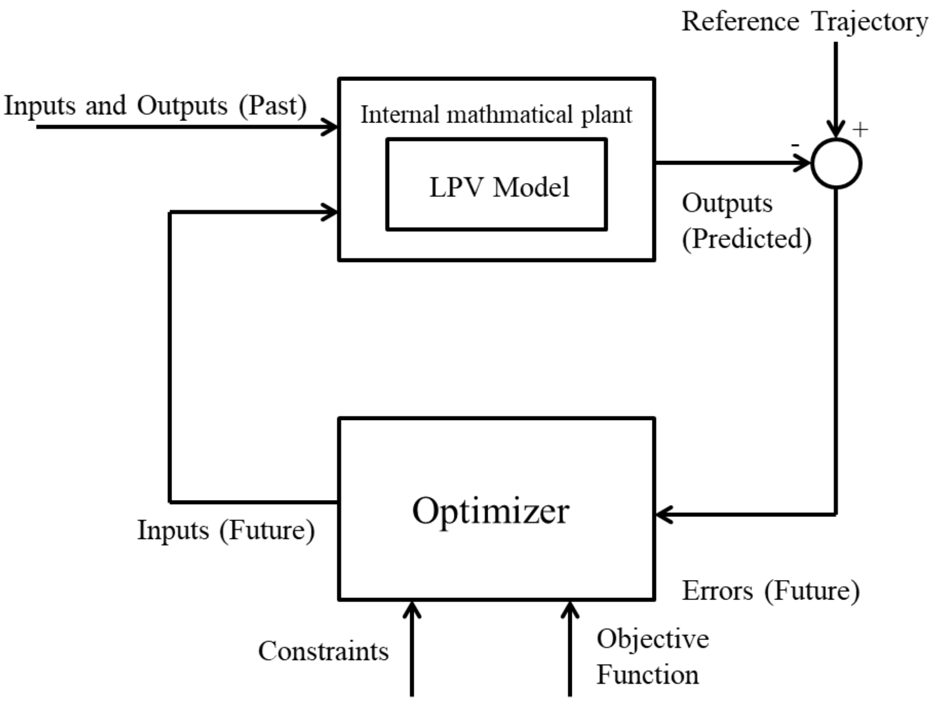

Figure 5.1: Structure of NMPC using LPV model

In Figure 5.2, an extract of the signal-flow scheme for the purposed NMPC application is shown which is characterised by a torque-required structure. It starts with the driver demand, which is typically entered via the fuel injection m_f and engine speed n by adjusting the drive pedal and is equivalent to a demanded engine torque and corresponding vehicle acceleration. To derive this torque, the required MAP and MAF, in dependence on operation point n and m_f are calculated by the engine-management system in ECU maps. These control functions provide the reference values of MAP_{ref} and MAF_{ref} for the NMPC. The chosen reference values, which are derived via the model-based optimisation of emissions and fuel, are provided more in detail in Chapter 6. In the close-loop control scheme, the precise control is realised by the proposed LPV-based NMPC controller, which regulates the position of the EGR and VGT to reach the required MAP and MAF. The block Kalman estimator consists of an estimator for calculating the states of the inputs and outputs of the air-path system for the NMPC controller. Other blocks in Figure 5.2 show the air path and the combustion process with the demanded torque and emissions. However, in a real automobile ECU, the engine-air-path control is more complex and is divided into several possible activities. The structure shown in Figure 5.2 can be considered the main part of the air-path control. The low-level control functions (e.g., the control variants of the special operation states in idle speed, cold start and warm up) are ignored here because they are not the focus of this study.

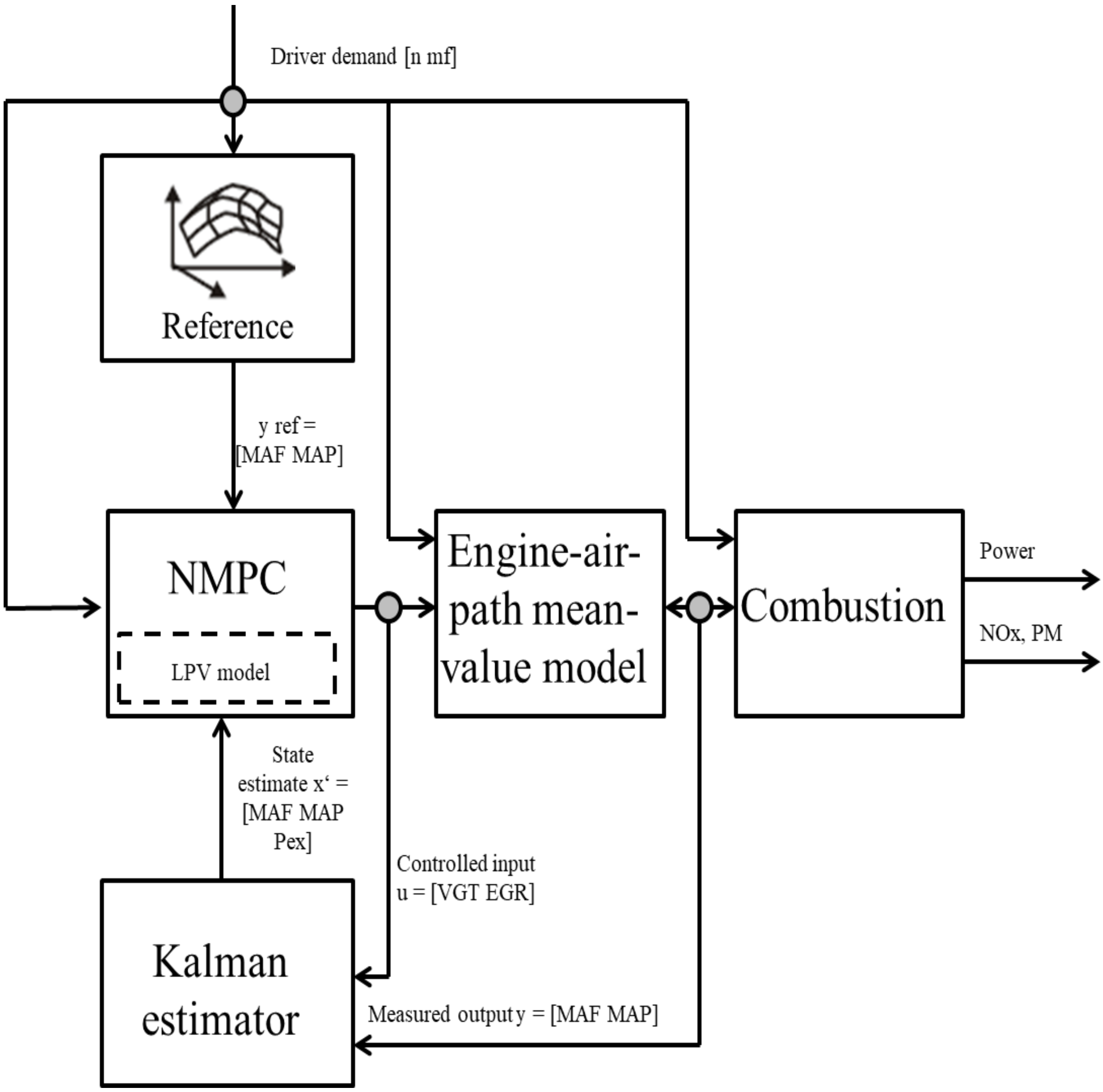

Figure 5.2: NMPC close-loop control scheme in engine-air-path system

The structure of this chapter is as follows. The new LPV-based NMPC approach for the engine-air-path is first given in Section 5.1 with particular emphasis on modelling suitable for NMPC control. This is followed by consideration of an NMPC application of a diesel engine-air-path in Section 5.2. The simulation results of the NMPC controller performance in the engine-air-path are presented, discussed and compared with a linear MPC and a standard ECU at different operation areas in Section 5.3.

5.1 Non-linear Model Predictive Control (NMPC)

As is discussed in the literature review, which follows in Chapter 2, the linear MPC became one of the leading control techniques in the process control industry in the last thirty years, (Langthaler, 2007; Alberer, 2009; Afram & Janabi, 2014). Although most processes encountered in the industry are in practice non-linear, MPC algorithms are generally based upon linear systems. In many applications, the use of a linear MPC can be equate. Many successful applications of linear MPC can be found in the chemical process and refinery industry (Camacho & Bordons, 2007; Richalet, Rault, Testud, & Papon, 1978). Unfortunately, in practice, system non-linearities are very crucial to the closed-loop stability. Studies (Abidi, Bosche, & El Hajjaji, 2013; Casavola, Famularo, & Franze, 2003) have shown that a linear MPC is not effective enough in a complex non-linear system control such as an engine-air-path. This is because a linear model may be restricted in the amount of information it can contain about a process, thereby compromising achievable control quality. An overview of engine-air-path simulation and control approaches is presented in Chapter 2. Compared with most other control techniques, non-linear MPC generally provides superior performance in terms of better transient response, robustness to disturbances and consistent performance under varying conditions. Therefore, NMPC could be a very interesting research area for those who are interested in overcoming the problems raised in the context of engine-air-path control. However, so far as the author is aware, the reported applications of NMPC are still limited. Theoretically, the extension of MPC fundamentals to the non-linear case is straightforward, but in practice, the following challenges have to be faced: 1) the generation of accurate model of non-linear system, 2) the integration of non-linear modelling methods for use in NMPC, and 3) the integration of fast and powerful optimisation techniques for NMPC QP-Solver.

Hence this study seeks a fast, non-linear control application with a special focus on compensation of the non-linearities and the computational burden. In this section, first, the overview of the MPC concept is by presented with the focus on cost functions, QP problems, MPC formulations and stability. In the second part, based on the derived LPV model, an

NMPC is created for the non-linear system-control problems to improve the control performances with respect to tracking, robustness and stability during disturbances caused by operation state changes. The definitions of NMPC are described, and the determination of the LPV model, non-linear control optimisation algorithms and NMPC close-loop representation are given. Finally, the controller layout is presented, and the results are analysed and evaluated.

5.1.1 Model Predictive Control

MPC is an optimal control method based mainly on certain optimisation methods. It uses a model of the process and minimises an objective function to obtain an optimal control action. In contrast to classical feedback controllers, MPC is able, due to its predictive character, to take future reference signals and known future disturbances into account. In addition, input and output constraints can be handled relatively easily. As discussed in Chapter 2, a lot of literature can be found on the theories and practices of MPC (Camacho & Bordons, 2007; Ortner, 2006; Richalet, Rault, Testud, & Papon, 1978). In this study, MPC theory is to be extended to NMPC. To better understand the calculation basis of NMPC, a brief introduction to the general MPC definition and notation shall be given within this section.

The main concept of MPC can be summarised as follows:

- It involves the use of a mathematical model to predict the future output of a determined horizon called Predication Horizon (PH). The model can be a state-space system, a transfer function or any other mathematic representation.
- It also involves the calculation of an optimal control sequence for a shorter horizon called a Control Horizon (CH) by minimising an objective function. The optimisation problem is solved by predicting the future system output by using a model of the plant. This can be done either online during run time or offline.
- It also involves the use of a receding-horizon strategy: i.e., at each time instance, the optimisation is achieved for a finite horizon, which involves the application of the first control signal of the optimised sequence at each step. At next time instance, the horizons move ahead, and iteration processes repeat until the optimal solution is reached.

To present this concept, the basic structure of general MPC is shown in Figure 5.3. An internal mathematical model is used to predict future plant outputs. The future control actions are calculated by the optimiser taking the objective function and the constraints into account.

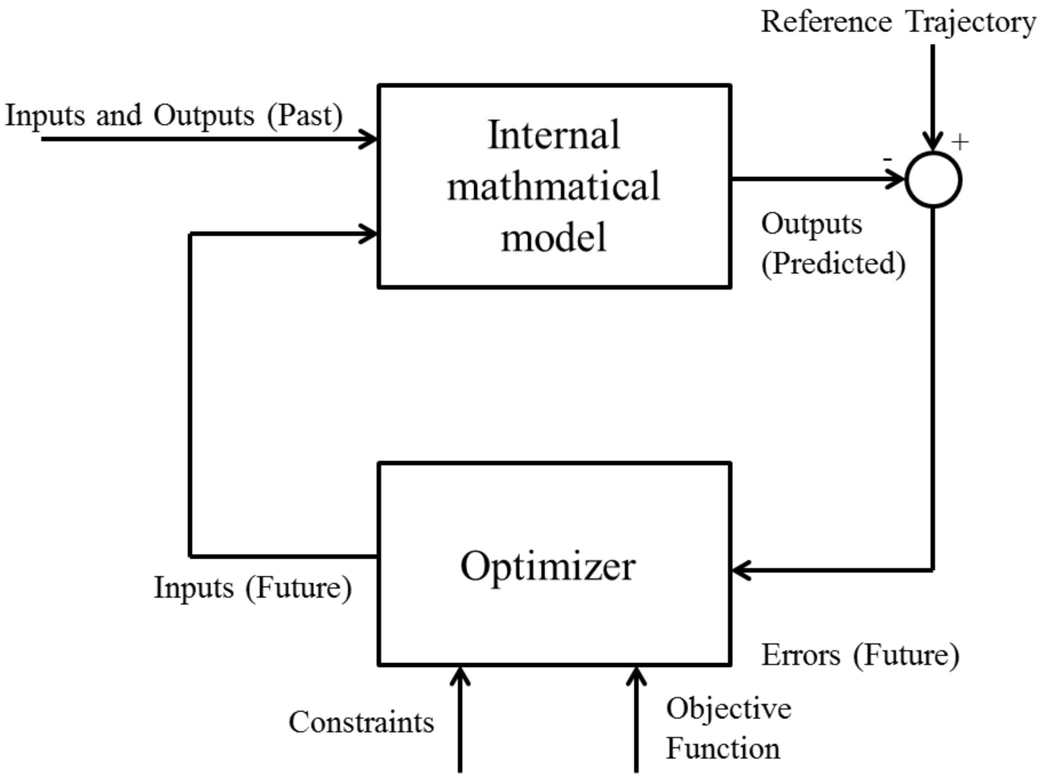

Figure 5.3: Basic structure of a general MPC (Camacho & Bordons, 2007)

When considering engine-air-path control-system characteristics, the MPC approach has several advantages over other control strategies (Nieuwstadt & Kolmanovsky, 2000; Liu & Wei, 2007; Zhao & Pan, 2012):

- Handling of constraints: There are (nearly) always constraints involved in real systems such as the control actuators. In case the engine-air-path controls are constrained, the control values of VGT and EGR must be within the physical limitations of 0% and 100%. The MPC is able to include such constraints on the control value. Besides, MPC can also deal with constraints of changing rates on the control parameters in the optimisation task.
- Handling of MIMO system: Because the optimisation can be done by solving the state-space system representation, coupled MIMO systems can also be considered.

- Handling of future disturbance: By extending the state-space system, a future disturbance approach can be implemented.

Despite many advantages and considerable work on MPC development, areas that may require further investigation still exist and are summarised as follows:

- MPC requires an accurate model for prediction, and the model must be able to reflect the real dynamics in a sufficient way.
- The optimisation task in MPC controller has to be solved, where a unique solution can only be obtained in some special cases. Besides the computational burden, caused by the optimisation task, has to be done at every sampling time instant. The formulation of the optimisation problem of an MPC leads to a QP; this has to be solved to obtain the optimal control sequence.

5.1.1.1 MPC Internal Model

First, MPC requires a proper internal model for calculating the prediction. A survey of MPC in theory is given in (Camacho & Bordons, 2007). This section presents the definition and notation related to the MPC approach, as presented in (Camacho & Bordons, 2007). The classical state-space representation (Equation 5-1) of linear time-invariant systems is a widely accepted form of the MPC internal model (Camacho & Bordons, 2007),

$$\begin{gathered} x(t+1) = A \cdot x(t) + B \cdot u(t) \\ y(t) = C \cdot x(t). \end{gathered} \tag{5-1}$$

In discrete cases, the following formulation in the form of a discrete state-space representation of the process model can be used (Camacho & Bordons, 2007):

$$\begin{gathered} x_{i+1} = A \cdot x_i + B \cdot u_i \\ y_i = C \cdot x_i, \end{gathered} \tag{5-2}$$

where x_i is the state $x \in R^{n_x}$ at time instant i, i is the time-instant number and u and y denote the system input and output, respectively. A is the system state matrix and $\dim[A] = n_x \times n_x$;

B is the system input matrix $\dim[B] = n_x \times n_u$. C represents the system output matrix and $\dim[C] = n_x \times n_y$. Equation 5-2 is subject to the following constraints on inputs and outputs:

$$u_i \in [u_{min}, u_{max}], y_i \in [y_{min}, y_{max}], \forall\, i \geq 0\,. \tag{5-3}$$

5.1.1.2 Receding-horizon Strategy

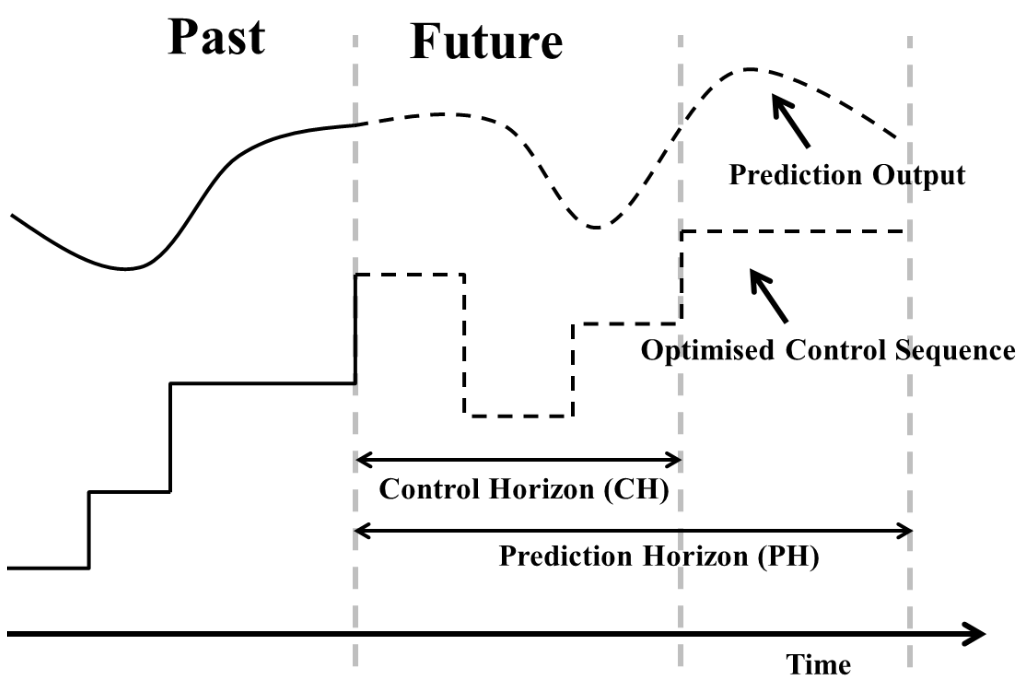

Figure 5.4: MPC receding-horizon strategy (Camacho & Bordons, 2007)

It has been known in (Camacho & Bordons, 2007; Maciejowski, 2000) that making the horizons constrained in predictive control leads to guaranteed stability. This idea basically consists of deriving a future control sequence so that the predicted output over some future time range is constrained to be exactly at a reference value. The receding-horizon strategy in MPC is illustrated in Figure 5.4. There are two temporally significant horizons in MPC: the PH, with length n_{PH}; and the CH, with length n_{CH}. At each time instant, the output of the process is predicted for the next n_{PH} steps within the prediction horizon, depending on the future input sequence. As a receding-horizon strategy is used, only if the first element of the control sequence,u_i or Δu_i, is sent to the plant and all the computation is repeated at the next sampling time. If PH is infinity and there are no constraints, the predictive controller becomes the well-known Linear Quadratic Regulator (LQR). The optimal control sequence is generated by a steady-state feedback law, as the feedback gain matrix is computed via the solution of an algebraic equation. In many applications, the n_{CH} is chosen to be much smaller than the n_{PH} so that the number of variable input signals and therefore the number of optimisation variables is reduced. This leads to less computing time with respect to the optimisation.

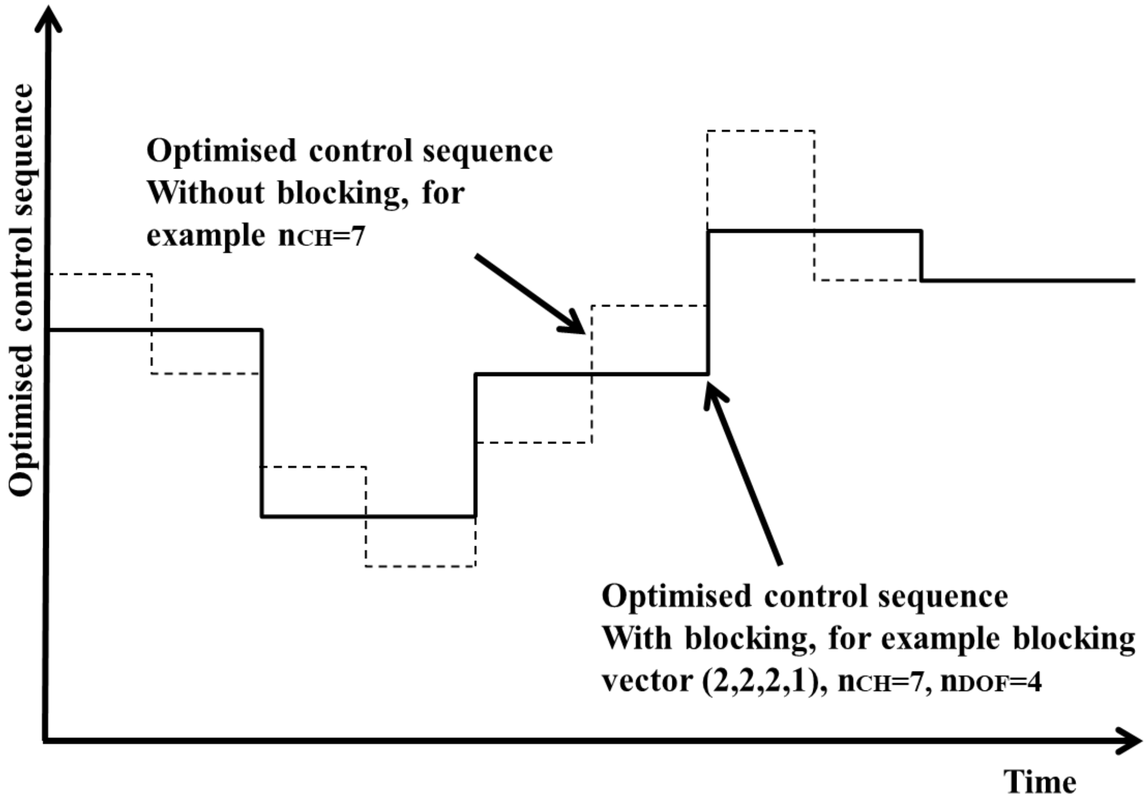

Figure 5.5: Input blocking (Camacho & Bordons, 2007)

Due to these receding horizons, a kind of feedback approach is introduced such that the MPC is able to react to disturbances. In (Camacho & Bordons, 2007), an input-blocking approach is applied to optimise the input sequence. In MPC, to reduce the degrees of freedom of optimisation variables, the predicted control input trajectory is forced to remain constant over some steps (Longo, Kerrigan, & Ling, 2011).

Figure 5.5 depicts the optimised input sequence during the control horizon. This obviously shows that blocking leads to fewer optimisation variables and consequently to a reduced computational burden.

5.1.1.3 MPC Objective Functions

It is widely accepted that an objective function is used in an MPC as a scalar, non-negative measure of controller performance which usually has a quadratic formulation (Ferreau, 2014). Based on the objective function, the MPC solves the quadratic optimisation problem at each control interval (Camacho & Bordons, 2007). Equation 5-4 provides a formulation of the objective function *J* for solving the MPC tracking problem, and this formulation is called a quadratic programming (QP) problem (Alberer, 2009; Zhang, Xue, & Gao, 2018). In Equation 5-4, x_i is the system state at time *i*, and this objective function requires the constrains: system output $[y_{min}, y_{max}]$, system input $[u_{min}, u_{max}]$ and system input change rate $[\varDelta u_{min}, \varDelta u_{max}]$, and the tracking results difference $y_i - y_{ref}$ between system outputs y and given references y_{ref}.

$$J = \quad min_u \frac{1}{2} \sum_{i=0}^{n_{PH}} (y_i - y_{ref})^T Q \left(y_i - y_{ref}\right) + \sum_{i=0}^{n_{CH}} \Delta u_i^T \, R \Delta u_i \tag{5-4}$$

$$subject\ to$$

$$y_{min} \leq y_i \leq y_{max}, i = 0 \dots PH$$

$$u_{min} \leq u_i \leq u_{max}, i = 0 \dots PH$$

$$\Delta u_i = u_i - u_{i-1}$$

$$\varDelta u_{min} \leq \varDelta u_i \leq \varDelta u_{max}, i = 0 \dots CH - 1$$

$$\Delta u_i = 0, i = CH \dots PH.$$

In MPC, a QP-solver involves the minimisation of Objective Function 5-4 subject to constraints, tracking reference and internal mathematical model structure.

Based on Equation 5-2, the predictions for the future system outputs are recursively calculated with the actual system states and future system inputs (Alberer, 2009) :

$$\begin{aligned}
& y_0 = Cx_0 && (5\text{-}5) \\
& y_1 = Cx_1 = C(Ax_0 + Bu_0) = \ CAx_0 + CBu_0 \\
& y_2 = Cx_2 = C(Ax_1 + Bu_1) = \ CA^2x_0 + CABu_0 + CBu_1 \\
& y_3 = Cx_3 = C(Ax_2 + Bu_2) = \ CA^3x_0 + CA^2Bu_0 + CABu_1 + CBu_2 \\
& \vdots \\
& y_{CH} = \ CA^{CH}x_0 + CA^{CH-1}Bu_0 + \cdots + CABu_{CH-2} + CBu_{CH-1}
\end{aligned}$$

$$y_{CH+1} = CA^{CH+1}x_0 + CA^{CH}Bu_0 + \cdots + CA^2Bu_{CH-2} + CABu_{CH-1} + CBu_{CH-1}$$

$$\vdots$$

$$y_{PH} = CA^{PH}x_0 + CA^{PH-1}Bu_0 + \cdots + CA^{PH-CH+1}Bu_{CH-2} + CA^{PH-CH}Bu_{CH-1} + \cdots + CABu_{CH-1} + CBu_{CH-1}.$$

Equation 5-5 can be written in a matrix notation (Alberer, 2009):

$$\begin{bmatrix} y_0 \\ y_1 \\ y_2 \\ y_3 \\ \vdots \\ y_{CH} \\ \vdots \\ y_{PH} \end{bmatrix} = \begin{bmatrix} C & 0 & 0 & \cdots & 0 \\ CA & CB & 0 & \cdots & 0 \\ CA^2 & CAB & CB & \cdots & 0 \\ CA^3 & CA^2B & CAB & \cdots & 0 \\ & & & \ddots & \\ CA^{CH} & CA^{CH-1}B & \cdots & & CB \\ \vdots & & & & \vdots \\ CA^{PH} & CA^{PH-1}B & & A^{PH-CH+1}B & CA^{PH-CH}B + \cdots + CAB + CB \end{bmatrix} \cdot \begin{bmatrix} x_0 \\ u_0 \\ u_1 \\ u_2 \\ \vdots \\ u_{CH-1} \end{bmatrix}. \tag{5-6}$$

The error equation, $e = y - y_{ref}$, can be written in a matrix equation as follows:

$$\mathcal{G} = \mathcal{K} \cdot \mathcal{T}\ , \tag{5-7}$$

where

$$\mathcal{G} = \begin{bmatrix} e_0 \\ e_1 \\ e_2 \\ e_3 \\ \vdots \\ e_{CH} \\ \vdots \\ e_{PH} \end{bmatrix}, \mathcal{T} = \begin{bmatrix} x_0 \\ u_0 \\ u_1 \\ u_2 \\ \vdots \\ u_{CH-1} \\ y_{ref} \end{bmatrix}, \tag{5-8}$$

$$\mathcal{K} = \begin{bmatrix} C & 0 & 0 & \cdots & 0 & -1 \\ CA & CB & 0 & \cdots & 0 & -1 \\ CA^2 & CAB & CB & \cdots & 0 & -1 \\ CA^3 & CA^2B & CAB & \cdots & 0 & -1 \\ \vdots & & & \ddots & & \vdots \\ CA^{CH} & CA^{CH-1}B & \cdots & & CB & -1 \\ \vdots & & & & & \vdots \\ CA^{PH} & CA^{PH-1}B & & A^{PH-CH+1}B & CA^{PH-CH}B + \cdots + CAB + CB & -1 \end{bmatrix}.$$

For tracking control, the rate of input change Δu has to be considered. Thus, in Equation 5-9, the variations of the input signals are defined as $\Delta u_i = u_i - u_{i-1}$.

The vector of Δu from time instant 0 to CH-1 are recursively calculated:

$$\begin{bmatrix} \Delta u_0 \\ \Delta u_1 \\ \vdots \\ \Delta u_{CH-1} \end{bmatrix} = \begin{bmatrix} -1 & 1 & 0 & \cdots & 0 \\ 0 & -1 & 1 & & 0 \\ & & \ddots & \ddots & \\ 0 & & & -1 & 1 \end{bmatrix} \cdot \begin{bmatrix} u_{-1} \\ u_0 \\ u_1 \\ \vdots \\ u_{CH-1} \end{bmatrix}. \tag{5-9}$$

Defining the ΔU, E and $\mathcal{S}$ as follows:

$$\Delta U = \begin{bmatrix} \Delta u_0 \\ \Delta u_1 \\ \vdots \\ \Delta u_{CH-1} \end{bmatrix}, E = \begin{bmatrix} -1 & 1 & 0 & \cdots & 0 \\ 0 & -1 & 1 & & 0 \\ & & \ddots & \ddots & \\ 0 & & & -1 & 1 \end{bmatrix} and\ \mathcal{S} = \begin{bmatrix} u_{-1} \\ u_0 \\ u_1 \\ \vdots \\ u_{CH-1} \end{bmatrix}. \tag{5-10}$$

Integrating Equation 5-10 into the Equation 5-9 yields the following:

$$\Delta U = E \cdot \mathcal{S}. \tag{5-11}$$

Defining the weightings $\mathcal{Q}$ and $\mathcal{R}$ as follows:

$$\mathcal{Q} = diag(Q, \cdots, Q), \tag{5-12}$$
$$\mathcal{R} = diag(R, \cdots, R),$$

thereby yielding the following optimisation:

$$min_u \frac{1}{2}(\mathcal{K}\mathcal{T})^T \mathcal{Q}(\mathcal{K}\mathcal{T}) + (E\mathcal{S})^T \mathcal{R}(E\mathcal{S}). \tag{5-13}$$

Furthermore, Equation 5-13 can be rewritten as follows:

$$min_u \frac{1}{2}\mathcal{T}^T \mathcal{K}^T \mathcal{Q}\mathcal{K}\mathcal{T} + \mathcal{S}^T E^T \mathcal{R}E\mathcal{S}. \tag{5-14}$$

As given in (Alberer, 2009), the $\mathcal{K}^T \mathcal{Q}\mathcal{K}$ in Equation 5-14 has the following dimension:

$$\mathcal{K}^T \mathcal{Q}\mathcal{K} = \begin{bmatrix} \dim x \times \dim x & \dim x \times \mathrm{CH} \dim u & \dim x \times \dim y \\ \mathrm{CH} \dim u \times \dim x & \mathrm{CH}\ \dim u \times \mathrm{CH} \dim u & \mathrm{CH} \dim u \times \dim y \\ \dim y \times \dim x & \dim y \times \mathrm{CH}\ \dim u & \dim y \times \dim y \end{bmatrix}. \tag{5-15}$$

And the $E^T \mathcal{R}E$ in Equation 5-14 has the dimension:

$$E^T \mathcal{R}E\ = \begin{bmatrix} \dim u \times\ \dim u & \dim u \times \mathrm{CH} \dim u \\ \mathrm{CH}\ \dim u \times\ \dim u & \mathrm{CH}\ \dim u \times \mathrm{CH} \dim u \end{bmatrix}. \tag{5-16}$$

According to (Alberer, 2009) and (Ferreau, 2014), the Hessian matrix H and matrix f of the linear inequality related to the QP-solver are expressed as follows:

$$\begin{gathered} H = \mathcal{K}^T \mathcal{Q}\mathcal{K}\ (2,2) + E^T \mathcal{R}E(2,2) \\ f = [\mathcal{K}^T \mathcal{Q}\mathcal{K}\ (1,2) \quad E^T \mathcal{R}E(1,2) \quad \mathcal{K}^T \mathcal{Q}\mathcal{K}\ (3,2)], \end{gathered} \tag{5-17}$$

where $\mathcal{K}^T \mathcal{Q}\mathcal{K}$ (2,2), $\mathcal{K}^T \mathcal{Q}\mathcal{K}$ (1,2) and $\mathcal{K}^T \mathcal{Q}\mathcal{K}$ (3,2) mean the blocks (2,2), (1,2) and (3,2) of $\mathcal{K}^T \mathcal{Q}\mathcal{K}$ in Equation 5-15; $E^T \mathcal{R}E$ (2,2) and $E^T \mathcal{R}E(1,2)$ mean the blocks (2,2) and (1,2) of $E^T \mathcal{R}E$ in Equation 5-16.

These matrices are now suitable for the QP-solver. The vector f is multiplied with a vector $\Theta = [x_i\ u_{i-1}\ y_{ref}]$, which includes information on the current state x_i, the output reference y_{ref} and the previous optimal input signal u_{i-1}. And this vector f is updated at every instant. Ortner, Langthaler, Ortiz and del Re (2006) have shown that, in practice, all processes are subject to constraints: 1) physical limits (actuators have a limited range of action and a limited slew rate), 2) safety limits (pressure or temperature limits), and 3) operating conditions (due to technological limits or economic or environmental reasons). In MPC, the input (manipulated) variables can be kept in-bound by clipping, and its constraints are integrated straightforwardly in the matrices in minimal input lb and maximal output ub:

$$lb \leq \ U \ \leq ub. \tag{5-18}$$

It is common with rate-of-change constrains on the input signal, Δu_{min} and Δu_{max}, that the following calculations are achieved (Alberer, 2009):

$$\Delta U_{min} \leq \Delta U \leq \Delta U_{max} \ , \tag{5-19}$$

where

$$\Delta U = \begin{bmatrix} \Delta u_0 \\ \Delta u_1 \\ \vdots \\ \Delta u_{CH-1} \end{bmatrix}, \Delta U_{min} = \begin{bmatrix} \Delta u_{min} \\ \Delta u_{min} \\ \vdots \\ \Delta u_{min} \end{bmatrix} \ and \ \Delta U_{max} = \begin{bmatrix} \Delta u_{max} \\ \Delta u_{max} \\ \vdots \\ \Delta u_{max} \end{bmatrix}. \tag{5-20}$$

Output constraints must be controlled in advance, as output variables are affected by process dynamics. The neglect of output constraints can reduce economic profit and cause damage to actuators (Alberer, 2009).

Considering Equation 5-7, the output is calculated with

$$Y = [\mathcal{K}_1 \ \mathcal{K}_2] \cdot \begin{bmatrix} x_0 \\ U \end{bmatrix} = \ \mathcal{K}_1 \cdot x_0 + \mathcal{K}_2 \cdot U, \tag{5-21}$$

where

$$U = \begin{bmatrix} u_0 \\ u_1 \\ \vdots \\ u_{CH-1} \end{bmatrix}. \tag{5-22}$$

The constraints are then

$$Y_{min} - \mathcal{K}_1 \cdot x_0 \leq \mathcal{K}_2 \cdot U \leq Y_{max} - \mathcal{K}_1 \cdot x_0. \quad (5\text{-}23)$$

A combination of input rate Equations 5-19 and output constraints Equation 5-23 results in

$$\begin{bmatrix} \Delta U_{min} \\ Y_{min} - \mathcal{K}_1 \cdot x_0 \end{bmatrix} \leq \begin{bmatrix} \Delta U \\ \mathcal{K}_2 \cdot U \end{bmatrix} \leq \begin{bmatrix} \Delta U_{max} \\ Y_{max} - \mathcal{K}_1 \cdot x_0 \end{bmatrix}. \quad (5\text{-}24)$$

5.1.1.4 Disturbance Model

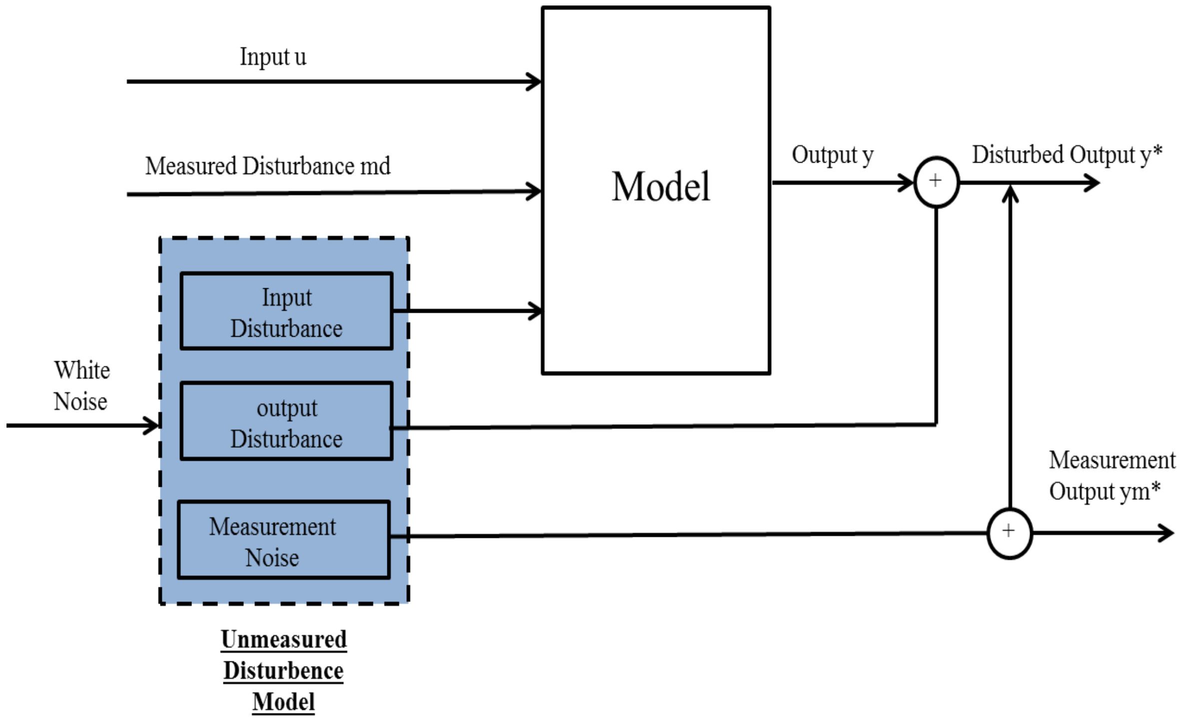

Figure 5.6: Disturbance model (Alberer, 2009)

Many processes are affected by external disturbances caused by variables that can be measured such as those governing the engine-air-path, where the MAF and MAP are controlled by manipulating the EGR and VGT. Any variation of the EGR and VGT will influence the MAF and MAP. These perturbations, also known as load disturbances, can be handled by using feed-forward controllers. Known disturbances can be taken explicitly into account in MPC. To get correct prediction results, this model can be augmented by a disturbance model, as shown in Figure 5.6. These disturbances can represent either input or output disturbances or mixed disturbances. Furthermore, measured disturbances can be considered. These disturbances may be uncontrolled inputs (i.e., inputs not used for control).

In case of the disturbance model, the augmented control model is given in Equation 5-25 (Alberer, 2009), where the plant denotes the state-space representation of the disturbance model. The disturbance can be integrated into the system representation with a manipulated variable u_i and a measured disturbance v_i. The calculation of the H and f matrices is performed as described in Equation 5-17,

$$\begin{bmatrix} x_{i+1} \\ v_{i+1} \end{bmatrix} = \begin{bmatrix} A & B \\ 0 & A_{dist} \end{bmatrix} \cdot \begin{bmatrix} x_i \\ v_i \end{bmatrix} + \begin{bmatrix} B \\ B_{dist} \end{bmatrix} \cdot u_i \qquad (5\text{-}25)$$
$$y_i = [C\ C_{dist}] \cdot \begin{bmatrix} x_i \\ v_i \end{bmatrix},$$

where A, B and C are system matrices, and A_{dist}, B_{dist} and C_{dist} are disturbance matrices.

5.1.1.5 Stability

Stability is one of the more complicated issues in the analysis of a control system. Generally, the stability of a control system can combine Lyapunov stability criteria (Vidyasagar, 1993) and concepts from convergence theory (Bemporad, 2001):

Theorem (Bemporad, 2003) Assume the *V(x)* as a Lyapunov function. Optimal control sequence at time i, $U_i = [\,u_0\, u_1\, u_2\, \cdots\, u_{i-1}]^T$. The feasible sequence at time *i+1 is* $\overline{U}_{i+1} = [\,u_0\, u_1\, u_2\, \cdots\, u_{i-1}\ 0]^T$. The cost function of $\overline{U}_{i+1}$ becomes $V^*(x_i) - {x_i}^T Q x_i - {u_i}^T R u_i \geq V^*(x_{i+1})$, where $V^*(x_i) \geq 0$ and monotonically decreasing, so $\exists \lim_{t\to\infty} V^*(x_i) \triangleq V_\infty$. Hence $0 \leq {x_i}^T Q x_i + {u_i}^T R u_i \geq V^*(x_i) - V^*(x_{i+1}) \to 0$ with $t \to \infty$.Since $R > 0, Q > 0$, therefore $\lim_{t\to\infty} x_i = 0, \lim_{t\to\infty} u_i = 0$.

Theorem (Vidyasagar, 1993) The equilibrium points at the origin of system $x_{i+1} = f_i(x_i)$. Assume X is a positively invariant set in this system, which contains a neighbourhood of the origin in its interior. A function V is called a Lyapunov function in X if for all $x \in X$,

$$V(x) > 0 \; \forall \, x \neq 0, V(0) = 0 \qquad (5\text{-}26)$$
$$V(x_{i+1}) - V(x_i) \leq 0.$$

If a system admits a Lyapunov function in X, then the equilibrium point at the origin is Lyapunov stable in X.

The MPC objective function can be considered as a Lyapunov function. The guarantee of stability can be provided by a finite horizon. In (Cheng & Allgoewer, 1998), the terminal region and stabilising control method with quasi-infinite horizon is given, but only for the computation of the terminal cost. A terminal state equality states a stability constraint, $x_{i+N} = 0$, which leads to initial conditions $X_f = 0$. But for short-prediction horizons, the control action may become very high and performance can be decreased because of this addition constraint (Langthaler, 2007). Furthermore, in (Mayne, 2001), the asymptotic stability theorem is explained. The study shows that, based on Lyapunov theory, one can prove that asymptotically stable systems do not need stability constraints for an infinite prediction horizon. Wang and Steiner (2011) show that the stabilising properties of constrained MPC can be summarised as follows: the unconstrained optimal performance should be retained in the control scheme; the number of decision variables should be kept as small as possible and the set of initial conditions X_0 should be as large as possible.

5.1.1.6 Kalman Estimator

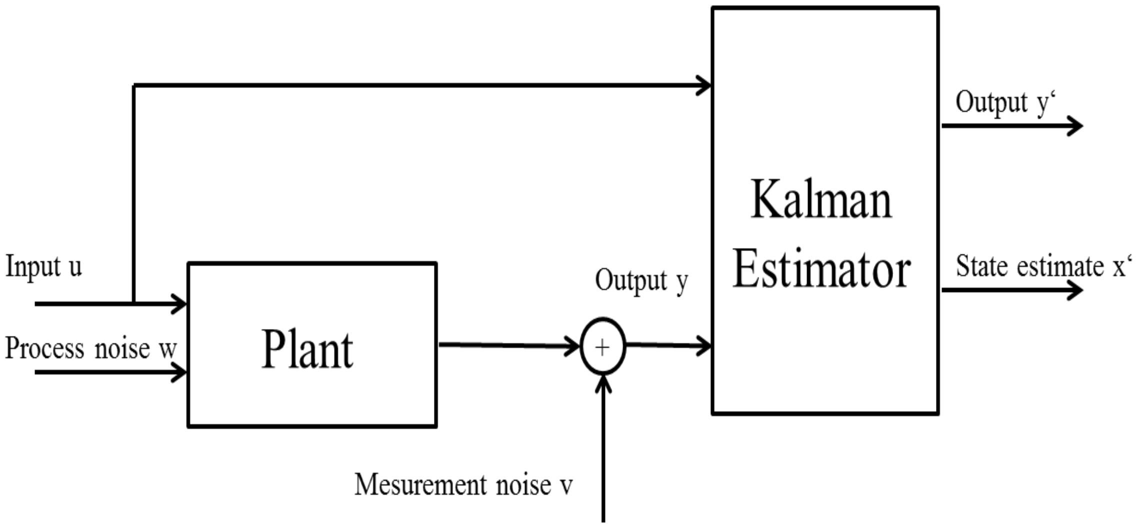

Figure 5.7: Kalman Estimator

For prediction of the system outputs, the MPC controller should use the actual system states as initial values in each iteration. With the help of an observer, as shown in Figure 5.7, Kalman estimator (also called a Kalman filter), the actual states of the MPC internal model can be estimated. This section presents the definition and notation related to the Kalman filter approach, as presented in (Welch & Bishop, 2006).

In general, a Kalman filter is used to estimate states given a plant in discrete time:

$$x_{i+1} = f(x_i, u_i, i) + w_i \qquad (5\text{-}27)$$
$$y_i = g(x_i, u_i, i) + v_i,$$

where x_i denotes the system states, u_i represents the system inputs, w_i represents process noise and v_i represents measurement noise.

The expectations of the two noise terms satisfy the following: $E(w) = E(v) = 0; E(w \cdot w^T) = Q$; $E(v \cdot v^T) = R$; $E(w \cdot v^T) = N$.

The task is to minimise the steady-state error covariance using a state estimate $\hat{x}$:

$$P = \lim_{n \to \infty} E(\{x - \hat{x}\} \cdot \{x - \hat{x}\}^T). \qquad (5\text{-}28)$$

Here, the observer error must be as small as possible to guarantee the stability of the closed loop.

As given in (Welch & Bishop, 2006), the estimator obeys the following equation:

$$\hat{x}_i = A \cdot \hat{x}_{i-1} + B \cdot u_i + L \cdot (y_i - C \cdot \hat{x}_{i-1}). \qquad (5\text{-}29)$$

By solving Equation 5-29, the matrix L can be derived:

$$L = (A \cdot P \cdot C^T + \bar{N}) \cdot (C \cdot P \cdot C^T + \bar{R})^{-1}, \qquad (5\text{-}30)$$

where A, B and C are system matrices $\bar{R} = R + H \cdot N + N^T \cdot H^T + H \cdot Q \cdot H^T$ and $\bar{N} = G \cdot (Q \cdot H^T + N)$.

5.1.2 Non-linear Model Predictive Control

Based on the general definition of MPC given in Section 5.1.1, a new formulation of the NMPC using the LPV system class is proposed in this section. The main difference between the linear and non-linear MPCs is the inclusion of a non-linear prediction model in the NMPC algorithm (Herceg, Raff, Findeisen, & Allgoewer, 2006). This improves the prediction accuracy over that of the linear MPC. In both cases, a QP problem has to be solved in each step of the prediction horizon. As mentioned, the use of non-linear models also complicates the solution of the optimisation problem. For non-linear problems, the output prediction and the condensing have to be re-performed for each instance of the prediction horizon. In contrast, in the linear MPC, there is just one calculation step for the optimisation procedure. The additional computing effort for each time instant in NMPC significantly increases the required computational power. Ortner and Wang (2009), Wang, Waschl, Alberer and Del Re (2012) and Wang, Zhang and Bechkoum (2016) review numerical methods for the solution of optimal control problems in real-time, as they arise in NMPC. It is shown that fast QP-solvers can be used successfully for NMPC engine-control applications.

In this section, a special class of LPV system is employed for NMPC formulation. Bamieh and Giarre (2002), Wei and Del Re (2003), Wang and Steiner (2011) and Wang, Zhang and Bechkoum (2019) have studied the LPV formulation problem. Consider an LPV model represented in the state-space formulation by the following system equations:

$$\begin{aligned} x_{i+1} &= A_i(\rho) \cdot x_i + B_i(\rho) \cdot u_i + M \cdot v \\ y_i &= C_i(\rho) \cdot x_i, \end{aligned} \tag{5-31}$$

where $x_i \in R$ represents the system state, $u_i \in R$ represents the system inputs, $y_i \in R$ represents the system outputs and $\rho \in R$ is exogenous input parameters that are measureable in real-time by sensors. The matrix M multiplied by measured disturbances v denotes the input of the measured disturbances.

The LPV system matrices A_i, B_i and C_i are evaluated at each instant with the current external parameters ρ. Hence, the system turns into a linear state-space formulation at each time step. The formulation and evaluation of the system matrices A_i, B_i and C_i in LPV system are given in (Wang & Steiner, 2011). The LPV system in Equation 5-31 can be described as follows:

$$\dot{x} = f(x, u, t, \rho) \qquad (5\text{-}32)$$
$$y = g(x, u, t, \rho).$$

The system identification algorithms always deal with discrete measurement (Wang & Steiner, 2011), so the Equation 5-32 can be rewritten as following:

$$(1 + A(q^{-1}, \rho_i)) \cdot y_i = B(q^{-1}, \rho_i) \cdot u_i + m_i, \qquad (5\text{-}33)$$

where q^{-1} is the backward shift operator; m_i denotes the modelling error. The polynomials $A(q^{-1}, \rho_i)$ and $B(q^{-1}, \rho_i)$ in Equation 5-33 have the following formulations (Wang & Steiner, 2011):

$$A(q^{-1}, \rho_i) = a_1(\rho_i) \cdot q^{-1} + a_2(\rho_i) \cdot q^{-2} + \cdots + a_{na}(\rho_i) \cdot q^{-na}\ , \qquad (5\text{-}34)$$

$$B(q^{-1}, \rho_i) = b_1(\rho_i) \cdot q^{-1} + b_2(\rho_i) \cdot q^{-2} + \cdots + b_{nb}(\rho_i) \cdot q^{-nb}\ . \qquad (5\text{-}35)$$

The coefficients $a(\rho)$ and $b(\rho)$ are linear combinations of a set of known functions $[f_1, f_2, \dots, f_{N-1}]$ as following:

$$a_\alpha(\rho_i) = a_\alpha^0 + f_1(\rho_i) \cdot a_\alpha^1 + \cdots + f_{N-1}(\rho_i) \cdot a_\alpha^{N-1}, \qquad (5\text{-}36)$$

$$b_\beta(\rho_i) = b_\beta^0 + f_1(\rho_i) \cdot b_\beta^1 + \cdots + f_{N-1}(\rho_i) \cdot b_\beta^{N-1}, \qquad (5\text{-}37)$$

where $\alpha = 1,2, \dots, na$ and $\beta = 1,2, \dots, nb$.

Integrating equations 5-36 and 5-37 into equations 5-34 and 5-35 yields the following:

$$\begin{gathered} A(q^{-1}, \rho_i) = (a_1^0 q^{-1} \cdots + a_{na}^0 q^{-na}) + f_1(a_1^1 q^{-1} \cdots + a_{na}^1 q^{-na}) + \\ \cdots f_{N-1}(a_1^{N-1} q^{-1} \cdots + a_{na}^{N-1} q^{-na}), \end{gathered} \qquad (5\text{-}38)$$

$$\begin{gathered} B(q^{-1}, \rho_i) = (b_1^0 q^{-1} \cdots + b_{nb}^0 q^{-nb}) + f_1(b_1^1 q^{-1} \cdots + b_{nb}^1 q^{-nb}) + \\ \cdots f_{N-1}(b_1^{N-1} q^{-1} \cdots + b_{nb}^{N-1} q^{-nb}). \end{gathered} \qquad (5\text{-}39)$$

Using the definitions

$$\varphi_i = [-y_{i-1}\ - y_{i-2} \cdots - y_{i-na} \cdots u_{i-1}\ u_{i-2} \cdots u_{i-nb}], \qquad (5\text{-}40)$$

$$\theta^k = [a_1^k\ \ a_2^k \cdots\ a_{na}^k\ \ b_1^k\ \ b_2^k \cdots\ b_{nb}^k]^T, \qquad (5\text{-}41)$$

$$F_i = [1\ f_1(p_i) \dots f_{N-1}(p_i)], \qquad (5\text{-}42)$$

where $k = 1,2,\dots,N-1$.
Equation 5-33 can be rewritten as following:

$$y(i) = \varphi_i\theta^0 + f_1\varphi_i\theta^1 + \dots + f_{N-1}\varphi_i\theta^{N-1} + m_i$$
$$= [\varphi_i \ f_1\varphi_i \cdots f_{N-1}\varphi_i] \cdot \begin{bmatrix} \theta^0 \\ \theta^1 \\ \vdots \\ \theta^{N-1} \end{bmatrix} + m_i = [F_i \otimes \varphi_i\,] \cdot \Theta + m_i = \Gamma_i \cdot \Theta + m_i, \tag{5-43}$$

where $\otimes$ denotes Kronecker product, and $\Theta = [(\theta^0)^T(\theta^1)^T \cdots (\theta^{N-1})^T]^T$ and $\Gamma_i = F_i \otimes \varphi_i$.

The Equation 5-43 leads to the least squats system identification approach for estimation of the parameter vector as following:

$$\hat{\Theta} = (\Gamma^T\Gamma)^{-1}\Gamma^T Y. \tag{5-44}$$

The Equation 5-44 can be shown to converge to the real parameter vector under the assumption of white noise for m_i (MathWorks, 2018).

Please refer to (Wang & Steiner, 2011; Wei, 2006) for more details about LPV system identification algorithm.

The validation results of the LPV identification in Section 5.2.1 clearly show that, compared to linear models, LPV models offer several advantages which make them sensible alternatives for non-linear systems. Once the LPV model is identified, the design of an NMPC can be implemented.

An extension of the Equation 5-31 to an incremental state-space formulation is done in Equation 5-45:

$$\begin{bmatrix} x_{i+1} \\ u_i \end{bmatrix} = \begin{bmatrix} A_i & B_i \\ 0 & I \end{bmatrix} \cdot \begin{bmatrix} x_i \\ u_{i-1} \end{bmatrix} + \begin{bmatrix} 0 & M \\ I & 0 \end{bmatrix} \cdot \begin{bmatrix} \Delta u_i \\ v \end{bmatrix} \tag{5-45}$$
$$y_i = C_i \cdot x_i,$$

where in NMPC, this formulation allows a limitation of the rate of change for the input variables $\Delta u_i \in [\Delta u_{min}, \Delta u_{max}]$. In Equation 5-45, I denotes the identity matrix. Based on the

LPV model formulation, a cost function needs to be defined. Assume that the state x_i is available at the current instant *i*. Then the cost function of optimisation in NMPC has the following formulation:

$$J_{nmpc} = \quad min_u \frac{1}{2} \sum_{i=0}^{n_{PH}} (y_i - y_{ref})^T Q (y_i - y_{ref}) + \sum_{i=0}^{n_{CH}} \Delta u_i^T R \Delta u_i \tag{5-46}$$

$$subject\ to$$

$$x_{i+1} = A_i(\rho) \cdot x_i + B_i(\rho) \cdot u_i + M \cdot v$$

$$y_i = C_i(\rho) \cdot x_i,$$

$$y_{min} \leq y_i \leq y_{max}, i = 0 \dots PH$$

$$u_{min} \leq u_i \leq u_{max}, i = 0 \dots PH$$

$$\Delta u_i = u_i - u_{i-1}$$

$$\Delta u_{min} \leq \Delta u_i \leq \Delta u_{max}, i = 0 \dots CH - 1$$

$$\Delta u_i = 0, i = CH \dots PH.$$

Equation 5-46 is initialised in each time instant with x_0, which is a vector of the estimated system states calculated by a Kalman filter using the LPV form. The fundamentals of the Kalman filter are described in detail in Section 5.1.1.6. This cost function is normally desired to have a quadratic structure, which can be solved by efficient algorithms. However, in this case, the LPV model structure includes a non-linear dependency between the plant inputs and outputs. During this integration along the predicted trajectory, the LPV system matrices A_i, B_i and C_i are also evaluated for each step of the prediction horizon. This can be done by calculating the current coefficients of the matrices with the polynomial dependency. To reduce the computation time, in the algorithm of (Ferreau, 2014), this sequential-quadratic-programming (SQP) procedure is replaced by a "stand-alone" QP-solver in each step of the prediction horizon. The system state x_i can be iteratively calculated for the whole prediction horizon. The predictions along the horizons are given by,

$$\begin{aligned}
x_1 &= A_0 x_0 + B_0 u_0 + Mv \\
x_2 &= A_1 A_0 x_0 + A_1 B_0 u_0 + B_1 u_1 + A_1 M v + Mv \\
x_3 &= A_2 A_1 A_0 x_0 + A_2 A_1 B_0 u_0 + A_2 B_1 u_1 + B_2 u_2 + A_2 A_1 M v + A_2 M v + Mv \\
&\vdots \\
x_{CH} &= A_{CH-1} A_{CH-2} \cdots A_0 x_0 + A_{CH-1} A_{CH-2} \cdots A_1 B_0 u_0 + \cdots + B_{CH-1} u_{CH-1} + A_{CH-1} \cdots A_1 M v \\
&\quad + \cdots + Mv
\end{aligned} \tag{5-47}$$

$$\vdots$$

$$x_{PH} = A_{PH-1}A_{PH-2}\cdots A_0x_0 + A_{PH-1}A_{PH-2}\cdots A_1B_0u_0 + \cdots + B_{PH-1}u_{CH-1} + A_{PH-1}\cdots A_1Mv + \cdots + Mv,$$

where the LPV system matrices A_i and B_i are calculated iteratively. The procedure for output prediction starts with an estimation of current system states by an observer. These states are used at the beginning of each optimisation step to initialise the cost function with the actual system states. Starting with the initial value x_0, the discrete time LPV model is integrated over the whole prediction horizon PH. This is used to calculate x_{i+1} at each time instant based on the current system states x_i. As explained in (Ortner, Bergmann, Ferreau, & Del Re, 2009) and (Wang, Waschl, Alberer, & Del Re, 2012), v represents the measured disturbances which are assumed to be constant over the whole prediction horizon. Equation 5-47 can be formulated in a state-space matrix representation for a control horizon of *CH*:

$$\underbrace{\begin{bmatrix} x_0 \\ x_1 \\ x_2 \\ x_3 \\ \vdots \\ x_{CH} \\ \vdots \\ x_{PH} \end{bmatrix}}_{\tilde{X}} = \underbrace{\begin{bmatrix} I & 0 & \cdots & \cdots & 0 \\ A_0 & B_0 & 0 & \cdots & 0 \\ A_1A_0 & A_1B_0 & 0 & \cdots & 0 \\ A_2A_1A_0 & A_2A_1B_0 & & \cdots & 0 \\ \vdots & \vdots & & \ddots & \\ A_{CH-1}A_{CH-2}\cdots A_0 & A_{CH-1}A_{CH-2}\cdots A_1B_0 & \cdots & & A_{CH}B_{CH-1} \\ \vdots & \vdots & & & \vdots \\ A_{PH-1}A_{PH-2}\cdots A_0 & A_{PH-1}A_{PH-2}\cdots A_1B_0 & & \cdots & A_{PH}B_{PH-1} \end{bmatrix}}_{[\tilde{A}0\ \tilde{A}1]} \cdot \underbrace{\begin{bmatrix} x_0 \\ u_0 \\ u_1 \\ u_2 \\ \vdots \\ u_{CH-1} \end{bmatrix}}_{\begin{bmatrix} x_0 \\ \tilde{U} \end{bmatrix}} \tag{5-48}$$

$$+ \underbrace{\begin{bmatrix} 0 \\ M \\ (A_1+1)M \\ (A_2A_1+A_1+1)M \\ \vdots \\ (A_{CH-1}\cdots A_1 + A_2A_1 + A_1 + 1)M \\ \vdots \\ (A_{PH-1}\cdots A_1 + A_2A_1 + A_1 + 1)M \end{bmatrix}}_{\tilde{M}} \cdot v\,,$$

where

$$\tilde{X}=\begin{bmatrix} x_0\\ x_1\\ x_2\\ x_3\\ \vdots\\ x_{CH}\\ \vdots\\ x_{PH}\end{bmatrix}, \tilde{A}0=\begin{bmatrix} I\\ A_0\\ A_1A_0\\ A_2A_1A_0\\ \vdots\\ A_{CH-1}A_{CH-2}\cdots A_0\\ \vdots\\ A_{PH-1}A_{PH-2}\cdots A_0\end{bmatrix}, \widetilde{M}=\begin{bmatrix} 0\\ M\\ (A_1+1)M\\ (A_2A_1+A_1+1)M\\ \vdots\\ (A_{CH-1}\cdots A_1+A_2A_1+A_1+1)M\\ \vdots\\ (A_{PH-1}\cdots A_1+A_2A_1+A_1+1)M\end{bmatrix},$$

$$\tilde{A}1=\begin{bmatrix} A_0 & B_0 & 0 & \cdots & 0\\ A_1A_0 & A_1B_0 & 0 & \cdots & 0\\ A_2A_1A_0 & A_2A_1B_0 & & \cdots & 0\\ \vdots & \vdots & & \ddots & \\ A_{CH-1}A_{CH-2}\cdots A_0 & A_{CH-1}A_{CH-2}\cdots A_1B_0 & \cdots & & A_{CH}B_{CH-1}\\ \vdots & \vdots & & & \vdots\\ A_{PH-1}A_{PH-2}\cdots A_0 & A_{PH-1}A_{PH-2}\cdots A_1B_0 & & \cdots & A_{PH}B_{PH-1}\end{bmatrix}. \quad (5\text{-}49)$$

Furthermore, the Equation 5-48 can be expressed as follows:

$$\tilde{X}=\tilde{A}0\cdot x_0+\tilde{A}1\cdot\widetilde{U}+\widetilde{M}\cdot v. \quad (5\text{-}50)$$

Integrating Equation 5-50 into the QP formulation 5-46 yields the following:

$$\mathrm{J}=min_u\frac{1}{2}(C_i\cdot\tilde{X}-C_i\cdot\tilde{I}\cdot X_{ref})^TQ\big(C_i\cdot\tilde{X}-C_i\tilde{I}\cdot X_{ref}\big)+\widetilde{U}^T R\widetilde{U} \quad (5\text{-}51)$$

$$\rightarrow min_u\frac{1}{2}C^T{}_i(\tilde{A}0\cdot x_0+\tilde{A}1\cdot\widetilde{U}+\widetilde{M}\cdot v$$

$$-\tilde{I}\cdot X_{ref})^T\tilde{Q}C_i\big(\tilde{A}0\cdot x_0+\tilde{A}1\cdot\widetilde{U}+\widetilde{M}\cdot v-\tilde{I}\cdot X_{ref}\big)+\widetilde{U}^T R\widetilde{U}\quad ,$$

$$subject\ to$$

$$\tilde{X}_{min}\leq\tilde{A}0\cdot x_0+\tilde{A}1\cdot\widetilde{U}+\widetilde{M}\cdot v\leq\tilde{X}_{max}$$

$$\widetilde{U}_{min}\leq\widetilde{U}\leq\widetilde{U}_{max}$$

Re-formulation of the condition for the state constraints $\tilde{A}0\cdot x_0+\tilde{A}1\cdot\widetilde{U}+\widetilde{M}\cdot v$ leads to

$$\tilde{X}_{min} - \left(\tilde{A}0 \cdot x_0 + \widetilde{M} \cdot v\right) \leq \tilde{A}1 \cdot \widetilde{U} \leq \tilde{X}_{max} - \left(\tilde{A}0 \cdot x_0 + \widetilde{M} \cdot v\right). \tag{5-52}$$

Leaving the constant parts of the objective function away and using the new state constraint formulation as conditions yields,

$$J = min_u \frac{1}{2} \widetilde{U}_i^T (\tilde{A}1^T \tilde{Q} \tilde{A}1 + \tilde{R})^T \widetilde{U}_i \quad + \widetilde{U}_i^T \tilde{A}1^T \left(\tilde{A}0 x_0 + \widetilde{M} - \tilde{I} X_{ref}\right), \tag{5-53}$$

$$subject\ to$$

$$\tilde{X}_{min} - \left(\tilde{A}0 \cdot x_0 + \widetilde{M} \cdot v\right) \leq \tilde{A}1 \cdot \widetilde{U} \leq \tilde{X}_{max} - (\tilde{A}0 \cdot x_0 + \widetilde{M} \cdot v)$$

$$\widetilde{U}_{min} \leq \widetilde{U} \leq \widetilde{U}_{max}.$$

The condensed QP problem, defined in Equation 5-46, can now be solved by means of the QP-solver, qpOASES, (Ferreau, 2014). By assuming $w_0 = f(x_0, \rho)$, the QP problem can be written as a parametric quadratic problem which can be solved by any QP-solver. This yields the following solution in qpOASES:

$$\text{QP } (x_0): \qquad min_{\widetilde{U}} \frac{1}{2} \widetilde{U}^T H \widetilde{U} + \widetilde{U}^T g(w_0), \tag{5-54}$$

$$subject\ to$$

$$lb(w_0) \leq \widetilde{U} \leq ub(w_0)$$

$$lb_G(w_0) \leq G\widetilde{U} \leq ub_G(w_0).$$

where $G = \tilde{A}1$ (Equation 5-49) is a part of the system matrix (Equation 5-48); The Hessian matrix H has been given in Equation 5.17.

The implementation of Equation 5-54 in QP-Solver is based on the open-source package qpOASES (Ferreau, 2014). The optimal solution U_{opt} of the QP is given in (Ferreau, 2014) as follows:

$$U_{opt} = -H^{-1} \cdot f \cdot \theta, \tag{5-55}$$

$$subject\ to$$

$$\theta = [x_i, u_{i-1}, y_{ref}]^T.$$

With the U_{opt}, the control actions in the CH are calculated, and the first control is applied to the system. Matrices H and f are affine representations of the NMPC, and they can be defined by a new gain matrix $F_{nmpc} = -H^{-1} \cdot f = [F_{nmpc-xi}, F_{nmpc-u_{i-1}}, F_{nmpc-y_{ref}}]$. Now the affine control law for the NMPC can be written in a matrix form as follows:

$$u_i = F_{nmpc} \cdot \theta = [F_{nmpc-x}, F_{nmpc-u_{i-1}}, F_{nmpc-y_{ref}}] \cdot [x_i, u_{i-1}, y_{ref}]^T. \tag{5-56}$$

In practice, the NMPC controller and real plants are coupled with each other. The question is whether this configuration leads to growing of numerical errors and a destabilised closed loop. As discussed in Section 5.1.1.5, the MPC objective function can be considered as a Lyapunov function, and the guarantee of stability can be provided by a finite horizon (Cheng & Allgoewer, 1998; Langthaler, 2007; Mayne, 2001; Wang & Steiner, 2011). A detailed proof of the stability and the real-time iteration scheme for non-linear optimisation is given in (Diehl, Bock, & Schloeder, 2005). In this case, the qpOASES, active set strategy, provides an efficient online optimisation algorithm that has already been successfully tested in several fast-process control applications (Ferreau, 2006; Ferreau, 2008; Wang, Waschl, Alberer, & Del Re, 2012). Studies show that the fast QP-solver guarantees closed-loop robust stability in the proposed control law. The application of the closed-loop NMPC control in the engine-air-path is described in Section 5.2.

5.2 Implementation of the NMPC on the Engine-air-path System

5.2.1 LPV Model of Engine-air-path

As mentioned above, the LPV model is chosen as an internal model for this NMPC control problem. The engine-air-path system has a significant influence on the fuel consumption and emissions of an engine. This section presents LPV modelling techniques for the air-path system of a diesel engine. Since NMPC controllers are model-based, a non-linear model is required from the overall system. The engine system is highly non-linear. However, an operation point change means discrete switching in the overall compressor clearance for a short time; i.e., it is a non-linear sequential switching process. In reality, an operation point change means a change in the physical system: the clearance volume changes in the engine cylinder. Del Re (2011) shows that frequent switching need not be modelled, as an approximation of the relevant frequency spectrum by an LPV dynamical system is sufficient. Using simulation data from a Matlab/Simulink virtual test-bench, which is developed in Chapter 4, an LPV model is introduced for the identification of the MAF, MAP and P_{ex} of an engine-air-path system in this section.

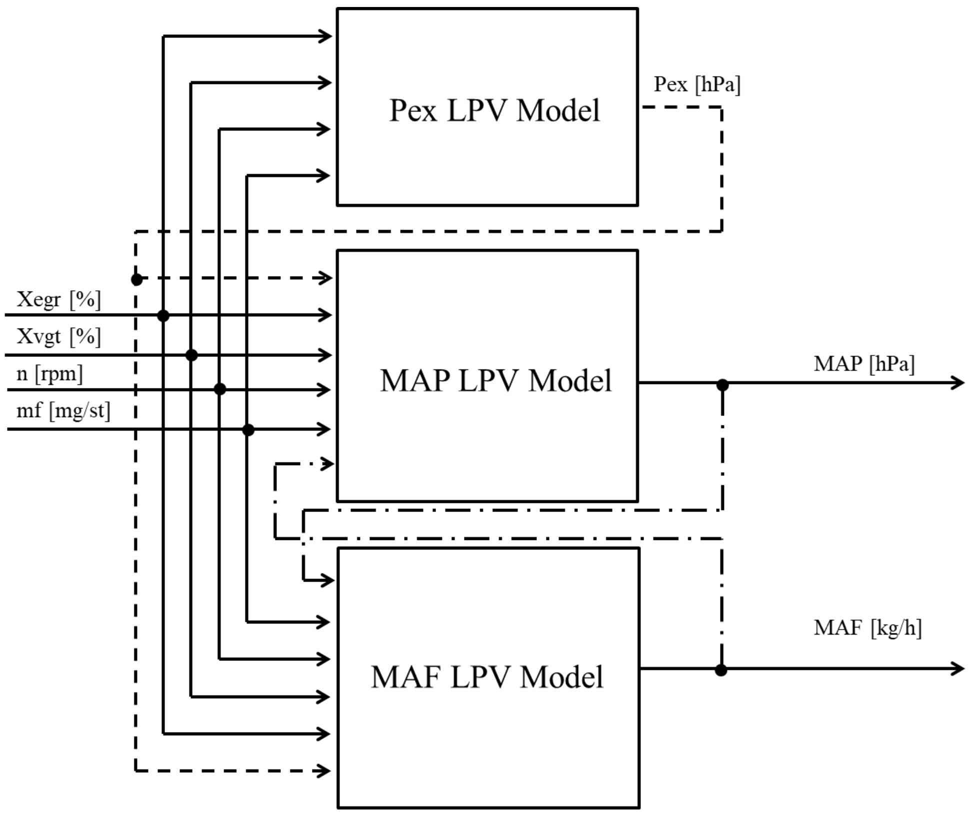

Input/output	Description	Unit	Range
X_{egr}	EGR actuator	%	0~100
X_{vgt}	VGT actuator	%	0~100
n	Engine speed	rpm	0~4000
m_f	Fuel injection	mg/st	>0
MAF	Intake manifold air flow	Kg/h	>0
MAP	Intake manifold air pressure	hPa	>0
P_{ex}	Exhaust manifold pressure	hPa	>0

Figure 5.8: Overall LPV engine-air-path model structure and input/output descriptions

As depicted in Figure 5.8, the considered system is the air-path of a diesel engine with EGR and VGT. Three partly consecutive, connected sub-models are displayed: P_{ex}, MAP and MAF.

The advantage of the purposed model structure is the opportunity for the separate and independent identification of the target sub-model, which imposes the reliability of the estimates. Finally, these sub-models are merged in a whole block to an overall MIMO model. Moreover, the model degree for each subsystem can be chosen according to the individually required level of complexity. Furthermore, the verification is simplified, as the overall system can be validated and every single sub-model can be verified.

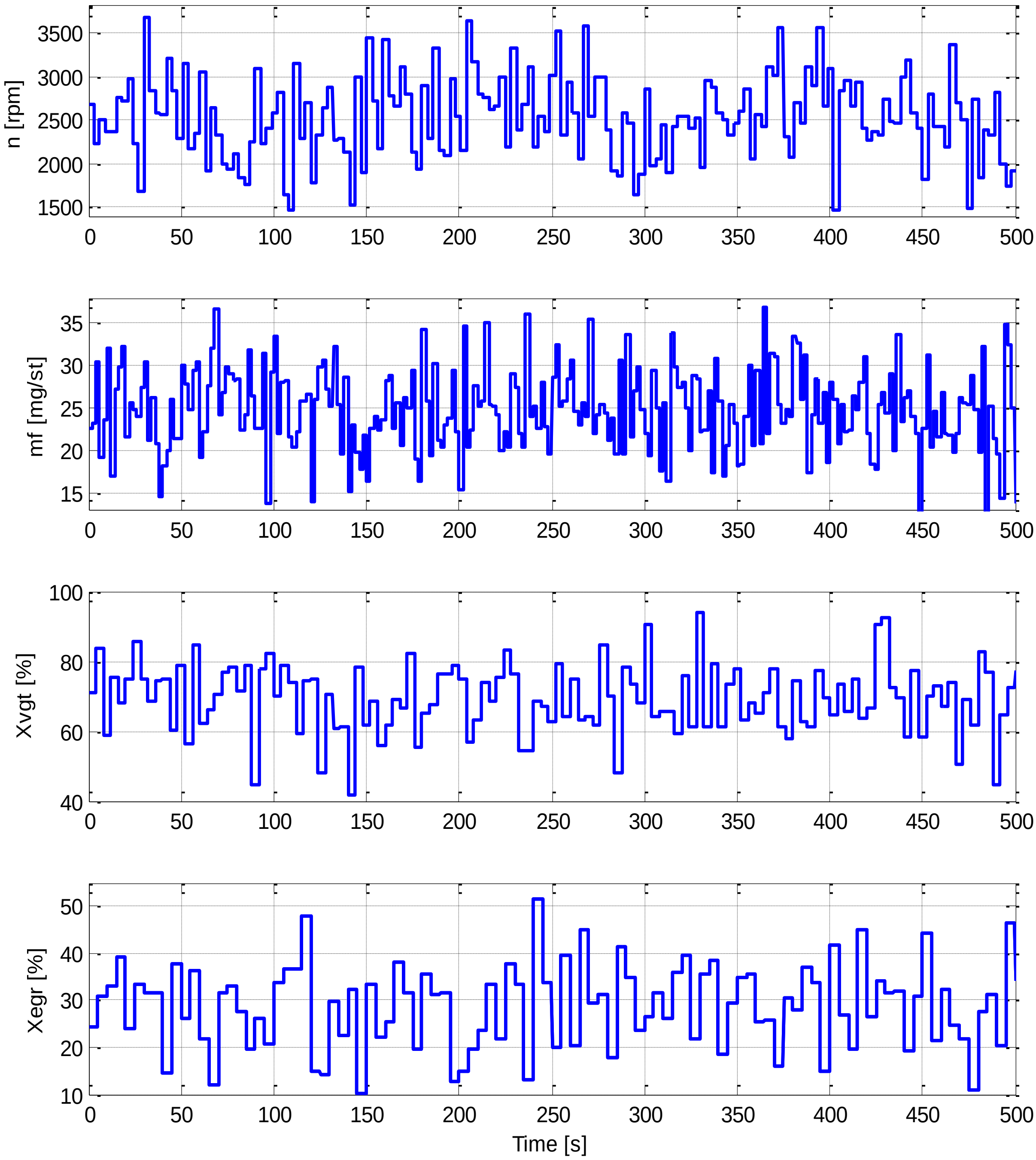

Figure 5.9: Input excitation for identification

The LPV identification method is introduced in Section 5.1.2. The engine-air-path systems are identified as state-space LPV form. The engine-air-path system is a typical MIMO system. As mentioned, for the purpose of MAF and MAP controls, the system can be considered to be a three-coupled MISO model in which the inputs are X_{egr}, X_{vgt}, n, m_f and an intermediated quantity: exhaust manifold pressure P_{ex}. The identification experiments are performed at different operation states. The identified models are used for the NMPC control design. To have persistent excitation, the inputs X_{egr}, X_{vgt}, n and m_f are excited by a pseudorandom binary signal, which is illustrated in the Figure 5.9. In the simulation, a sampling frequency of 20 Hz is performed. In the following, the sub-model structures and an analysis of the simulation are depicted.

This section is organised as follows. First, the LPV model configuration is defined. This configuration will be used to define the model structure. Next, the identification experiments are carried out on the virtual engine tech bench. Finally, the results of the LPV model and linear state-space model are compared and discussed.

5.2.1.1 LPV Modelling of Sub-systems

Nguyen-Schaefer (2013) has shown that the P_{ex} exhibits strong coherence dependency on the MAF and MAP. As it is desirable to consider the influence of P_{ex}, a MISO LPV model is needed. As shown in Figure 5.10, the MISO LPV model has VGT, EGR, n and m_f as inputs and P_{ex} as output.

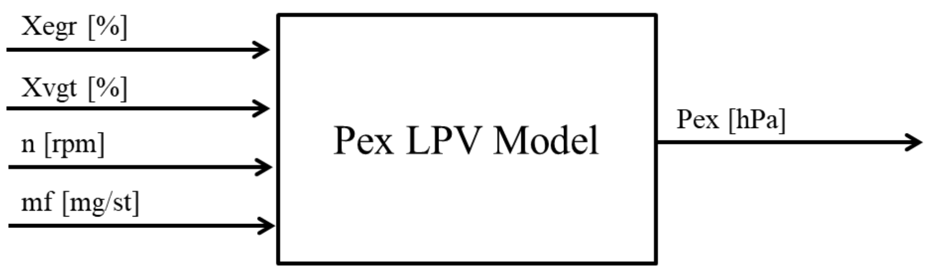

Figure 5.10: Structure of the P_{ex} model

The VGT and EGR valve positions correspond to the actuator signals X_{egr} and X_{vgt}; therefore, in the identification, X_{egr} and X_{vgt} are used as inputs. As mentioned in Section 5.1.2, the scheduling parameters have to be defined. Consider the engine operation points: It turned out that n and m_f can be valuable choices for scheduling parameters. To take this into account for the P_{ex} model, the inputs n and m_f are used in addition to X_{egr} and X_{vgt}.

As shown in Figure 5.10, the P_{ex} model consists of four parallel transfer functions (one for each input) of the type:

$$G_{pex,i}(\rho) = \frac{A_i(\rho) \cdot q^{-1}}{1 + B_i(\rho) \cdot q^{-1}} . \tag{5-57}$$

The formulation of polynomial functions $A_i(\rho)$ and $B_i(\rho)$ are given in (Wang, Waschl, Alberer, & Del Re, 2012) as follows:

$$A_i(\rho) = A_{pex,i}(n, m_f) = a_i^0 + a_i^1 \cdot n + a_i^2 \cdot m_f + a_i^3 \cdot n \cdot m_f, \tag{5-58}$$

$$B_i(\rho) = A_{pex,i}(n, m_f) = b_i^0 + b_i^1 \cdot n + b_i^2 \cdot m_f + b_i^3 \cdot n \cdot m_f. \tag{5-59}$$

The approach of identification of $A_i(\rho)$ and $B_i(\rho)$ have been explained in Section 5.2.1.

The whole model structure is depicted for the P_{ex}:

$$\Sigma P_{ex} = G_{pex,egr} + G_{pex,vgt} + G_{pex,n} + G_{pex,mf} . \tag{5-60}$$

where $G_{pex,egr}, G_{pex,vgt}, G_{pex,n}$ and $G_{pex,mf}$ are the four parallel system transfer functions from inputs to output.

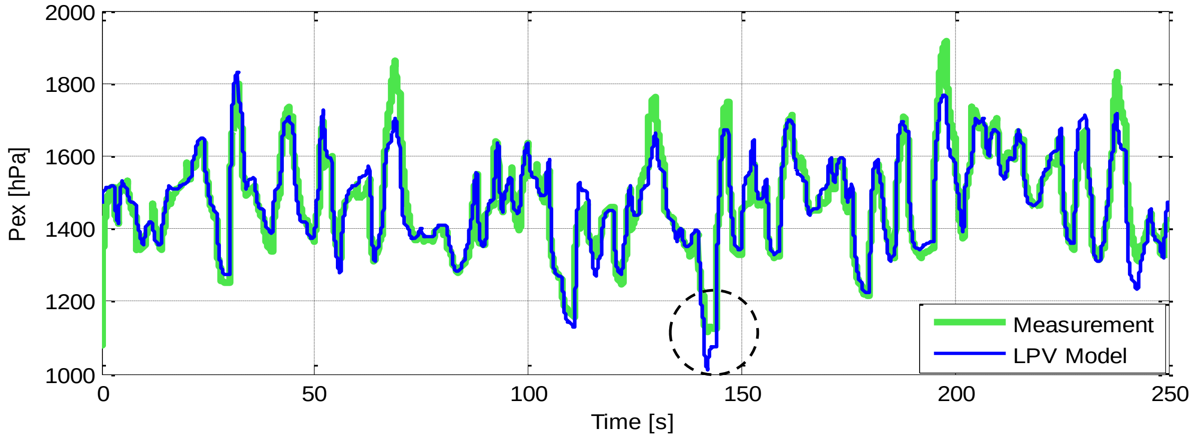

Figure 5.11: Identification of the P_{ex} model (VAF=91%)

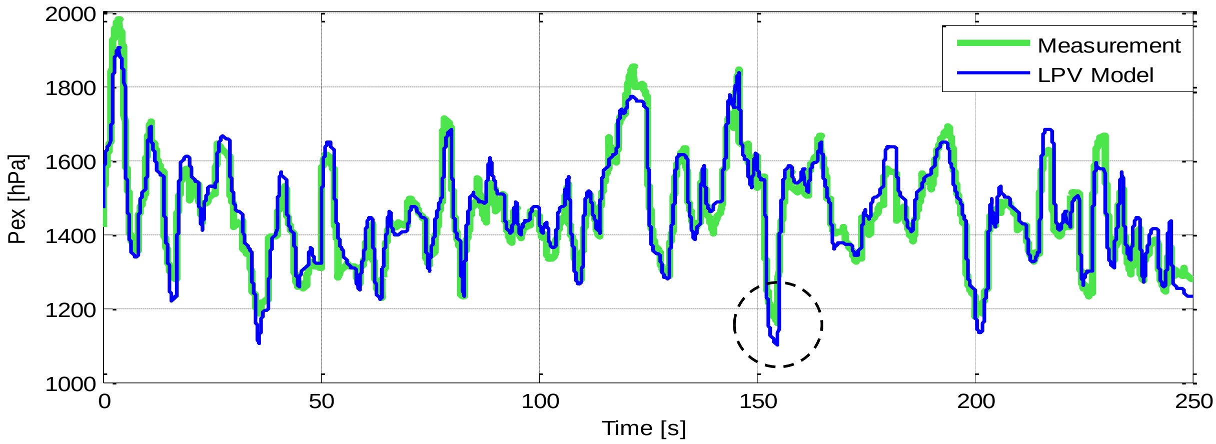

Figure 5.12: Validation of the P_{ex} model (VAF=86%)

The results of the identification and validation of an LPV model are shown in figures 5.11 and 5.12, where the model with the simulation outputs is compared with the measurement from the simulation. As shown in the validation results, the main system dynamics are captured with a reasonable precision thanks to the LPV structure. The most non-linearity agrees well with measurement; however, slight dynamic deviations can still be noticed at about 140s (the circle in Figure 5.11) and 160s (the circle Figure 5.12) for the case in which the combustion engine operates primarily in low-load areas, where it is very hard to predict the system dynamics.

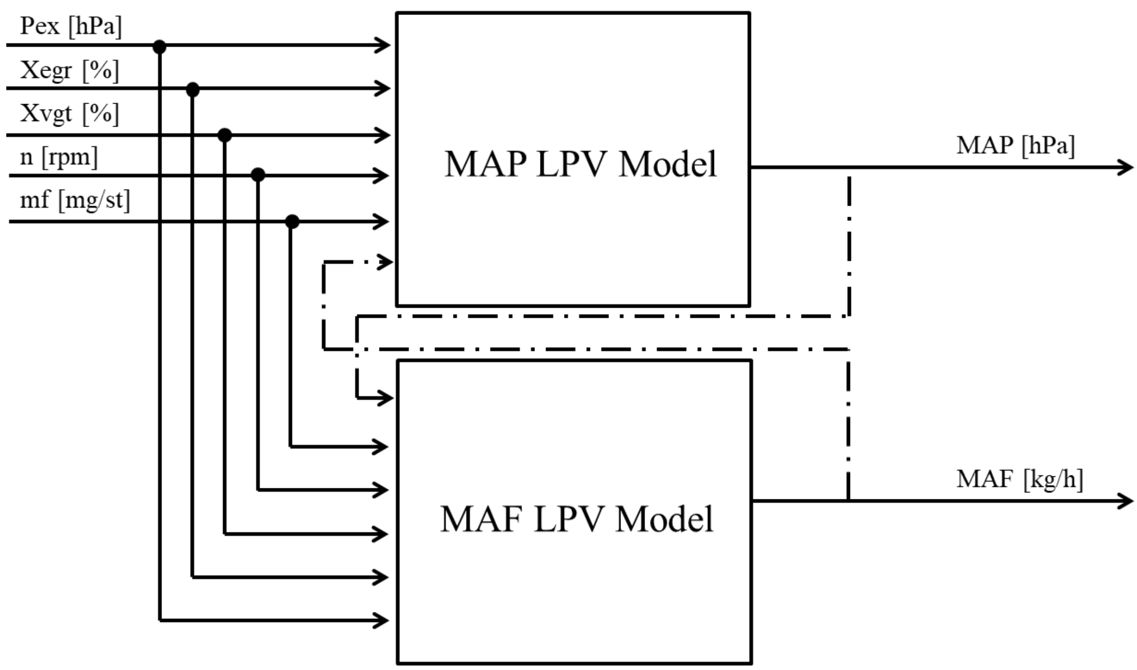

Figure 5.13: Structure of the cross coupled MAP and MAF model

As illustrated in Figure 5.13, the control model consists of two coupled sub-models—MAP and MAF—whose characteristics have been discussed in Section 2.1. The model inputs are VGT, EGR and the intermediate quantity P_{ex}, and the model outputs are MAF and MAP. To consider the description of the engine's actual operation state, the engine speed n and fuel injection m_f are chosen as the external scheduling parameter ρ. In addition, the cross-coupled feedbacks from MAP to MAF and from MAF to MAP must be considered. In the identification, to have persistent excitation, the inputs X_{egr}, X_{egr}, n, m_f and P_{ex} are excited by a pseudo random binary signal, as shown in Figure 5.9.

The similar mathematical descriptions shown in equations 5-58 and 5-59 are applied to model the MAP and MAF. For MAP, the polynomial function describes the effects of the inputs and external disturbances to the MAP. The dependencies in the quasi-MIMO transfer-function coefficients from the external parameters for the description of the non-linear model behaviour are as follows:

$$A_i(\rho) = A_{map,i}\big(n, m_f, MAF\big) = a_i^0 + a_i^1 \cdot n + a_i^2 \cdot m_f + a_i^3 \cdot MAF + a_i^4 \cdot n \cdot m_f \cdot MAF, \tag{5-61}$$

$$B_i(\rho) = B_{map,i}\big(n, m_f, MAF\big) = b_i^0 + b_i^1 \cdot n + b_i^2 \cdot m_f + b_i^3 \cdot MAF + b_i^4 \cdot n \cdot m_f \cdot MAF. \tag{5-62}$$

For MAF, the decided output has the following structure:

$$A_i(\rho) = A_{maf,i}\big(n, m_f, MAP\big) = a_i^0 + a_i^1 \cdot n + a_i^2 \cdot m_f + a_i^3 \cdot MAP + a_i^4 \cdot n \cdot m_f \cdot MAP, \tag{5-63}$$

$$B_i(\rho) = B_{maf,i}\big(n, m_f, MAP\big) = b_i^0 + b_i^1 \cdot n + b_i^2 \cdot m_f + b_i^3 \cdot MAP + b_i^4 \cdot n \cdot m_f \cdot MAP. \tag{5-64}$$

The formulation of polynomial functions $A_i(\rho)$ and $B_i(\rho)$ are given in (Wang, Waschl, Alberer, & Del Re, 2012). The approach of identification of $A_i(\rho)$ and $B_i(\rho)$ have been explained in Section 5.2.1.

The identification and validation results for MAP and MAF are shown in figures 5.14 and 5.15. As the VAF-results show, the LPV model is the appropriate model structure, as it is sufficient to capture the main dynamics of the engine-air-path system.

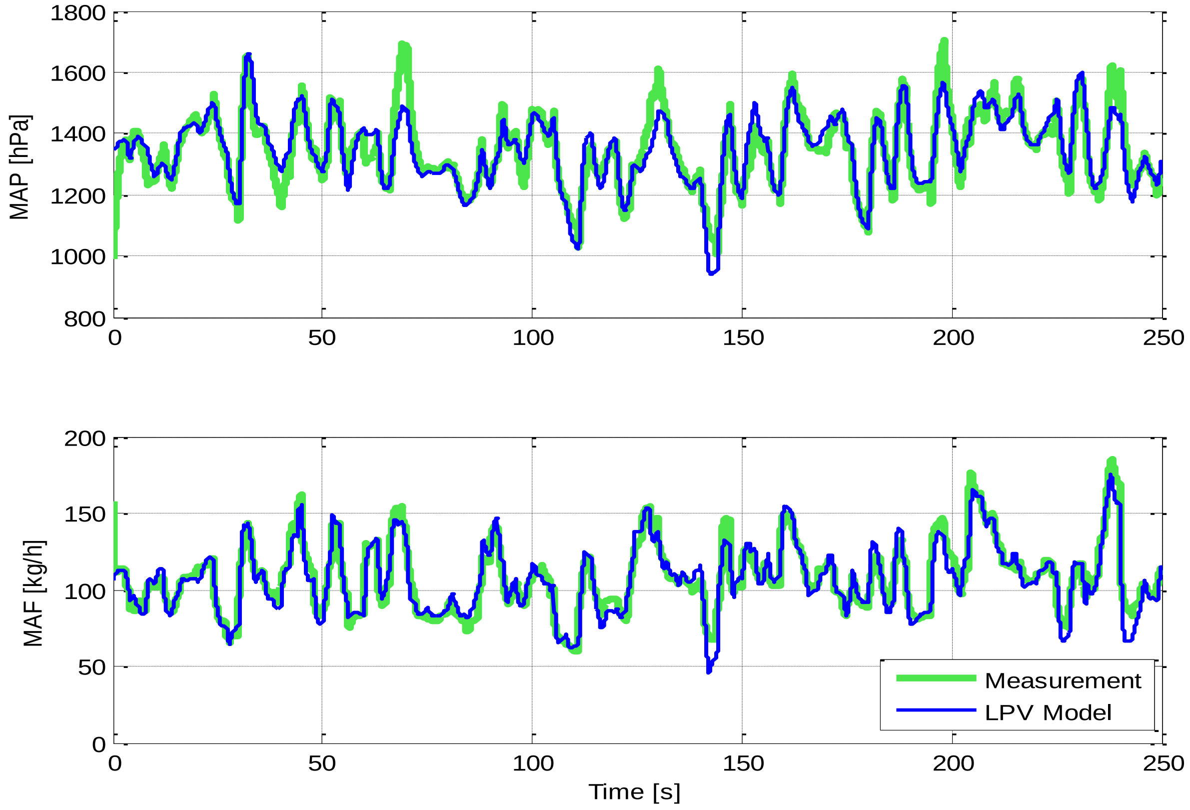

Figure 5.14: Identification of the MAP and MAF model (VAF_{map}=88%, VAF_{maf}=86%)

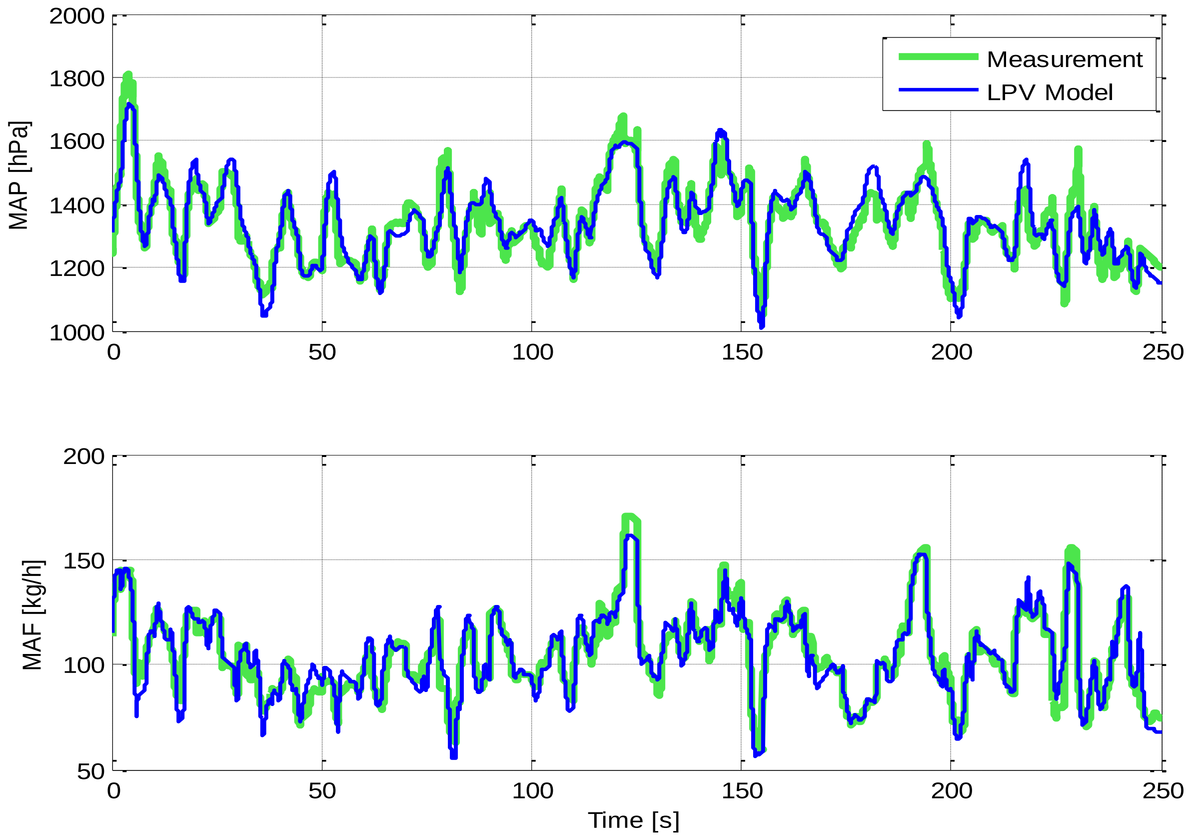

Figure 5.15: Validation of the MAP and MAF model (VAF_{map}=83%, VAF_{maf}=81%)

5.2.1.2 Simulation Results

As mentioned above, the engine-air-path system can be described via an LPV MIMO model. The model is identified with following input parameters: X_{egr}, X_{vgt}, n and m_f. The output is split into MAF, MAP and p_{ex}. The model structure is defined, and the input signals are proposed. The sub-models P_{ex}, MAP and MAF are finally cross-connected according to the structure depicted in Figure 5.8. In addition, for benchmark purpose, a corresponding state-space linear model is used to compare with the LPV model. The results obtained from the identification experiments are analysed in what follows.

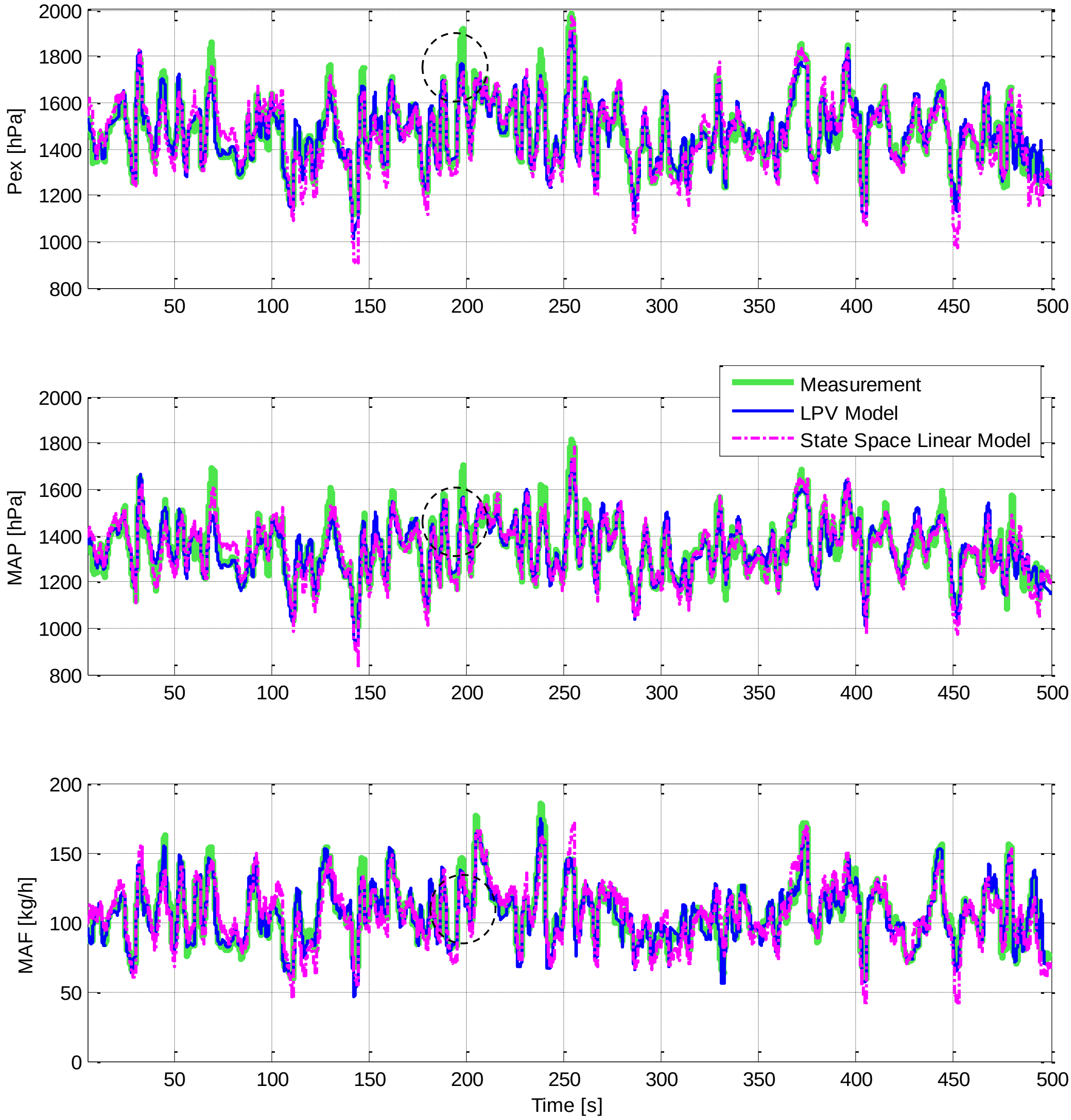

Figure 5.16: Simulation results for LPV and state-space linear model (0-500s)

The simulation results are shown in Figure 5.16. Obviously, the overall model quality can at the most be as good as the quality of the sub-models, as a cascading error might occur (the circle in Figure 5.16): in particular, the modelling error due to the cross-coupling effects on MAF and MAP might occur. This already indicates the need for a coupled MIMO treatment of the VGT and EGR during control. Further control considerations and discussions can be found in Section 5.3. To show the feasibility of the LPV approach, it is compared to a state-space linear model, which is estimated by the Matlab/Simulink system identification toolbox (MathWorks, 2018). This state-space model is given in the following form:

$$x_{i+1} = A \cdot x_i + B \cdot u_i \qquad (5\text{-}65)$$
$$y_i = C \cdot \ x_i,$$

where (1) y_i , x_i and u_i denote the system output, state and input at time step i respectively, and

(2) A, B and C are system matrices, which are identified by the Matlab/Simulink system identification toolbox.

A part of the NEDC driving cycle at different engine operation points is used for model validation. In Figure 5.16, the main dynamics of MAP and MAF are well captured by the LPV model, which in turn allows us to use LPV model as prediction models in the NMPC. This LPV model is further use for an optimised NMPC to reduce the emissions and thus the operating range of the engine.

Figure 5.17 shows the quality bar graphs and a comparison of LPV and state-space linear methods for different operation points. The VAF values in Figure 5.17 are calculated by Equation 3-6. Obviously, the LPV method can achieve a nearly precise model of MAF and MAP, and it has been shown that the linear model deviates from the measurements—especially in the operation points strong changing areas, e.g. at 190s in Figure 5.16. These model mismatches could decrease the control performance or even cause instability of the close-loop control. Experimental results show that the LPV model delivers a very high accuracy for the MAF and MAP estimation that cannot be reached by classical identification methods. Some discussions of the model structure and its application are presented and a non-linear LPV model structure is proposed. However, the LPV model is identified only with limited range of inputs and outputs. A further potential improvement is to identify a model suitable for a broader operating range.

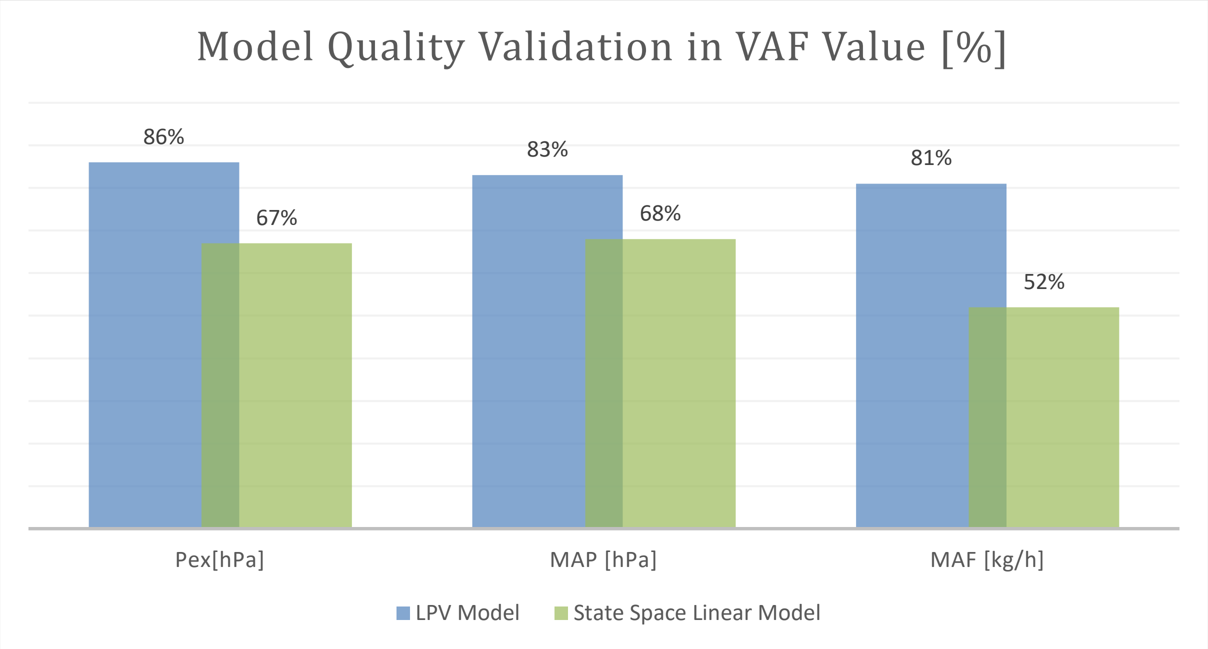

Figure 5.17: Comparison of the quality VAF of LPV and state-space model

For use in NMPC, the LPV model can be rewritten into state-space formulation. Studies discussed in Section 5.1.2 show that the constraints of change of the manipulated X_{egr}, X_{egr} and P_{ex} and the external disturbances n and m_f have to be taken into account. Therefore, similar to the previously work in (Wang, Waschl, Alberer, & Del Re, 2012), the whole output prediction model for use in the non-linear controller is expressed as follows:

$$\begin{bmatrix} x_{i+1} \\ u_i \end{bmatrix} = \begin{bmatrix} A_{MAF,MAP,Pex,i} & B_{MAF,MAP,Pex,i} \\ 0 & I \end{bmatrix} \cdot \begin{bmatrix} x_i \\ u_{i-1} \end{bmatrix} + \begin{bmatrix} 0 & M \\ I & 0 \end{bmatrix} \cdot \begin{bmatrix} \Delta u_i \\ v \end{bmatrix} \tag{5-66}$$
$$y_i = C_{MAF,MAF,Pex,i} \cdot x_i,$$

where

$$A_{MAF,MAP,Pex,i} = \begin{bmatrix} A_{MAF,i} & 0 & 0 \\ 0 & A_{MAP,i} & 0 \\ 0 & 0 & A_{Pex,i} \end{bmatrix}, \; B_{MAF,MAP,Pex,i} = \begin{bmatrix} B_{MAF,i} \\ B_{MAP,i} \\ B_{Pex,i} \end{bmatrix}, \tag{5-67}$$
$$C_{MAF,MAP,Pex,i} = \begin{bmatrix} C_{MAF,i} \\ C_{MAP,i} \\ C_{Pex,i} \end{bmatrix}.$$

The system matrices $A_{MAF,MAP,Pex,i}$, $B_{MAF,MAP,Pex,i}$ and $C_{MAF,MAP,Pex,i}$ in Equation 5-66 consist of matrices $A_{MAF,i}$, $A_{MAP,i}$, $A_{Pex,i}$, $B_{MAF,i}$, $B_{MAP,i,}B_{Pex,i}$, $C_{MAF,i}$ and $C_{Pex,i}$ which are respectively derived from the equations 5-58, 5-59, 5-61, 5-62, 5-63 and 5-64.

5.2.2 NMPC Constraints and Control Horizons

In case of air-path control, the target of the NMPC is to control both MAF and MAP via the inputs X_{egr} and X_{vgt}. The physical constraints of the manipulated actuators, EGR and VGT, are the minimum and maximum valve positions and the rate for opening and closing. Usually, the EGR valve can vary between 0 and 100% without damaging the engine; however, contrary to the EGR, the characteristic of VGT are more complex. Too much closing of the VGT at full load areas can damage the manifolds by high pressure or the turbocharger itself, due to the high rotor-operation speed. To ensure the durability of materials, the maximum speed of the rotor is predetermined, which depends on the materials, production techniques and driving statues used. For these reasons, the operation point is defined in accord with the VGT position. As mentioned in (Ortner, Langthaler, Ortiz, & del Re, 2006), there is a non-minimal phase behaviour from VGT to MAF. To guarantee the correct control action in steady conditions, the PH must be chosen to be much greater than the CH. Otherwise, the prediction model has too little information about the plant and causes wrong valve directions when controlling the MAF with the VGT.

The CH defines the number of sampling instants in which the manipulated variables are being changed by the QP-solver. The manipulated variables are either kept constant in time between PH minus CH or they are controlled by a state feedback controller in the qpOASES. In case of air-path control, due to the computation burden, the CH is fixed to a small number in qpOASES which ensure very good controller performance. If a longer CH is chosen, the controller has too many search regions for the optimal solution and a huge amount of memory is required.

5.2.3 NMPC State Observer

In the implemented NMPC, all the states must be estimated at each sampling instant if we are to evaluate the control law by the QP-solver, and the states must be updated at every time instant in real-time. To reduce the computational demands, an extended Kalman estimator is chosen as a state observer, as explained in Section 5.1.1.6. The model for the Kalman estimator has a same structure seen in Equation 5-27, including the measured disturbance *v*. The Kalman filter update equations remain identical, as above. As explained in (Wang, Waschl, Alberer, & Del Re, 2012), at each time instant, only the system matrices $A_{MAF,MAP,Pex,i}$ and $C_{MAF,MAP,Pex,i}$ are derived by a linearisation of the operating point:

$$A_{MAF,MAP,Pex}(x_i, u_i, i) = \frac{\partial f(x_i,u_i,i)}{\partial x_i}, \tag{5-68}$$

$$C_{MAF,MAP,Pex}(x_i, u_i, i) = \frac{\partial g(x_i,u_i,i)}{\partial x_i}, \tag{5-69}$$

where $f(x_i, u_i, i)$ and $g(x_i, u_i, i)$ are the system dynamics, as in Equation 5-27. This structure can be turned in real-time, and the complexity of the Kalman filter and thus the memory and computational demands can be reduced significantly.

5.2.4 Implementation of the NMPC Controller

It can be deduced that, in Section 5.1.2, use of the qpOASES with the previously introduced turning parameters leads to the following control law:

$$\text{QP } (x_0): \qquad min_{\widetilde{U}} \frac{1}{2} \widetilde{U}^T H \widetilde{U} + \widetilde{U}^T g(w_0) \tag{5-70}$$
$$subject\ to$$
$$lb(w_0) \leq \widetilde{U} \leq ub(w_0)$$
$$lb_G(w_0) \leq G\widetilde{U} \leq ub_G(w_0).$$

Now the matrices *H* and *f* are suitable for the QP-solver, qpOASES. In case of NMPC air-path control, the optimal solution U_{opt} of the QP can be described in a quasi-linear feedback form:

$$U_{opt} = -H^{-1} \cdot f \cdot \theta, \tag{5-71}$$

where $\theta = [x_{MAFi}, x_{MAPi}, x_{Pexi}, v_{mfi}, v_{ni}, v_{MAFi}, v_{MAPi}, u_{egri-1}, u_{vgti-1}, MAF_{ref}, MAP_{ref}]$ is the state vector of the controller. Research in (Ferreau, 2014) shows that the θ space is divided into polyhedral partitions; the boundary of this space is defined in the structure range. It includes the maximum and minimum values of the states, the control values and the reference trajectory. In air-path control, the $x_{MAFi}, x_{MAPi}, x_{Pexi}$ stand for the states of the LPV model. $v_{mfi}, v_{ni}, v_{MAFi}, v_{MAPi}$ are measured disturbances. u_{egri-1}, u_{vgti-1} are the last inputs. And MAF_{ref}, MAP_{ref} stands for the reference trajectories for MAF and MAP. According to the actual state vector θ, the actual region is searched and the optimal solution according to online active set strategy (Appendix B) is found.

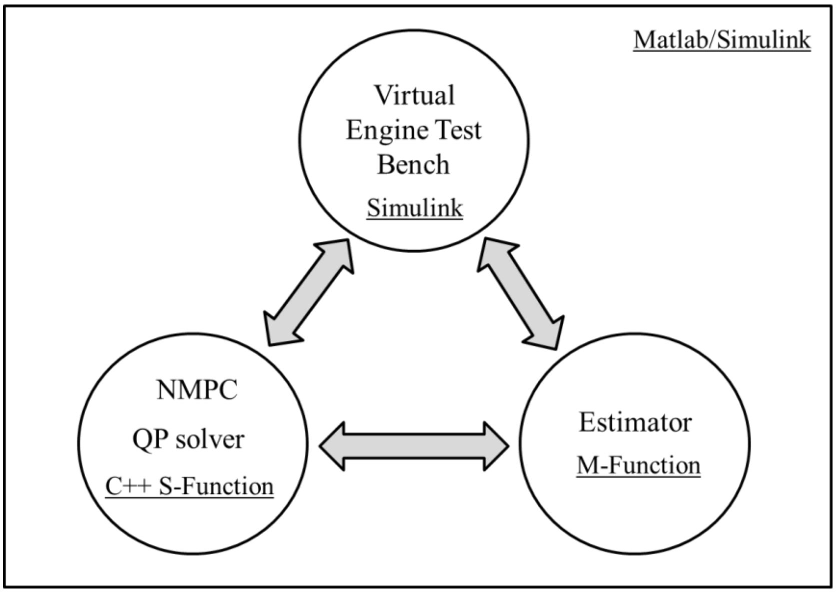

Figure 5.18: Software components on the virtual engine test-bench

The implementation of the NMPC controller in a virtual engine test-bench is realised by means of a C++ S-function in a Matlab/Simulink environment, which provides the interface between the Matlab function (M-Function), S-function (QP-solver) and the standard Simulink blocks. Figure 5.18 describes relations between the different software components for the implementation of the NMPC controller on the virtual engine test-bench. Control performance is evaluated during a run of the simulation in subsequent sections.

5.3 NMPC Simulation Results and Analysis

In this section, the NMPC controller is evaluated under different controller configurations and is compared to the linear MPC and standard PID controller function of vehicle ECU on the virtual engine test-bench, which is created by Matlab/Simulink from the previous Chapter 4.

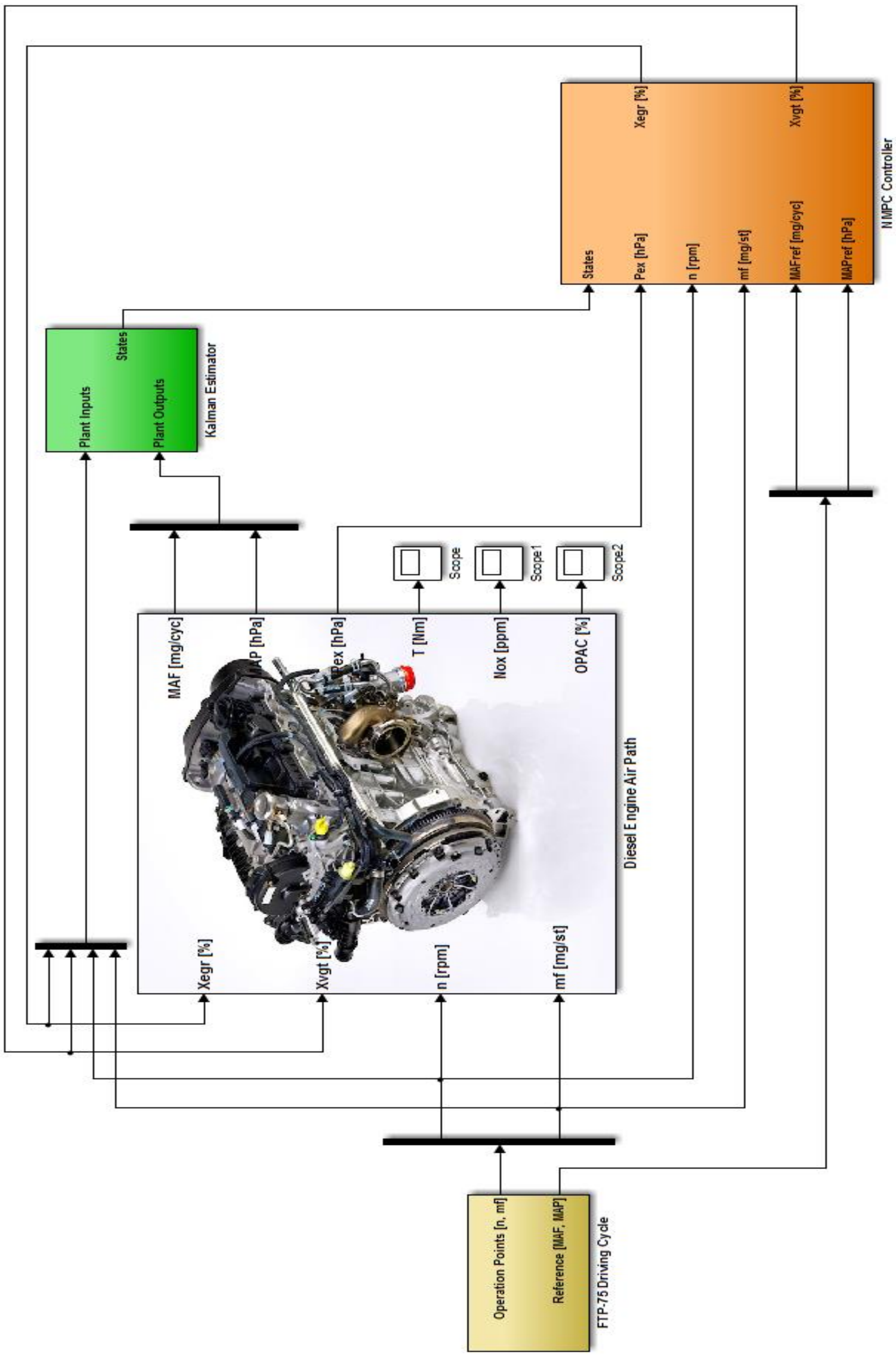

Figure 5.19: NMPC closed-loop scheme in Matlab/Simulink

In this section, first, the control performance of different NMPC controller configurations are validated, thereby comparing the NMPC at different configurations and test scenarios. Furthermore, the controller configurations which yield the best improvements are shown by the investigation of different control parameters and their impacts on the closed-loop behaviour. Finally, the NMPC is to be compared to the standard ECU and linear MPC, which work with the same engine model. The performance of the NMPC controllers against other control methods is then discussed in detail. Figure 5.19 illustrates the closed-loop structure of the whole simulation model in Matlab/Simulink environment. The virtual engine test-bench is represented by the mean-value model. The Kalman estimator and the NMPC controller are programmed using Matlab M-Function and S-Function and are saved in Simulink Function blocks.

5.3.1 Controller Configurations

Table 5-1: Setups of the NMPC controller

Turing Parameters	Value
Q_{NMPC}	[1 0; 0 1]
R_{NMPC}	[40 0; 0 40]
Δu_{NMPC}	[-8 -8;8 8]
PH	100; 120; 140; 160; 180
CH	2; 4; 6; 8; 10
$Q_{KalmanFilter}$	Diagonal [0.01, ….0.01]
$R_{KalmanFilter}$	[1 0; 0 1]

The NMPC approach has a set of tuning parameters. These parameters are as follows: CH, PH, weighting matrixes (Q_{NMPC} and R_{NMPC}) on MAF and MAP, weighting matrixes (Δu_{NMPC}) on Xegr and Xvgt rates and weighting matrixes ($Q_{KalmanFilter}$ and $R_{KalmanFilter}$) on the Kalman filter. All of the necessary setups of the controller are listed in Table 5-1. In this section, different CHs and PHs are compared based on tracking performance. In order to assess the impact of NMPC on engine transient performance, it is necessary to define benchmark scenarios to provide the corresponding inputs and reference values for the simulation. The experiments are separated into the following types: 1) step response tracking: The controller tracking performance under different load disturbances (operation point changing) is an important criterion. For step response simulation, the scenario should contain at least one load change. The chosen of a reachable set-point set has to be considered. In this case, the default input profile is defined as 150 seconds overall runtime, and the load-changes consist in step changes in engine speed from 1250 to 2300 rpm and fuel injection from 13 to 27 mg/cyc. The time between the set-point changes is set to 15s to ensure that the air-path system researches steady-state. Furthermore, from the step response, the transient behaviour can be compared with different configurations of NMPC. The trajectories for step response tracking are presented in Figure 5.20. The simulation results are given in figures 5.21 and 5.22. The left column shows the desired values of MAF and MAP for tracking with the initial dataset, and the right column shows the corresponding actuator signals: VGT and EGT. 2) FTP-75 driving cycle tracking: the FTP-75 cycle provides a standard emission test with different operation points. The sample time is defined as 0.05 s in whole simulations. The results of the different test types are presented in the following sections.

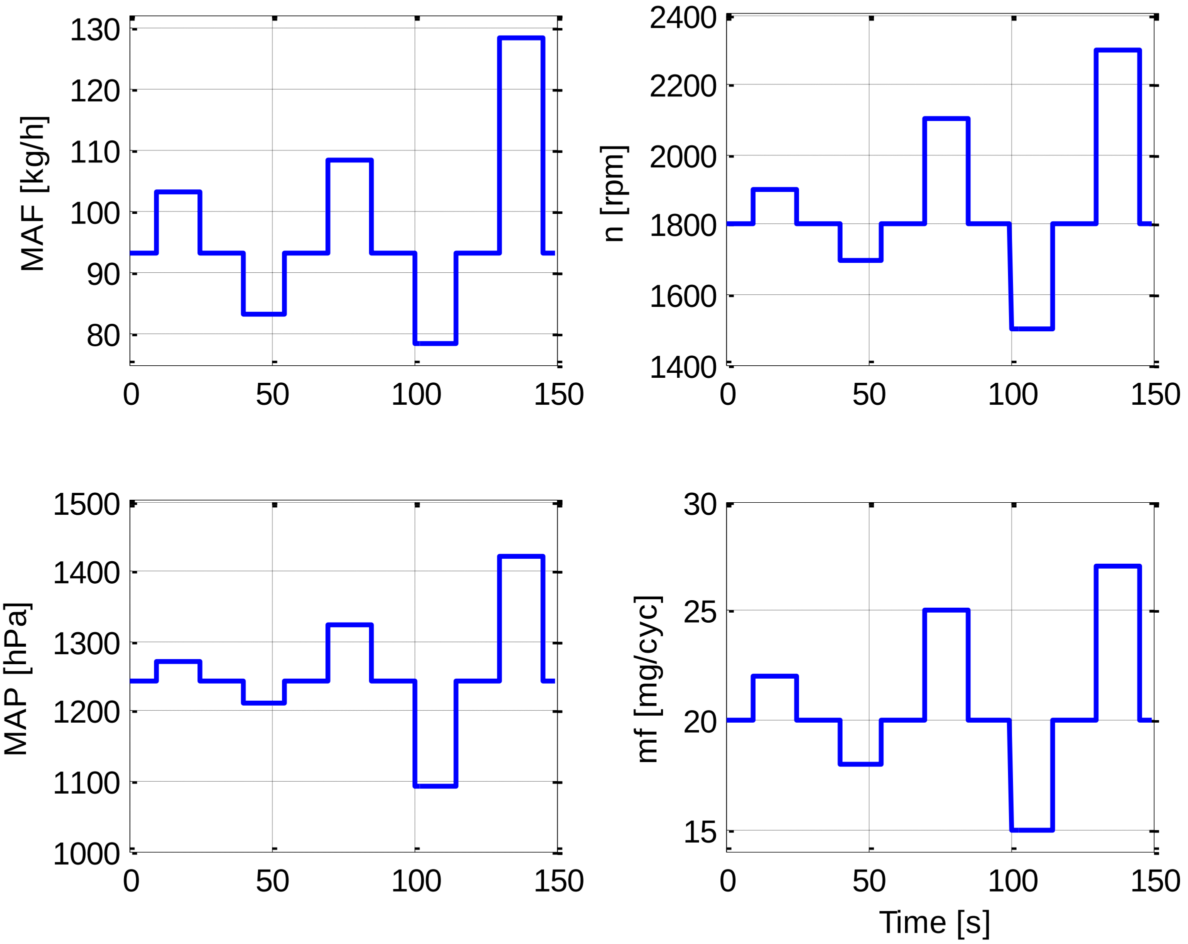

Figure 5.20: Test scenario for step response and tracking
(Left: reference MAF and MAP, right: operation points n and m_f)

5.3.2 Validation of NMPC Performance

Comparisons of the performance of different PH and CH configurations are performed in the same benchmark scenarios and under the same operating conditions. In the first experiment, the influence of PH variation is investigated, as mentioned in Section 5.2.2, to keep the computational burden as low as possible. Usually, the CH is chosen as a small number during the whole experiments; therefore, the control horizon is fixed by CH = 2 during the variation of the PH. The difference of the controller performance is derived from the prediction results encountered at different prediction horizons whereas the PH= [100 120 140 160 180]. As expected in Figure 5.21, all the PH variations are capable of reference value tracking to compensate for the load disturbances. Note that, despite different PH parameters, the obtained tracking performances and the actions of the actuators of VGT and EGR are similar.

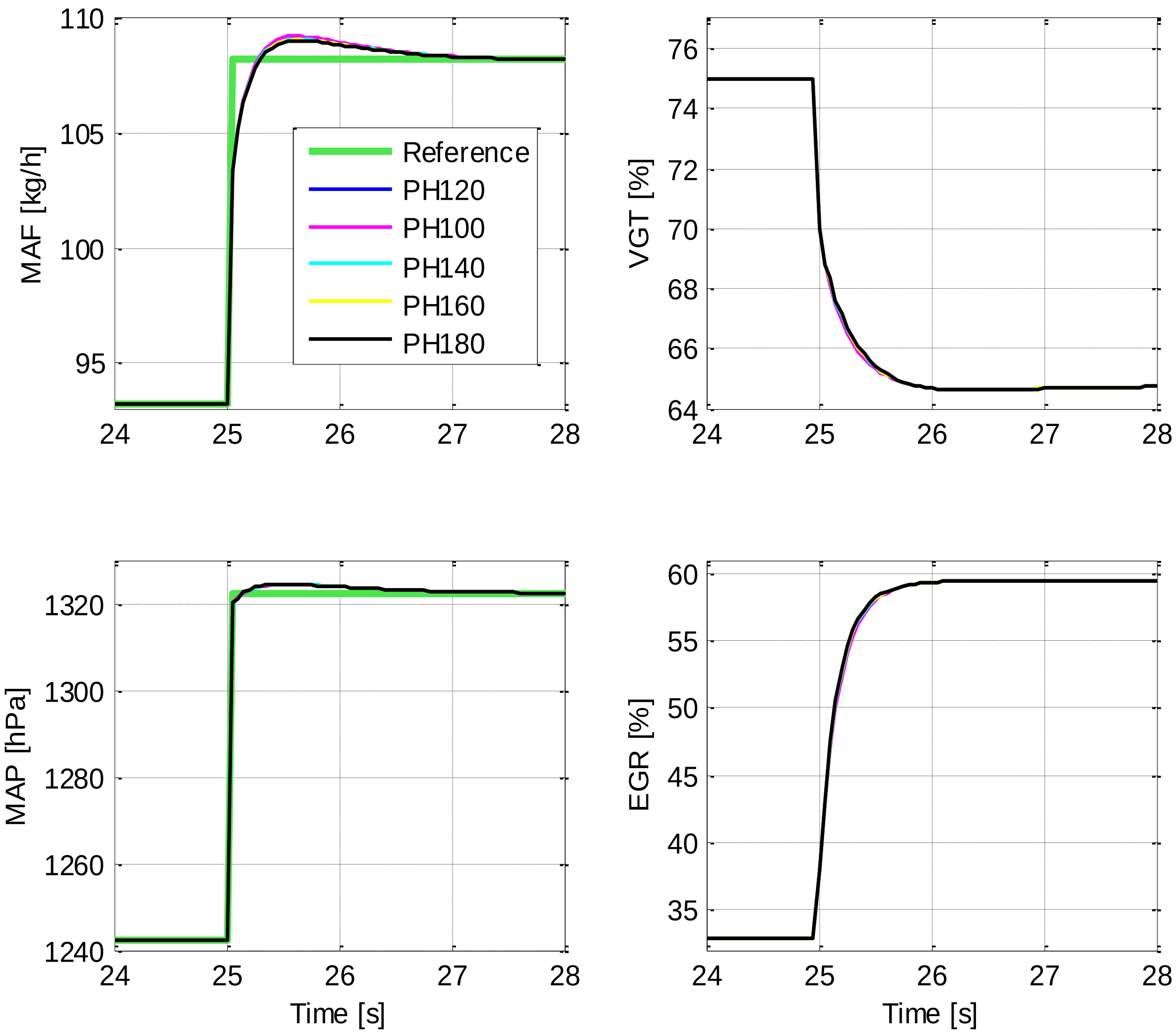

Figure 5.21: Evaluation of MAF and MAP over PH variation

The results in Figure 5.21 clearly show that the choice of PH has a very limited influence on the output of the NMPC controller and, for the considered case, increasing the PH clearly cannot improve the control performance. This behaviour is also confirmed by the MPC theory: The PH parameter determines the number of predicted outputs by means of the integrated mathematical model, and it must have a certain length to cover all model dynamics (Camacho & Bordons, 2007). Although the changes in performance with different prediction horizons from 100 to 180 are very limited in Figure 5.21, PH = 120 gives the best results; therefore, the PH is chosen as 120. Furthermore, according to (Camacho & Bordons, 2007), significantly shorter prediction horizons (for example PH= 20) cannot lead to improved performance, as the NMPC requires enough estimated information over the prediction horizons to optimise the inputs.

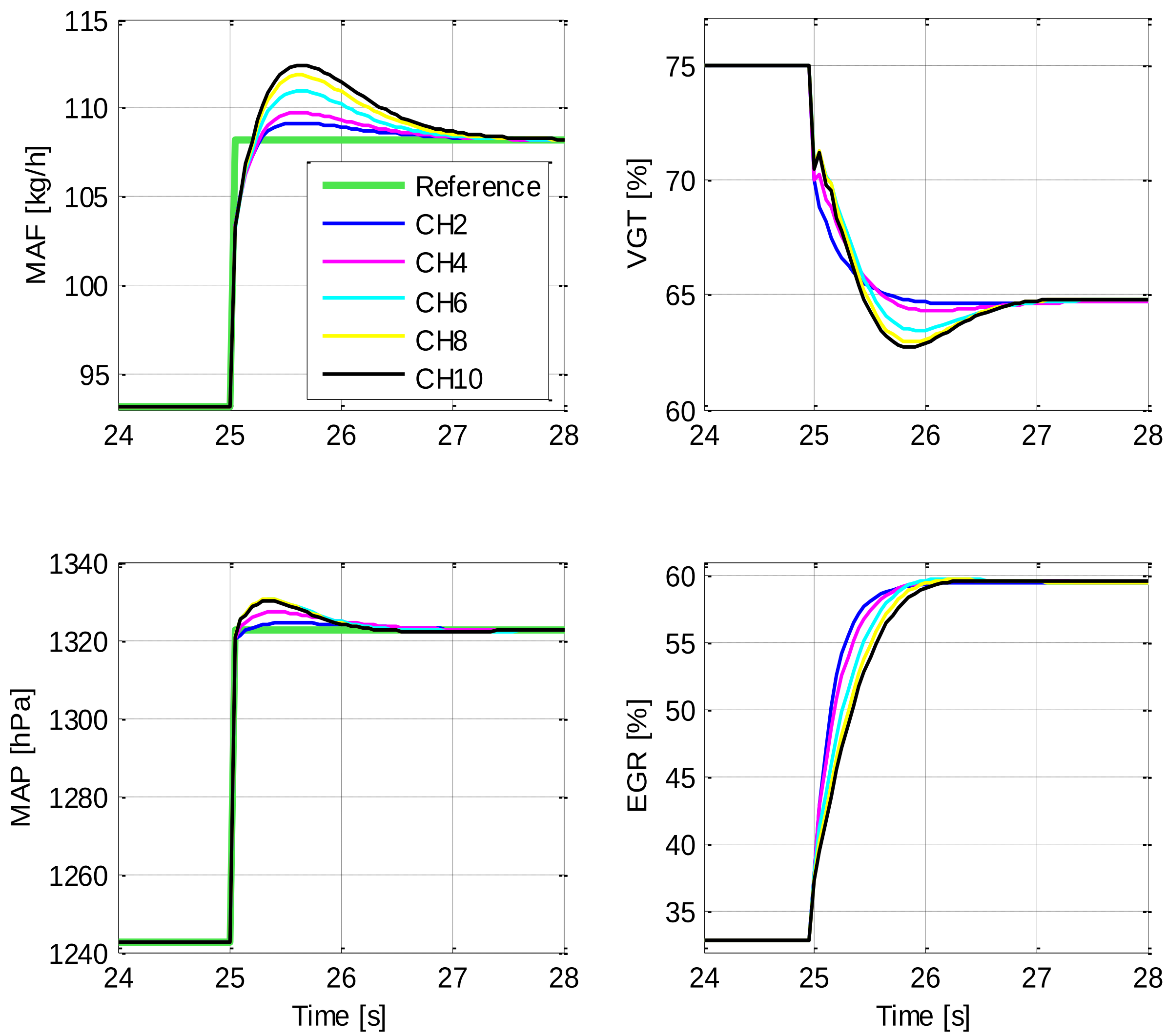

Figure 5.22: Evaluation of MAF and MAP over CH variation

According to the MPC theory, choice of a CH parameter has a significant influence on both the close-loop control performance and on the required computation time. To test the influence of the CH variation, different setups of CH have been investigated in the simulation whereas the PH is kept constant as 120. As can be seen in Figure 5.22 and Table 5-2, this obviously shows that all the CH variations are able to follow the desired value and compensate for the load disturbance. In contrast to PH, the CH has much more influence on the system behaviour.

The CH variation shows rather different step responses for MAF and MAP control. For different operation points, the actions of both actuator VGT and EGR differ. The results clearly show that the CH=2 succeeds in tracking the reference value in a shortest setting time, 2.5 seconds. The significance of the overshoot and the setting time to steady-state can be explained easily by appealing to the different CH setups [2, 4, 6, 8 10].

As shown in Figure 5.22 and Table 5-2, the shorter CH can lead a faster response to the required steady-state, as the longer CH permits more variations of the manipulated variables, which create additional degrees of freedom for the optimisation. Nevertheless, it should be noted that, as indicated by the fast QP method, all the optimisations in CH must be achieved in a short time, as longer control increases the computational effort. This behaviour is also confirmed by the MPC theory (Camacho & Bordons, 2007). Therefore, for this considered case, CH = 2 is chosen.

Table 5-2: CH value and time constant

CH Values	**Setting Time (second)**
2	2.5
4	2.7
6	2.8
8	2.9
10	3

Figure 5.23 shows the best NMPC closed-loop step response performance of the tracking with the configuration CH=2 and PH = 120.

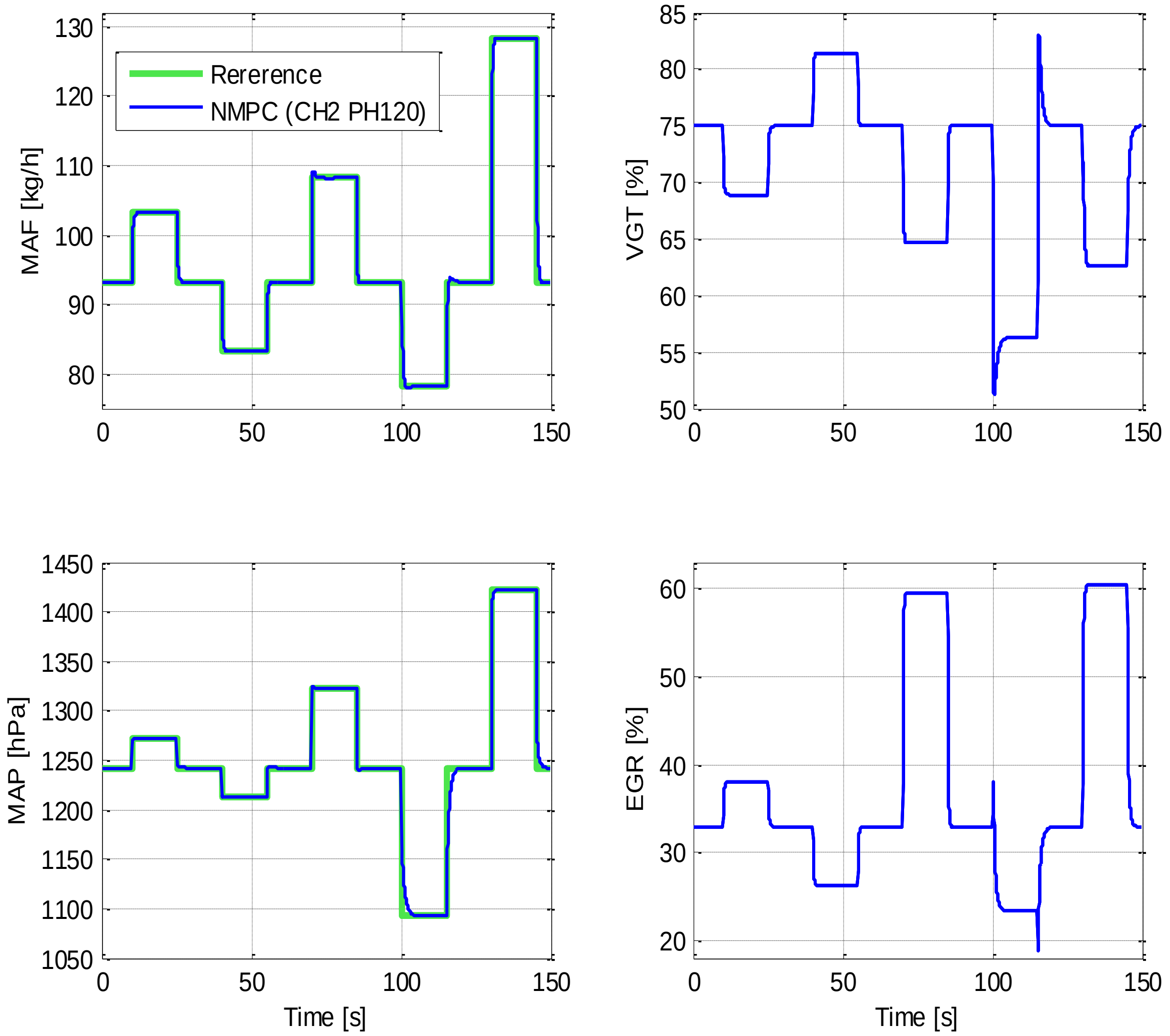

Figure 5.23: Overview of NMPC's closed-loop step response with best configuration

Both the results of PH and CH studies show that the NMPC controller is able to control the MAF and MAP under given set-point change. The question arises how this advantage affects emissions over a vehicle driving cycle. Therefore, the next reference profile to be tracked is the FTP-75 driving cycle. To make the tests clearly, the best CH and PH value are chosen from analysis of the simulation results presented above: PH=120 and CH = 2. Indeed, at steady-state, the MAF and MAP can be determined primarily by the operation point of fuel m_f and engine speed *n*. For a fixed operation point, the reference MAF and MAP value [MAF, MAP] = map (m_f, n). Therefore, to guarantee the same engine performance, the reference MAF and MAP have been kept unchanged with respect to the original ECU for the FTP-75 simulations. Figure 5.24 shows the simulation results for the FTP-75 tracking. The results lead us to the conclusion that the overall tracking performance of MAF and MAP is adequate; however, some local results on the peak are privileged, thus the reference cannot be followed due to possible unfeasible set points—especially for MAP around 200s and 450s in Figure 5.24. The results clearly show that the tracking performance strongly depends on the definition of set points. Such tracking errors can be reduced by optimising the set points to achieve requested performances regarding different operating points according to emission requirements. This optimisation issue of the reference values is discussed in Chapter 6.

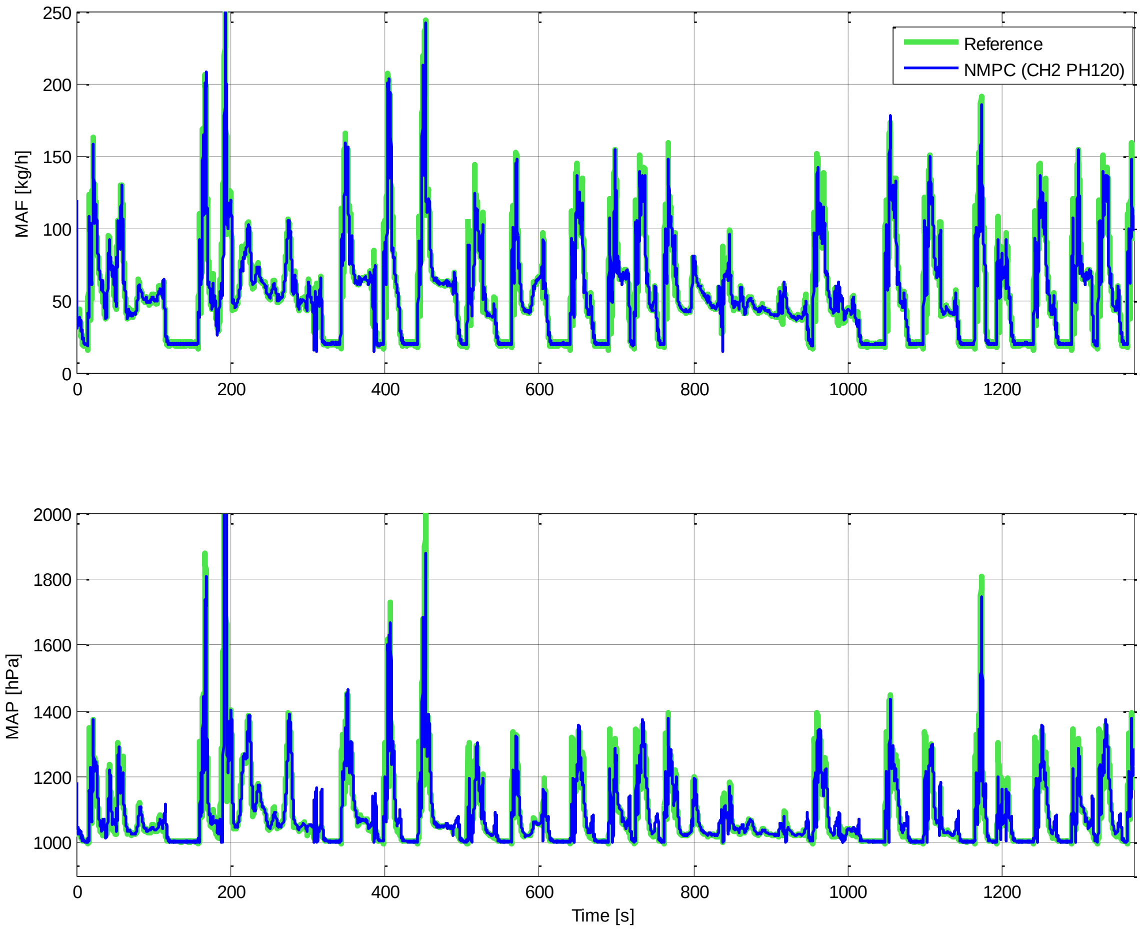

Figure 5.24: Overview evaluation of MAF and MAP over FTP-75 (0~1372s) (VAF_{maf}=87%, VAF_{map}=86%)

In Figure 5.25, 180s ~ 230s, the six main variables are presented. The upper cells show the trajectory of MAP and MAF and their tracking performance, in the middle the two cells show the manipulated variables X_{egr} and X_{vgt} and the emissions are shown in the lower cell. As is shown in Figure 5.25, the peak of the FTP-75 cycle is at about 195s, where the different reference values of the MAP and MAF are obvious. In this region, the engine operates at full load, while the emissions from engines which track high values of MAP and MAF produce a peak in NOx and OPAC due to high combustion temperature and high fuel consumption. One can see that the move direction of VGT and EGR are in contrast and that both actuators are nearly in saturation areas. This effect can be explained with the cross-coupling problem. For this case, at about 195s, the full load operation causes higher MAP and MAF. Therefore, the NMPC controller tries to increase the VGT vane position to compensate for the excessively high pressure in the intake manifold, and the closing of the EGR valve causes less exhaust gas to flow into the EGR valve. The tracking performance approves the results achieved previously; the NMPC is able to track their reference during the transient operation. However, at 190s, a shift operation causes a huge change in the VGT and EGR positions, so the NMPC fails to compensate for the disturbance and causes a small vibration on MAF and MAP.

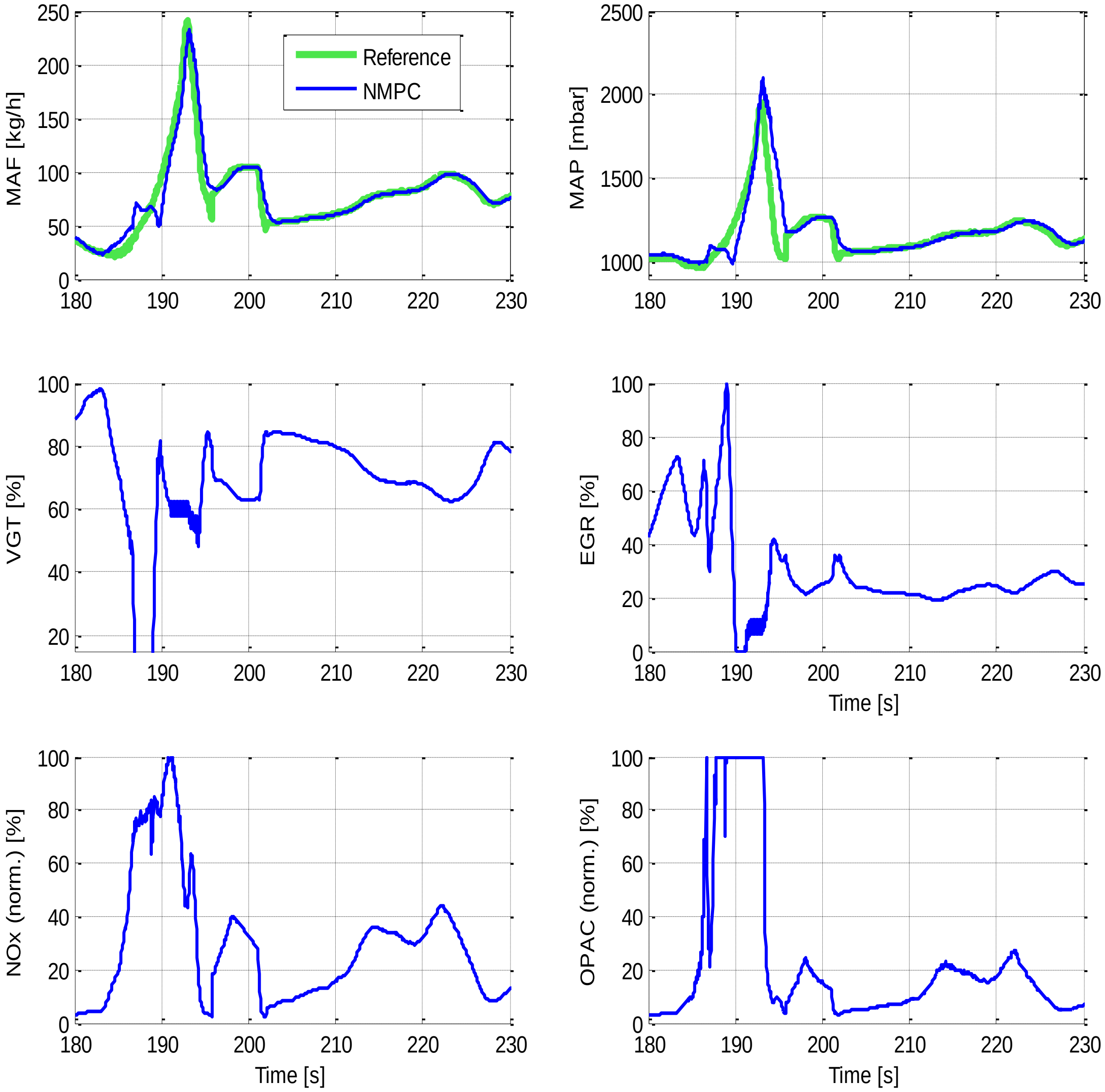

Figure 5.25: Evaluation of MAF and MAP over the FTP-75 (180s -230s)

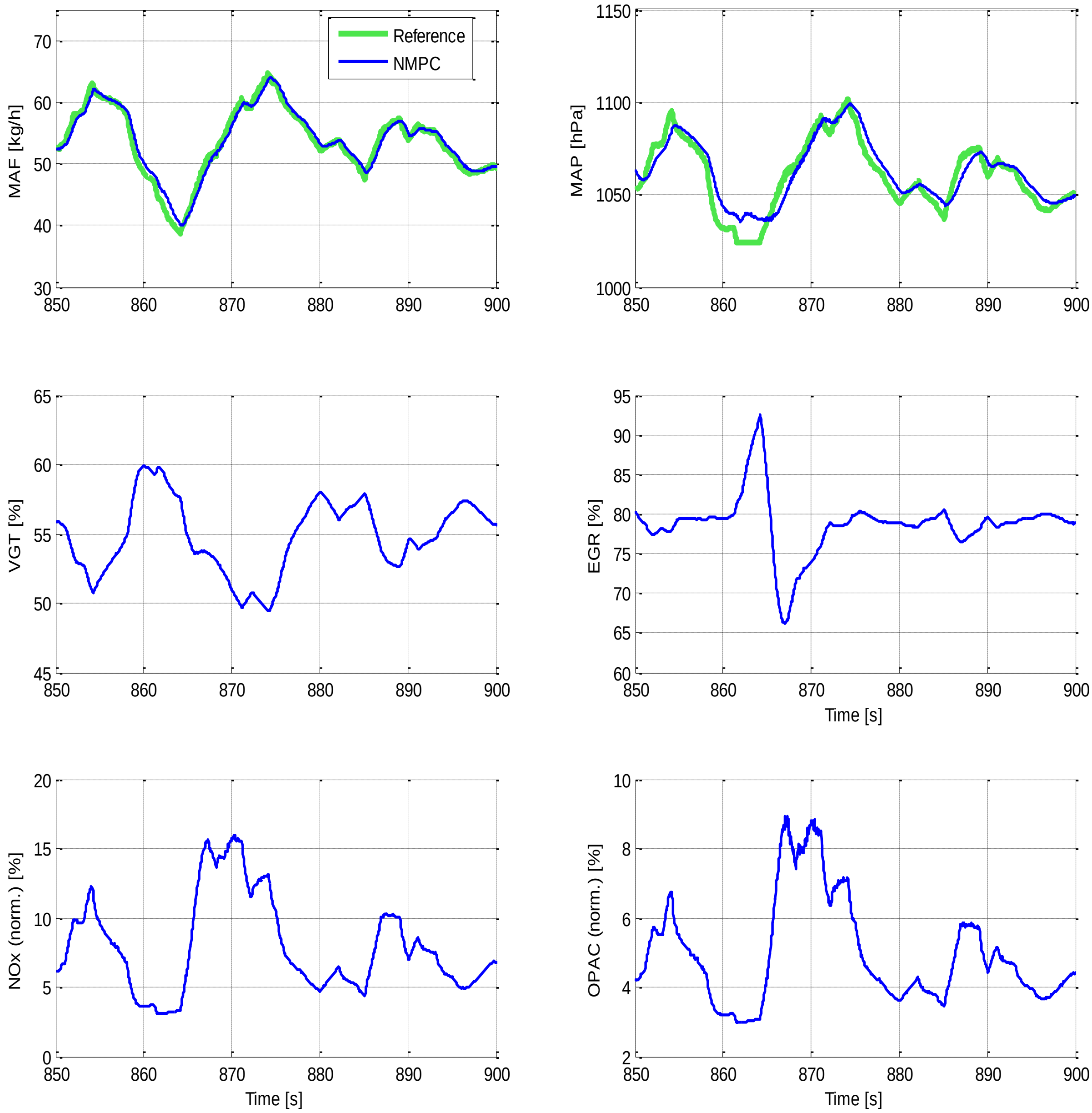

Figure 5.26: Evaluation of MAF and MAP over the FTP-75 (850s -900s)

As is shown in Figure 5.26, 850s ~ 900s, the NMPC increases the amount of EGR to 80%, which decreases the combustion temperature and can lead to less NOx. An interesting aspect of this process is that, despite the lower NOx, the OPAC obtained is not excessive. It seems that the engine operates in idle areas and has a very limited fuel injection on a lean condition. This effect can be confirmed by the advantage of the diesel engine in contrast to a gasoline engine (Reif, 2014). The simulation results show the NMPC, closed-loop, step-response performance of the tracking for desired MAF and MAP and the according engine actuator signals of VGT and EGR. Thanks to the internal non-linear LPV model and the well-posed optimisation QP-solver as presented in (Ferreau, 2014), the NMPC controller is able to track the reference signals quite fast without offset and compensate for the load disturbance.

5.3.3 Comparison with Existing Control Approaches

To show the advantage of the proposed NMPC method, in the comparison of the control performance of NMPC, linear MPC and standard ECU function (simulated functions in Matlab/Simulink), the experiments are performed under the same operating conditions on a step response and FTP-75 driving cycle. For benchmark purposes, the standard ECU air-path control function is implemented into the virtual engine test-bench, which essentially contains feed-forward loop up tables and a PID controller, as depicted in Figure 2.12. The configurations of the NMPC and MPC are set to PH = 120 and CH = 2. The performances of the different controllers are presented in the following.

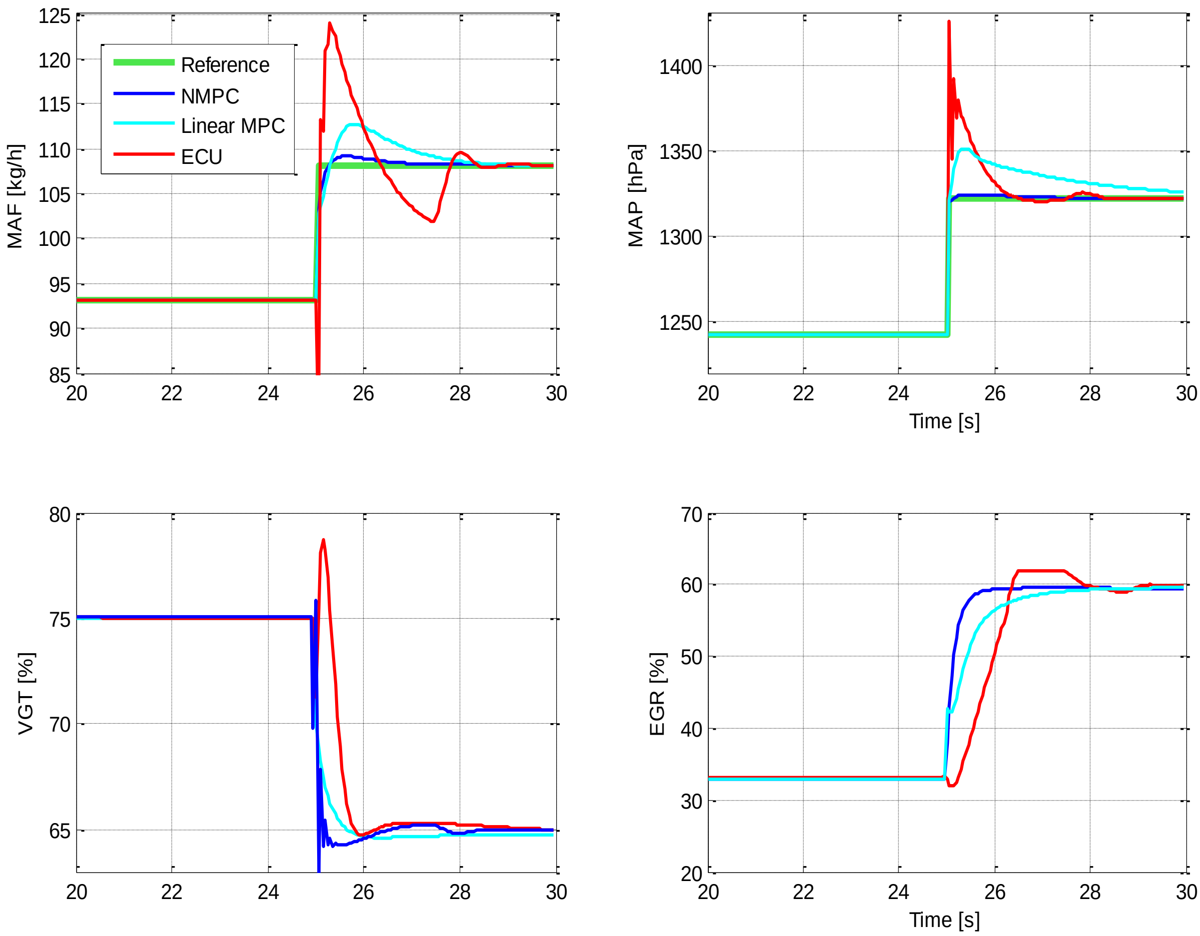

Figure 5.27: Set point change NMPC, Linear MPC and ECU

As shown in Figure 5.27, the results clearly show that all the controllers are able to follow the step trajectory without offset. On the transient areas, the NMPC controller has much better performance. The linear MPC and ECU have poor results in operation changing and get transient invisible, whereas the NMPC can solve the problem very well and arrive quickly at the steady-state, rejecting all disturbances.

We may conclude that the linear MPC based on the linear model shows an overshoot and a slower reaction to the actuator positioning, which causes a large error in tracking the MAF and MAP. The main reason for this behaviour is that the internal mathematical model is linearised only in the near-of-one operation point in linear MPC.

The overshoot comes from the large internal model mismatch. This problem leads to the model description in Section 5.2.1.2, where the linear state-space air-path model is not the best model with respect to MPC application compared to LPV model. Furthermore, in transient areas, the ECU controlled EGR and VGT valves have great overshoots at every larger change of operating point (for example at 25s in Figure 5.27), although the PID controller (in the ECU) is a very strong linear controller, but it is difficult to tune its parameters in order to well regulate the high non-linear systems in transient areas, such as operation changing of engine-air-path system. Therefor in the transient areas, the ECU causes strong overshoots in the MAF and MAP.

In Figure 5.28, the FTP-75 tracking performance is shown in detail from 390 to 420s. At about 403s, a change of engine operation causes a huge increase in the MAF and MAP so that the linear MPC and ECU fail in fast-tracking the reference value. For linear MPC, this is caused by the large mismatch of the internal model. It is certain that, without change of the engine operation and disturbances, both NMPC and linear MPC would deliver similar tracking behaviour. For this case, a comparison with the ECU controller is not fair, as the ECU control loops include a feed-forward part which is exactly optimised to the MAF and MAP set-point maps. But when changing the set points, the relationship between the feed-forward part and the set point is no longer correct and leads to bad results.

The large deviation of ECU shows that the PID controller parameter used in the FTP-75 cycle is not optimised and results in large oscillations of MAF and MAP. In contrast, the NMPC produces relatively small offsets and overshoots in MAF and MAP tracking.

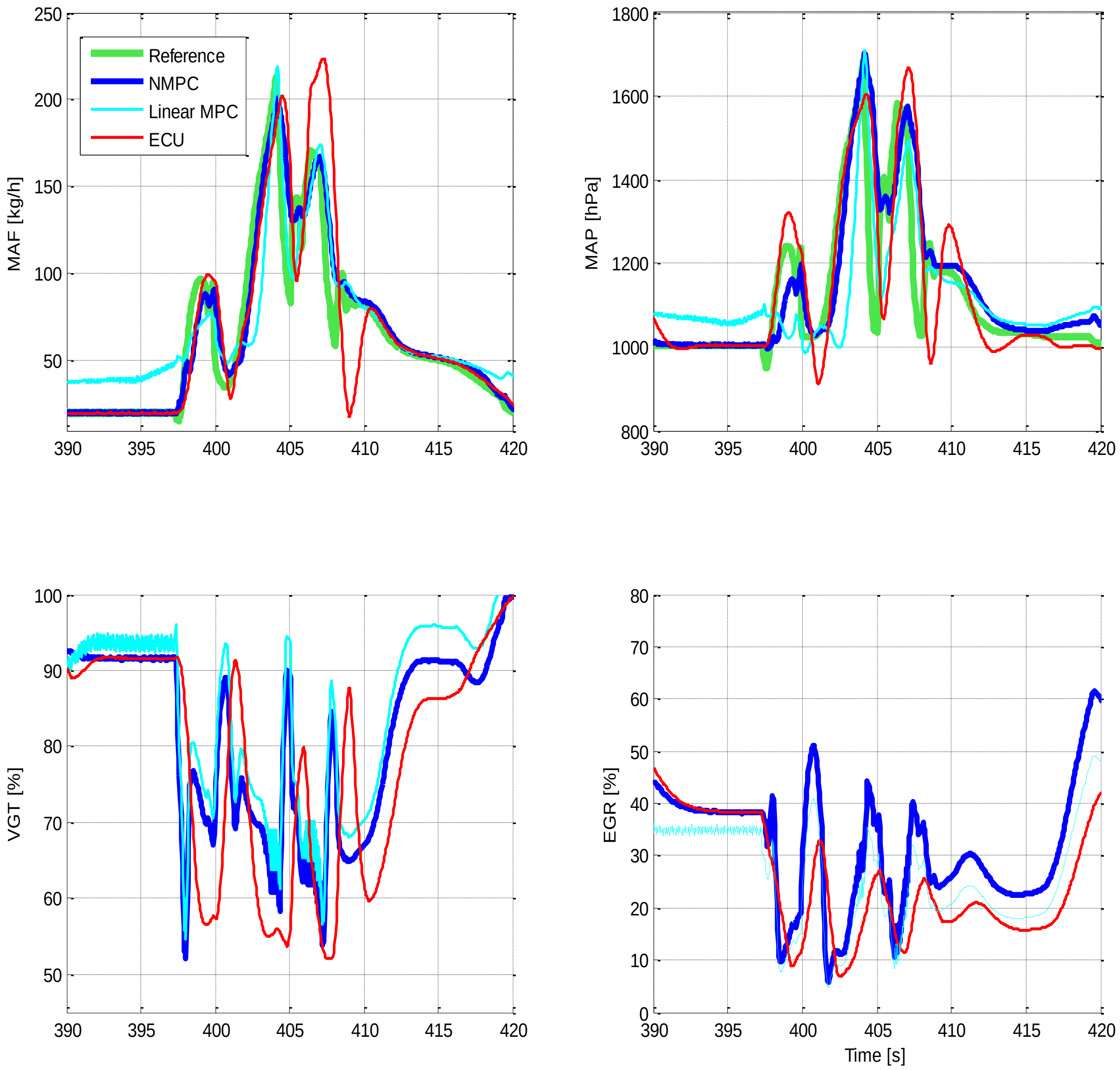

Figure 5.28: FTP-75 tracking- NMPC, Linear MPC and ECU (390s-420s)

Figure 5.29 shows the simulation results of the FTP-75 cycle, in which the performance of the difference controllers is obvious.

In Table 5-3, the tracking performance in VAF is shown; the results lead us to the conclusion that the NMPC is able to keep the MAF and MAP to the references better than the liner MPC and ECU. All three controllers can track the references satisfactorily during the FTP-75; however, their handles on the operation point’s change are very different. The results above clearly show that tracking performance strongly depends on the combination of the MPC internal model and the choice of the reference trajectories.

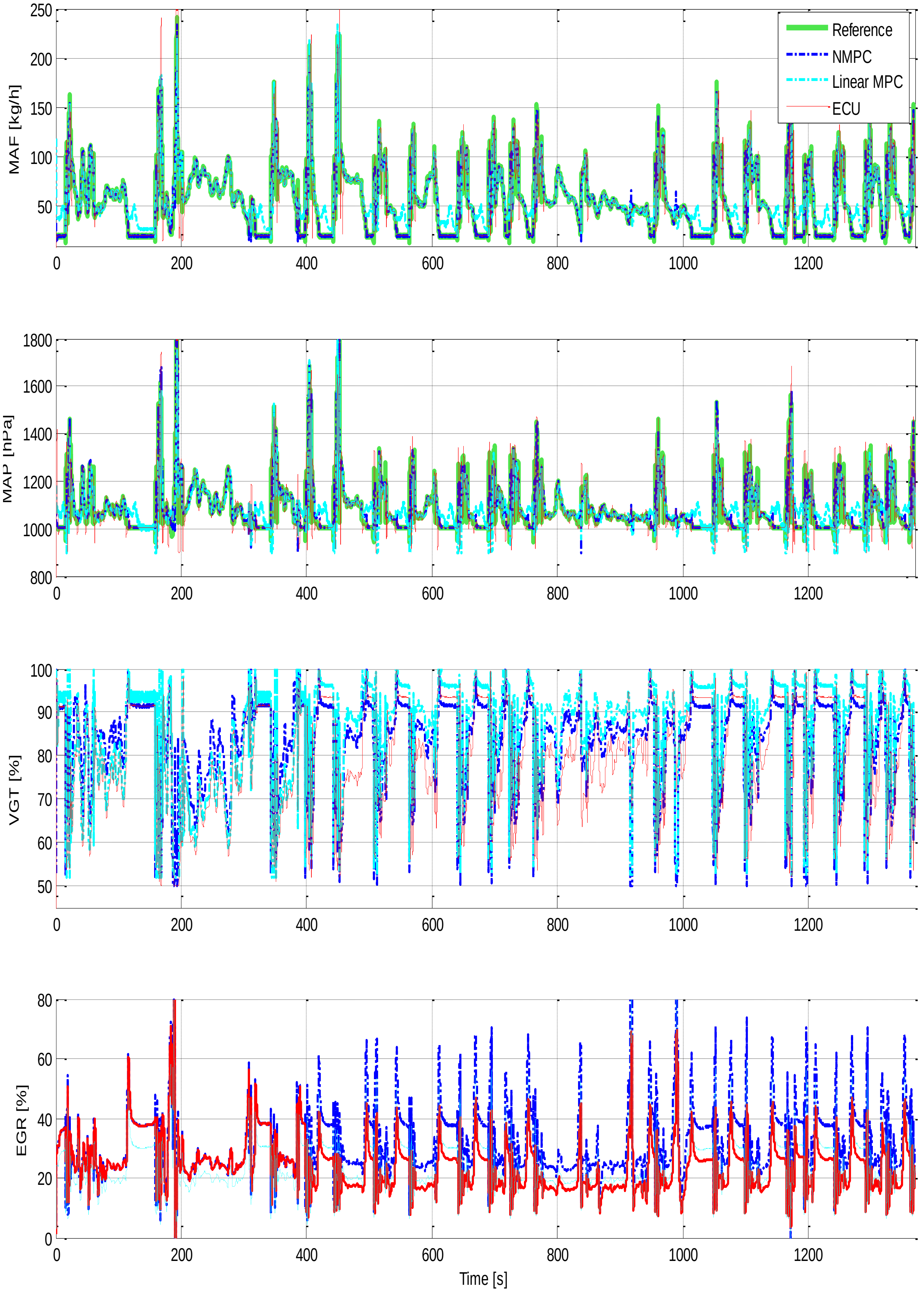

Figure 5.29: Overview of FTP-75 tracking- NMPC, Linear MPC and ECU (0~1372s)

Table 5-3: Comparison of the tracking performance in VAF (norm) in FTP-75

	Tracking results relative VAF value (Norm) [%]	
	MAP	MAF
NMPC	100%	100%
Linear MPC	85%	83%
ECU	87%	85%

As illustrated in figures 5.30 and 5.31, in FTP-75, the cumulative value of NOx and OPAC obviously shows that NMPC performs slightly better than the ECU with respect to both cumulative NOx and OPAC value. The main reason could be the improvement on the transient behaviour of EGR and VGT control, which results in reduced transient emissions. The results are actually not surprising, the improvement on emissions using NMPC are very limited, because using the same reference values in the case of NMPC cannot essentially change the overall emission output due to the un-optimised reference values, although the NMPC delivers a better tracking performance. It should be interesting to note that, by using the NMPC approach, it could be possible to reduce the overall driving-cycle emission-output result by optimising the reference values.

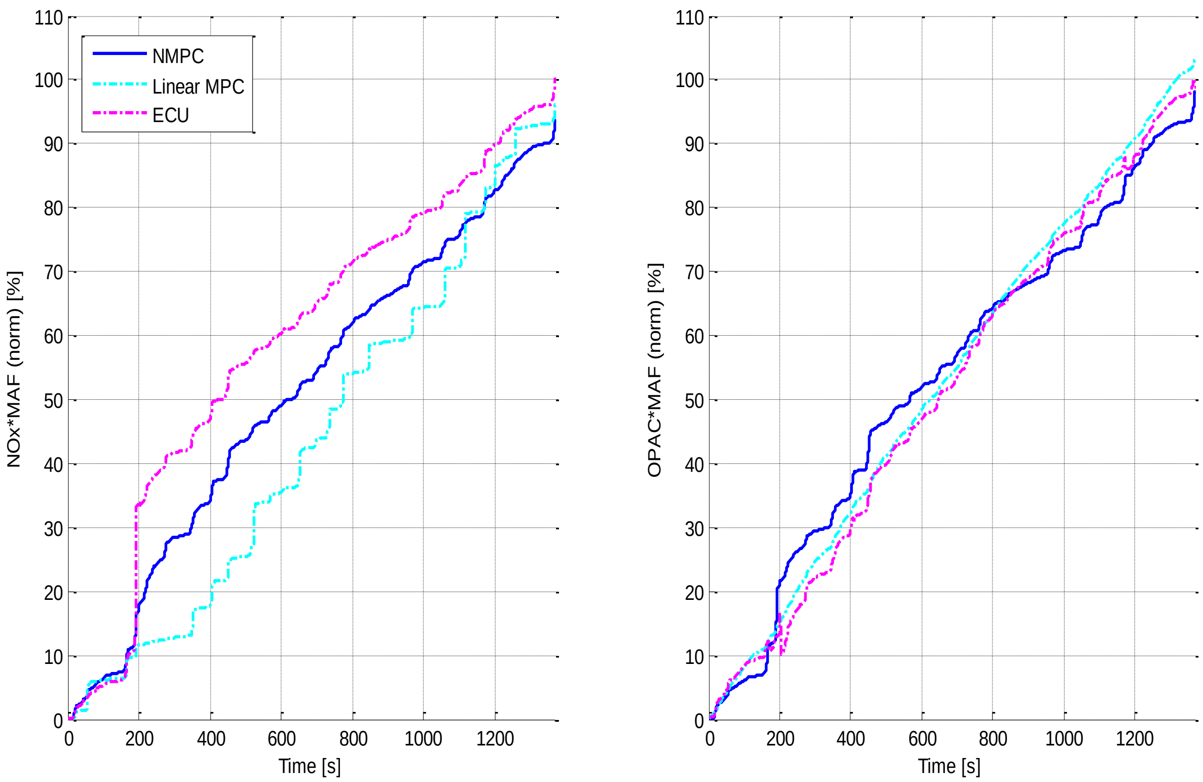

Figure 5.30: Cumulative values of NOx and OPAC (norm) in FTP-75

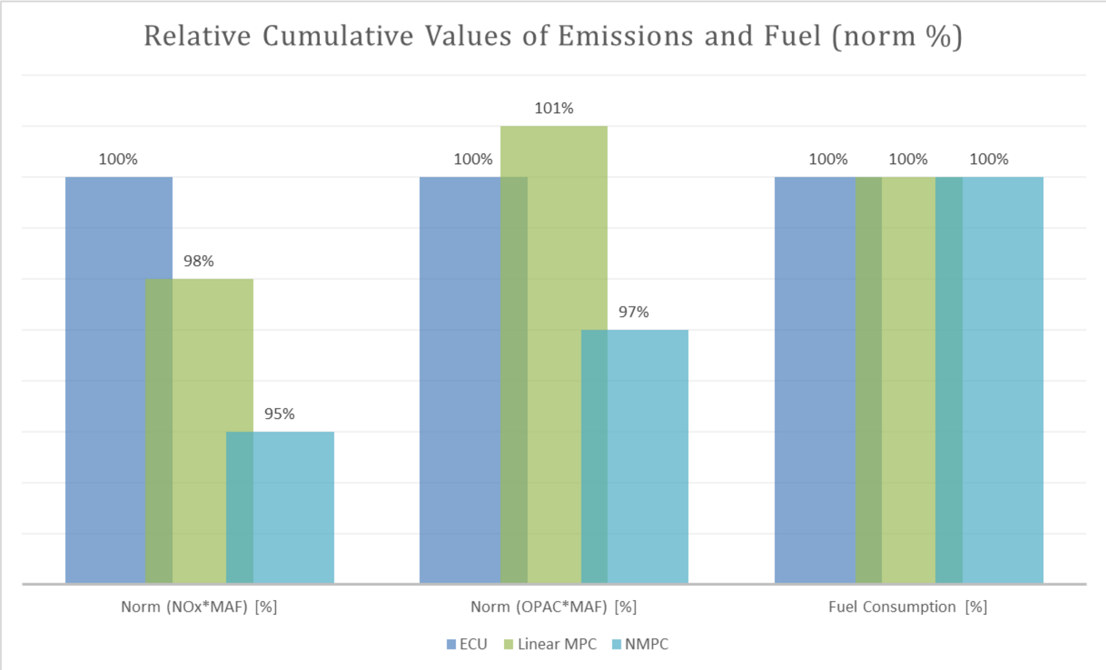

Figure 5.31: Relative cumulative values of Fuels, NOx and OPAC (norm) in FTP-75

Furthermore, the simulation results and control performance discussed in Chapter 5 show that nominal stability is given under realistic assumptions and the closed-loop NMPC scheme is not critical to stability in fast process controls such as engine-air-path control. In Chapter 6, the method of choosing MAF and MAP references in an optimal way will be presented.

Chapter 6. Application of Model-based Emissions and Fuel Optimisation on Engine-air-path Control

Modern internal-combustion engines have to meet constantly increasing demands in terms of the reduction of fuel consumption and abatement of emissions. The progress of hardware design leads to engines with more degrees of freedom and with the capability of achieving better performance in favourable directions. Control is one component which makes the possibility of design-optimisation come true (Del Re, 2011). In modern diesel engines, besides the classic manipulated variables of fuel-injection quantity and fuel-injection timing, the ECU interfaces are expended by further manipulated variables such as valve position of EGR, guide-vane position of VGT, injection pressure in common-rail systems and variable valve train (VVT). Unfortunately, the rising number of engine-control variables makes it increasingly difficult to find the optimal engine calibration and control solution at an acceptable time (Malikopoulos, Assanis, & Papalambros, 2008). As an enormous number of control options is available from table- (or map-) based heuristic control to optimal model-based control, the choice is not always easy. Consequently, engine-control design has often been boiled down to a large number of parameters, which are calibrated in the course of tiring work, thereby yielding what may be the most complex and least systematic feed-forward design structure available today.

In modern diesel-engine development, this problem is even more evident. As shown in Figure 6.1, to analyse the influence of individual manipulated variables on steady-states in all operating ranges quantitatively, the time-consuming grid measurement and operation costs required at engine test-benches increases considerably. The traditional approach, which is limited to a purely steady-states assignment of inputs and outputs, has been obsolete for a long time and can no longer meet all the current legal requirements. On the other hand, consideration of system dynamic behaviour is indispensable—especially for engines with turbochargers. The dynamic behaviours of exhaust emissions from the driving cycle must be studied to optimise the transient engine operation. As illustrated in Figure 6.1 regarding the signal-flow scheme for the optimisation of control functions for combustion engines, model-based methods are therefore necessary for the further development of engine-management systems that allow the steady and dynamic behaviour of combustion engines to be determined as accurately as possible by means of computer simulation and optimisation based on a mathematical model (Isermann, Hafner, Schaffnit, Schueler, & Sinsel, 1998; Mitterer & Zuber-Goos, 2002).

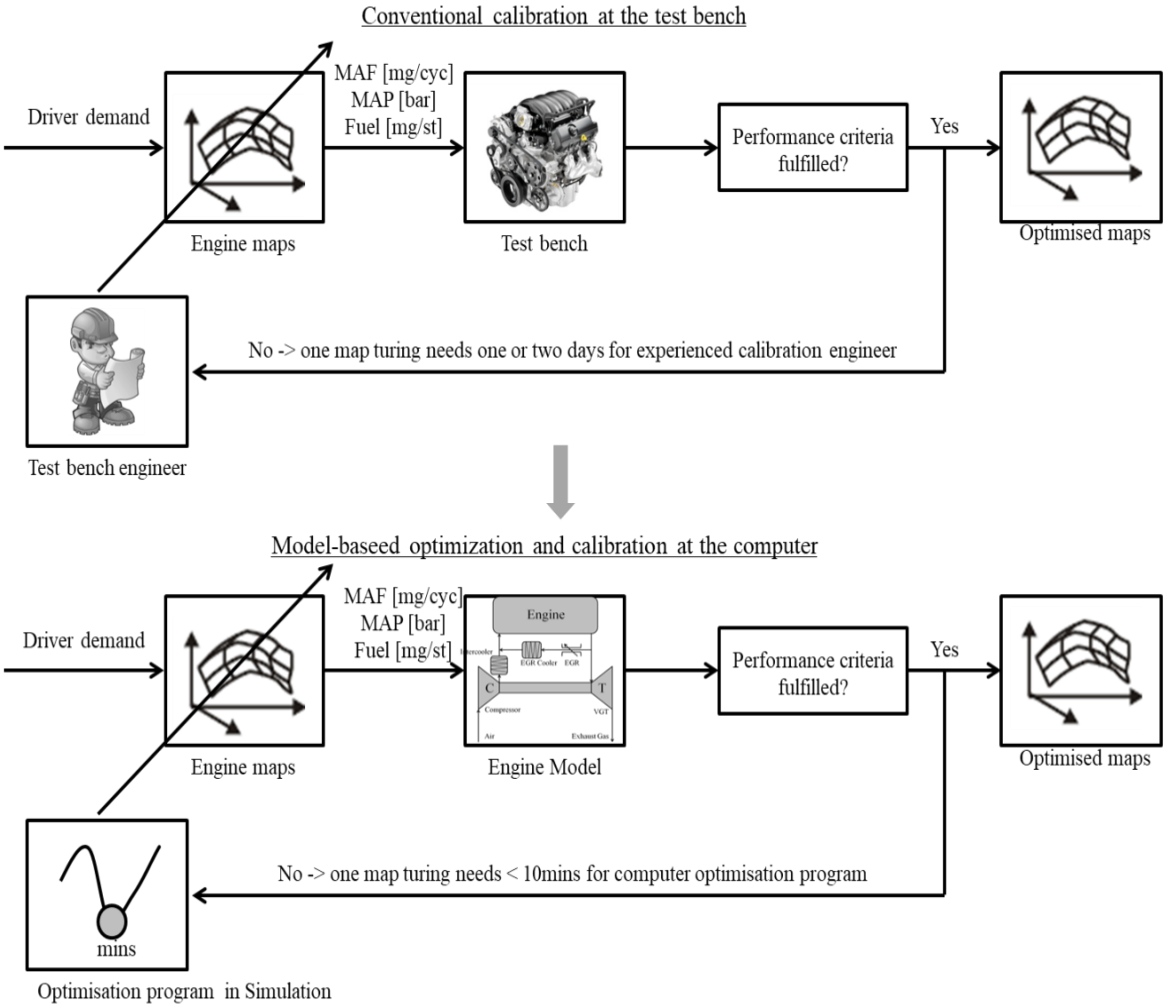

Figure 6.1: Trends in model-based optimisation and calibration

As mentioned in Chapter 5, simulation results in Table 5-3 and Figure 5.31 lead to the conclusion that, nevertheless, there is a strong coupling of VGT and EGR, and a significant improvement regarding VGT and EGR controls is achieved by using NMPC control in the engine-air-path. However, by using an advanced control method in the engine-air-path, no clear improvement of emissions is found in a systematic way even though a significant improvement of dynamical behaviour is achieved (Alberer, 2009). Ortner, Langthaler, Ortiz and Del Re (2006) show that the minimisation of emissions can be achieved by considering the optimised control reference values. This chapter presents an approach which is based on the virtual engine test-bench to optimise the emission behaviours and fuel consumption of internal combustion engines. A new, model-based, multi-criteria optimisation is presented, compared and discussed. The reference values of MAF and MAP are optimised for a driving cycle case based on the emission models from the first part and further evaluated for an NMPC engine-air-path control on the virtual engine test-bench with the target of reducing the emissions and fuel consumption. The optimisation results are then compared to the default ECU and un-optimised NMPC.

6.1 Model-based Multi-criteria Optimisation on Emissions and Fuel Consumption

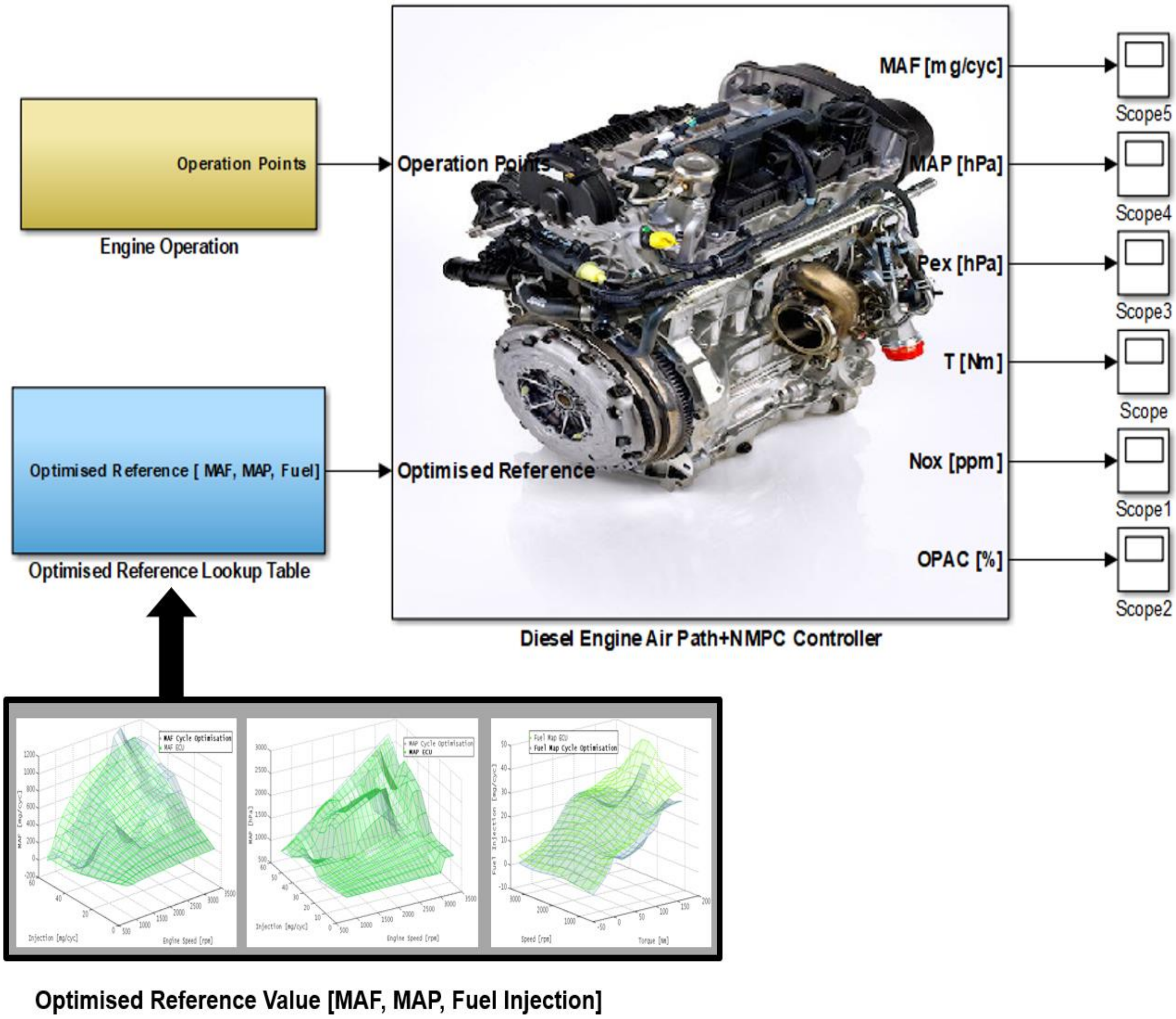

Figure 6.2: Model structure for optimisation in Matlab/Simulink

To benefit from the advantages over conventional diesel engines, the operating strategy implemented in modern diesel engines has to be optimised. This includes the reference strategy, which for air-path control means the reference values of MAF and MAP at each operation point. Unfortunately, there is no universal algorithm for the optimisation of control references due to the huge diversity of control functions and their complexity. Hence, it is obligatory to carefully study the characteristics of each configuration to imagine the best setup. In this section, different methods are introduced which aid the optimisation of the emissions based on the engine model. These methods concern air-path, torque and emission models from Chapter 4 (Figure 6.2).

The first approach here aims to determine the optimised reference maps for the engine-control variables, MAP and MAF, independent of a specific driving cycle. A driving cycle-based optimisation of emission behaviour and fuel consumption is then discussed. It is difficult to perform engine optimisation for emissions and fuel consumption on a real test-bench due to the complex controls. To obtain the optimal solution, the influences of the control variables have to be balanced at all operating points against each other with the consideration of the engine dynamics. In ECU, these are values, curves and maps based on engine operation points. For optimisation tasks on air-path control, the target would be the reference maps of MAF and MAP. In practice, on the real test-bench, the MAF and MAP reference values have to be calibrated so that, on the one hand, the exhaust emissions are minimised during the driving cycle and, on the other hand, the exhaust temperature is not be heated too much and the fuel consumption is minimal. The calibration optimisation task is to find, for every operation point, a combination of MAF and MAP that leads to minimal emissions.

To optimise the controls maps in ECU, several approaches are presented in (Malikopoulos, Assanis, & Papalambros, 2008), which are based on the selection of several main operating areas that represent the most of the emission driving cycle, and the engine has to be optimised as much as possible in these areas. The influence of the control variables is measured in these operating points on the test-bench. The main weakness of this approach is in the limitation of the number of operating points for optimisation; the reason is that online optimisation of a wide range of operating points on the test-bench is often expensive and time consuming.

In the following, a model-based method for engine optimisation is presented which can consider a large number of emission driving cycle operating points. The first issue of this optimisation task is to find the ideal reference value of MAF and MAP for the emission reduction. The outputs of this optimisation are references of MAF and MAP. Therefore, a mathematical cost function J has to be defined, which needs to be minimised by the optimisation algorithm. This function consists of several summands, each of which reflects a certain feature. Each of these summands can be weighted by weight factors k1 and k2 to consider its influence on the optimisation result. The cost function defining the minimisation problem is as follows:

$$J = k1(norm(NOx))^2 + k2(norm(OPAC))^2. \tag{6-1}$$

NOx and OPAC specify the emissions at each operation point. All the terms are considered to be quadratic in form, and their minimisation is important for whole emission cycles. The quadratic cost functions are mapped by emissions in compliance with the legal emission limits found by using a non-linear optimisation process. To solve the optimisation problem, the Matlab command fmincon is used. Using fmincon allows for a minimum of a constrained, non-linear multivariable functions. However, it is not trivial to find a setup of weight factors and it therefore has to be done with care. Moreover, it is important to understand that the dimensions of different weight factors cannot be directly compared, as they are coefficients to values of different units: e.g., NOx in ppm and OPAC in %. Therefore, the weight factors k1 and k2 have to be specified, depending on the normalised ratio of NOx (norm(NOx)) and OPAC (norm(OPAC)), as shown in Equation 6-1, before starting the optimisation algorithm. The used variables in Equation 6-1 are defined in the following table:

Table 6-1: Elements of cost function

Summand	Weight factor	Target
NOx	K1	Low NOx Emission
OPAC	K2	Low OPAC Emission

The optimisation algorithm then starts the simulation and varies the target parameters MAF and MAP, which are then determined by the minimisation of the cost function. As mentioned above, the MAF is the amount of air required to support oxygen as much as necessary to react hydrogen into water in a stoichiometric way. In general, a diesel engine runs with $\lambda > 1$, and its normal operation areas are overall $\lambda > 1.1$. For optimisation, some variations in an area around this value are possible and necessary. To get the two constraints, minimum MAF and maximum MAF, a multiplication with is performed with λ, factor 14.5 and fuel injection. The value of λ is defined as λ = 1.1 to calculate the minimum MAF. It is defined as λ = 2 to calculate the maximum MAF. Factor 14.5 is the value of the stoichiometric equivalence factor for diesel engines. Therefore, the applied lower and upper boundaries of MAF are [$14.5 \times m_f \times 1.1$] mg/cyc and [$14.5 \times m_f \times 2$] mg/cyc, which are estimated by the required lambda and fuel consumption. The MAP is the manifold pressure, which describes the pressure of intake manifold. Its boundaries have been set to ambient pressure up to 2.2 bars because of safety reasons.

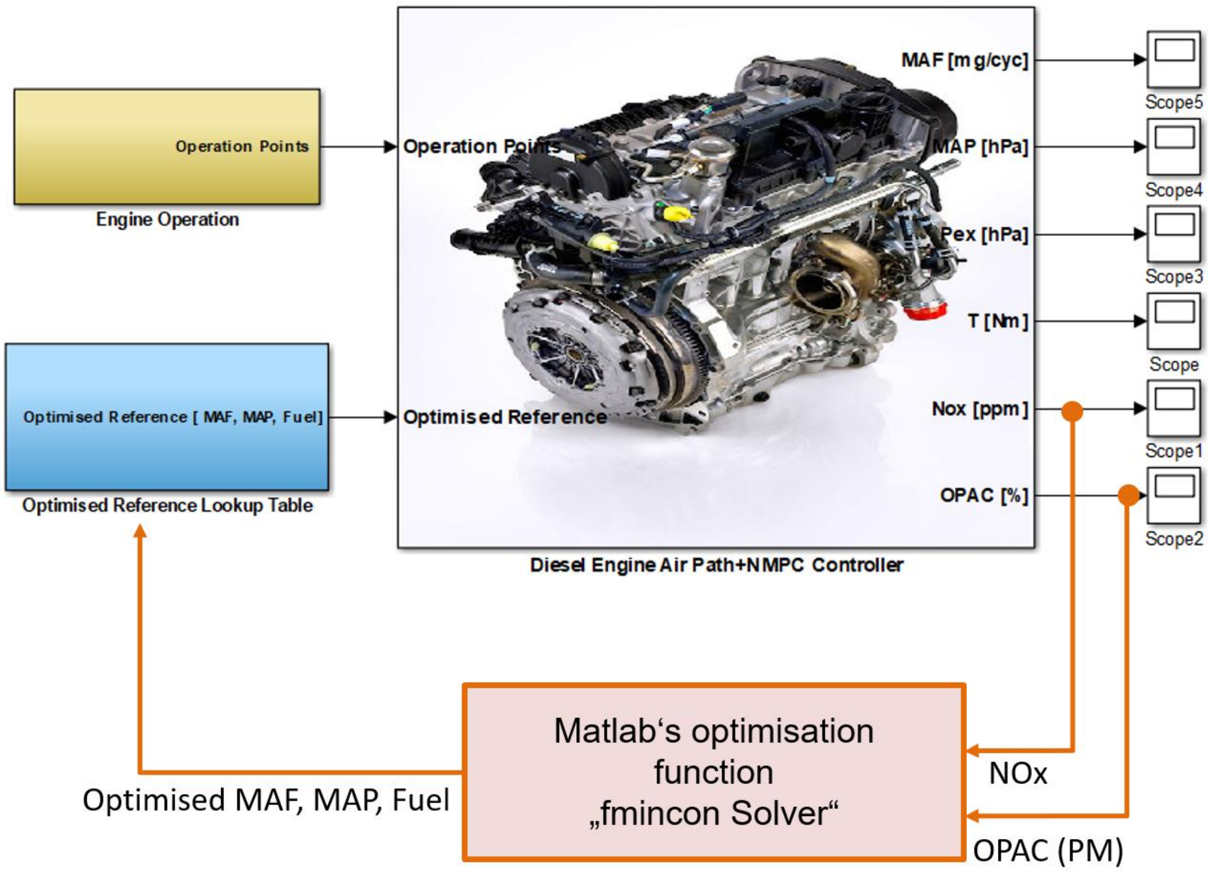

Figure 6.3: Optimisation loop and function blocks

As mentioned above, the optimisation of the references required several steps of refinement whereas, due to the lack of convexity of the problem, it is important to have an appropriate point to start. The Matlab function fmincon is initialised via the specification of optimisation parameters MAF and MAP and their upper and lower boundaries, as mentioned above. The optimisation method varies both parameters simultaneously according to the underlying algorithm. Figure 6.3 shows what the objective and optimisation functions are called by the Matlab's fmincon solver. The Matlab function fmincon attempts to find a constrained minimum of Cost Function J (Equation 6-1). In every iteration step, the emissions are calculated by the engine-air-path model in Figure 6.3 with the given constant inputs, which are engine speed, fuel injection, MAF and MAP, and Cost Function J. Equation 6-1 is evaluated by the Matlab function fmincon until the results of Cost Function J reach the stop criterion. To start the optimisation process, an initial estimate of the set of parameters must be made. In practice, this is done by trial and error, which means that the initial estimate is adjusted manually to achieve the best result. In this case, the initial estimate which provides the optimum solution for using the Matlab command fmincon is found to be MAF = 650 mg/cyc and MAP = 1.013 bar.

The value of weight factors is also important to the final results. This is the main degree of freedom in the optimisation program, as one can determine the importance of each summand of the cost function and the corresponding optimisation target by adjusting the appropriate weight factor. In the series ECU, higher EGR positions are applied at low operation points. Accordingly, the NOx emissions increase strongly at high operation points. If only the NOx emissions are weighted in the cost function *J*, the engine tends to exhibit higher EGR rates in the main entire operation areas. This can significantly reduce the NOx, but not for opacity. As shown in the Table 4-4, the engine has more NO_x emissions than expected; therefore, in order to achieve better comprehensive performance and further reduce the NO_x emission of this diesel engine, more weight is given to the NO_x weight factor k1. With a consideration of more weight on NO_x in the cost function, a variation of the weight factors is achieved for benchmark purposes as shown in the Table 6-2, and the weightings of NO_x are varied from 1 to 100. Applying the presented setup to the optimisation of the references results in the following figures (Figures 6.4 and 6.5). The optimised MAF and MAP references using different weight factors are very different, which clearly shows that the weight factors have a great influence on the optimisation results.

Table 6-2: Setting of weight factors

Weight factor	Value
K1/ k2	1/1
K1/ k2	10/1
K1/ k2	75/1
K1/ k2	100/1

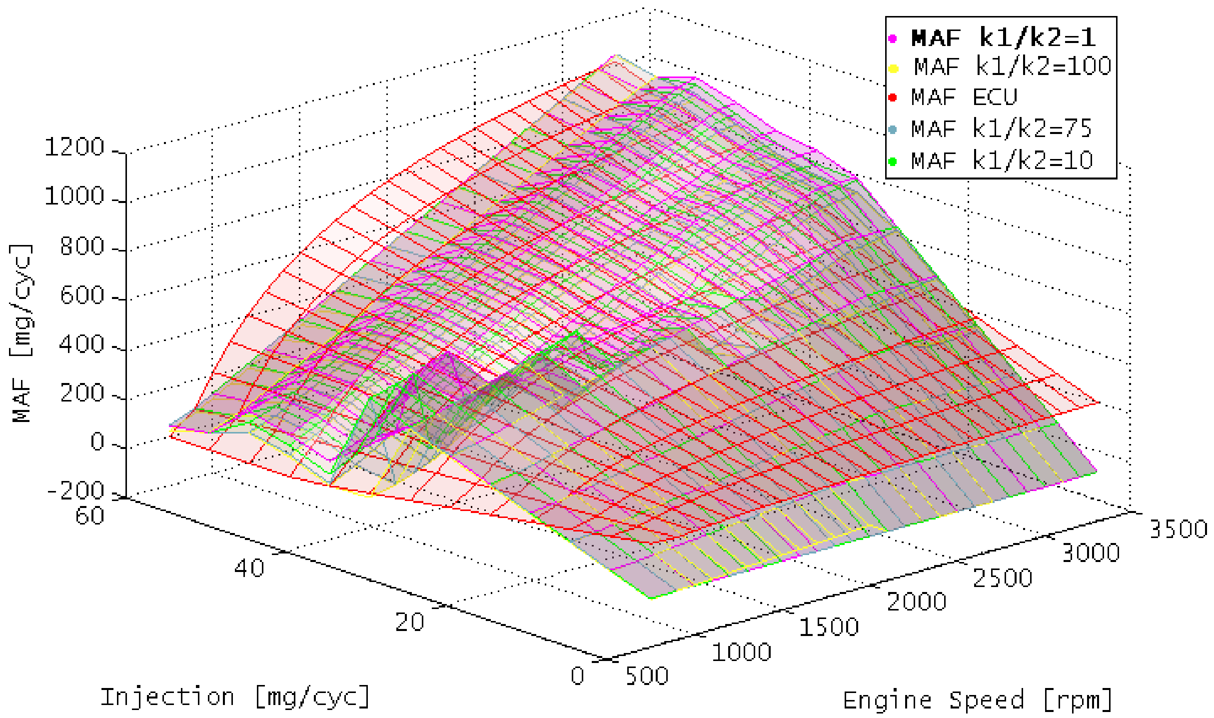

Figure 6.4: Optimisation of MAF in different weight factors

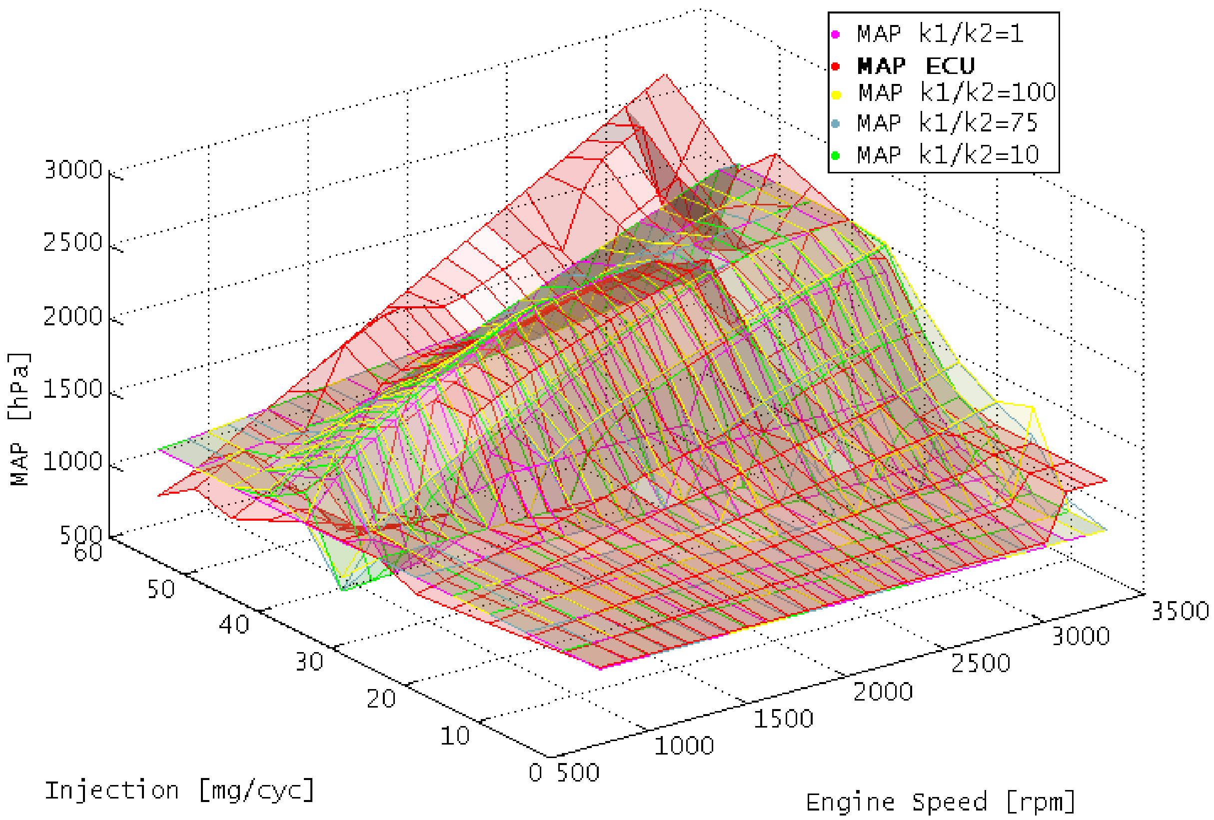

Figure 6.5: Optimisation of MAP in different weight factors

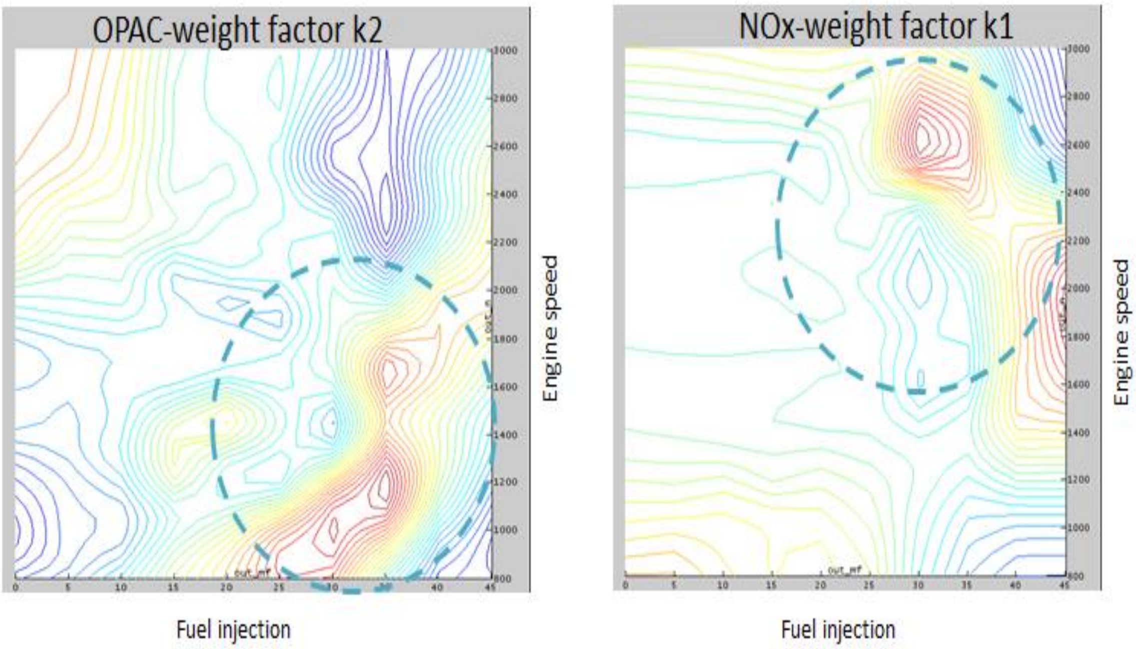

Figure 6.6: FTP-75 Cycle based weight factors for OPAC (left) and NOx (right)

In this study, an optimisation of the FTP-75 driving cycle is carried out. Since the raw exhaust emissions directly reflect the influence of the control variables independently of an exhaust after treatment system, the raw emissions are used for the optimising models (Figure 6.3). In combination with the manipulated variable models and the emission models, the optimisation scheme in Matlab/Simulink can be seen in Figure 6.3. The model-based approach makes it possible to calculate the optimal solution in a matter of minutes rather than via tests on the test-bench. Related to the cycle optimisation methods, first, the emissions in the driving cycle can be considered as an operation point's map of stationary points that are weighted according to their emission intensities in the FTP-75 driving cycle, as shown in Figure 6.6. The weight factors k1 and k2 are normalised values. These values stand for the relative intensities of the NOx and PM emissions at different operation points.

Each of the summands in Equation 6-2 can be weighted based on the operation points (n,mf) differently by cycle-based weight factors k1 (n,mf) and k2 (n,mf) to consider their influence on the optimisation result. The corresponding emissions are calculated from the engine emission models (Figure 6.3) with these manipulated variables as model inputs. Under the medium and heavy load, the air-fuel ratio in the cylinder is relatively high, due to the low temperature and un-optimal combustion conditions, the PM emissions are relatively high, as shown in Figure 6.6 left. And under the medium and high engine speed, the air-fuel ratio is close to one and the EGR open rate is lower, due to the high temperature, the NOx emissions are high, as shown in Figure 6.6 right. The optimisation must focus on these high emission areas. The non-linear optimisation method now has the task of adapting the parameters of the manipulated variables in Equation 6-2 in such a way that emission is minimal in compliance with the global emission limits and other local constraints:

$$J = k1(n, mf)(norm(NOx))^2 + k2(n, mf)(norm(OPAC))^2, \tag{6-2}$$

where *n* is the engine speed and *mf* is the fuel injection.

For emission limit values, the raw emission level of the engine is used with the serial setting to show the relative improvement in emission under the same fuel-consumption characteristics, figures 6.7 and 6.8 compare the series setting of the manipulated variables and the results of the optimisation parameters of the manipulated variable models as a 3D grid over the entire operating range.

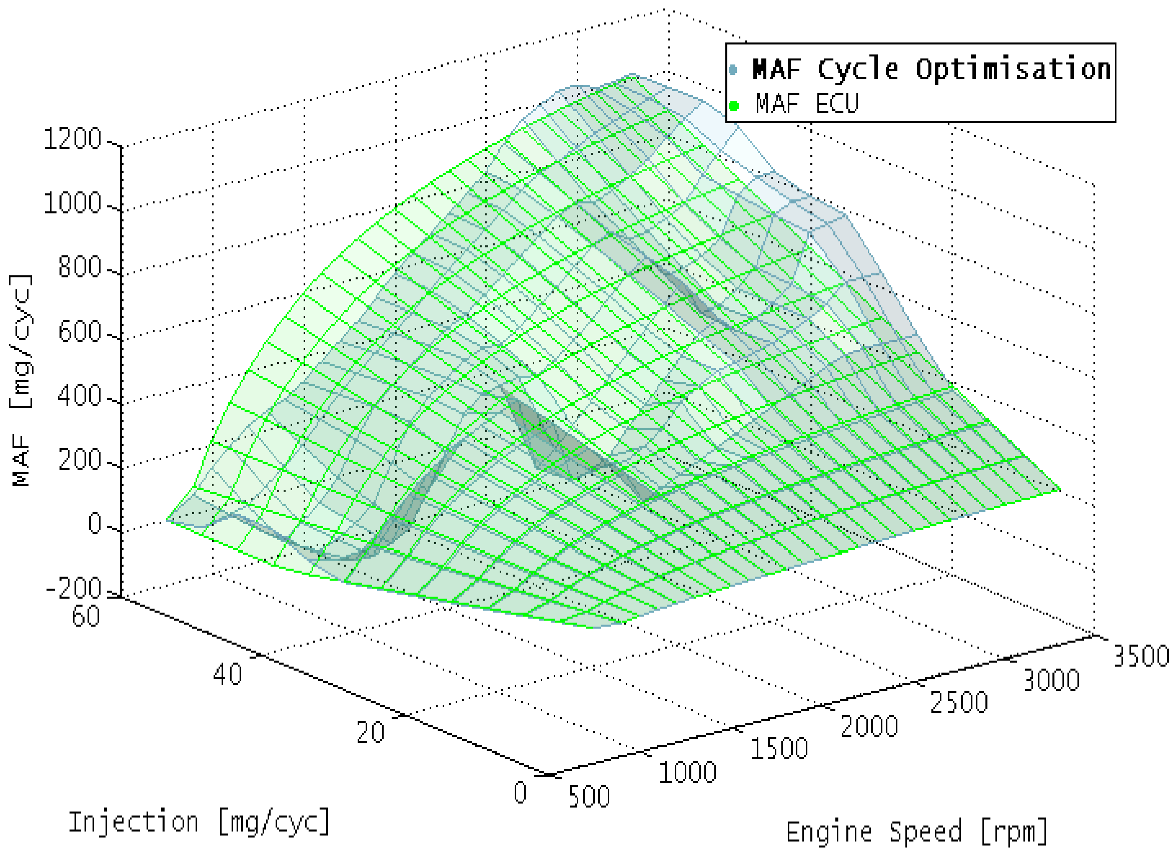

Figure 6.7: MAF FTP-75 Cycle based optimisation-Emissions

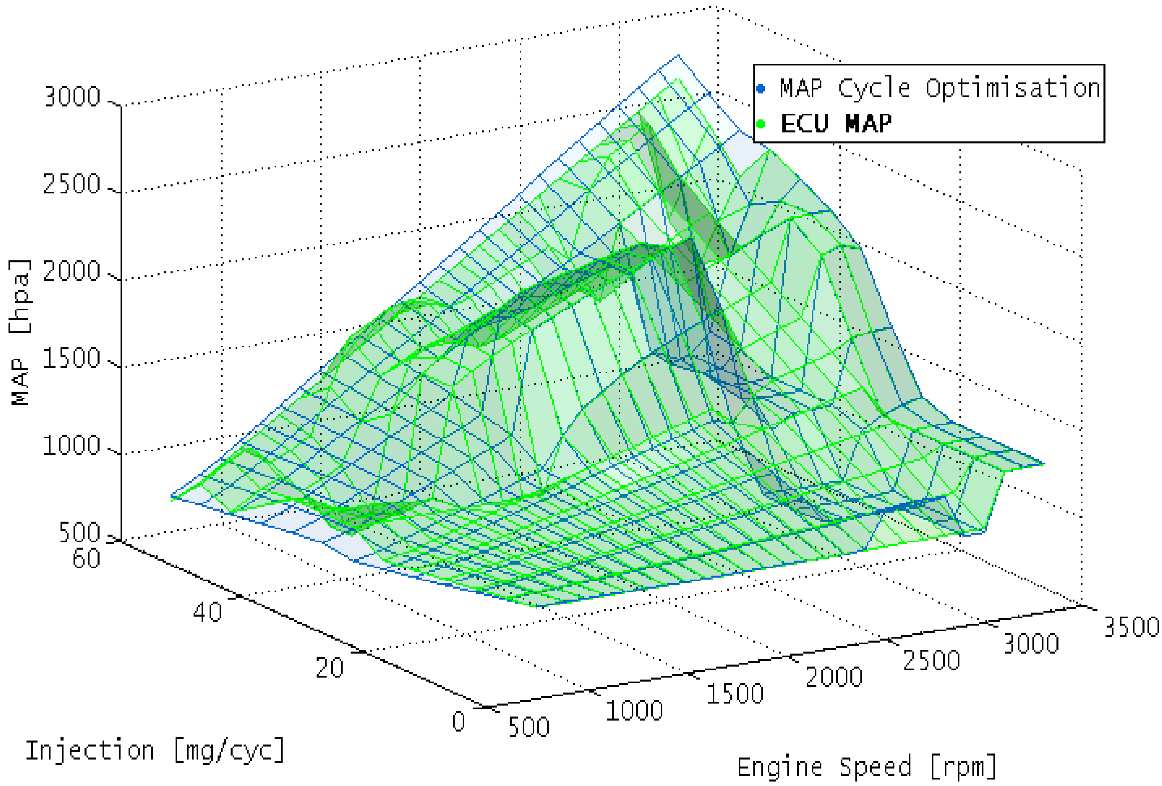

Figure 6.8: MAP FTP-75 Cycle based optimisation-Emissions

A further optimisation is to find the ideal reference value of fuel injection, MAF and MAP for the emissions and fuel consumption reduction together. Like Equation 6-2, each of these summands can be weighted differently by cycle-based weight factors k1, k2 and k3 to consider their influence on the optimisation result. The cost function defining the minimisation problem is as follows:

$$J = k1(n,T)(norm(NOx))^2 + k2(n,T)(norm(OPAC))^2 + k3(n,T)(norm(fuel))^2, \quad (6\text{-}3)$$

where *n* is the engine speed and *T* is the engine torque. The used weight factors in Equation 6-3 are defined in the following Table 6-3:

Table 6-3: Elements of cost function

Summand	**Weight factor**	**Target**
NOx	K1(n,T)	Low NOx Emission
OPAC	K2(n,T)	Low OPAC Emission
Fuel	K3(n,T)	Low Fuel Consumption $_{\text{Equivalent Power}}$

In a combination of the manipulated variable models with the emission models, the scheme can be seen in Figure 6.3 to be related to the cycle optimisation methods. The non-linear optimisation method now has the task of adapting the parameters of the manipulated variables in Equation 6-3 in such a way that emission and fuel are minimal in compliance with the global emission limits and other local constraints. This algorithm then starts the simulation and varies the manipulated parameters Fuel, MAF and MAP, which are then determined by the optimisation of the cost function.

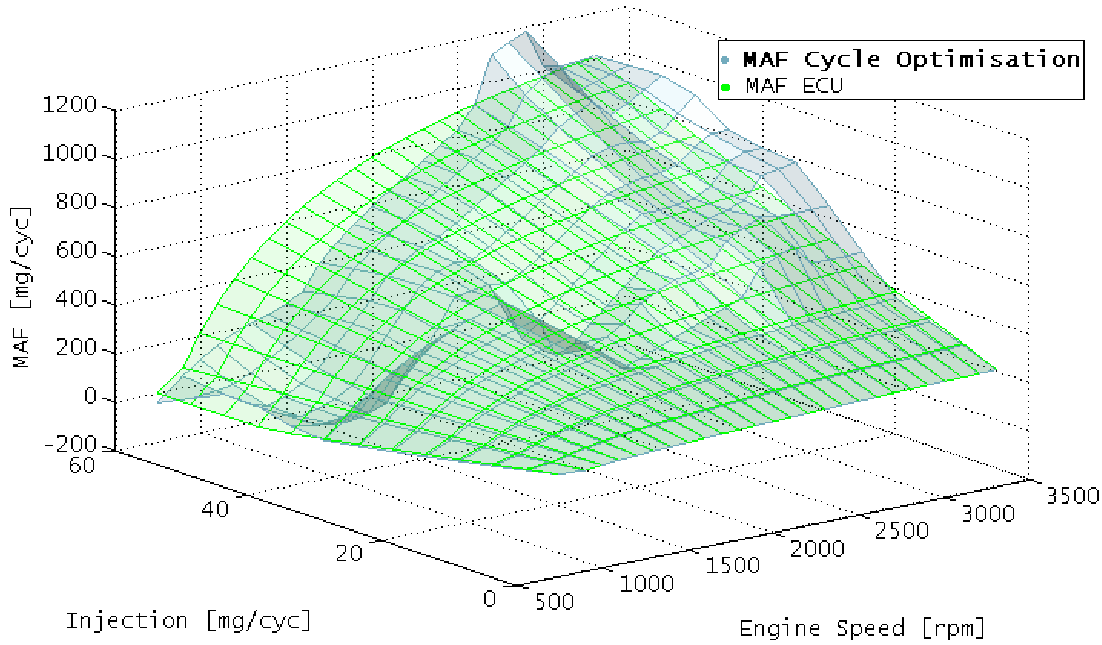

Figure 6.9: MAF FTP-75 Cycle based optimisation-Emissions and Fuel

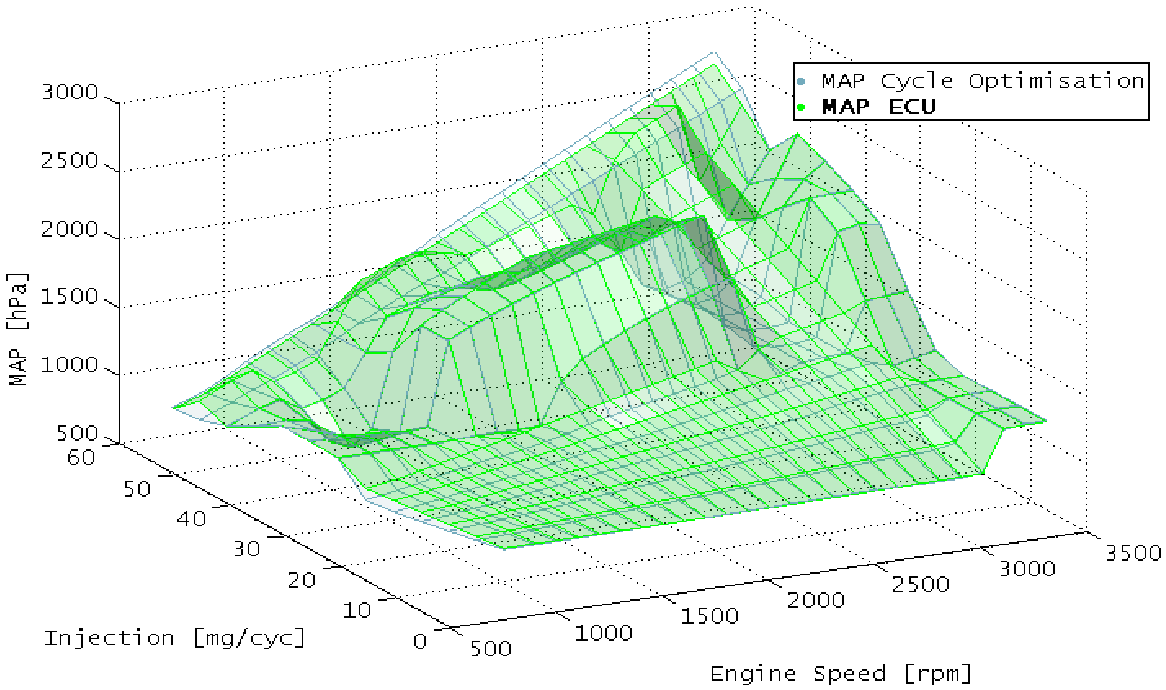

Figure 6.10: MAP FTP-75 Cycle based optimisation-Emissions and Fuel

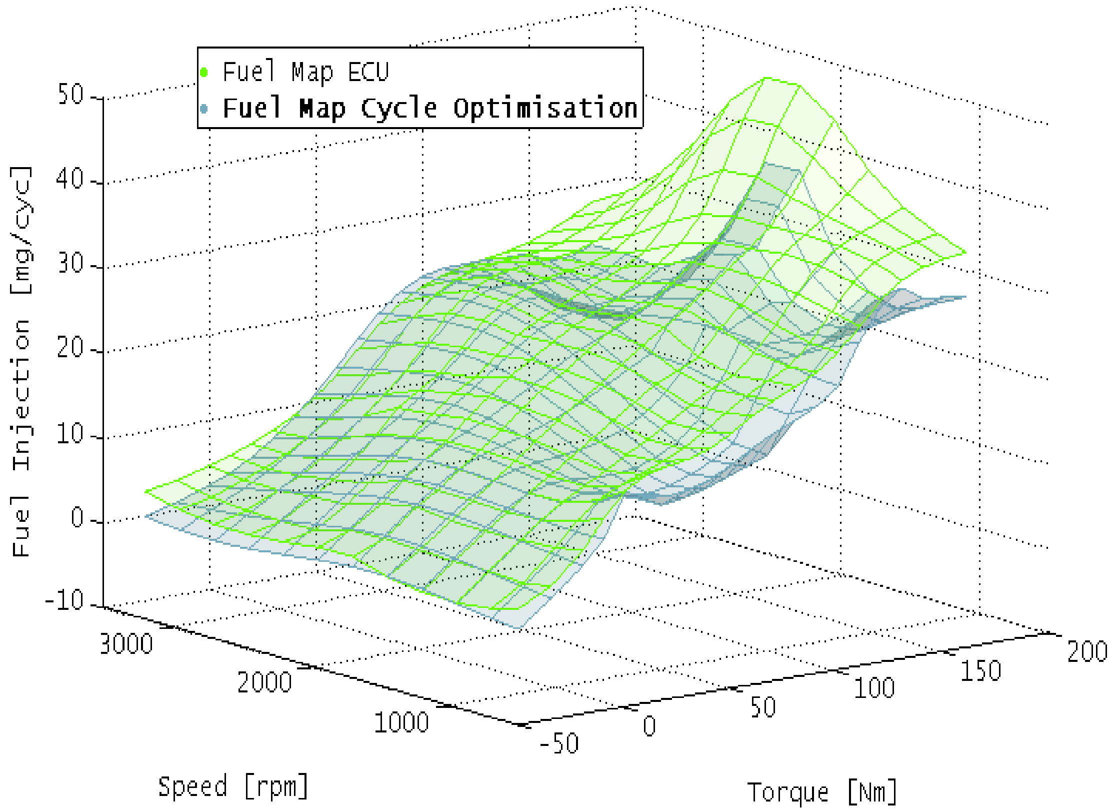

Figure 6.11: Fuel consumption FTP-75 Cycle based optimisation- Emissions and Fuel

In this case, the minimal and maximal values of fuel consumption use the default, as in the ECU. As mentioned above, and the boundaries of MAF and MAP are $[14.5 \times mf \times 1.1$ mg/cyc, $14.5 \times mf \times 2$ mg/cyc] and [1.013 bar, 2.2 bar] respectively. Figures 6.9, 6.10 and 6.11 compare the series setting of the manipulated variables and the results of the optimisation.

6.2 Optimised NMPC Engine-air-path Control Simulation Results and Analysis

The optimised references of fuel injection, MAF and MAP are evaluated during the FTP-75 cycle by using the diesel-engine model with the NMPC air-path controller (Figure 6.12). The emissions and fuel-consumption results are demonstrated both in the stationary test and in the dynamic test. The results in Table 6-5 clearly show that the applied optimised fuel-consumption map and MAF and MAP references result in a significant improvement of emissions during the driving cycle while the fuel consumption is reduced.

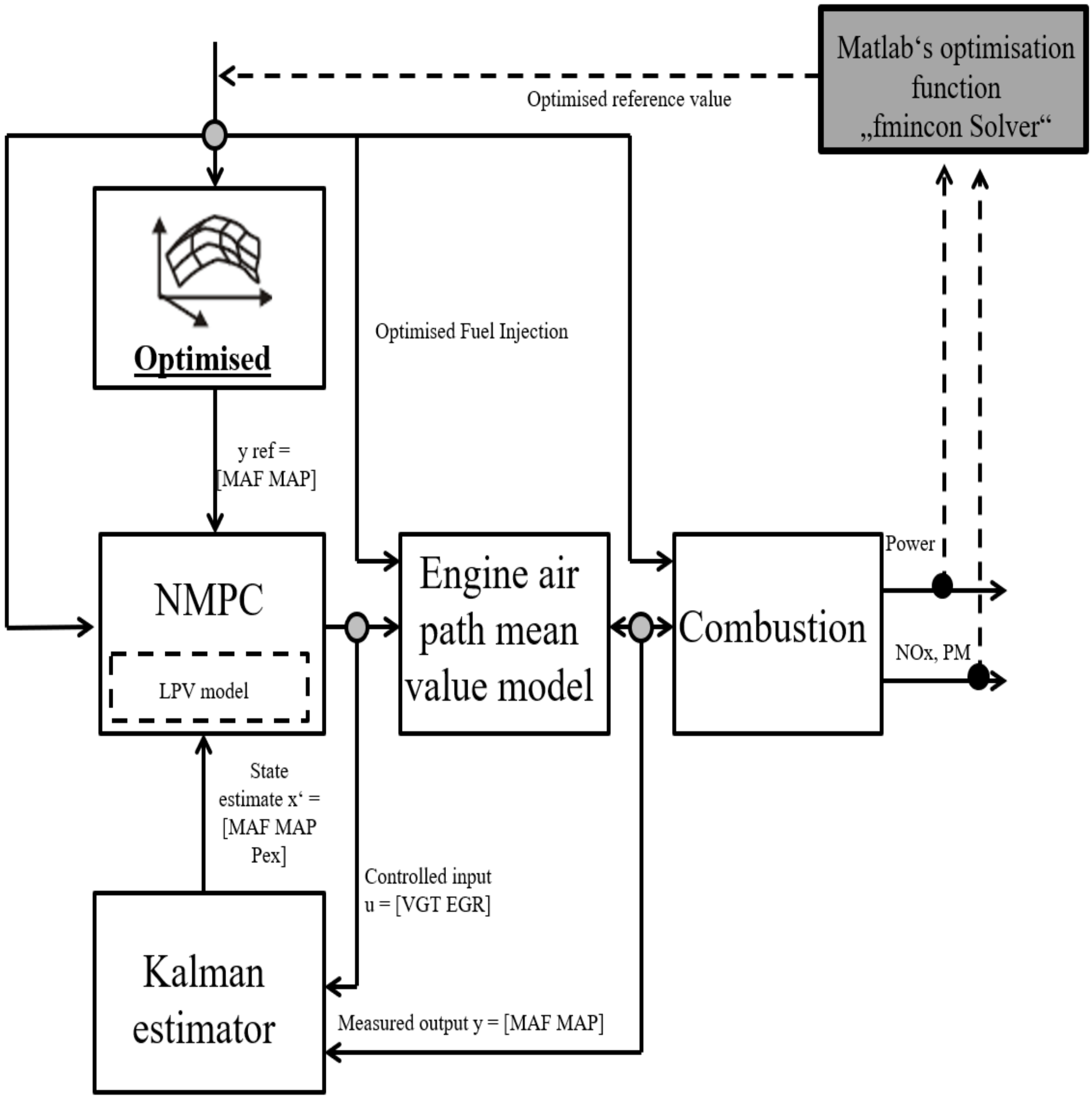

Figure 6.12: Engine-air-path control using optimised references

In the ESC stationary simulation, the implementation of the engine air-path model in Simulink represents the model structure presented in Figure 4.6. The setup of the Matlab/Simulink simulation model is given in Section 4.5. During the simulation, not all of the simulated data are stored. The areas with constant values are not useful for analysis, so they are omitted. The selected simulation inputs and outputs are given in Table 6-4. All of the mode simulations (see Table 4-6) are treated in this way by using stationary inputs. The simulation data set is stored in a Matlab mat-file with the time vector. Please refer to Section 4.5.1 for more details about the ESC stationary simulation in Matlab/Simulink. For benchmark purposes, simulations using different reference values and different air-path controllers are achieved. In Table 6-5, an overview of the simulation results is given.

Table 6-4: Inputs and outputs of the simulation model

Inputs	Outputs
Engine Speed	MAF
Engine Torque	MAP
VGT Position	BSFC
EGR Position	NOx Emission
	OPAC Emission
	VGT Position
	EGR Position

Table 6-5: Comparison of weighted value of BSFC, NOx and OPAC in ESC simulation

	BSFC [g/kWh]	NOx [g/kWh]	PM [g/kWh]
Simulation ECU	233.27	3.19	0.049
Simulation Unoptimised NMPC	233.27	3.19	0.049
Simulation Optimised NMPC	233.27	2.55	0.039
Simulation Optimised NMPC-fuel	228.61	2.48	0.040

As shown in Table 6-5 and Figure 6.13, at the ESC stationary simulation, the optimised NMPCs in this study could significantly improve the EGR rate and emissions. Due to the same reference value on MAP and MAF, the un-optimised NMPC has the same EGR and VGT positions and emissions as the ECU at the stationary test. Under the small and medium load, the air-fuel ratio in the cylinder is relatively large and the EGR tolerance is high, so the larger EGR rate can significantly reduce the NOx emissions without causing the significant decline in the economic efficiency. There is about 2% improvement on the BSFC in $\text{NMPC}_{(\text{NOx,PM and Fuel})}$, the reason is that a combination of VGT and EGR position causes better combustion efficiency of the engine and consequently the torque output is increased (Alberer, 2009). The optimised VGT-EGR diesel engine has a smaller VGT opening than the initial VGT-EGR diesel engine. The reduced VGT opening causes the increase in the exhaust back pressure, and the pressure difference between the exhaust pipe and the intake pipe also rises, thereby increasing the flow rate of the circulating exhaust gas as well as the EGR rate. VGT opening has greater decline in the small load areas (points 1, 2, 3 and 4 in Figure 6.13.b) than in the heavy load areas (points 9, 10, 11 and 12 in Figure 6.13.b), and due to the increased air mass flow in the exhaust, the turbocharger can better make use of the exhaust energy and the engine efficiency is relatively higher.

a) EGR

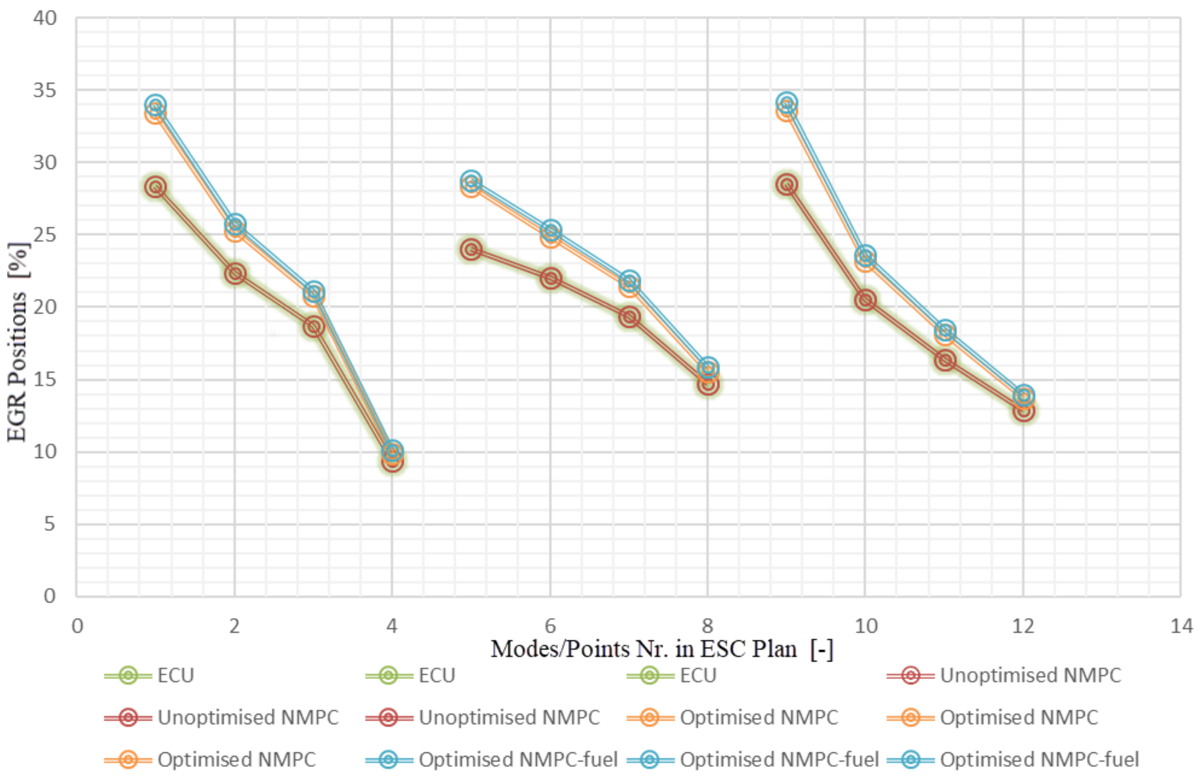

b) VGT

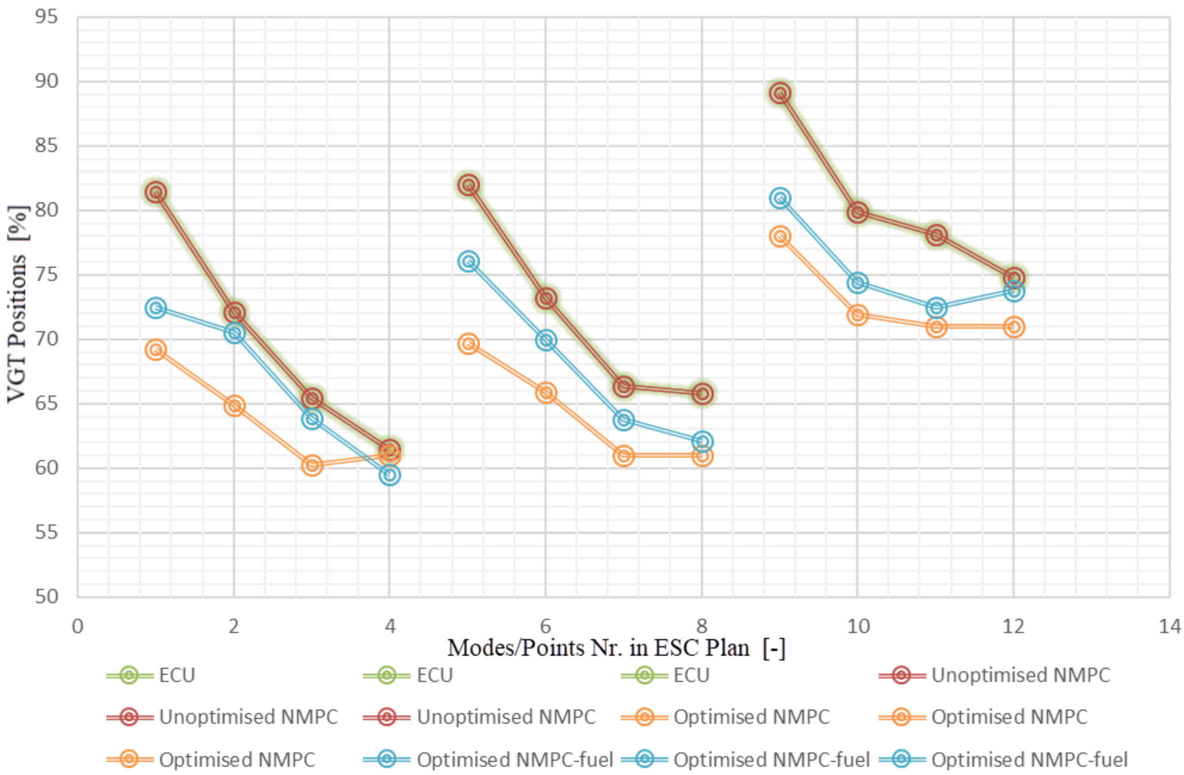

Figure 6.13: a) EGR and b) VGT positions in ESC test

The emission performance is the main optimisation target of this diesel engine, followed by the fuel efficiency. Compared to the default ECU engine, in the optimisation cost function, the weight factors assigned to the NOx emission are larger than those for the PM emissions, so the NOx emission optimisation is more obvious. The analysis of its results at stationary ESC test in Table 6-5 indicates that the EGR rate of the optimised engine is significantly greater than the un-optimised NMPC engine and the default ECU engine. The increase in EGR rate reduces the in-cylinder combustion temperature and reduces local oxygen enrichment conditions in the cylinder, which thus reduces NOx emissions but also deteriorates the in-cylinder combustion conditions, thereby resulting in a slight decrease in fuel consumption in $NMPC_{(NOx,PM\ and\ Fuel)}$. At the same time, in the optimised $NMPC_{(NOx,PM)}$ and $NMPC_{(NOx,PM\ and\ Fuel)}$, the optimisation of the VGT opening improves the gas flow in the intake system, which offsets the decline in the combustion conditions and has a positive effect on PM emissions, compared with the default ECU engine.

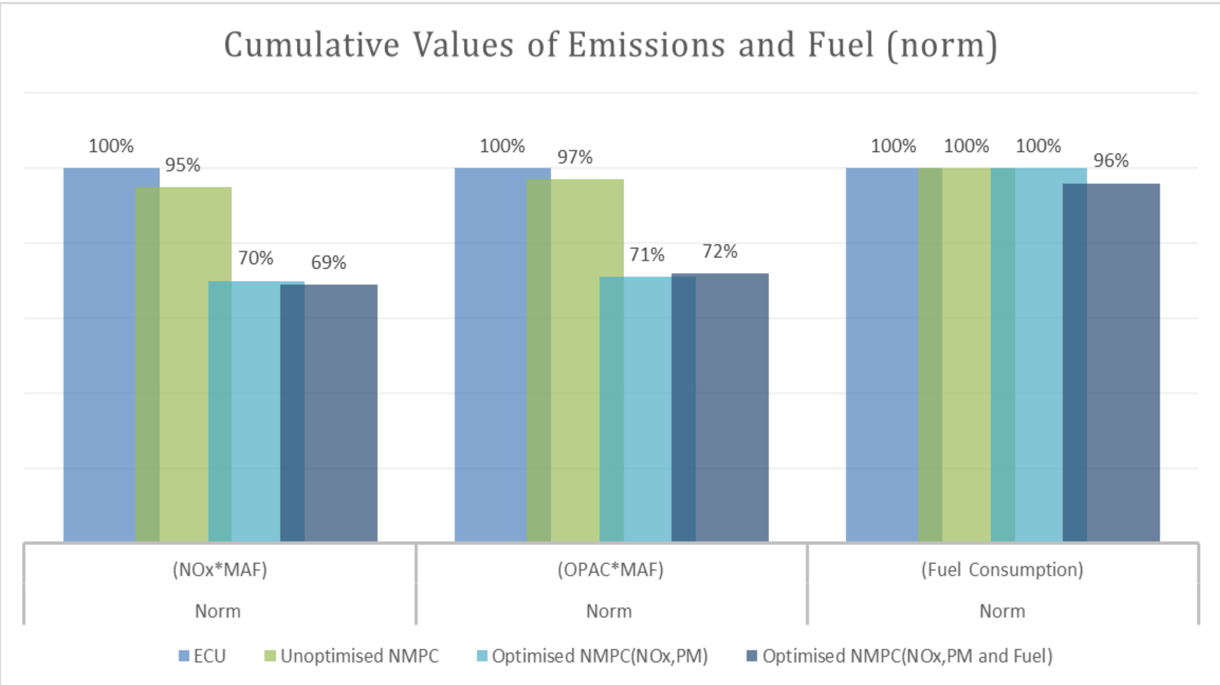

Figure 6.14: Comparison of cumulative values Fuel, NOx and OPAC in FTP-75

In the following study, the optimisation is demonstrated in the FTP-75. To calculate the mass flow of the emissions, the simulated emissions are derived from the actual cumulated MAF. The conventional ECU air-path control is taken as a reference for the comparison purpose. It is therefore considered to be 100% and is highlighted in light blue in Figure 6.14. The un-optimised NMPC shows a similar NOx and OPAC emissions as the default ECU engine, although it has an advanced air-path controller. This is caused by its same reference value, which results in good tracking performance but no improvement in emissions due to the unfavourable partial load operation and greater MAF values. The optimised $\text{NMPC}_{(\text{NOx, PM})}$ and $\text{NMPC}_{(\text{NOx, PM and Fuel})}$ have better results referred to the NOx and OPAC emissions due to the favourable reference on MAP and MAF. In total FTP-75, the optimised $\text{NMPC}_{(\text{NOx, PM})}$ and $\text{NMPC}_{(\text{NOx, PM and Fuel})}$ produce 30% and 31% less NOx than the default ECU engine. In OPAC, the optimised $\text{NMPC}_{(\text{NOx, PM})}$ and $\text{NMPC}_{(\text{NOx, PM and Fuel})}$ produce 29% and 28% less than the default ECU engine. At the same time, in $\text{NMPC}_{(\text{NOx,PM and Fuel})}$ simulation, the cumulative fuel consumption under the same engine power condition is reduced by 4%, which can be explained by a better transient behaviour, better combustion efficiency and the optimised fuel consumption map.

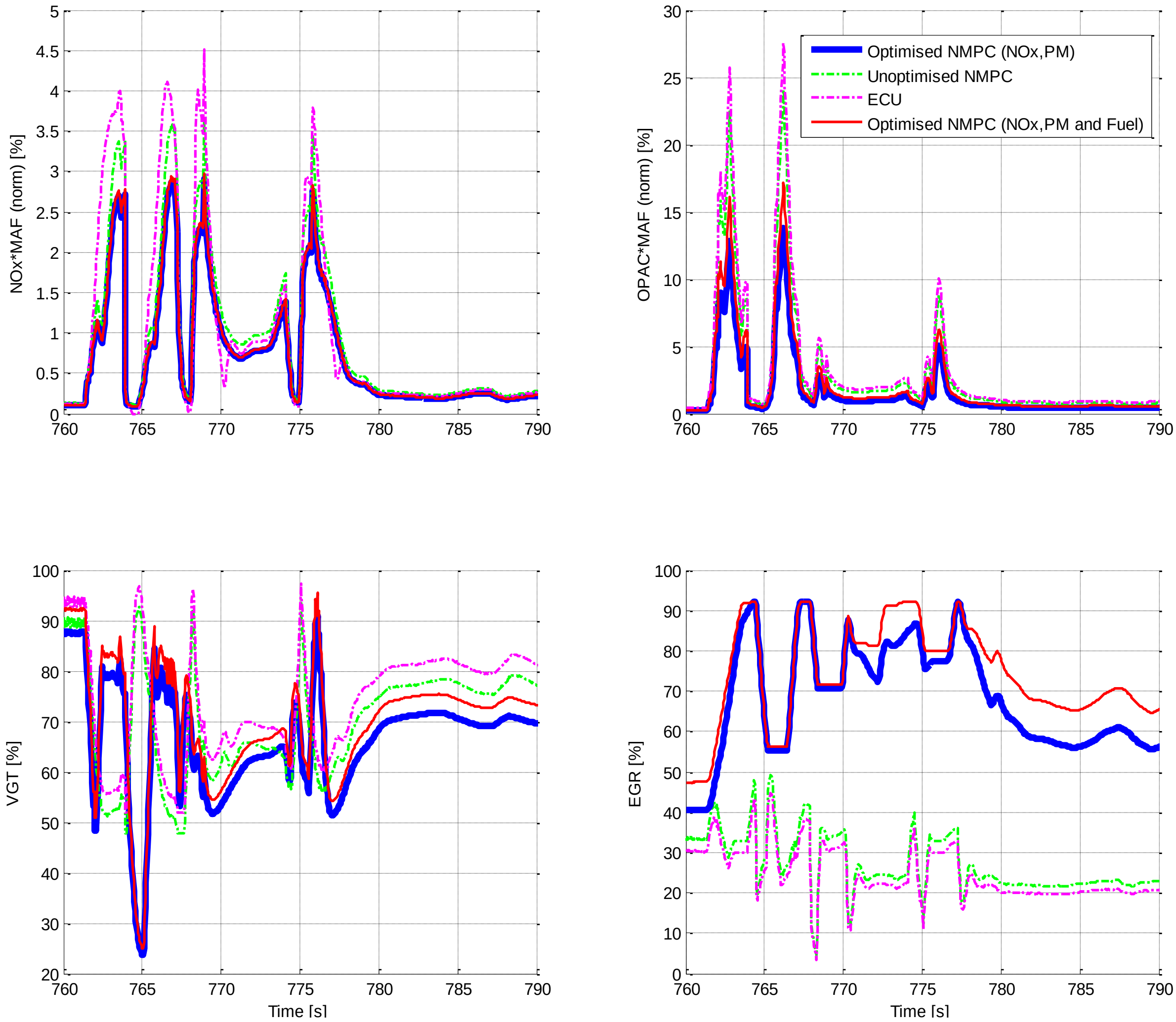

Figure 6.15: Comparison of NOx, OPAC, VGT and EGR positions- FTP-75 (760s ~790s)

To fully understand the simulation results in Figure 6.14, it is necessary to illustrate the EGR and VGT results in more detail. As can be seen in Figure 6.15, for example, the time between 760 and 790 seconds represents urban traffic driving conditions and the EGR in optimised NMPC are driven higher than un-optimised NMPC and the default ECU engine. These can lead to a lower emission, as most of the required optimised MAP and MAF are reached. Between 760 and 790 seconds, the emissions benefits are more significant with higher VGT and more EGR than the initial, un-optimised diesel engine. At the same time, the optimisation algorithm in the lower speed range provides an expansion of the EGR rate for NOx reduction, while an earlier start of injection is selected in the upper speed range to reduce fuel consumption. Operating areas that are not covered by the driving cycle remain unchanged. Besides being able to consider a larger number of operating points in the cycle optimisation, this approach has the further advantage that a smooth map is automatically created from the manipulated variable models.

Under the FTP-75 driving cycle, the rate of change of NOx emissions and PM emissions of this diesel engine using optimised NMPC are around 30% compared with those of the default ECU engine. The effective fuel consumption rate is about 4% reduced. This means that the NMPC approach could improve the trade-off between NOx emissions and PM emissions with better fuel efficiency or without significantly affecting fuel efficiency.

This study mainly changes the EGR and VGT opening rate, with no changes to the engine hardware. The optimised NMPCs in this study can significantly improve the EGR rate. As shown in Figure 6.16, under a medium to heavy load, the air-fuel ratio in the cylinder is relatively small and the EGR tolerance is lower; thus, a higher EGR rate can significantly reduce NOx emissions. The dynamic performance of the VGT turbocharger has been improved by NMPC in the following ways compared with the MAF and MAF reference values: The VGT turbocharger is more efficient, and it could make better use of the exhaust energy than the wastegate turbocharger. The exhaust flow is smoother, and the flow loss is reduced. The intake pressure increases, and the pumping loss decreases.

The VGT has a more rapid dynamic response and the hysteresis loss is reduced. To benefit from the advantages over conventional WG diesel engines, the advanced NMPC controller has been implemented in this study. Using the NMPC, the VGT opening and the exhaust back pressure can be accurately controlled and finely adjusted for different working conditions.

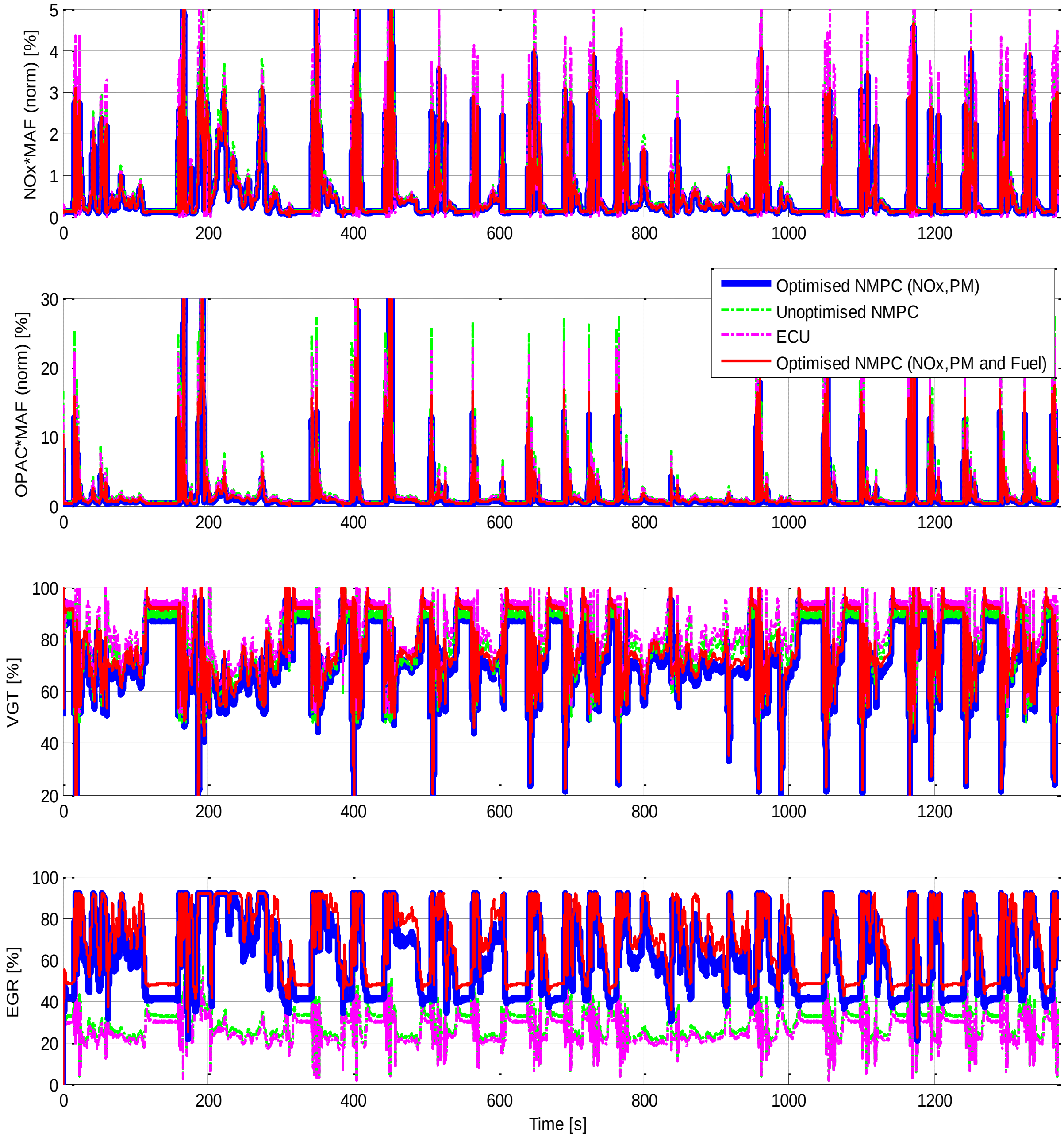

Figure 6.16: Comparison of NOx, OPAC, VGT and EGR positions-FTP-75 (0~1372s)

The results of the optimisation are shown as examples of the air-path control. Here, the effects of different weights for NOx and OPAC are shown. The results lead us to the conclusion that, based on the advanced NMPC controller and model-based approach, the optimisation and calibration can be performed in a virtual environment by using different criteria. The purposed model-based optimisation approach combined with the advanced NMPC controller provides a way to efficient reduce emissions for a given driving cycle and vehicle with minimum fuel consumption.

Chapter 7. CONCLUSIONS AND FURTHER WORK

7.1 Main Achievements

The increasing variability and complexity of advanced internal combustion engines requires a systematic model-based development of control functions and their optimisation. Therefore, this study analyses the model-based method for optimising emissions of diesel engines through nonlinear model predictive control (NMPC). In this study, the goal of the purposed NMPC control system is to simultaneously achieve a low fuel consumption and low NOx and PM emissions. The modelling of the engine-air-path system using the LPV method is emphasised. The identification of nonlinear multivariable models with an LPV structure allows for precisely describing the stationary and dynamic behaviour of the engine air path. The idea behind the proposed NMPC strategy is to represent the plant model as an LPV model. The control-objective function used to search for the optimal solution to the QP problem is then extended to the parameter-varying cost function by utilising the given LPV model. On the basis of the engine-air-path model and the NMPC controller, an optimisation can be performed on computer, by using different criteria for emissions and fuel consumption.

The originality of this work can be summarised as:

1. Using LPV model as a prediction model for the NMPC

In NMPC, a mathematical non-linear model was used for the prediction of future system outputs based on past inputs and outputs. The deviation between reference trajectory and predicted outputs was then minimised by means of an optimisation algorithm that considers possible constraints and the defined objective function. This study reveals that there are many perceived benefits to using an LPV model as a ‘predictor’. The LPV identification approach delivered in this thesis is successfully applied to the modelling of a diesel engine-air-path. In the NMPC application, the air-path dynamic model is investigated based on an input-output data set. As shown in previous chapters, it is indeed possible to build a low-order model which can describe the dynamic properties of the MAF and MAP only by means of pure data measurements such as n, m_f, VGT and EGR signals from an FTP-75 cycle. While the average performance of the model could be increased by optimising the model and the membership functions, it is nevertheless clear that the model will not be able to provide 100% exact MAF and MAP predictions. However, it is still an adequate basis for model-based engine-control synthesis. This means the LPV identification algorithms can be applied to non-linear system like engines, in which the operation states can be defined as some discrete values for scheduling the systems. From the results shown in chapters 4, 5 and 6, we can safely draw the conclusion that LPV identification techniques provide a new way of modelling dynamical systems. Moreover, it is suggested that good LPV system identification results can be reached by combining non-linear optimisation methods. These advantages make the LPV model for NMPC control application possible.

2. Integrating LPV model in the cost function of NMPC that helps ensure quality outcomes and deliverables

This point is related to the NMPC controller performance. The performance criteria most commonly used to evaluate the performance of various controllers are stabilisation and reference tracking of a dynamic system. From the results shown in chapters 5 and 6, compared to the linear MPC and standard ECU, the control performance of an engine-air-path could be significantly improved by the LPV-based NMPC. The critical factors affecting NMPC performance were reviewed from different aspects, concerning the prediction model, cost function, optimisation, constrains and QP problem. Based on the progress of this study, some improvements regarding the critical factors have been made to create an NMPC for providing a quality controller in an air-path system. In NMPC, the optimisation of the LPV cost function can be transformed into a time-varied quadratic program problem of a form which can be solved by a QP-solver. In the linear case, algorithms for QP-solver configurations are state-of-the-art. The QP describes the standard convex quadratic optimisation problem. However, the complex structure of a non-linear problem can complicate the formulation of a NMPC. In (Ferreau H. J., Ortner, Langthaler, Del Re, and Diehl, 2007) an alternative fast method of QP-solver is presented. In this study the fast method of QP-solver was used. The results of this study lead us to the conclusions that an upper computation bound of an optimal problem can be ensured in a real-time simulation, which is very suitable for the LPV model in the NMPC cost function.

3. Using the LPV-based NMPC overcome the cross-coupling and tracking problem in the diesel engine-air-path control, thereby reducing emissions and maintaining engine performance

Due to the possibility of treating constraints and non-linear MIMO systems directly, an NMPC was chosen for this feedback control problem, where the cross-coupling problem of VGT and EGR was considered by the MIMO model structure. The output prediction model, required by the NMPC, was designed by using an LPV approach. This structure can be interpreted as a special case of a gain-scheduling system in which the coefficients of the transfer function are re-calculated and varied in each time step. A mean-value diesel-engine model has been used to validate the effects of the predictive control strategy. The simulation and comparison of various configurations in chapters 5 and 6 show a satisfying, closed-loop performance of the two target quantities, MAF and MAP. Compared to linear MPC, this new NMPC approach provides good tracking performance even during plant operations in regions far from the linearisation point. Due to limited time and resources, the NMPC is evaluated only in the simulation platform for this study. A further step for the analysis and evaluation of the NMPC performance is controller implementation on a real-world test-bench, which provides validation under real conditions. Under real conditions, the ability of the NMPC to reduce emissions during a driving cycle and the quality of the LPV model prediction can be investigated and validated.

7.2 The Contribution to the New Knowledge Generation

Besides the results presented in this study, a summary of the contribution to the new knowledge generation is given here.

1. A new non-linear model predictive control of diesel engine-air-path system

This is the first time an LPV-based NMPC has been developed for control of engine-air-path system. In this study, three different kinds of engine-air-path controllers—NMPC, linear MPC and standard ECU—have been proposed and validated by experiments on the virtual engine test-bench as a solution to the problem of engine-air-path control while satisfying the tracking of the control references. The results presented lead us to the conclusion that the LPV model can be used to predict the air-path behaviour of a diesel engine. The LPV model used for the prediction MAF and MAP gives qualitatively correct, reproducible behaviour at variations in engine speed and fuel injection. Furthermore, it was found that the NMPC controller gives better results than linear MPC and standard ECU, as it combines robustness and acceptable tracking ability. The problems of the computational burden in QP, and thus the non-applicability to fast processes, are overcome by the online active QP-solver, qpOASES. The tracking performance and stability of NMPC can be guaranteed in LPV representations, which can be evaluated by the step-response simulation. From this study, the following conclusions can be drawn: First, NMPC has the opportunity to include LPV model, MIMO control technique and constraints in the optimisation problem. These advantages make the NMPC very useful for the interaction of EGR and VGT control in engine-air-path system, compared with other approaches like linear MPC and standard ECU. It has been shown experimentally that an LPV model in combination with an MPC can compensate for the disturbances more quickly than the linear method. Another advantage of the NMPC is to include more precise future prediction in the optimisation problem. This can clearly be found in the nature of the engine system. During the operation point's change, the optimal solution of the next instant will be known in advance, which makes the engine-air-path control more efficient. Second, the FTP-75 cycle simulation has been presented with the default MAF and MAP reference maps of the ECU. As mentioned in Section 5.3, although MAF and MAP can be tracked better by using NMPC than by using the standard ECU, the overall emissions cannot be improved significantly if the set points are not optimised with respect to emissions. This optimisation issue was investigated in Chapter 6. Generally speaking, the results confirm the use of NMPC as an engine-air-path controller. Moreover, the control concept is not restricted to use of engine-air-path control; it therefore provides the potential for numerous control applications of non-linear systems.

2. A new simulation model for diesel engine-air-path

A mean-value engine-air-path model—including intake and exhaust manifolds, torque, emission, etc.—is developed in Matlab/Simulink as a virtual engine test-bench in this study. First, the engine-air-path characteristics are described by physical equations; then the emissions and torques are modelled via a data-based approach. Nevertheless, some simplification concerns the modelling of turbocharger and combustion, the combination of a physical description and data-based approach seems a promising method for a reduced complexity modelling with a sufficient precision for model-based controller design.

The following conclusions can be drawn from this study. The model development for model-based development is characterised by a trade-off between model accuracy, computational requirements and parametric effort. First, the model must meet the requirements for a correct physical representation of a real engine. Next, the real-time capability of the engine model is required due to closed-loop simulation with the control unit. This point significantly limits the quantity of the modelling approach. The clear parametric effort then decides on a productive use of the simulation model in the further development process. An increase in efficiency within model-based development—especially in a large-scale development process—is in accord with the availability and reusability of the model's parameters with fewer test-bench efforts.

3. A new model-based emissions and fuel optimisation method on engine-air-path control

To meet the increasing demands on modern diesel engines control in terms of satisfied dynamic performances and low exhaust emissions and fuel, it is necessary to determine a suitable control reference. The proposed new optimisation methods have therefore been developed in this study. The optimised NMPC-controlled diesel-engine system makes use of the EGR and the VGT to improve the combustion situation, thereby improving the power and fuel efficiency of the diesel engine. Compared with the initial diesel engine, in the optimised NMPC(NOx,PM), the fuel consumption is basically the same, and the NOx exhibits a decrease of about 30% coupled with a 29% reduction in PM emissions.

In this approach, one of the emphases is on the mathematical MIMO modelling of emissions using a data-based approach. For this particular optimisation task, the non-linear and dynamic behaviours of emissions are well interpreted by DOE data-based modelling. Based on these models, different methods for model-based optimisation and calibrations are performed on the virtual engine test-bench. The following conclusions can be drawn from Chapter 6: The presented optimisation methods can be carried out by computer simulation for multi-manipulated variables and multi-objectives with selected weighting factors. Using the optimised control reference, the NMPC shows a significant potential for the improvement of emissions and fuel. This obviously shows that the optimisation results strongly depend on the quality of the emissions models. If the emission behaviour can be described more precisely, this optimisation method could provide a very practical and efficient solution which can help the optimisation and heuristic intermediate variables to be calibrated in a relatively short time. Once the optimal calibration is determined in a virtual environment, only a validation test run on the real test-bench for confirmation is necessary.

7.3 Limitation and Further Work

In this thesis, the research findings for solving non-linear control problems in fast process shown for instance in the engine-air-path control give a very promising perspective, that the purposed NMPC algorithms will be able to run in combustion engine systems in near future. Such kinds of application of LPV-based NMPC approach will greatly increase the attractiveness of NMPC for engine control. The further research steps should continue to prioritise this work to strengthen the understanding of the combustion engine and emission behaviours to obtain more precise models and maintain up-to-date and effective NMPC approach to solve the proposed problems and ensure that the Euro VI even further emission legal standards can be appropriately and effectively fulfil with continuously increasing computation power of the available hardware. In this context, highlighted below are those areas where the research limitations exit and where further progresses should be achieved.

Engine Modelling

Even though the purposed engine model gave satisfactory results for the approximation of the MAF and MAP, there are still some concerns. A practical modelling method for model-based development needs to be configurable to a wide variety of engines for instance naturally aspirated engine, mechanical boost engine, even for more complicated engine layouts, such as multiple turbocharger engines. So far in this thesis the modelling efforts have only accomplished VGT EGR diesel engine for air-path control function development and performance optimisations.

The development of more sophisticated engine models (e.g., with detail fuel injection models and more precise emission models) to allow NMPC engine constitute challenges in issues of overall non-linear engine modelling, model-based optimisation and calibration, remains a core challenge for the future of model-based control deign for engine systems. Another point which should be investigated is the reproducibility and extension of the measured data used here for validation and further optimisation purpose. This means that the data have to be analysed such that all the necessary signals have to be figured out. In this work only the MAF, MAP, exhaust pressure, NOx and OPAC have been considered, but to ensure the reproducibility of the data, to build a model, it can be necessary that other signals, for instance exhaust temperature and fuel injection, must be considered.

Engine Non-linear Model Predictive Control

Due to the limited time and resources, the NMPC is only evaluated in the simulation platform. Some of the issues will be next overviewed involved when considering implementing the NMPC air-path controller within production ECU on a real test-bench, particularly paying attention to balancing the trade-off between computing burden and controller performance. Under the real conditions, the ability of the NMPC on the emissions reduction during a driving cycle and the quality of the LPV model prediction could be investigated and validated. Another interesting issue is to transfer this idea of air-path to other engine control applications—for instance, to investigate the NMPC on the engine thermal management and to study the impact of the cylinder temperature on the emissions, in particular on the NOx. We found that it is possible to reduce the NOx peaks during the driving cycle when the temperature of the cylinder head is stabilised. Furthermore, in the thesis, two intermediary parameters, MAF and MAP, are selected to impact the emissions. It will be very interesting to develop and implement a direct emission control method. The LPV identification algorithms could be applied to the modelling issue of emissions, and this LPV model could be integrated into the NMPC controller. The high potentials of this LPV NMPC application can be expected in the combination of the LPV emission models for prediction and thus to directly penalise the emissions within the bounds of the legal requirements and optimised the emission behaviour on the transient operation areas. Finally, the results of this thesis lead us to the conclusion that this LPV NMPC approach is feasible, reasonable and effective for non-linear system control and is of great value for practical application in the automotive industry is shown. Therefore, it makes sense to develop a commercial software toolbox with which to provide a systematic, efficient development processes to facilitate the control-development process and to offer the possibility of efficiently designing a real-time capable NMPC in combination with QP-solver qpOASES.

Model-based Engine Optimisation and Calibration

The presented optimisation methods are carried out for multiple manipulated variables and evaluating outputs with selectable weights such as fuel consumption and emissions. This is to be done in a relatively short time with the simulation engine models, whereby any driving cycles and either stationary or transient engine test cycles can be applied. However, solving these optimisation problems is usually not a choice for multi-domain combustion (mechanical, thermal, two-phase fluid) optimisation, though attempts have been made in this direction for a very long time. There are a number of reasons for this, among which is the fact that several effects are not well known. In addition, the computational effort is too high for actual ECUs—especially in view of the highly dimensional and mostly non-convex problems caused by the complex and non-linear nature of most applications. The improved computational power of ECUs and optimisation approaches are expected to allow for the use of more sophisticated control techniques such as those encountered in multi-variable, optimal control paired with multi-domain combustion and emissions models for control.

REFERENCE

Aarenstrup, R. (2015). *Managing Model-Based Design.* Natick: Mathworks.

Abidi, I., Bosche, J., & El Hajjaji, A. (2013). Air path control of a Turbocharged diesel engine: Fuzzy approach. *Proceedings of the 3rd International Conference on Systems and Control* (pp. 401 - 407). Munich: IEEE.

ACEA. (2018). *NEW PASSENGER CAR REGISTRATIONS EUROPEAN UNION.* Brussels: ACEA.

Afram, A., & Janabi, F. (2014). Theory and application of HVAC control systems - A review of MPC. *Building and Environment 72*, 343-355.

Ahmed, F. S. (2013). *Modeling, simulation and control of the air-path of an internal combustion engine.* Technical University Belfort Montbeliard.

Alberer, D. (2009). *Fast Oxygen Based Transient Diesel Engine Control.* Linz: Trauner Verlag.

Ammann, M., Fekete, N. P., Guzzella, L., & Glattfelder, A. H. (2003). Model-Based Control of the VGT and EGR in a Turbocharged Common-Rail Diesel Engine: Theory and Passenger Car Implementation. *SAE 2003 World Congress & Exhibition* (pp. 675-699). USA: SAE.

Andersson, H. (2012). *Variability and Customisation of Simulator Products A Product Line Approach in Model Based Systems Engineering.* Linköping, Sweden: Linköping University.

Aran, V., & Unel, M. (2017). Data driven disturbance observer design and control for diesel engine airpath. *11th Asian Control Conference (ASCC)* (pp. 2600-2605). Australia: IEEE.

Atam, E. (2018). Advanced Air Path Control in Diesel Engines Accounting for Variable Operational Conditions. *IEEE Access. 6*, pp. 42165-42176.

Atkinson, A., & Donev, A. (1992). *Optimum Experimental Designs.* Oxford: Oxford University Press.

AVL GmbH. (2008). *AVL PRODUCT DESCRIPTION: Emission Test Instruments AVL 439 Opacimeter*. Graz: AVL.

AVL GmbH. (2014). *Engine PUMA Open User Manual*. Graz: AVL.

AVL GmbH. (2017). *Drive Cycle Optimisation Using Global DOE.* Graz: AVL.

Azam, A., Ali, S., & Iqbal, A. (2016). Emissions from Diesel Engine and Exhaust After Treatment Technologies. *4th International Conference on Energy, Environment and Sustainable Development*. Jamshoro, Sindh, Pakistan.

Bacic, M., & Cannon, M. K. (2003). *Constrained NMPC via state-space partitioning for input-affine nonlinear systems.* Proceedings of American Control Conference, Denver, Colorado.

Baines, N. (2005). *Fundamentals of Turbocharging.* Wilder Publications.

Baines, N. (2006). *The Turbocharging Challenge.* Concepts NREC.

Bamieh, B., & Giarre, L. (2002). Identification of linear parameter varying models. *International Journal of Robust and Non-linear Control*, 589-630.

Batteh, J., Tiller, M., & Newman, C. (2003). Simulation of Engine Systems in Modelica. *The Modelica Association* (p. 350). Prague: Modelica.

Bemporad, A. (2001). The explicit linear quadratic regulator for constrained systems. *Automatica*, pp. 3-20.

Bemporad, A. (2003). *Min-max control of constrained uncertain discrete-time linear systems.* IEEE Transactions on Automation.

Bengea, S., DeCarlo, R., Corless, M., & Rizzoni, G. (2002). *A. Polytopic System Approach for the Hybrid Control of a Diesel Engine Using VGT/EGR.* Prudue: Prudue University e-Pubs.

Bengtsson, J. (2007). Hybird modeling of HCCI engine dynamics - a survey. *International Journal of Control*, 61-78.

Bennett, S. (2014). *Modern Diesel Technology: Diesel Engines.* Cengage Learning.

Bock, H., Diehl, M., Leineweber, D., & Schloeder, J. P. (2000). A Direct Multiple Shooting Method for Real-Time Optimisation of Nonlinear DAE Processes. *Progress in Systems and Control Theory Volume 26*, pp. 245-267.

Bodenstein, C., Lohse, F., & Zimmermann, A. (2010). Executable specifications for model-based development of automotive software. *Systems Man and Cybernetics (SMC), 2010 IEEE International Conference* (pp. 727 - 732). Istanbul: IEEE.

BorgWarner. (2018). *Turbocharger*. Retrieved 06 10, 2018, from Borgwarner: http://www.turbos.borgwarner.com/en/products/turbochargerHistory.aspx

Bruckner, M., Grünbacher, E., Alberer, D., del Re, L., & Atschreiter, F. (2006). Predictive Thermal Management of Combustion Engines. CCA conference 2006.

Bryman, A., & Bell, E. (2011). *Business Research Methods.* Oxford: Oxford University Press Publishing.

California Environmental Protection Agency. (2015). *LOWER NOX HEAVY-DUTY DIESEL ENGINES.* California: State of California.

Camacho, E. F., & Bordons, C. (2007). *Model Predicitve Control.* London: Springer.

CAMBUSTION. (2018). *Ultra fast-response gas analysers user manual.* Cambridge, UK: Cambustion.

Casavola, A., Famularo, D., & Franze, G. (2003). Predictive control of constrained nonlinear systems via LPV linear embeddings. *International Journal of Robust and Nonlienar Control*.

Chai, T., & Draxler, R. (2014). Root mean square error (RMSE) or mean absolute error (MAE)? *Geosci. Model Dev. Discuss*.

Chapman, K. (2002). *Development of Turbocharger Reciprocing Engine Simulation.* Kansas: Kansas State University.

Chen, F., Jiao, J., Liu, S., Yu, Y., & Xu, S. (2018). Control-oriented LPV Modeling for the Air Supply System of Proton Exchange Membrane Fuel Cells. *Fuel Cells*, 433-440.

Chen, W. H., Ballance, D. J., & Gawthrop, P. J. (2003). *Optimal Control of Nonlinear Systems: A Predictive Control Approach.* Automatica 39: 633-641.

Chen, Y., Frison, G., Duijkeren, N., Bruschetta, M., Beghi, A., & Diehl, M. (2018). Efficient Partial Condensing Algorithms for Nonlinear Model Predictive Control with Partial Sensitivity Update. *IFAC-PapersOnLine,Volume 51, Issue 20*, pp. 406-411.

Cheng, H., & Allgoewer, F. (1998). A Quasi-Infinite Horizon Nonlinear Model Predictive Control Scheme with Guaranteed Stability. *Automatica*, 72-99.

Cheng, R., & Maloney, P. (2018). *www.mathworks.com.* Retrieved 03 10, 2018, from http://de.mathworks.com/videos/model-predictive-control-of-diesel-engine-airpath-81995.html

Chou, C., & Verhaegen, M. V. (1997). Subspace algorithms for the identification of multivariable dynamic errors-in-variables models. *Automatica*, pp. Vol. 33, 10, 1857-1869.

CIMAT. (2018). *Turbo test static and dyanmic measurements user manual.* Poland: Burke porter group.

Cook, D., Pitsch, H., Chen, H., & Haweks, E. (2007). Falmelet based modeling of auto-ignition with thermal inhomogeneities for application to HCCI engines. *Process Combustion Insitute*, 2093-2911.

Cornetti, G. (2014). Simulation of diesel engine emissions by coupling 1-D with data-based models. *14. Internationales Stuttgarter Symposium* (pp. 125-150). Stuttgart: Springer Fachmedien Wiesbaden .

Corno, M., Wingerden, J., & Verhaegen, M. (2012). Linear Parameter-Varying System Identification: The Subspace Approach. In *Identification for Automotive Systems* (pp. 53-65). London: Springer.

Cray, C., & Malins, J. (2004). *Visualizing Research: A Guide to the Research Process in Art and Esign.* England: ASHGATE Publishing Limited.

Criens, C. (2014). *Air-path control of clean diesel engines : for disturbance rejection on NOx, PM and fuel efficiency.* Eindhoven: Technical University Eindhoven.

Cutler, C. R., & Ramaker, B. L. (1980). Dynamic matrix control- A computer control algorithm. *Joint Automatic ControlConference.* San Francisco, CA, USA.

Czerwinski, J., & Zimmerli, Y. (2015). Emission Reduction with Diesel Particle Filter with SCR. *Emiss. Control Sci. Technol*.

Dahl, J., Wassén, H., Santin, O., Herceg, M., Lansky, L., Pekar, J., & Pachner, D. (2018). Model Predictive Control of a Diesel Engine with Turbo Compound and Exhaust After-Treatment Constraints. *IFAC-PapersOnLine, Volume 51, Issue 31,* pp. 349-354.

De, S., Agarwal, A., Chaudhuri, S., & Sen, S. (2018). *Modeling and Simulation of Turbulent Combustion.* Springer Singapore.

Dekker, H., & Sturm, W. (1996). Simulation and control of a HD diesel engine equipped with new EGR technology. *SAE Conference* (pp. 81-89). Detroit: SAE.

Del Re, L. (2011). *Engine Control System.* Linz: University Linz.

Diehl, M. (2007). *Dynamic Process Optimisation.* Leuven: K.U.Leuven.

Diehl, M., Bock, H., & Schloeder, J. P. (2005). Nominal stability of the real-time iteration scheme for nonlinear model predictive control. *SIAM J. CONTROL OPTIM*, pp. 56-73.

Dimitris, K., Gianluca, F., Andrea, Z., & Moritz, D. (2018). Recent Advances in Quadratic Programming Algorithms for Nonlinear Model Predictive Control. *Vietnam Journal of Mathematics*, pp. 456-488.

Dorling, J. (2016). *Global NRMM Markets and the Legislative Framework - 2016 update.* Integer.

Duprez, D., & Cavani, F. (2014). *Handbook of Advanced Methods and Processes in Oxidation Catalysis: From Laboratory to Industry.* World Scientific.

Durea, M. (2014). *An Introduction to Nonlinear Optimisation Theory.* De Gruyter Open.

Eichlseder, H., Baumann, E., & Müller, P. (2000). Chancen und Risiken von Ottomotoren mit Direkteinspritzung. *MTZ*, 30-36.

Engl, H., Hanke, M., & Neubauer, A. (1996). *Regularisation of Inverse Problems.* Dordrecht: Kluwer Academic Publishers.

Eriksson, L. (2002). Modeling of a Turbocharged SI Engine. *Annual Reviews in Control*, 50-62.

ETAS. (2017). *ETAS solutions for fast control functions*. Retrieved 09 15, 2017, from https://www.etas.com/en/products/applications_electric_hybrid_drive-designing_new_functions.php

European Union. (2011). COMMISSION REGULATION (EU) No 582/2011. *Official Journal of the European Union*, 566-590.

Felici, F., Van Wingerden, J., & Verhaegen, M. (2007). Subspace identification of MIMO LPV systems using a periodic scheduling sequence. *Automatica*, 78-99.

Ferrari, A., Fantechi, A., Gnesi, S., & Magnani, G. (2013). Model-based development and formal methods in the railway industry. *The IEEE Computer Society*, 28-34.

Ferreau, H. (2006). *An Online Active Set Strategy for Fast Solution of Parametric Quadratic Programs with Applications to Predictive Engine Control.* Heidelberg: University of Heidelberg.

Ferreau, H. (2008). *Predictive Engine Control using an Online Active Set Strategy.* Annual Reviews in Control.

Ferreau, H. (2014). *qpOASES: a parametric active-set algorithm for quadratic programming.* Baden-Daettwil: ABB Corporate Research .

Ferreau, H., Ortner, P., Langthaler, P., Del Re, L., & Diehl, M. (2007). Predictive control of a real-world Diesel engine using an extended online active set strategy. *Annual Reviews in Control*, pp. 293–301.

FEV. (2017). FEV Engineering Newsletter. Aachen: FEV.

Findeisen, R., & Allgoewer, F. (2006). *An Introduction to Nonlinear Model Predictive Control.* Stuttgart: University of Stuttgart.

Friedrich, C., Compera, Y., Auer, M., & Stiesch, G. (2017). An Efficient Test Methodology for Combustion Engine Testing: Methods for Increasing Measurement Quality and Validity at the Engine Test Bench. *SAE Technical Paper*, 604-625.

Gelso, E., & Dahl, J. (2016). Air-Path Control of a Heavy-Duty EGR-VGT Diesel Engine. *IFAC-PapersOnLine,Volume 49, Issue 11*, pp. 589-595.

Gregg, D., & Kulkarni, U. (2001). Understanding the Philosophical Underpinnings of Sofware Engineering Research in Information Systems. *Information Systems Frontiers 3:2*, pp. 169-183.

Grimm, K. (2010). Exhaust Gas Mass Flow Sensor for Car and Commercial Vehicle Applications. *ATZ*, 45-51.

Gruenbacher, E., & Schrems, A. (2007). *Identifikation und adaptive Regelung.* Linz: Johannes Kepler University Linz.

Gruene, L., & Pannek, J. (2017). *Nonlinear Model Predictive Control Theory and Algorithms.* Springer International Publishing.

Gundmalm, S. (2009). *CFD modeling of a four stroke S.I. engine for motorcycle application.* Stockholm, Sweden: University KTH.

Gunes, B., Wingerden, J., & Verhaegen, M. (2018). Tensor networks for MIMO LPV system identification. *International Journal of Control* , pp. 133-145.

Guzzella, L., & Onder, C. (2004). *Introduction to Modeling and Control of Internal Combustion Engine Systems.* Berlin: Springer.

Hafner, M., Schueler, M., & Isermann, R. (2000). Einsatz schneller neuronaler Netze zur modellbasierten Optimierung von Verbrennungsmotoren. *Motortechnische Zeitschrift*.

Hamarashid, L. (2008). *GT-Power modeling of a 6-Cylinder natural Gas Egnine and Investigation fo the Possbile Performance Improvements by Studying the Miller Cycle.* Lund: Lund University.

Hanema, J., Lazar, M., & Toth, R. (2017). Stabilizing tube-based model predictive control: Terminal set and cost construction for LPV systems. *Automatica, Volume 85*, pp. 137-144.

Hanke, M., & Hansen, P. (1993). Regularisation Methods for Large-Scale Problems. *Surveys on Mathematics for Industry*, pp. 253-315.

Hellestrand, G. (2005). Model-Based Development with Virtual Prototypes. *VaST Systems Technology*, 74-88.

Herceg, M., Raff, T., Findeisen, R., & Allgoewer, F. (2006). Nonlinear Model Predictive Control of a Turbocharged Diesel Engine. *International Conference on Control Applications*, (pp. 234-255). Munich.

Hirsch, M. (2011). *Identification of a Virtual Sensor Model for Diesel Egnine Emissions by Means of Optimal Input Design.* Linz: Trauner Verlag.

Hochschwarzer, H. (1990). *Automatische Motorparameteroptimierung.* Graz: Technical University Graz.

Huang, H., Zaseck, K., Butts, K., & Kolmanovsky, I. (2016). Rate-Based Model Predictive Controller for Diesel Engine Air Path: Design and Experimental Evaluation. *IEEE Transactions on Control Systems Technology, vol. 24, no. 6*, pp. 1922-1935.

Huang, M., Nakada, H., Polavarapu, S., & Choroszucha, R. (2013). Towards Combining Nonlinear and Predictive Control of Diesel Engines. *American Control Conference*, (pp. 2846 - 2853). Chicago.

Hubert, L. (1997). *Identification and Robust Control of Linear Parameters-Varying Systems.* Berkley: University of California at Berkley.

Integer Research. (2018). *Market Overview Emissions Control in Europe 2018.* London: Integer Research.

Isermann, R. (2014). *Engine Modeling and Control.* Berlin: Springer Verlag.

Isermann, R., Hafner, M., Schaffnit, J., Schueler, M., & Sinsel, S. (1998). Modellbildung und Simulation des statischen und dynamischen Verhaltens von Dieselmotoren mit Turbolader. *Proceedings of the GMA Congress*, (pp. 1210-1235). Baden-Baden.

Jaeskelaeinen, H. (2018). *Emission Formation in Diesel Engines*. Retrieved 08 23, 2018, from https://www.dieselnet.com/tech/diesel_emiform.php

Jacob, D., Goettel, H., Kotlarski, S., Lorenz, P., & Sieck, K. (2008). *Klimaauswirkungen und Anpassung in Deutschland – Phase 1: Erstellung regionaler Klimaszenarien für Deutschland.* Hamburg: Max Planck Institute for Meteorology.

Jaeskelaeinen, H. (2017). *EGR Systems and Components*. Retrieved 06 15, 2017, from DieselNet: https://www.dieselnet.com/tech/engine_egr_sys.php

Jankovic, M., & Kolmanovsky, I. (2000). Constructive Lyapunov control design for turbocharged diesel engines. *IEEE Transactions on Control Systems Technology*, pp. 288 - 299.

Johansson, R. (1993). *System Modeling and Identification.* Chicago: Prentice Hall.

Jones, M. J., & Parker, J. K. (2014). *Informed consent form.* UK: University of Gloucestershire.

JRC. (2016). *Science for environmental sustainability.* Brussels: The European Commission science service.

Jung. (2003). *Mean-Value Modelling and Robust Control of the Airpath of a Turbocharged Diesel Engine.* Cambridge: University of Cambridge.

Kamaruddin, T., & Darus, I. (2012). System Identification for Internal Combustion Engine Model. Bali, Indonesia: Modelling Symposium (AMS).

Kiefer, J., & Wolfowitz, J. (1960). The equivalence of two extremum problems. *Canadian Journal of Mathematics 12*, pp. 363-366.

Kiencke, U., & Nielsen, L. (2005). *Automotive Control Systems For Engine, Driveline, and Vehicle.* Berlin Heidelberg: Springer-Verlag.

Kim, S., Choi, S., & Jin, H. (2016). Pressure model based coordinated control of VGT and dual-loop EGR in a diesel engine-air-path system. *International Journal of Automotive Technology*, pp. 193–203.

Kouvaritakis, B., Cannon, M., & Rossiter, J. A. (1999). Non-linear model based predictive control. *International Journal of Control*, 919-928.

Kristoffersson, I. (2006). *Model Predictive Control of a Turbocharged Engine.* Master thesis, Royal Institute of Technology.

Kumar, R. (2014). *Research Methodology:A Step-by-Step Guide for Beginners Fourth Edition.* New York: SAGE Publications Ltd.

Kuzmych, O., Aitouche, A., Hajjaji, A., & Bosche, J. (2014). Nonlinear control for a diesel engine: A CLF-based approach. *International Journal of Applied Mathematics and Computer Science*, pp. 821–835.

Ladommatos, N., Balian, R., Horrocks, R., & Cooper, L. (1996). The Effect of Exhaust Gas Recirculation on Soot Formation in a High-Speed Direct-injection Diesel Engine. *SAE World Congress and Exhibition* (pp. 58-71). Detroit: SAE Technical Paper.

Lammersen, T., Stoehr, K., Peters, N., & Abel, D. (2013). Model Predictive Control of Dimethyl Ether Combustion in a Jet Stirred Reactor under Low Temperature Conditions. *American Control Conference 2013*, (pp. 1636-1641). Washington.

Landweber, L. (1951). An iteration formula for Fredholm integral equations of the first kind. *Amer. J. Math.*, pp. 615–624.

Langthaler, P. (2007). *Model Predictive Control of a Diesel Engine Air Path.* Linz: University Linz.

Langthaler, P., & Del Re, L. (2007). *Fast Predictive Oxygen Charge Control of a Diesel Engine.* Linz: University Linz.

Lauer, F. (2018). *Hybrid System Identification: Theory and Algorithms for Learning Switching Models.* Springer.

Lennart, L. (1999). *System Identification - Theory for the User 2nd Edition.* New Jersey: Pearson Prentice Hall.

Li, D., Li, F., Huang, X., Lai, Y., & Zheng, S. (2010). A mode lbased integration framework for computer numerical control system development. *Robotics and Computer-Integrated Manufacturing*, pp. 333–343.

Liu, L., & Wei, X. (2007). LPV Control for the Air Path System of Diesel Engines. *IEEE International Conference on Control and Automation* (pp. 873-878). China: IEEE.

Ljung, L. (2001). *System Identification.* New Jersey: John Wiley & Sons, Inc.

Ljung, L., Zhang, Q., Lindskog, P., & Juditski, A. (2007). *Estimation of grey box and black box models for non-linear circuit datas.* Linköpings university.

Longo, S., Kerrigan, E., & Ling, K. V. (2011). Parallel Move Blocking Model Predictive Control. *2011 50th IEEE Conference on Decision and Control and European Control Conference.* Orlando, FL, USA: IEEE.

Lu, A., & Arkun, Y. (2000). A Quasi-min-max MPC Algorithm for Linear Parameter Varying Systems with Bounded Rate of Change of Parameter. *American Control Conference*, (pp. 56-77). New York.

Maciejowski, J. M. (2000). *Predictive Control with Contrains.* London: Prentice Hall.

Malikopoulos, A., Assanis, D., & Papalambros, P. (2008). Optimal Engine Calibration for Individual Driving Styles. *SAE International*, pp. 1367-1374.

Mareels, I., & Polderman, J. (1996). *Adaptive Systems - An Introduction.* Boston: Birkhaeuser.

Martyr, A., & Plint, M. (2011). *Engine Testing: Theory and Practice.* Butterworth-Heinemann.

Maruyama, T., Shimura, T., Ejiri, A., & Ikai, Y. (2011). Model predictive control applied to a diesel engine-air-path system with dead time. *2011 Proceedings of SICE Annual Conference* (pp. 2628 - 2633). Osaka: SAE.

MathWorks. (2014). *Matlab and Simulink for control design acceleration.* Natick: MathWorks.

MathWorks. (2018). *System Identification Toolbox User's Guide.* Natick: Mathworks.

Mayne, D. Q. (2001). Control of constrained dynamic systems. *European Journal of Control*, 85-92.

Mayne, D. Q., & Michalska, H. (1993). Adaptive receding horizon control for constrained nonlinear systems. *Proceedings 32nd IEEE Conference on Decision* (pp. 485-492). Munich: IEEE.

Meeks, E. (2014). ANSYS Strategy for Internal Combustion Engine Simulations World Congress. *Automotive Simulation.* Tokyo, Japan.

Mertl, R., Otto, E., & Beckmann, R. (1998). Die neue Motorsteuerung von Siemens für die BMW Sechszylinder-Ottomotoren. *MTZ*, 820-825.

Miller, F., Vandome, A., & McBrewster, J. (2009). *Beer-Lambert Law.* VDM Publishing.

Minnesota, U. (2003). *A Guide to Research Ethics.* USA: University of Minnesota.

Mitterer, A., & Zuber-Goos, F. (2002). Modellgestütze Kennfeldoptimierung – Ein neuer Ansatz zur Steigerung der Effizienz in der Steuergeräteapplikation. *ATZ*, 188-196.

Moon, J. (1974). *Rudolf Diesel and the Diesel Engine.* London: Priory Press.

Nemani, M., & Ravikanth, R. (1995). Identification of Linear Parameter Varying Systems. *Proceedings of the 34th Conference on Decision & Control*, (pp. 2990-2995). Chicago.

Nguyen-Schaefer, H. (2013). *Aero and Vibroacoustics of Automotive Turbochargers.* Berlin: Springer.

Ni, J., Liu, Y., & Shi, X. (2016). Variable nozzle turbine combined with Venturi exhaust gas recirculation system improving emission performance of diesel engines. *Transactions of the Chinese Society of Agricultural Engineering*, pp. 82-88.

Nickmehr, N. (2015). *System Identification of an Engine-load Setup Using Grey-box Model.* Linköping: Linköping University.

Nieuwstadt, M. J., & Kolmanovsky, I. V. (2000). EGR-VGT control schemes: Experimental comparison for a high-speed diesel engine. *IEEE Control Systems Magazine*, pp. 63-79.

Nieuwstadt, M., Moraal, P., Kolmanovsky, I., & Stefanopoulou, A. (1998). Decentralized and multivariable designs for EGR-VGT control of a diesel engine. *IFAC Workshop, Advances in Automotive Control*, (pp. 61-68). Karlsruhe.

Nocedal, J. (2006). *Numerical Optimisation.* Berlin: Springer.

Nova, I., & Tronconi, E. (2014). *Urea-SCR Technology for deNOx After Treatment of Diesel Exhausts.* Springer Science & Business Media.

Oates, B. J. (2006). *Researching Information Systems and Computing.* London: SAGE Publication.

Oh, B., & Lee, M. (2013). VGT and EGR Control of Common-rail Diesel Engines using an Artificial Neural Network. *Journal of Engineering for Gas Turbines and Power*.

Olenev, N. (2008). *Systems Analysis and Modeling of Intergreated World Systems- Vol. I Modelling and Simulation Techniques.* Encyclopedia of Life Systems .

Oravec, J., Jiang, Y., Houska, B., & Kvasnica, M. (2017). Parallel Explicit MPC for Hardware with Limited Memory. *IFAC-PapersOnLine, Volume 50, Issue 1*, pp. 3301-3306.

Ortner, P., Bergmann, R., Ferreau, H., & Del Re, L. (2009). Nonlinear Model Predictive Control of a Diesel Engine Airpath. *IFAC Workshop on Control Applications of Optimisation, vol. 7,* (pp. 550-556).

Ortner, P. (2006). MPC for a diesel engine air path using an explicit approach for constraint systems. *IEEE International Symposium on Intelligent Control.* Germany: 2760 - 2765.

Ortner, P., & Wang, X. (2009). NMPC for EGR/VGT control. *Automotive Model Predictive Control* (pp. 45-71). Linz: University Linz.

Ortner, P., Langthaler, P., Ortiz, G., & del Re, L. (2006). MPC for a Diesel Engine Air Path using an Explicit Approach for Constraint Systems. *Proceedings of the 2006 IEEE* (pp. 270-2765). Munich: IEEE.

Pluymers, B., Rossiter, J. A., Suykens, J. A., & Moor De, B. (2005). Interpolation Based MPC for LPV Systems using Polyhedral Invariant Sets. *American Control Conference* (pp. 124-133). California: ACC.

Purao, S. (2002). *Design Research in the Technology of Information Systems:Truth or Dare.* Atlanta: The Pennsylvania State University.

Qin, S. J., & Badgwell, T. A. (1997). An Overview of Industrial Model Predictive Control Technology. *Fifth International Conference on Chemical Process Control*, (pp. 232–256).

Qu, S. (2010). Modeling and Simulation of the Proportional Valve Control System for the Turbocharger. *IEEE*, 43-52.

Rakopoulos, C. (2009). *Diesel Engine Transient Operation: Principles of Operation and Simulation Analysis.* Berlin: Springer.

Rasol, M. (2012). *Analysis of Diesel Particulate Matter on Single Cylinder Diesel Engine Using Waste Plastic Fuel.* UMP.

Reif, K. (2014). *Diesel Engine Management: Systems and Components.* Berlin: Springer Vieweg.

Reis, S. (2005). *Costs of Air Pollution Control: Analyses of Emission Control Options for Ozone Abatement Strategies.* Springer.

Renninger, P., Daudel, H., & Hohenberg, G. (2000). Das DaimlerChrysler-Konzept zur computergestützten Motoroptimierung. *4. International Symposium on Combustion Diagnostics*, (pp. 231-239). Baden-Baden.

Research Committe. (2008). *Ethics Handbook.* UK: University of Gloucestershire.

Richalet, J., Rault, A., Testud, J. L., & Papon, J. (1978). Model predictive heuristic control:applications to industrial processes. *Automatica*, pp. 413-428.

Robert Bosch GmbH. (2006). *Diesel-Engine Management.* Stuttgart: John Wiley & Sons.

Saggese, R. (2012). *Combustion Control for Diesel Engines: Model Based Feedforward Approach for Direct Injection.* Saarbruecken: LAP LAMBERT Academic Publishing.

Santos, P., Romano, R., Azevedo-Perdicoulis, T., & Ramos, J. (2017). LPV system identification using the matchable observable linear identification approach. *2017 IEEE 56th Annual Conference on Decision and Control* (pp. 4626-4631). Melbourne: IEEE .

Schueler, M. (2000). *Stationäre Optimierung der Motorsteruerung von PKW-Dieselmotoren mit Abgasturbolader druch Einsatz schnellr neuronaler Netze.* Technical University Damstadt.

Schulz, E., Bussa, A., & Werner, H. (2016). Identification of linear parameter-varying systems via IO and subspace identification - a comparison. *2016 IEEE 55th Conference on Decision and Control (CDC)* (pp. 7147-7152). Las Vegas: IEEE.

Schwerdt, C. (2006). *Modelling NOx-Formation in Combustion Processes.* Lund: Lund University.

Sequenz, H. (2013). *Emission Modelling and Model-Based Optimisation of the Engine Control.* Darmstadt: Technical University Darmstadt.

Serrano, D. (2014). *Combustion Engine Identification and Control.* Lund: Lund University.

Sher, E. (1998). *Handbook of Air Pollution from Internal Combustion Engines.* London: Academic Press Limited.

Shi, X., & Seiser, R. (2015). Fuel-Dithering Optimisation of Efficiency of TWC on Natural Gas IC Engine. *SAE International Journal of Engines*.

Sjoeberg, M., & Dec, J. (2003). A parametric study of HCCI combustion the sources of emissions at low loads and the effects of GDI fuel injection. *SAE technical Papers*, 735-755.

Skarke, P., Auerbach, C., Bargende, M., & Berner, H.-J. (2017). Multivariable air path and fuel path control for a Diesel engine with homogeneous combustion. *17. Internationales Stuttgarter Symposium* (pp. 143-155). Stuttgart: Springer.

Song, C. (2015). *Chemistry of Diesel Fuels.* Boca Raton, FL, USA: CRC Press.

Srinivasan, C. (2014). Increasing the Efficiency of an Engine by the use of Variable Geometry Turbochargers. *International Journal of Innovative Research in Science, Engineering and Technology*.

Tangirala, A. K. (2014). *Principles of System Identification: Theory and Practice.* CRC Press.

The European Parliament. (2007). REGULATION on type approval of motor vehicles with respect to emissions from light passenger and commercial vehicles and on access to vehicle repair and maintenance information. *Journal of the European Union*, pp. 171-187.

Thoma, M., Allgöwer, F., & Morari, M. (2009). *Nonlinear Model Predictive Control - Towards New Challenging Applications.* Springer-Verlag Berlin Heidelberg.

Tikhonov, A. N. (1963). Solution of incorrectly formulated problems and the regularisation. *Dokl. Akad. Nauk. SSSR*, pp. 1035–1038.

Transport Resources Interational Limited. (2017). *The European Union moved to the introduction of Euro 6 emission limits on buses and coaches (and other vehicles) from the start of 2014.* Retrieved 10 09, 2017 from http://www.dougjack.co.uk/bus-industry-euro-6-emissions-limits.html

Truscott, T., & Porter, B. (1997). Die Simulation modellbasierter Regelalgoritmen für einen VTG Dieselmotor. *MTZ*, 58-62.

Unland, S., Stuhler, H., & Stuber, A. (1998). Neue effiziente Applikationsverfahren für die physikalisch basierte Motorsteuerung ME7. *MTZ*.

Unver, B., Koyuncuoglu, Y., & Gokasan, M. (2016). Modeling and validation of turbocharged diesel engine airpath and combustion systems. *International Journal of Automotive Technology*, 13–34.

Van Basshuysen, R., & Schäfer, F. (2004). *Lexikon Motorentechnik.* Wiesbaden: Friedrich Vieweg & Sohn Verlag.

Verdult, V. (2000). Identification of Multivariable Linear Parameter-Varying Systems Based on Subspace Techniques. *Proceedings of the 39th IEEE Conference on Decision and Control*, (pp. 2000-2005). Sydney.

Verdult, V. (2001). *Nonlinear System Identification A State-Space Approach.* Twente: University of Twente.

Verdult, V., & Verhaegen, M. (2001). Identification of Multivariable LPV State-space Systems By local Gradient Search. *Proceedings of the Europe Control Conference*, (pp. 3675-3680). Porto.

Vidyasagar, M. (1993). Nonlinear Systems Analysis. *Classics in Applied Mathematics*, 567-577.

Wahlstroem, J. (2006). *Control of EGR and VGT for emission control and pumping work minimisation in diesel engines.* Linkoeping: Linkoeping University.

Wahlstrom, J., Eriksson, L., Nielsen, L., & Pettersson, M. (2005). PID controllers and their tuning for EGR and VGT control in diesel engines. *IFAC World Congress*, (pp. 1922-1922). Czech Republic.

Wan. (2017). *Variable Turbine Geometry*. Retrieved 06 23, 2017, from Autozine: http://www.autozine.org/technical_school/engine/tech_engine_3.htm#VTG

Wan, Z., & Kothare, M. V. (2003). Efficient Robust Constrained Model Predictive Control with a Time Varying Terminal Constraint Set. *Systems and Control Letters*, 375-383.

Wang, X., & Steiner, A. (2011). Linear Parameter-Varying Modeling of Electric Vehicle Air Conditioning System. *Applied Mechanics and Materials*, pp. 318-325.

Wang, X., Waschl, H., Alberer, D., & Del Re, L. (2012). A Design Framework for Predictive Engine Control. *Oil & Gas Science and Technology – Rev. IFP Energies nouvelles*, pp. 599-612.

Wang, X., Zhang, S., & Bechkoum, K. (2016). Data-Based Gain-Scheduled Modeling and Nonlinear Control of Engine Intake and Exhaust System. *Advances in Engineering Research Proceedings of the 5th International Conference on Mechanical Engineering, Materials and Energy* (pp. 230-235). Atlantis Press.

Wang, X., Zhang, S., & Bechkoum, K. (2019). Model-based multi-critical optimisation of combustion engine fuel consumption and emissions. *Proceedings of 2nd International Conference on Robotics and Mechantronics* (pp. 260-263). IOP Conference Series: Materials Science and Engineering.

Wang, Y. (2015). Model-based calibration: A case study for calibrating control systems of downsized boosted engines. *2015 American Control Conference (ACC)* (pp. 2112-2122). Chicago: IEEE.

Wei, X. (2003). LPV Identification of a Diesel Engine Torque Model. *13th IFAC Symposium of System*, (pp. 1448-1453). Netherland.

Wei, X. (2004). LPV Dynamical Models of Diesel Engine NOX Emission. *First IFAC Symposium on Advances in Automotive Control*, (pp. 262-267). Italy.

Wei, X. (2006). *Advanced LPV Techniques for Diesel Engines.* Linz: University Linz.

Wei, X., & Del Re, L. (2003). LPV Identification of a Diesel Engine Torque Model. *13th IFAC Symposium of System Identification*, 654-660.

Welch, G., & Bishop, G. (2006). *An introduction to the Kalman filter.* Carolina: University of North Carolina.

Willmott, C., & Matsuura, K. (2005). Advantages of the Mean Absolute lute Error (MAE) over the Root Mean Square Error (RMSE). *Clim. Res*, 79–82.

Wissel, D., Talon, V., Grangier, B., Lansky, L., & Uchanski, M. (2016). Linking model predictive control (MPC) and system simulation tools to support automotive system architecture choices. *8th European Congress on Embedded Real Time Software and Systems,* (pp. 2078-2081). Toulouse, France.

WWF. (2018). *Auswirkungen des Klimawandels Weltweit*. Retrieved 07 09, 2018, from www.wwf.at/de/menu471/subartikel1282/

Xie, Y., Kistner, A., & Bleile, T. (2018). Optimal Automated Calibration of Model-Based ECU-Functions in Air System of Diesel Engines. *SAE Technical Paper*, 556-580.

Yan, F., Benjamin, H., & Wang, J. (2009). Optimal Control of Complex Air-Path Systems for Advanced Diesel Engines. *ASME 2009 Dynamic Systems and Control Conference,* (pp. 67-71). California.

Yang, Z., Winward, E., Zhao, D., & Stobart, R. (2016). Three-Input-Three-Output Air Path Control System of a Heavy-Duty Diesel Engine. *IFAC-Papers OnLine, Volume 49, Issue 11*, pp. 604-610.

Yao, M., & Zhang, Q. (2009). Experimental study of effects of oxygen concentration on combustion and emissions of diesel engine. *Science in China Series E: Technological Sciences*.

Yin, J., Su, T., Guan, Z., Chu, Q., & Meng, C. (2017). Modeling and Validation of a Diesel Engine with Turbocharger for Hardware-in-the-Loop Applications. *Energies,* 445-460.

Yin, L., Ingesson, G., Johansson, R., Tunestal, P., & Hedrick, J. K. (2017). Nonlinear air-path control of a heavy-duty diesel engine - a Receding Horizon Sliding Control approach. *2017 American Control Conference (ACC)* (pp. 3619-3624). Seattle, WA, USA: IEEE.

Yule, G. (1927). On a Method of Investigation Peroodicities in Disturbed Series with Special References to Wolfers Sunspot Numbers. *Philos. Trans. R. Soc. London*.

Zeng, T., Upadhyay, D., & Zhu, G. (2017). Linear quadratic air-path control for diesel engines with regenerative and assisted turbocharger. *IEEE 56th Annual Conference on Decision and Control (CDC).* Melbourne, VIC, Australia: IEEE.

Zhang, R., Xue, A., & Gao, F. (2018). *Model Predictive Control.* Singapore: Springer.

Zhao. (2010). *Advanced Direct Injection Combustion Engine Technologies and Development: Diesel Engines.* Woodhead Publishing Limited.

Zhao. (2013). Explicit model predictive control on the airpath of turbocharged diesel engines. *American Control Conference*, (pp. 5213 – 5218). New York.

Zhao, W., & Pan, H. (2012). A Fuzzy PID Controller for Exhaust Gas Recirculation System. *International Conference on Mechanical Engineering and Automation*, (pp. 34-55). Munich.

Zheng, Z., & Yao, M. (2009). Mechanism of Oxygen Concentration Effects on Combustion Process and Emissions of Diesel Engine. *Energy Fuels*.

Zhou, J., Fiorentini, L., & Canova, M. (2016). Model-based optimisation and predictive control of a turbocharged diesel engine with variable geometry compressor. *International Journal of Powertrains*, pp. 167 - 190.

Zhu, J., Ren, H., & Luo, Y. (2015). Simulation Research on EGR Reducing NOx Emission of Diesel Engine. *International Journal of Energy and Power Engineering*, pp. 275-279.

Appendix A- Design of Experiment

The following definitions of DOE mainly coincide with those of (Hirsch, 2011) and (Ljung, System Identification, 2001). First of all, it is assumed that a mathematical model (sensor dynamics is known) is sufficient for approximation:

$$\hat{y}(k) = f\big(u(k)\big) = \theta_0 + \theta_1 u_1(k) + \theta_2 u_2(k) \ldots \theta_4 u_4(k) u_4 \,. \qquad \text{(a-1)}$$

As presented in (Hirsch, 2011), the independently and identically distributed Gaussian error *ε~ N (0, σ²)* on the transformed measurement *y* is expressed as follows:

$$y(k) = \ f(u(k), \theta) + \varepsilon(k). \qquad \text{(a-2)}$$

We define the least squares estimators as well as the maximum likelihood estimators $\hat{\theta}$ as follows,

$$\hat{\theta} = (\textstyle\sum_{k=1}^{N} \frac{\partial f(u(k),\theta)}{\partial \theta} \frac{\partial f(u(k),\theta)}{\partial \theta^T})^{-1} \sum_{k=1}^{N} \frac{\partial f(u(k),\theta)}{\partial \theta} y, \qquad \text{(a-3)}$$

and the variance of $\hat{\theta}$ can be written as follows,

$$var\hat{\theta} = \partial^2 (\textstyle\sum_{k=1}^{N} \frac{\partial f(u(k),\theta)}{\partial \theta} \frac{\partial f(u(k),\theta)}{\partial \theta^T})^{-1} = \frac{\partial^2}{N} \bar{M}(u, \theta)^{-1}. \qquad \text{(a-4)}$$

$\bar{M}(u, \theta)^{-1}$ is the normalised information:

$$\bar{M}(u, \theta) = \frac{1}{N} (\textstyle\sum_{k=1}^{N} \frac{\partial f(u(k),\theta)}{\partial \theta} \frac{\partial f(u(k),\theta)}{\partial \theta^T}) \,. \qquad \text{(a-5)}$$

Hirsch (2011) states that the idea of input design is to have an input sequence *u(k)* that persistently excites the system. This means that the input signal should be conditioned that way column of $X = \frac{\partial f(u(k),\theta)}{\partial \theta^T}$ (regressors) are uncorrelated and separable. To minimise the influence of the noise $\varepsilon(k)$, amplitudes of repressor in X should become maximal which implies that the entire input range Ω should be utilised. Furthermore, critical model extrapolations can be avoided by maximising the amplitudes to the boundaries of Ω.

Optimal input design algorithms define input signal such that inputs operate within the pre-defined continuous but bounded input range Ω and thereby maximise a scalar criterion, usually related to the size of $\bar{M}(u,\theta)$, a common one being the D-criterion, defined as follows:

$$J(M) = \det(\bar{M}(u,\theta)) \ . \tag{a-6}$$

For some alternative criteria see e.g. Optimum Experimental Designs (Atkinson & Donev, 1992). The input sequence can be computed by solving:

$$u(k) = argmax\Big(det\big(\bar{M}(u,\theta)\big)\Big), u(k) \in \Omega, k = 1 \ldots N. \tag{a-7}$$

This Equation a-7 for an input sequence of length *N* will have *r = 4* (number of inputs) times *N* parameters for optimisation. Direct optimisation of more than 10-20 parameters would overstrain optimisation routines especially as the optimisation should be a global one, since the problem is non-convex. Using approximate design algorithms, where next inputs are defined sequentially is considering the already obtained measurements, parameters for optimisation can be reduced. The used algorithm here is based on the Kiefer-Wolfowitz Equivalence Theorem (Kiefer & Wolfowitz, 1960) which relates optimality in the parameter space to optimality in the space of observations. For D-optimality this theorem does this in the following sense:

Let $\hat{\theta}$ be the estimated parameter vector for a data series (measured inputs as well as outputs) of length *k*. The error for the estimation of *y(k)* according to $\hat{\theta}$ is given by the output variance which depends on the location of *u(k+1)* within *Ω*:

$$var(y\big(u(k+1),\hat{\theta}\big) = \frac{\partial^2}{N} X(k+1)^T \bar{M}(k)^{-1} X(k+1), \tag{a-8}$$

where $\bar{M}(k)$ defines the normalised information matrix at the sampling instance k and therefore includes all measurements up to that point. Mostly the standardised prediction variance $d(y(u(k+1), \overline{M}(k))$ is used for optimsation as this value does not depend on N and ∂^2:

$$d(u(k+1), \overline{M}(k)) = X(k+1)^T \overline{M}(k)^{-1} X(k+1)\ . \tag{a-9}$$

The D-optimal design is sequentially approximated, if the next input *u(k+1)* is defined such that $d(y(u(k+1), \overline{M}(k))$ becomes maximal (For more details see e.g. (Atkinson & Donev, 1992)):

$$u(k+1) = argmaxX(k+1)^T \overline{M}(k)^{-1} X(k+1) u(k+1) \in \Omega. \tag{a-10}$$

This optimisation presents a non-convex problem with several local maxima within Ω. In this task, a multi-shot optimisation is used to cope with this issue. There, several optimisations start at random points within Ω and the best is considered as the optimum.

APPENDIX B- ONLINE ACTIVE SET STRATEGY

An online active set strategy, namely the qpOASES, for the fast solution of QP problem is developed in (Ferreau, 2014); it is shown that this active set strategy turned out to be significantly faster than a standard QP-solver while overcoming the prohibitive limitations of the explicit approach to MPC optimisation. This software provides us with mathematical methods for the handling of QP problems. A parametric online active set method is applied where in each major iteration step a quadratic approximation of the Hessian of the Lagrange function is calculated to determine the direction of search for the next iteration, while the step length is determined by an appropriate line search procedure such that a sufficient decrease in a merit function is obtained. This is done repeatedly until the stop condition is fulfilled, i.e. the cost function is sufficiently minimised.

The qpOASES using following QP formulation in the solver:

$$\text{QP } (x_0): \qquad min_w \frac{1}{2} w^T H w + w^T \underbrace{F^T x_0}_{=:g(x_0)} . \tag{b-1}$$

$$subject\ to$$

$$Gw \geq \underbrace{\bar{b} + E x_0}_{=:b(x_0)}$$

$$w \coloneqq [u_0, \cdots, u_{N-1}]^T.$$

This idea behind this QP-solver is a process of finding the best achievable result according to various parameters. The optimum is specified by the extreme of a defined function which can be either the maximum or – as it is in this case – the minimum of a cost function, which is referred to the objective function *f(x)* in the following.

Therefore, a general optimisation problem can be defined according to (Nocedal, 2006) and (Durea, 2014) as follows:

$$\min f(x), \quad x \in R^n. \tag{b-2}$$

As in general *x* is a vector, the derivation of *f(x)* according to each element of *x* has to be determined. In detail the gradient *g(x)* of a scalar function *f(x)* can be computed by solving:

$$g : R^n \to R^n \ , \quad g(x) = \nabla f(x) = \begin{bmatrix} \frac{\partial f}{\partial x_1}(x_1, \cdots, x_n) \\ \vdots \\ \frac{\partial f}{\partial x_n}(x_1, \cdots, x_n) \end{bmatrix}. \tag{b-3}$$

The second derivative is written as a Hessian matrix as follows:

$$H : R^n \to R^{n\times n} \ , \quad g(x) = \nabla f(x) = \begin{bmatrix} \frac{\partial^2 f}{\partial x_1^2} & \cdots & \frac{\partial^2 f}{\partial x_1 \ x_n} \\ \vdots & \ddots & \vdots \\ \frac{\partial^2 f}{\partial x_1 \ x_n} & \cdots & \frac{\partial^2 f}{\partial x_n^2} \end{bmatrix}. \tag{b-4}$$

Because of the commutability of the differentiation this matrix is always symmetric. The first order necessary condition for a local minimum $x*$ is defined by,

$$g(x^*) = \nabla f(x^*) = 0. \tag{b-5}$$

For an unconstrained optimisation problem, this first order condition is necessary but not sufficient as a turning point also fulfills $g(x^*) = \nabla f(x^*) = 0$ although it is not a global extreme point. Hence, in order to obtain a sufficient optimality condition, it is required that $H(x^*)$ is positive definite. In the case of a constrained optimisation problem constraint functions $c_i(x)$ are given by,

$$c_i(x) = 0, \qquad i \in E, \tag{b-6}$$

where E is the index set of equality constraints and I is the set of inequality constraints. The constraint functions $c_i(x)$ have to be considered in the objective function (x) , which can be done by introducing the Lagrange function of $f(x)$ written as,

$$L(x, \lambda) = f(x) - \lambda^T \cdot c(x), \tag{b-7}$$

where $\lambda^T$is the vector of Lagrange multiplier. Using the Lagrangian function instead of the original objective function $f(x)$ the condition of the extreme point can be written as:

$$\nabla L(x^*, \lambda^*) = 0, \tag{b-8}$$

and additionally, the Hessian of the Lagrange $\nabla L(x^*, \lambda^*)$ must be positive definite.

The following is applied to the optimisation process in the solver of qpOASES. **Theorem** (Diehl, 2007)**:** *Let $QP(x_0)$ be a strictly convex and feasible quadratic program, then there exists a unique $w^* \in R^n$ and at least one working set A and a vector $y^* \in R^n$ which satisfy the following conditions:*

$$\text{QP }(x_0): \qquad \begin{aligned} & H\,w^* - G_A^T y_A^* = -g(x_0) \\ & subject\ to \\ & G_A w^* = b_A(x_0) \\ & y_\Pi^* = 0, (\,\Pi := [1, \cdots, m]^T \backslash A) \\ & G_\Pi w^* = b_\Pi(x_0). \end{aligned} \tag{b-9}$$

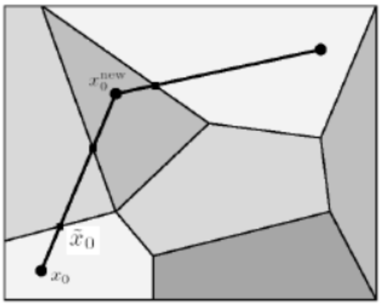

Figure b.1: Search for optimal solution in qpOASES (Ferreau, 2014)

In the optimisation process, as shown in Figure b.1 the solver of qpOASES calculate the $\Delta x_0, \Delta g$ and Δb at first and based on their results to calculate the primal and dual step directions Δw^* and Δy^*. Then determine the maximum homotopy step length $\tau_{max} := \min\{\,1, \tau_{max}^{prim}, \tau_{min}^{prim}\}$ in order to obtain optimal solution of QP (x_0) as follows:

$$\begin{aligned} & x_0 + \tau_{max}\Delta x_0 \rightarrow \tilde{x}_0 \\ & w^* + \tau_{max}\Delta w^* \rightarrow \widetilde{w}^* \\ & y^* + \tau_{max}\Delta y^* \rightarrow \tilde{y}^*, \end{aligned} \tag{b-10}$$

where if $\tau_{max} = 1$, the final optional solution of QP (x_0^{new}) can be found; if $\tau_{max} = \tau_{max}^{prim}$, a dual blocking constraint $j(\tau_{max}^{prim} = -\frac{y_j^*}{\Delta y_j})$ should be removed from the working set; in all other situations a primal blocking constant $j(\tau_{max}^{prim} = \frac{b_j(x_0) - G_j^T w^*}{G_j^T \Delta w^* - \Delta b_j})$ will be added to ensuring the linear independence. Finally set

$$\begin{aligned} x_0 &\to \tilde{x}_0 \\ w^* &\to \widetilde{w}^* \\ y^* &\to \tilde{y}^*, \end{aligned} \tag{b-11}$$

and all the computation is repeated at the next sampling time.

In the case of a convex optimisation problem every local minimum is a global minimum too. This is not valid in the case of a non-convex problem and therefore convex optimisation problems are relatively easy to solve. The purposed optimisation in QP problem is a constrained optimisation problem, as there are some limitations e.g. to the VGT and EGR. Furthermore, the derivatives of the cost function cannot be determined analytically, as described above. Thus, to evaluate the derivatives of the cost function, the simulation is performed using different parameters and the different results caused by the cost functions have compared each other.